



PARTY SUBMISSION

TO THE
NATIONAL TRANSPORTATION
SAFETY BOARD

FIU University City Prosperity Pedestrian Bridge
Construction Accident
Miami, Florida | March 15, 2018

Submitted by - Figg Bridge Engineers, Inc.

September 20, 2019

TABLE OF CONTENTS

PARTY SUBMISSION

TO THE NATIONAL TRANSPORTATION SAFETY BOARD
FIU UniversityCity Prosperity Pedestrian Bridge Construction Accident
Miami, Florida | March 15, 2018
Submitted by - Figg Bridge Engineers, Inc.

1. Executive Summary

2. Introduction

3. Project Description

4. Project Participants

5. Summary of Events

- 5.1. Prior to Bridge Move
- 5.2. Bridge Move and De-Stressing
- 5.3. March 11 through March 14
- 5.4. Day of Accident (March 15)

6. Factual Information

- 6.1. NTSB Factual Report
- 6.2. Design
 - 6.2.1. Calculations
 - 6.2.2. Plans
 - 6.2.3. Specifications
 - 6.2.4. Construction Phasing
 - 6.2.5. FDOT Reviews
- 6.3. Redundancy
- 6.4. Independent Peer Review
- 6.5. Construction
 - 6.5.1. Main Span Fabrication
 - 6.5.2. Bridge Move
 - 6.5.3. Restressing Member #11
 - 6.5.4. Communication With EOR
- 6.6. Road Closures
- 6.7. Construction QC/QA

TABLE OF CONTENTS CON'T

6.8. NTSB Testing

- 6.8.1. Post-Tensioning Jack
- 6.8.2. Concrete and Reinforcing/Post-Tensioning Steel
- 6.8.3. Deck and Truss Members 11 & 12 Construction Joint
- 6.8.4. Roughness Measurements of Member 11/12 Construction Joint

6.9. Construction Joint Sliding Tests by WJE

7. Analysis

- 7.1. Collapse Sequence
- 7.2. Evaluation of Joint Below Members 11/12
- 7.3. Structural Analysis
 - 7.3.1. Factor of Safety
 - 7.3.2. Compliance with Design Requirements
- 7.4. Bridge Move
- 7.5. Restressing Member #11

8. Conclusions

- 8.1. Probable Cause
- 8.2. Contributing Causes
- 8.3. Excluded Causes

9. Safety Recommendations

- 9.1. Role of Engineer of Record (EOR) During Construction
- 9.2. Training for Contractors and Inspectors of Concrete Construction Joints
- 9.3. Personal Safety Equipment

10. Other Reports

- 10.1. NTSB Factual Report
- 10.2. NTSB Investigative Update 2
- 10.3. OSHA Investigation Report

Exhibits

- A. WJE Report
- B. TFHRC Factual Report "Concrete Interface Under Members 11 and 12"
- C. NTSB Materials Laboratory Study Report No. 19-043
- D. BDI Report (Excerpts)

1. EXECUTIVE SUMMARY

1. EXECUTIVE SUMMARY

BACKGROUND

At approximately 1:47 p.m. on March 15, 2018, a partially completed concrete pedestrian bridge spanning SW 8th Street in Miami, Florida, collapsed during construction fatally injuring six (6) individuals and injuring a number of others. The pedestrian bridge was part of the UniversityCity Prosperity Project that was intended by the Owner, Florida International University (FIU), to connect the FIU campus on the south to the City of Sweetwater on the north. The structure was to be a Signature Pedestrian Bridge with a creative and distinctive design to serve as a landmark.

After extensive competition, FIU entered into a contract with Munilla Construction Management, LLC (MCM) in January 2016 for \$9.4 million to design and build the signature pedestrian bridge. MCM had many subcontractors working for them during construction. Figg Bridge Engineers, Inc. (FIGG) designed the bridge as a consultant to MCM and was the Engineer of Record for the structure. Located 500 miles away from the project in Tallahassee, FIGG's scope did not include personnel at the project site during construction other than occasional visits.

Because the bridge was located in right-of-way owned by the Florida Department of Transportation (FDOT), they reviewed the design and confirmed they were satisfied with the Released for Construction (RFC) plans before construction started. FIU retained Bolton, Perez and Associates (BPA) to administer and oversee the design-build contract, and to provide construction engineering and inspection services at the site to ensure compliance with the project requirements.

BRIDGE DESIGN

The signature pedestrian bridge designed by FIGG consisted of a 174-foot main span over SW 8th Street and a 99-foot back span crossing a canal on the north, with access stairs and elevators at each end as shown in **FIGURE 1-1**. The superstructure was a concrete truss with a 30-foot wide walkway on the bottom and a canopy above, connected by a single row of truss members (diagonal supports). The center support featured a 109-foot tall pylon with steel pipes that connected to the bridge superstructure. Nearly all the load was carried by the concrete truss, with the steel pipes serving to reduce vibrations from pedestrian loads after the bridge was open.

The bridge design followed the American Association of State Highway Transportation Officials (AASHTO) Load and Resistance Factor Design (LRFD)

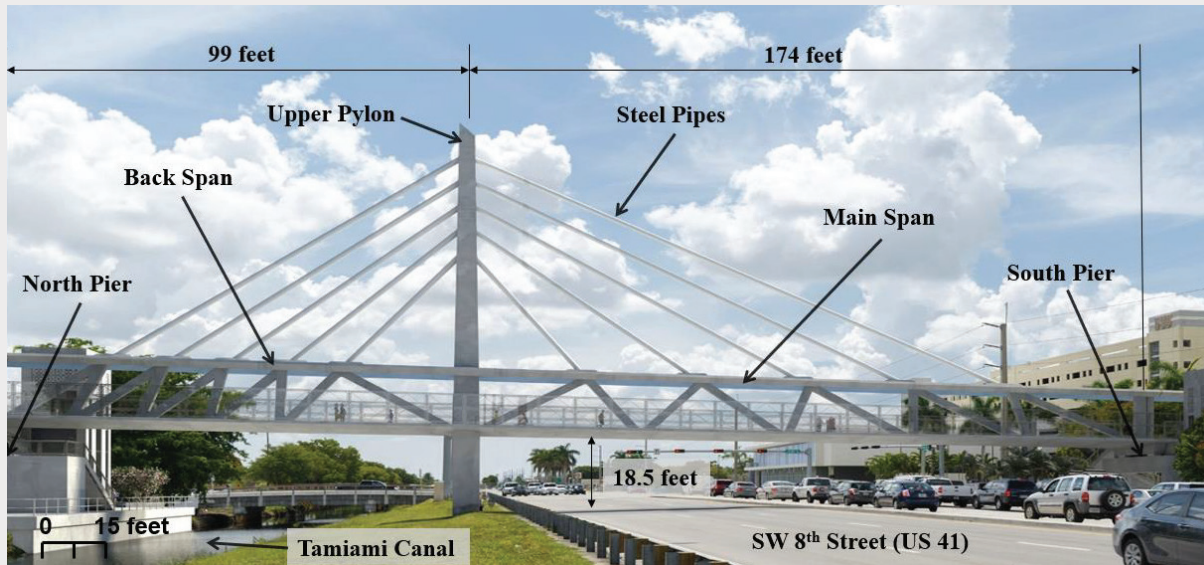


FIGURE 1-1 Rendering of what the signature pedestrian bridge would look like when completed looking to the east (Source: NTSB Factual Report)

Specifications, the FDOT Structure Design Guidelines and the contract design criteria for the project. Use of FDOT Standard Specifications for Construction was a contract requirement, and these were specified in the first note on the General Notes sheet at the front of the RFC plans.

Design submittals were reviewed before construction by a team of 37 individuals, including 32 from FDOT and their outside consultants and a structural reviewer from the Federal Highway Administration (FHWA). Over 340 comments were made and all were satisfactorily resolved before the RFC plans were issued for construction.

A construction sequence was included in the RFC plans that utilized Accelerated Bridge Construction (ABC), a technique supported by the Federal Highway Administration as “changing the ways State Departments of Transportation do business”. FIU is home to the Accelerated Bridge Construction University Transportation Center which has received Federal grants and promotes ABC. The goal of ABC is to minimize traffic disruptions during construction, in this case by precasting the main span truss adjacent to SW 8th Street and then moving the span into position over SW 8th Street during a weekend road closure.

EVENTS LEADING TO THE ACCIDENT

Main Span Fabrication

The concrete truss for the main span was precast on falsework in a staging area on the south side of SW 8th Street just west of the permanent bridge location. For

constructability, the span was cast in three pours: first the bottom slab (bridge deck), then the truss members and finally the canopy. Between each of the pours, the lower portion of concrete was allowed to harden before wet concrete was deposited above it for the next element. The interfaces between the prior pour and the subsequent pour are concrete construction joints which must transfer forces between the two concrete pours so that the span behaves as a continuous structure when completed. MCM cast the bridge deck on October 19, 2017 and the truss members on November 6.

The FDOT Standard Construction Specifications listed at the front of the RFC plans require that construction joints between concrete pours be roughened after the first pour has hardened, which is important to remove surface laitance and increase bond and shear capacity across the joint. This requirement was reiterated by FIGG in an e-mail exchange between MCM and BPA in June 2017 prior to construction. However, evidence obtained after the accident by NTSB from material samples, laboratory testing and worker interviews indicate that the concrete joint under the critical truss members at the north end of the main span (members 11/12) was left in an as-cast, un-roughened condition. This fact was unknown to FIGG until the post-accident investigation.

After the main span precasting was complete and the falsework removed in February 2018, BPA provided a report of some observed concrete cracking, including cracks in the chamfer between the end truss diagonal members and the bridge deck (**FIGURE 1-2**). These were evaluated by FIGG and deemed to be

FIGURE 1-2

Cracks in the base of member 11 near the bridge deck on February 28, 2018 after falsework removal. (Source: BPA)



FIGURE 1-2A

Crack in east side chamfer of member 11 connection to bridge deck.



FIGURE 1-2B

Crack in west side of truss member 11.



FIGURE 1-3C

Crack in west side chamfer of member 11 connection to bridge deck.

due to the boundary location between members. The self-supporting main span remained in the precast area, subject to the same loads and forces as at the time of the accident, for two weeks after the shoring was removed until the bridge move.

Bridge Move

MCM contracted with Barnhart Crane and Rigging (Barnhart) to lift and transport the main span from the precast area to the permanent location over SW 8th Street, rotating it 90 degrees and moving it approximately 70 feet to the east as seen in **FIGURE 1-3**. As part of this, Barnhart hired Bridge Diagnostics, Inc. (BDI) to electronically monitor the span during the move to ensure in part that the twist limits specified by FIGG to avoid damage to the span were not exceeded. The move took place during a road closure on Saturday, March 10 starting at 4:30 a.m. with completion around 12:30 p.m.

FIGG was present for the span move and was not informed either during or after the move that there were any recorded instances of span twist exceeding the established limits. However, a report prepared 20 days after the accident by BDI indicated that the twist limits had been exceeded during the move, and that the span had been subjected to at least 150% and possibly 168% of the maximum limit as seen in the graph in **FIGURE 1-4**. A post-accident structural analysis by forensic engineers Wiss, Janney, Elstner Associates (WJE) determined that this caused high stresses in the truss member connection region at the north end of the span.

FIGURE 1-3

Precast main span truss move by transporters on March 10, 2018 from casting area to permanent piers.
(Source: FIGG)



FIGURE 1-4

Figure 32 from BDI monitoring report on twist of the main span during the bridge move (as modified in WJE report). Twist limit of 0.5 degrees was substantially exceeded on multiple occasions.

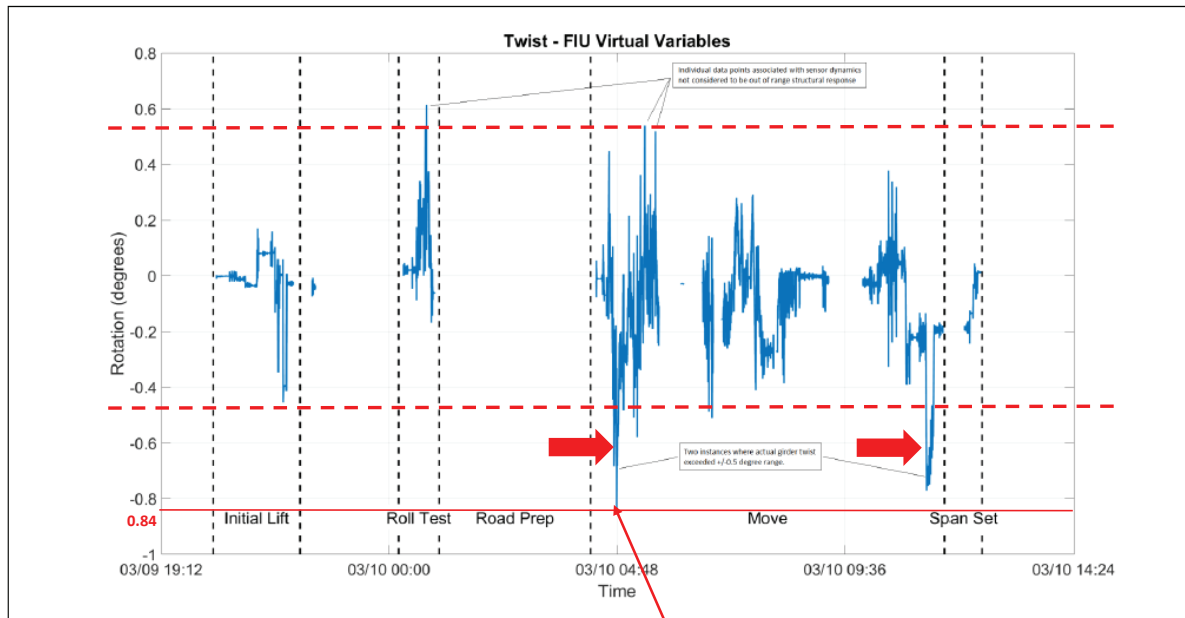


Figure 32 – Girder Twist – Difference in angle between Sections J & L

Difference in rotation between north and south supports: 0.84°

Days Prior to Accident

Photographs taken immediately after the bridge move on March 10 show that the cracking at the north end connection was similar to that observed before the move. However, several hours later and after FIGG had left the site, MCM and an inspector for Corradino (subconsultant to BPA) observed significantly worsened cracking, new cracking and spalled concrete at the north truss member connection. FIGG was not contacted, and the next construction step of distressing temporary steel prestressing bars in the end truss diagonals proceeded, after which SW 8th Street was reopened to traffic. The distressing was performed by a subcontractor to MCM, Structural Technologies (Structural or VSL). Shortly after the distressing operations were completed and an hour after traffic was opened, a worker for Structural texted a co-worker “It cracked like hell”. FIGG was not notified by anyone of worsening or additional cracking until two days later.

Late Monday afternoon March 12, MCM sent FIGG 16 photos, 13 of which were of the north diaphragm showing distress (**FIGURE 1-5**). After opening the e-mail on the morning of March 13, the MCM and FIGG project managers had two phone calls in which MCM told FIGG that the cracking had been noticed on Saturday prior to the distressing operation, the cracks had gotten slightly worse after the distressing, and the cracks had not increased in size since Saturday afternoon. FIGG sent

FIGURE 1-5

Photo of the member 11/12 node provided to FIGG. (Source: NTSB Factual Report Attachment #24 and Bridge Factors Photographs #'s 90, 83 and 76)



e-mails to MCM recommending installing additional shims beneath the diaphragm (to reduce stress in the diaphragm) and to restress the end diagonal truss member (to revert to the prior state of the structure where it had been reported there was less cracking). The restressing was to be performed in 12 steps with close monitoring of the cracks. If the cracks worsened, the restressing operation was to be halted immediately and FIGG notified.

The next afternoon (March 14), shortly before FIGG was leaving to travel to the site to present their analysis, MCM sent an e-mail to FIGG with photos attached without commentary. The e-mail also confirmed the meeting to be held at 9:00 a.m. the next day at the site where FIGG was to present a summary of their evaluation.

Based on photographs submitted to the NTSB by MCM, BPA and their respective subcontractors, the companies on-site were aware of changes in the cracks. No measurements of cracks, other than the appearance of a tape measure in certain photographs, were provided to FIGG since before the bridge move. No record of monitoring and no crack reports were provided for analysis to FIGG during this time, and no one called or e-mailed FIGG to say that anything had changed since Monday. There is no indication that MCM, BPA or other project participants who were on-site during this time actively observing the cracking expressed concern with the safety of the span suspended over SW 8th Street or suggested that the road should be closed until the situation was resolved.

Day of the Accident (March 15, 2018)

On the morning of March 15, two engineers from FIGG, together with representatives of MCM and BPA, went on the bridge deck and observed the north truss connection to the deck before going to MCM's office trailer for the 9:00 a.m. meeting. The meeting was attended by representatives from MCM, FDOT, FIU, BPA and FIGG. A presentation was made by FIGG focusing on the north end diaphragm which showed that there should be sufficient capacity to carry the applied loads.

No one at the meeting expressed concern with the safety of the span suspended over SW 8th Street or with leaving SW 8th Street open. FIGG left the site to return to Tallahassee to develop a way to enhance the north end truss member connection during this stage of construction.

Just before noon on March 15, Structural began the process of restressing the member 11 PT bars using the 12 step process. Site video and witness interviews indicate that the restressing was nearly complete when the bridge experienced a catastrophic failure and collapsed onto SW 8th Street at approximately 1:47 p.m. Post-accident analysis of FIU construction web cam video shows that the cracks were not closely monitored during re-stressing as stipulated by FIGG and by Structural shop drawings and that proper crack monitoring tools do not appear to have been in use. Had proper crack monitoring been performed, it is possible that a worsening condition could have been detected and the restressing operation halted before the accident occurred.

PROBABLE CAUSE

The FIU UniversityCity Prosperity Pedestrian Bridge construction accident occurred because the construction joint at the north end of the main span between the truss members and the bridge deck was not roughened as required by the Florida Department of Transportation (FDOT) Standard Specifications for Road and Bridge Construction. This failure to meet the construction specification requirements was not noticed by either the contractor's quality control personnel or by the construction inspectors under contract to FIU.

Supporting Analysis

Forensic engineers, Wiss, Janney, Elstner Associates performed analyses related to the FIU Pedestrian Bridge accident, including laboratory testing of full-size specimens designed to replicate the truss member 11 connection to the bridge deck. Key findings from the WJE studies presented in Exhibit A are:

- The design of the truss member 11 connection to the bridge deck as shown in the RFC plans prepared by FIGG was in compliance with the AASHTO LRFD design requirements.
- A debonding and sliding failure at the construction joint below truss member 11 led to a breakout failure of the north-end diaphragm and ultimately collapse, triggered by sudden crushing of member 11 near its base.
- For the observed failure pattern and as-built un-roughened condition of the member 11 construction joint (**FIGURE 1-6**) that was not in compliance with the FDOT Standard Specifications, the estimated connection resistance determined from testing and analysis is consistent with the calculated force in the deck connection at the time the failure. This explains the failure due to the un-roughened construction joint surface.

- Full-scale tests show that if the construction joints below Members 11 and 12 were roughened as required by the FDOT Standard Specifications, the collapse would not have occurred. This conclusion is valid for hardened concrete surfaces intentionally roughened in accordance with FDOT Standard Specifications even if the surface roughness is considered to be less than the 1/4 inch amplitude referenced in the AASHTO LRFD Design Code.
- The FDOT Standard Specifications, as proven by the project testing achieves the requirements of the AASHTO Code.

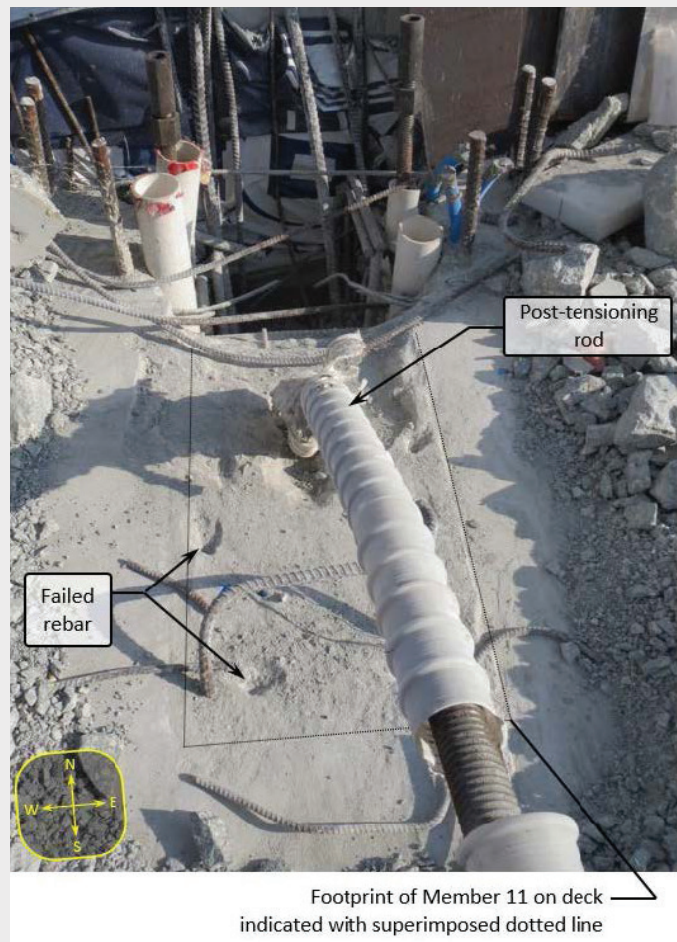
Contributing Causes

While the bridge collapse would not have happened if not for the failure to comply with FDOT specifications, several other factors contributed to the accident:

- Damage to the bridge from significantly exceeding the established twist limits during the bridge move, which was not revealed until weeks after the accident.
- Inadequate, inaccurate and untimely information provided by MCM and others at the project site to FIGG, who was off-site, concerning the crack growth, locations and extents.
- Failure of MCM, BPA, FIU and FDOT acting alone or collectively to close traffic on SW 8th Street while questions about the observed cracking were being investigated and while Structural was restressing the member 11 post-tensioning.
- Failure of Structural, MCM and BPA to closely monitor the existing cracking during restressing member 11 in accordance with instructions from FIGG and the Structural drawing.

FIGURE 1-6

Interface under member 11 showing smooth construction joint surface (Source: TFHRC Report “Concrete Interface under members 11 and 12”)



STRUCTURE REDUNDANCY

The FIU Pedestrian Bridge superstructure was designed as a single concrete prestressed and reinforced truss and was not a steel structure. While there are numerous provisions related to redundancy in the AASHTO LRFD design code for steel bridges, there are no provisions related to redundancy specifically for concrete bridges. According to FHWA, structural redundancy can be provided in several ways. The FIU pedestrian bridge design has redundant features such as multiple parallel reinforcing bars and/or prestressing tendons and a continuous superstructure at completion. The issue of redundancy in concrete structures will be outlined fully in our following submission.

SUMMARY

This detailed Submission presented by FIGG presents a very clear explanation of why this structure failed. The Released For Construction plans, approved by FDOT and independently peer reviewed required use of the FDOT Standard Construction Specifications, which require roughening the surface of concrete construction joints, a common practice in the industry. The northern truss member 11/12 connection to the deck was not roughened as required. The oversight of the concrete work was inadequate and missed that this common requirement was not completed per the RFC plans and FDOT specifications. When this weakened node is combined with the movement of the structure where twisting of the bridge significantly exceeded allowable limits, the cause of this tragedy is clear.

In this submittal, FIGG is providing a detailed review of the accident based on an analysis of the facts and standard bridge engineering concepts and standards. We are also offering proposed recommendations for the Board to consider adopting so that this tragedy is never repeated.

2. INTRODUCTION

2. INTRODUCTION

Figg Bridge Engineers, Inc. (FIGG) is an industry leader in the design of bridges. For over four decades, since 1978, using well accepted and established design and engineering principles, FIGG has studied, designed, or worked on more than 230 bridges in 42 states and six nations and has received more than 414 awards of excellence, including three Presidential Awards for bridges from Presidents of the United States.

The events of March 15, 2018 were, by any measure, a tragedy. However, contrary to incomplete prior accident updates, the design of the UniversityCity Pedestrian Bridge at Florida International University was neither the proximate cause, nor a contributing cause, of the construction accident.

The technique used for this bridge, referred to as Accelerated Bridge Construction (ABC), has been in wide use since 2010. Just seven days before this tragedy, the Federal Highway Administration confirmed that ABC technology, among other things, “Enhances Safety . . . Reduces Environment Impact . . .” and “help(s) improve motorist and worker safety . . .” (See EDC-2: Accelerated Bridge Construction, <https://www.fhwa.dot.gov/innovation/everydaycounts/edc-2/abc.cfm>, March 8, 2018).

If, however, the various parties constructing the bridge, inspecting the construction, or moving the bridge into position, fail to comply with the approved Released For Construction (RFC) Plans, routine standard state specifications, construction requirements, Construction Quality Control Procedures, and agreed boundaries, then even a safe design will be compromised.

As will be discussed in this submission, the proximate cause of the collapse was multiple failures, by multiple parties on site during construction, to comply with the approved Released for Construction Plans, routine standard state specifications, and other requirements.

None of these issues of non-compliance were known to FIGG at any time prior to the construction accident. At all times, FIGG believed that the design, specifications, quality control, and contract requirements were being complied with by all involved contractors and inspectors at the site. Had the failures of compliance been known to FIGG, FIGG would have objected to the bridge being moved, the highway being opened, and/or the highway remaining opened, and the tragic events of March 15, 2018, would never have occurred.

3. PROJECT DESCRIPTION

3. PROJECT DESCRIPTION

The UniversityCity Prosperity Project included a Signature Pedestrian Bridge crossing SW 8th Street (US 41 also known as Tamiami Trail) and the Tamiami Canal near the intersection of SW 109th Avenue. The pedestrian bridge would connect the Florida International University (FIU) campus on the south with the City of Sweetwater on the north. **FIGURE 3-1** from the NTSB Factual Report shows the bridge location with the red line and the orientation of the construction site on March 26, 2017.

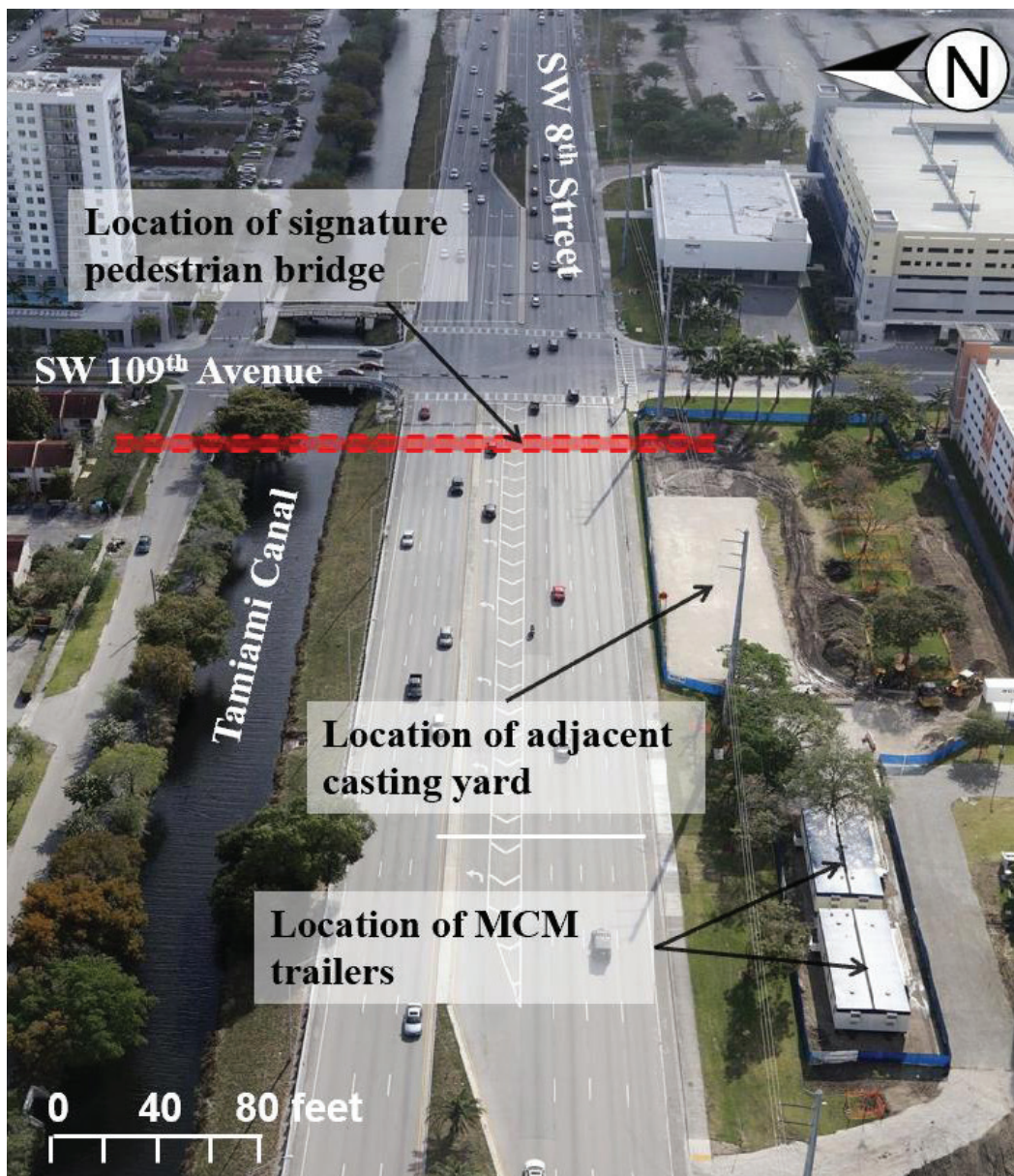


FIGURE 3-1
Location of the signature bridge in red and showing the contractor's adjacent casting yard and construction trailers on 3/26/2017 (Source: NTSB Factual Report)

The general project arrangement, conceptual signature bridge ideas, permitting, and funding were developed by FIU with support from their consultant TY Lin International. The Florida Department of Transportation (FDOT) also provided support to FIU. One of the cable-stayed bridge concepts during the early project development prepared by FIU is shown in **FIGURE 3-2** from the NTSB Factual Report. The location ultimately was changed to the west side of the SW 109th Avenue intersection.



FIGURE 3-2

Bridge rendering of what the new signature pedestrian bridge would look like as submitted by FIU as part of the 2013 TIGER grant application (Source: NTSB Factual Report)

On January 14, 2016, the contractor, MCM, entered into a design-build contract with FIU for a contract amount of \$9.4 million. The bridge design was accomplished by Figg Bridge Engineers, Inc. (FIGG) as a subconsultant to MCM. A signature pedestrian bridge design was created to meet FIU’s vision of a 30-foot walkway width with a canopy over part of the walkway, grand staircase, elevators and other special features. The NTSB Factual Report description of the signature pedestrian bridge is as follows:

“The signature pedestrian bridge designed by FIGG was an innovative design that was composed of a walkway and a canopy connected by a single row of diagonal supports that extended down the center of the bridge. The bridge also featured an upper pylon and steel pipes, as well as a grand staircase and

elevators. The signature pedestrian bridge was designed with the look of a cable-stayed bridge, where the deck is suspended from cables fanning out from a tall mast. The steel pipe supports were functional structural members that were designed to increase the natural frequency of the pedestrian bridge, which dampens vibrations from pedestrian traffic. According to the Project Design Criteria, the bridge vibrations shall be investigated in accordance with Section 6 of AASHTO Guide Specifications for Design of Pedestrian Bridges. To obtain the cable-stayed bridge look, it was selected that the diagonal members lined up with the steel pipes from the upper pylon. Each of the diagonal members were of different angles and lengths. The upper pylon was designed to extend approximately 109 feet tall, which happened to mark the location of the cross street, SW 109th Avenue. The resulting signature pedestrian bridge included 10 steel pipes that could be dramatically lit up at night, with an upper pylon capped with a beacon of light.

The signature pedestrian bridge consisted of a walkway that was approximately 30 feet wide. The single row of diagonal supports was centered in the middle of the walkway. The canopy, which partially covered the walkway, was approximately 16 feet wide. The vertical distance from the walkway to the canopy was approximately 15 feet. The concrete deck was post-tensioned in the longitudinal and transverse directions to maximize durability and achieve a design life that exceeded 100 years.”

FIGURE 3-3 below is a rendering of the proposed signature pedestrian bridge.

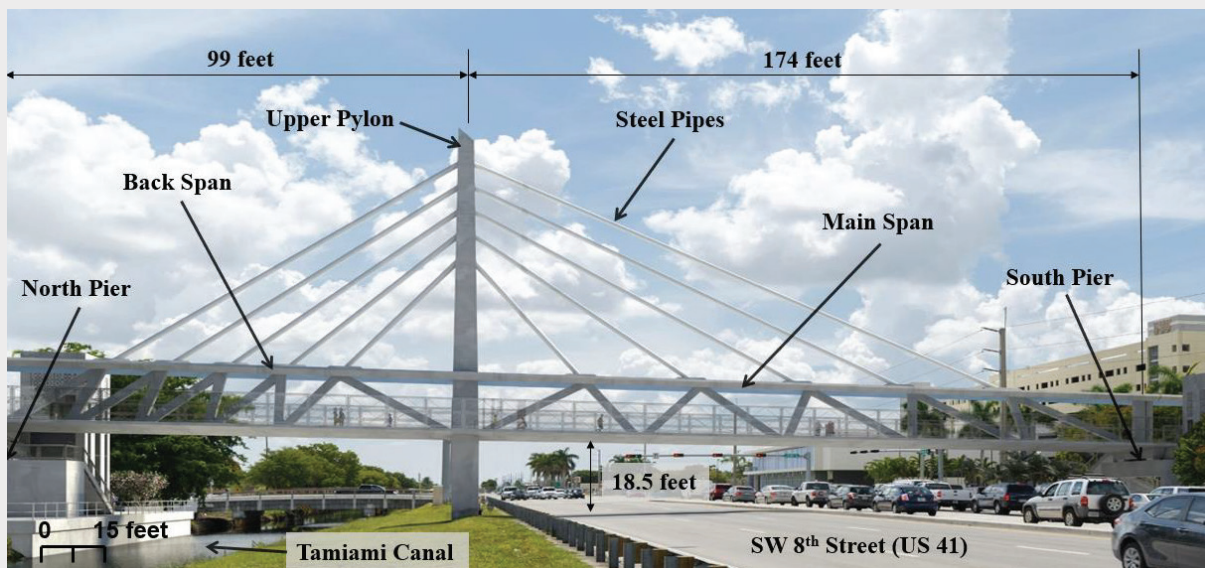


FIGURE 3-3 Rendering of what the signature pedestrian bridge would look like when completed looking to the east (Source: NTSB Factual Report)

The main span located to the right, in **FIGURE 3-3**, and **FIGURE 3-4**, is the span that was installed before the construction accident on March 15, 2018 over SW 8th Street (or US 41). The NTSB Factual Report states:

“The main span extended from the upper pylon to the south pier for a distance of approximately 174 feet. The back span over the Tamiami Canal, which had not been constructed, extended from the upper pylon to the north pier for a distance of 99 feet. The upper pylon and steel pipes also had not been constructed. The vertical distance from SW 8th Street to the bottom of the main span was approximately 18.5 feet.”

FIGURE 3-4 outlines the location of the main span, which was precast in the adjacent casting yard (location shown in **FIGURE 3-1**) and then moved into place over the piers.

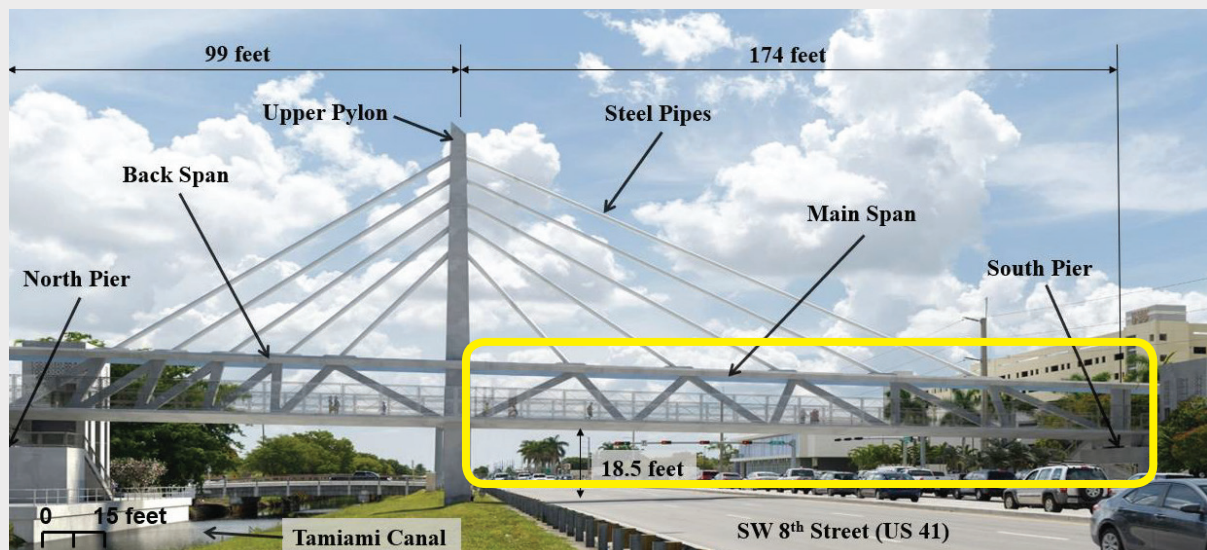


FIGURE 3-4 Rendering of what the signature pedestrian bridge would look like, showing the main span outlined (Source: NTSB Factual Report, with the added outline)

From the NTSB Factual Report, **FIGURE 3-5** on the following page:

“...illustrates the main span being moved on March 10, 2018, prior to placement on the south pier and pylon pier, looking to the west. The canopy, diagonal supports, and walkway are highlighted below on...” **FIGURE 3-5**

The main span accident occurred five days later, on March 15, 2018, during a construction operation.

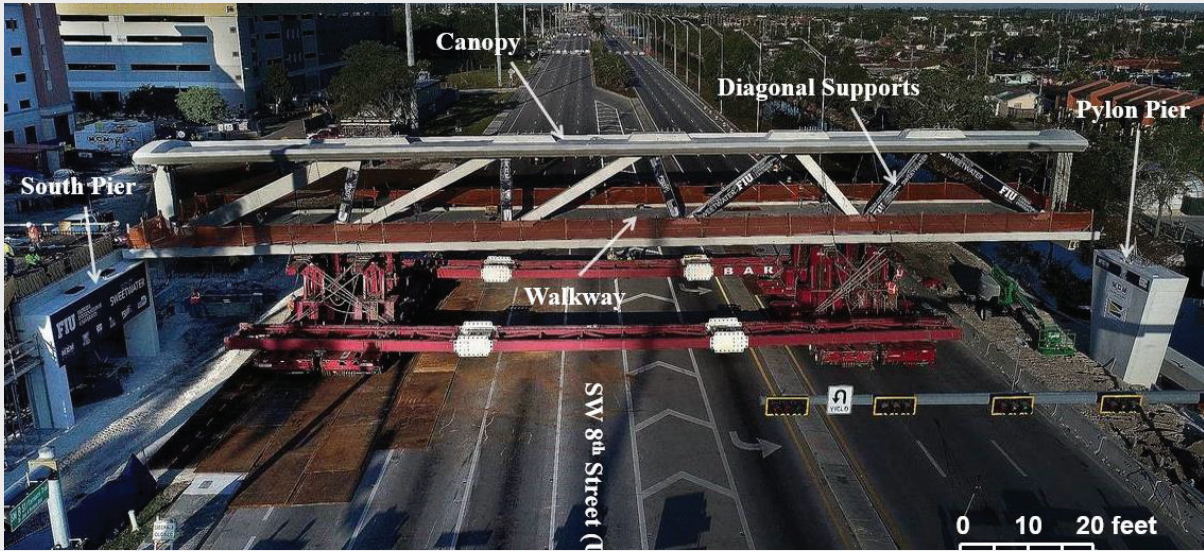


FIGURE 3-5 Main span being moved on March 10, 2018 prior to placement on the south pier and pylon pier, looking to the west (Source: NTSB Factual Report)

The main span of the bridge is a concrete truss, with a canopy on top and the deck on bottom, making it analogous to a large concrete beam, or I-beam, with struts running along the centerline.

From the NTSB Factual Report, **FIGURES 3-6** through **3-8**:

“...illustrate other renderings of what the signature pedestrian bridge would look like when completed.”

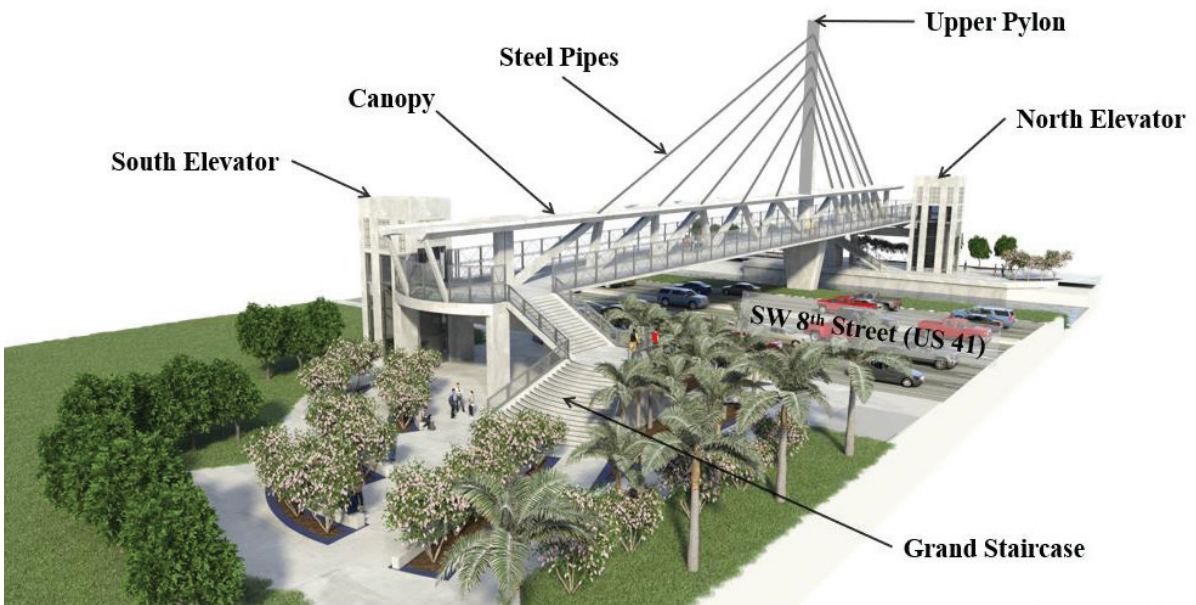


FIGURE 3-6 Rendering of what the signature pedestrian bridge would look like when completed, looking to the northwest (Source: NTSB Factual Report)

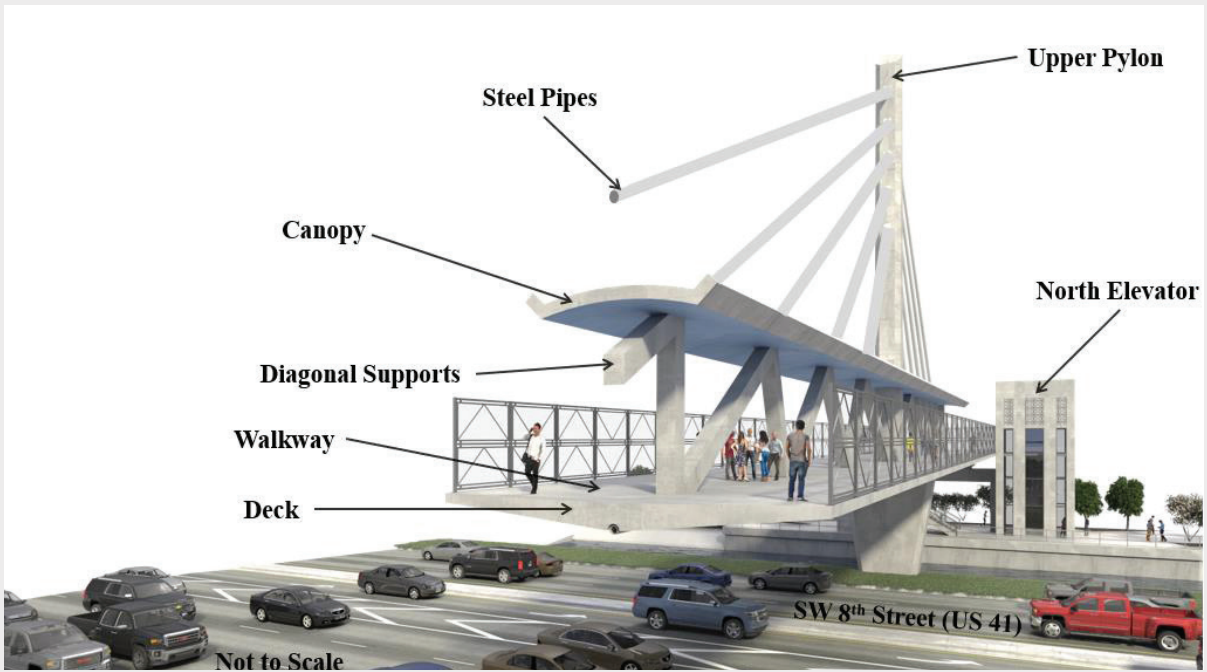


FIGURE 3-7 Rendering of what the cross section of the pedestrian bridge would look like when completed, looking to the northwest (Source: NTSB Factual Report)

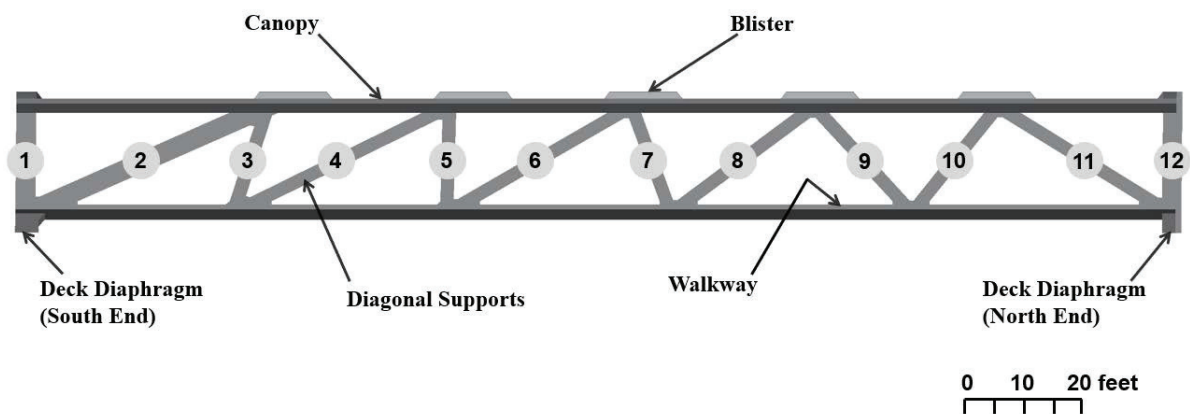


FIGURE 3-8 Rendering of what the pedestrian bridge walkway would look like when completed, looking to the north (Source: NTSB Factual Report)

From the NTSB Factual Report, **FIGURE 3-9**

“...illustrates the nomenclature of the diagonal and vertical members on the main span of the signature pedestrian bridge. There was a total of 12 diagonal and vertical members”. **FIGURE 3-9** “also illustrates the location of the canopy, blisters, walkway, and deck diaphragms located at the south and north end of the main span.”

FIGURE 3-9 Map illustrating nomenclature of the diagonal and vertical members on the main span of the signature pedestrian bridge, looking to the west (Source: NTSB Factual Report)



The bridge design stipulated use of Florida Department of Transportation standard construction specifications and followed national and state design criteria. The details of the required specifications and design criteria are part of the first two pages of the approved Released For Construction Plans. This is discussed further in Section 6.2 of this report. For approximately 14 months, the bridge design went through various stages of development and a detailed review with the Florida Department of Transportation and their consultants prior to approval and construction starting. The details of this review process are given in Section 6.2.5 of this report. Louis Berger was engaged to perform an independent peer review of the design, and certified compliance as described in Section 6.4 of this report.

KEY POINT(S)

All aspects of the initial design by FIGG were the subject of numerous governmental, contractor and peer reviews, over a long period of time, before construction ever started.

This submission includes the following:

- Description of the **Project Participants** and their roles, including whether participants were on-site during construction, or if their role was off-site, is given in Section 4.
- **Summary of Events** describing important information leading up to the construction accident on March 15, 2018, is given in Section 5.
- **Factual Information** describing important information in the investigation and the analysis is given in Section 6.
- Summary of the **Analysis** describing the results analyzing the factual information is given in Section 7.
- **Conclusions** describing how results of the facts and analysis led to the probable cause, contributing causes and items that did not contribute to the cause are given in Section 8.
- **Safety Recommendations** for various areas of improvement for the industry are given in Section 9.
- Supporting references are given in **Other Reports**, Section 10, and in the **Exhibits**. This includes a report of "Research and Analysis Related to the Collapse during Construction" by Forensic Engineering Specialist, Wiss, Janney, Elstner Associates, Inc. (WJE) in Exhibit A.

4. PROJECT PARTICIPANTS

4. PROJECT PARTICIPANTS

Below is a list of some of the Project participants with a brief description of roles. This provides general areas of responsibility. However complete details are contained in individual company contracts. The participant descriptions are followed by a simplified organization chart showing the contractual relationships between these participants.

Owner

The Florida International University (FIU) is the owner of the Project. As Owner, FIU hired the Contractor to design and build the project and FIU hired the Construction Engineering and Inspection Company to inspect the services provided by the Contractor to make certain that the services complied with the contract requirements.

Owner's Construction Engineering and Inspection (CEI)

Network Engineering Services, Inc. d/b/a Bolton, Perez and Associates (BPA) was hired by the Owner to provide oversight on the construction through Construction, Engineering, & Inspection services. Inspectors are required to have specific qualifications for the services they are inspecting so BPA hired The Corradino Group, Inc. (Corradino) as its subcontractor to inspect all post-tensioning work.

State Agency Support

The Florida Department of Transportation (FDOT) is an executive agency of the State of Florida. FDOT is responsible for design review for the Project. FDOT provided comments on the design and confirmed it was satisfied with the design and Released for Construction (RFC) Plans before construction started. FDOT is responsible for regulating the independent peer review requirements and performed an audit of the Independent Peer Review Documentation. FDOT attended meetings and provided support to the Owner, FIU.

Contractor for Design-Build Contract

Munilla Construction Management, LLC (MCM) is the construction contractor hired by the Owner to design and build the Project. MCM had standard contractor responsibilities for project management, construction quality control, management of subcontractors, and safety. MCM had a number of subcontractors, suppliers and consultants for various parts of the Project, some of these are given below.

Concrete Subcontractor

The Structural Group of South Florida, Inc. (Structural Group) is the company hired by the Contractor to assist with the placement of concrete for the Project which included the precast main span prior to the move.

Formwork Shoring Subcontractor

RC GROUP, LLC (RCGROUP) is the company hired by the Contractor to provide labor and services, including inspection and analysis, for temporary shoring in the precasting operation of the main span.

Post-Tensioning Subcontractor

Structural Technologies, LLC (Structural or VSL) is the company hired by the Contractor to perform all post-tensioning work for the Project.

Bridge Move Subcontractor

Barnhart Crane and Rigging, Co. (Barnhart) is the company hired by the Contractor to move the bridge span into place over SW 8th Street. Barnhart hired Bridge Diagnostics, Inc. (BDI) as its subcontractor to perform the monitoring of the effect of the move on the bridge span. Barnhart hired RLT Engineering Solutions, LLC to provide engineering support of analysis and design of the structural support system for the move and suitability of the ground surface.

Crane Subcontractor

George's Crane Service is the company hired by the Contractor to provide labor, equipment and services for various crane needs. Their crane and personnel were supporting the post-tensioning operations at the north end of the bridge span at the time of the bridge accident.

.....

Design Consultant/ Engineer of Record (EOR)

Figg Bridge Engineers, Inc. (FIGG) is the company hired by the Contractor as the Design Consultant and Engineer of Record for the bridge design. FIGG had a number of subconsultants for various design activities including roadway design, survey, geotechnical, lighting, landscaping, etc. FIGG's scope of work did not include having a representative at the construction site except for occasional visits and meetings.

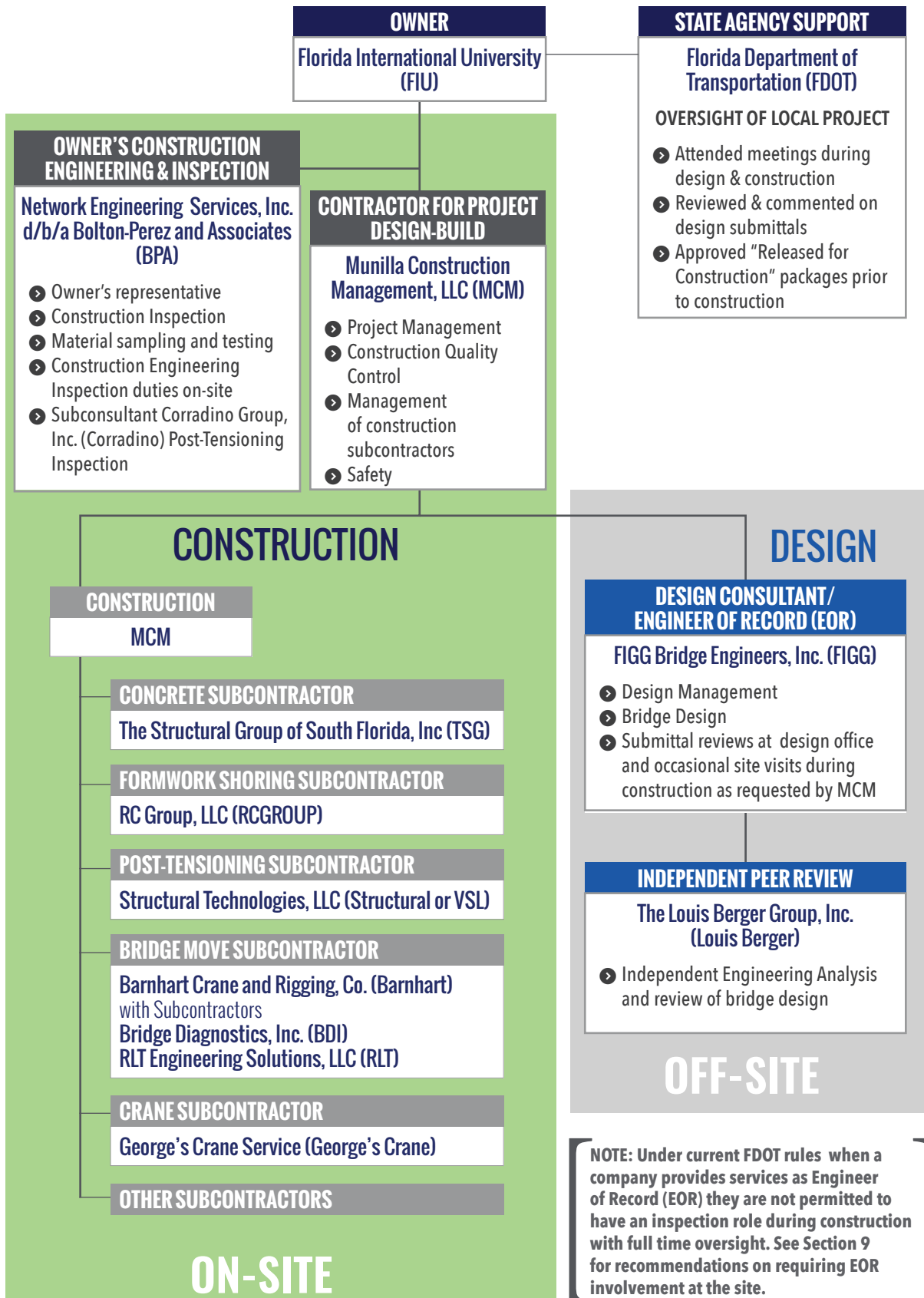
Independent Peer Reviewer

The Louis Berger Group, Inc. (Louis Berger) was the independent peer reviewer responsible for completing an independent review of the bridge design in accordance with the FDOT regulations and certifying compliance of the design with applicable regulations.

The organization chart on the following page shows the contractual relationships between these Project participants. This chart also shows whether Participants had on-site or off-site roles during construction.

PROJECT PARTICIPANT ORGANIZATION CHART

FIU UNIVERSITY CITY PROSPERITY PEDESTRIAN BRIDGE PROJECT



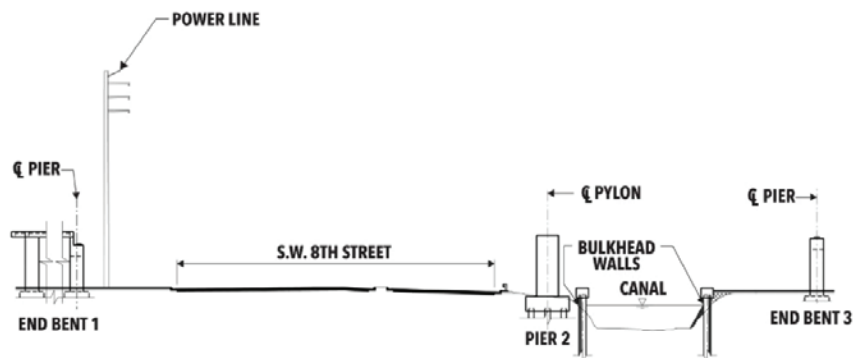
5. SUMMARY OF EVENTS

5. SUMMARY OF EVENTS

This section presents the summary of events up to the construction accident. The following section, Section 6, provides relevant facts that are then analyzed in Section 7.

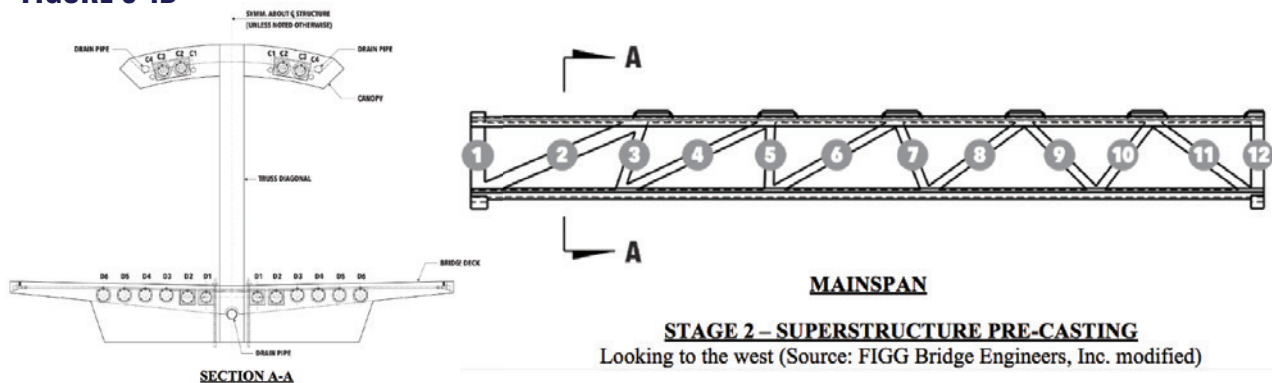
The FIU Pedestrian Bridge construction sequence is provided in the Released For Construction (RFC) Plans (sheets B-109 and B-110). Applying the principles of Accelerated Bridge Construction (ABC) to minimize disruption to traffic on SW 8th Street, the main span truss structure was precast on the south side of the road and then transported as a single piece overnight during a road closure to its permanent location spanning SW 8th Street. Stage 1 of the construction was installing the foundations and building the supporting piers. Stage 2 was precasting the main span truss and Stage 3 was moving the truss into position over SW 8th Street and setting it on the permanent piers (**FIGURE 5-1A, 5-1B, AND 5-1C**). The construction accident occurred during Stage 3,

FIGURE 5-1A
Bridge construction stages 1 through 3 (Source - NTSB Factual Report)



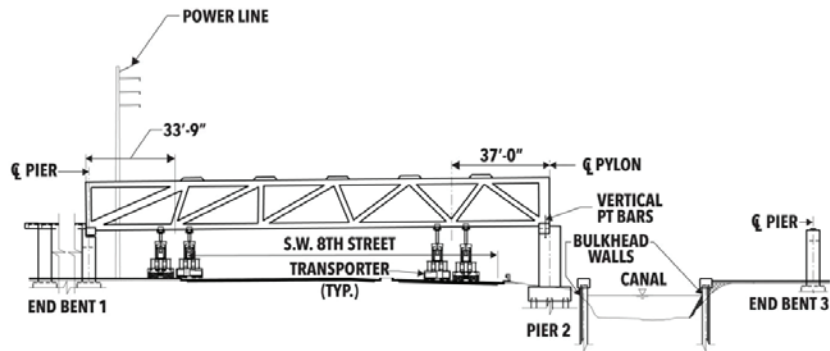
STAGE 1 – SUBSTRUCTURE CASTING
Looking to the west (Source: FIGG Bridge Engineers, Inc. modified)

FIGURE 5-1B



STAGE 2 – SUPERSTRUCTURE PRE-CASTING
Looking to the west (Source: FIGG Bridge Engineers, Inc. modified)

FIGURE 5-1C



STAGE 3 – ERECTION OF MAINSPAN
Looking to the west (Source: FIGG Bridge Engineers, Inc. modified)

after the main span truss had been set on the piers. Key events during construction Stages 2 and 3 preceding the accident are described in this section.

5.1. PRIOR TO BRIDGE MOVE

The 174-foot long concrete truss for the main span was precast in a staging area on the south side of SW 8th Street just west of the permanent bridge location (FIGURE 5-2). To enable the self-propelled modular transporters (SPMTs) to lift and move the span after precasting, the span was constructed on falsework approximately 17 feet above ground. For constructability, the span was cast in three pours: first the bottom slab (bridge deck), then the truss members and finally

FIGURE 5-2

Main span truss construction in precast area prior to casting the canopy.



the canopy. Between each of the pours, the lower portion of concrete was allowed to cure before wet concrete was cast for the next pour above it. The interfaces between the prior pour and the subsequent pour are concrete construction joints which must transfer forces between the two concrete pours so that the span behaves as a continuous structure when completed. MCM cast the bridge deck on October 19, the truss members on November 6, and the canopy on December 14 of 2017.

After the main span was precast, the next step in construction was to install and stress the post-tensioning. Post-tensioning tendons are high-strength steel cables or bars running through ducts in the concrete with anchors at the ends. These are stressed (elongated) with a hydraulic jack during construction and then anchored to the concrete to provide compression in the bridge. This compression then resists tension that is induced when loads are applied to the bridge. The main span had longitudinal tendons in the deck and canopy, transverse tendons in the deck and post-tensioning bars (PT bars) in most of the truss members. The post-tensioning was installed and stressed in the order specified in the RFC plans starting on January 16, 2018.

On February 2, 2018, while the tendons were being stressed, Bolt Perez & Associates (BPA) performed a visual inspection of the truss and identified hairline cracks in truss members 3 and 10 (**FIGURE 5-3**). This information was provided to FIGG in a Crack Inspection Report on February 13, and FIGG replied on February 15 that these were temporary in nature and would dissipate once the PT bars in these members were stressed. There is no mention in the record of cracks in members 3 and 10 after the PT bars in those members were stressed.

Post-tensioning was completed on February 18, and on February 22, MCM began removing the falsework supporting the main span. This involved removing the shoring starting from the center of the span and working both directions towards the ends of the span until the self weight of the bridge was fully transferred from the shoring to the truss. Removal of the shoring was completed on February 24, 2018. At this point the truss spanned between the falsework supporting the end diaphragms in a configuration similar to that after the move to the permanent piers (**FIGURE 5-4**).

FIGURE 5-3

Typical crack photo from BPA February 13, 2018 report. Cracks 0.004 inches wide noted on truss members 3 and 10 before all post-tensioning tendons were stressed. (Source: BPA)

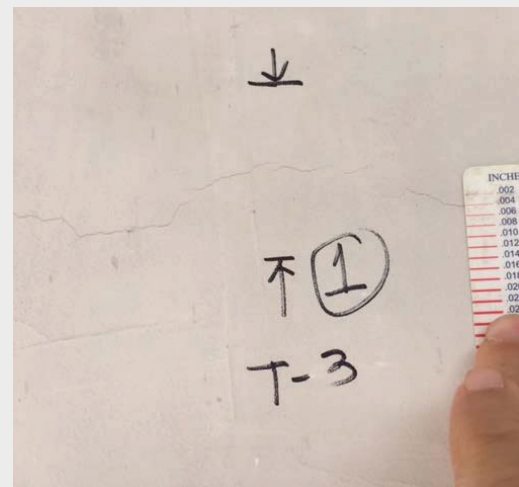


FIGURE 5-4

Completed precast main span truss supported on temporary shoring at both ends in casting area. Bridge was in this self supporting position for two weeks. (Source: Bridge Factors Photo 41)



In an interview with NTSB after the accident, the owner of Structural Group of South Florida, who was responsible for removing the shoring, reported that his work crew told him they heard a loud noise when the shoring removal was half to three-quarters of the way complete on February 24, 2018. He further stated that they noticed cracks near the ends of the span where the truss members connect to the deck.

On February 28, MCM sent FIGG a crack inspection report prepared by BPA along with additional photos taken by MCM (**FIGURE 5-5**). Some of the cracks shown were hairline cracks in truss members. The photos also showed cracks in the chamfer between the end diagonal truss members (2 and 11) and the bridge deck that were approximately 0.030 inches to 0.040 inches in width. Smaller cracks approximately 0.014 and 0.016 wide were shown in the top surface of the bridge deck at the end of the span near truss member 12. FIGG responded on March 7, requesting additional information and noting that in general, hairline cracks are not a concern. Also, FIGG noted that the cracks in the chamfers were at a boundary location between members and would need to be sealed per FDOT specifications.

The self-supporting truss main span remained in the precast area for two weeks from February 24 after the shoring was removed, until the bridge move on March 10, 2018.

FIGURE 5-5

Cracks in the base of member 11 near the bridge deck on February 28, 2018 after falsework removal. (Source: BPA)



FIGURE 5-5A

Crack in east side chamfer of member 11 connection to bridge deck.



FIGURE 5-5B

Crack in west side of truss member 11.



FIGURE 5-5C

Crack in west side chamfer of member 11 connection to bridge deck.

5.2. BRIDGE MOVE AND DE-STRESSING

Stage 3 of construction involved moving the main span truss from where it was precast on the south side of SW 8th Street to its permanent location crossing SW 8th Street. Barnhart Crane and Rigging (Barnhart) was contracted by MCM to perform the move. The approximately 950 ton span was transported by SPMTs while the road was closed, rotating the span in an arc from an east-west orientation to a north-south orientation and then moving it approximately 70 feet eastward to the permanent piers.

As part of the move planning, FIGG provided movement tolerances to MCM that were not to be exceeded during the bridge move to avoid damaging the precast span. Barnhart contracted with Bridge Diagnostics, Inc. (BDI) to perform electronic monitoring of the span using highly sensitive sensors capable of measuring displacements in 1/1000's of a foot, angles of tilt & twist in 1/100's of a degree and local changes in strain as Microstrains (1/1,000,000 inch/inch).

BDI installed their monitoring system on the main span in the precast area prior to the SPMT's lifting of the span from its end supports. Sensor readings from this initial baseline condition were the benchmark to which all later readings would be compared.

FIGURE 5-6

Precast main span truss move by transporters on March 10, 2018 from casting area to permanent piers.
(Source: FIGG)



During the evening of March 9, 2018, the SPMTs performed the initial lift of the span with hydraulic jacks from its end supports. Electronic data was collected which documented the change in vertical position, slope, tilt, twist and deflected shape of the span once lifted. After the span was lifted and initial data recorded, a “roll test” was performed. The roll test was done to verify twist measurement sensitivity of the installed monitoring system and Barnhart’s ability to control adjustments of twist during the upcoming movement of the span. Data from the sensors was collected during the roll test.

Traffic on SW 8th Street was closed the evening of March 9. The travel path for the SPMTs was prepared with gravel, timbers and composite grid mats as needed to reduce unevenness across the shoulder, curbs and median of the street. The actual move of the span began at approximately 4:30 a.m. on March 10 **(FIGURE 5-6)**.

Data from the electronic sensors was recorded by BDI during the move. Select data, principally span twist, was actively monitored by BDI relative to defined limits of permissible twist. There were multiple occurrences during the move when communication between the remote wireless sensors and the data acquisition/recorder unit were lost. Each time this happened, Barnhart stopped the SPMT movement until communications were restored. However, a complete set of data was not continuously reported during each of these events, between the time when communications were lost and the SPMT were fully stopped.

Upon completion of the move, the span was lowered on to bearings on each end of the span: temporary bearings on the North end of the span and permanent bearings on the South end of the span (FIGURE 5-7). Representatives of FIGG were on-site at the time to observe the span move, which was completed around noon. FIGG was not informed either during or after the move that there were any recorded instances of span twist exceeding the established limits.

KEY POINT

At no time was FIGG ever made aware of the fact that during the move, the bridge was twisted in excess of allowable limits on multiple instances. (FIGURE 5-7)

FIGURE 5-7

Main span on March 10, 2018 after placement on permanent piers. (Source: FIGG)



A FIGG representative reviewed the truss members at approximately 12:30 p.m. on March 10 immediately prior to leaving the site after the move. Photographs taken by him show that the cracks in the chamfers where members 2 and 11 connect to the deck were similar in size to the cracks at these locations shown in the photographs sent to FIGG by MCM on February 28 before the move, although some type of coating had been applied to the concrete surface by MCM at the crack locations (FIGURE 5-8).

FIGURE 5-8

Cracks in member 11 chamfer with deck on March 10, 2018 at approximately 12:30 p.m. (Source: FIGG)



East face of member 11 chamfer.



West face of member 11 chamfer.

During transport from the precast area to the permanent supports, the ends of the main span truss were cantilevered from the SPMT supports positioned about 35 feet from the truss ends. This resulted in tension in the truss end diagonal members 2 and 11 during the move which was resisted by the PT bars in these members. Since in the completed bridge these members are always in compression, these bars were to be destressed after the span move was complete. MCM arranged for their post-tensioning subcontractor, Structural Technologies LLC (Structural or VSL), to destress the PT bars the afternoon of March 10. Photographs, video and text messages from a Structural employee indicate that destressing of the PT bars in member 11 began about 3:00 p.m. and was completed around 4:30 p.m. The destressing operation was then performed for member 2 and completed about an hour later.

An inspector for the Corradino Group (Corradino), who was a subcontractor to BPA to inspect post-tensioning, was present for the PT bar destressing operation on March 10. In an interview with NTSB after the accident, the inspector stated that he observed more significant cracking around the time of destressing than was present in the bridge before the move. Photographs taken from 3:09 to 3:18 p.m. that afternoon by Corradino or MCM show significantly wider cracks at the member 11 chamfer at the deck connection and at the deck surface adjacent to member 12 than had been apparent in previous photos (**FIGURE 5-9**). In addition, a new crack had appeared in the west face of member

FIGURE 5-9

Cracking observed at north end of bridge at 3:16 p.m. on March 10, 2018 after bridge move and before member 11 PT bar destressing. (Source: Bridge Factors Photos 62 - 66)



FIGURE 5-9A

East side of member 11 at base near deck.



FIGURE 5-9B

West side of member 11 at base near deck.



FIGURE 5-9C

North edge of diaphragm west of member 12.



FIGURE 5-9D

North edge of diaphragm east of member 12.

FIGURE 5-10

Traffic reopens on SW 8th Street on March 10, 2018, at approximately 6:00 p.m. after members 2 and 11 PT bar destressing. (Source FIGG's Photo Submission FCA 23-6)



11 near the connection to the deck, and the top edge of the diaphragm on the north end near member 12 spalled off (approximately 2 inches wide and 5 feet long).

At approximately 6:00 p.m. on March 10, MCM and BPA re-opened SW 8th Street to traffic early (**FIGURE 5-10**). At 7:08 p.m., the Structural technician who had been working on the PT bar destressing texted another person within Structural stating "It cracked like hell". The EOR, FIGG, was not notified by anyone of worse or additional cracking until two days later on March 12, 2018 at 4:51 p.m. by email.

KEY POINT

FIGG was not told that "it cracked like hell" until two days after the cracking occurred and when they learned of it FIGG only knew there had been some additional cracking and not that "it cracked like hell."

5.3. MARCH 11 THROUGH MARCH 14

At 4:51 p.m. on Monday, March 12, MCM sent FIGG 16 photos. No phone calls were made from MCM or BPA to FIGG on March 12 regarding this issue. On the morning of March 13, FIGG opened the e-mail and reviewed the photographs. Of the 16 photos, 13 were of the north face of the north end diaphragm showing cracking starting from the top of the deck adjacent to member 12 and extending at a 45 degree downward angle to the bottom of the diaphragm. The spalling along the top edge of the diaphragm was also apparent. The three other photos showed cracking in the north side of member 12 and on the east face of member 11 near

the deck. A ruler in the photo indicated that the crack at the member 11 chamfer at the deck connection was approximately 1/2 inch wide. MCM requested in the e-mail that FIGG review the photos and respond as quickly as possible.

On Tuesday morning March 13, the FIGG project manager called the MCM project manager to discuss the situation. In his interview with NTSB after the accident, the FIGG project manager stated that MCM told him in the call that MCM had noticed cracking prior to destressing the PT bars in member 11 on Saturday and that the cracking had gotten slightly worse after the bars were destressed. FIGG's project manager sent an e-mail afterwards summarizing the conversation, which focused on the north diaphragm. It was noted that MCM said the cracks had not increased in size since Saturday afternoon. FIGG recommended placing shims between the pier and the bridge deck at member 12 to provide additional support and stated that further evaluation was ongoing. MCM acknowledged the e-mail around noon that day.

KEY POINT

The only thing FIGG knew was that the cracking had gotten slightly worse.

Late that same afternoon, the MCM and FIGG project managers had another phone call, where the FIGG project manager recommended restressing the PT bars in member 11. As he explained in the NTSB interview later, this recommendation was based on the observation relayed by MCM that the cracking worsened when the PT bars had been destressed, so the intent was to revert to the prior state of the structure. The stressing of the two bars was to be performed in 12 incremental steps while the cracks were being closely monitored. If the cracking worsened, the restressing was to immediately stop and FIGG notified. FIGG followed up the call with a summary e-mail to MCM.

The next afternoon (March 14) MCM sent an e-mail to FIGG with photos attached, but without commentary or a Crack Inspection Report. The e-mail also confirmed a meeting to be held at 9:00 a.m. the next day at the project site where FIGG was to present a summary of their evaluation.

Additional photos of cracking at members 11, 12 and 2 were taken by MCM and BPA on March 13 and 14, but FIGG was not aware of them prior to the accident. No measurements of cracks, other than the appearance of a tape measure in certain photographs, were provided to FIGG since before the bridge move. There is no indication that MCM, BPA or other project participants who were on-site during this time actively observing the cracking expressed concern with the safety of the span suspended over SW 8th Street or suggested that the road should be closed until the situation was resolved.

5.4. DAY OF ACCIDENT (MARCH 15)

Two engineers from FIGG arrived at the project site around 7:45 a.m. Thursday morning, March 15. Representatives of MCM, BPA and FIGG went on the bridge deck and observed the member 11/12 connection to the deck. Then one person from MCM and FIGG used a man-lift to review the north and south faces of the north diaphragm, before going to MCM's office trailer for the 9:00 a.m. meeting.

The meeting was attended by representatives from MCM, FDOT, FIU, BPA and FIGG. A FIGG engineer gave a presentation focusing on the calculations done thus far on the north end diaphragm which indicated that there was sufficient capacity to carry the applied loads and that the observed behavior was not replicated by the analyses performed. The main action items resulting from the meeting were for MCM to restress the PT bars in member 11 that afternoon and for FIGG to develop a temporary mechanism to capture the member 11/12 nodal zone, potentially using PT bars tied back to the member 10/9 truss node. MCM was also tasked with evaluating methods to accelerate the pylon construction, which would incorporate the nodal zone into the large reinforced concrete pylon per the RFC plans. No one at the meeting expressed concern with the safety of the span suspended over SW 8th Street or with leaving SW 8th Street open.

KEY POINT

Despite the Project Participants who were on-site (MCM, BPA, and others) having intimate knowledge of the construction, span move and cracking progression in the bridge, neither MCM, BPA, FIU or FDOT expressed concern about leaving SW 8th Street open to traffic.

Just before noon on March 15, Structural began the process of restressing the member 11 PT bars using the 12 step process. Site video and witness interviews indicate that the restressing was nearly complete when the bridge experienced a catastrophic failure and collapsed onto SW 8th Street at approximately 1:47 p.m. The accident resulted in six fatalities and multiple injuries.

The next section, Section 6, provides relevant facts that are then analyzed in Section 7.

6. FACTUAL INFORMATION

6. FACTUAL INFORMATION

6.1. NTSB FACTUAL REPORT

The NTSB has produced a “Bridge Factors Group Chairman’s Factual Report” (Factual Report) as part of its investigation into the FIU Pedestrian Bridge accident (last version provided to party members was April 8, 2019). This is in addition to a Preliminary Report and two Investigative Updates previously released by NTSB concerning the accident. The discussion below highlights some of the information presented in the Factual Report and provides additional insights and information relative to an analysis of the probable cause of the accident.

It is the position of FIGG that certain information presented in the Factual Report is incorrect or misleading. During the process of producing the report, the NTSB solicited comments from the investigation Party members including FIGG. However, many of the comments were either not incorporated or not incorporated in a manner that provided clarity to the facts of the matter. Party members to the investigation were not asked to signify agreement with the final Factual Report. A discussion of some important items in the final Factual Report needing correction or clarification is presented in Section 10.1 of this report.

Based on the evidence gathered during the NTSB investigation, it is clear that the collapse of the FIU Pedestrian Bridge originated with a failure in the nodal area at the north end of the span where truss members 11 and 12 connect to the bridge deck and north diaphragm. This report focuses on information relevant to that area of the structure.

6.2. DESIGN

The design-build contract for the FIU Pedestrian Bridge contained design criteria and reference documents that were to be followed in the design of the bridge. These include:

- ✓ American Association of State Highway and Transportation Officials (AASHTO) Load and Resistance Factor Design (LRFD) Bridge Design Specifications (current version at the time was 7th Edition with 2015 interims)
- ✓ AASHTO LRFD Guide Specification for Design of Pedestrian Bridges (current version at the time was 2nd Edition, 2009)
- ✓ Florida Department of Transportation (FDOT) Structures Design Guidelines (current version at the time was January 2015)

- ✓ FDOT Standard Specifications for Road and Bridge Construction (current version at the time was 2015)

6.2.1 Calculations

Design calculations document the analyses and process used to arrive at the information shown on the Released For Construction (RFC) plans. The actual construction, however, is performed using the information shown on the RFC plans and provided in the project construction specifications. Thus, the final design is that reflected in the RFC plans, which is a result of the design process including calculations, review comments, detailing preferences, and constructability practices, among other aspects. The calculations alone do not reflect the full design.

In this case, the superstructure design calculations for the connections between the bridge truss verticals and diagonals to the bridge deck and canopy (Superstructure-Longitudinal & Transverse; RFC Design Calculations; April 2017; starting on page 1282) do not completely represent either the loads or the capacities for the connections as shown in the Released For Construction (RFC) plans.

As noted in the Factual Report, the connection shear loads shown in the table on page 1283 of the calculations are significantly less than the loads from another design analysis model contained in the calculations.

At the same time, the capacity calculations are conservative due to substantial underestimation of the capacity of the truss member 11/12 connection to the deck. This is because the calculations do not include the contribution of the member 12 concrete and reinforcing and the capacity from cohesion that is recognized by the AASHTO LRFD design code.

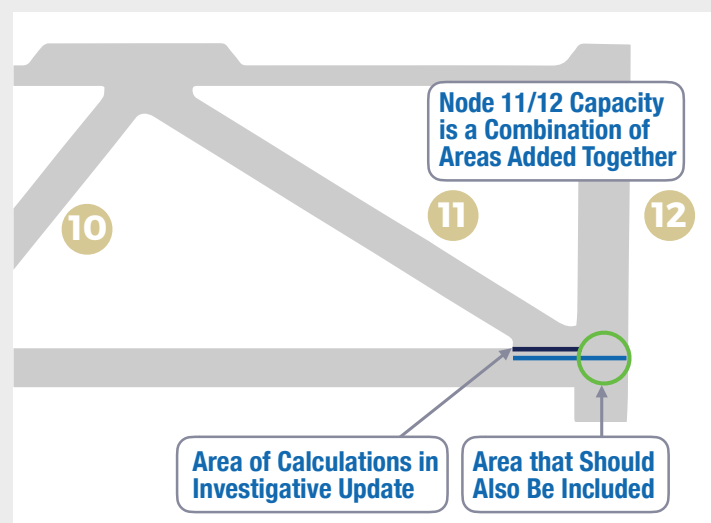
FIGURE 6-1 illustrates the portion of the connection included in the calculations versus the entire area of the connection.

KEY POINT

All appropriate and required design criteria/specifications were included in the Released For Construction plans from FIGG. The investigation has established that multiple contractors failed to comply with them.

FIGURE 6-1

Portion of member 11/12 nodal connection included in design calculation versus the entire connection.



The design of the member 11/12 nodal connection was based on AASHTO LRFD design specifications for shear friction (Section 5.8.4). The calculations used a friction coefficient of 1.0 which is specified in the design code for "normal weight concrete placed against a clean concrete surface, free of laitance, with surface intentionally roughened to an amplitude of 0.25 in."

Since the bridge was constructed using the RFC plans, the nodal applied loads and capacities are actually represented by the RFC plan details as opposed to the design calculations. Section 7.3 of this report provides an analysis of the design for the member 11/12 nodal connection as shown in the RFC plans.

6.2.2 Plans

Details of the member 11/12 nodal zone with the deck at the north end are shown in the RFC superstructure plans as follows:

- Main span truss dimensions – Sheet B-37 **(FIGURE 6-2)**
- Truss member post-tensioning – Sheet B-38
- Truss member reinforcing – Sheet B-40 **(FIGURE 6-3)**
- North end diaphragm (Type II) reinforcing – Sheets B-46 and B-47 **(FIGURE 6-4)**
- Deck reinforcing – Sheet B-60
- Member 11/12 nodal zone reinforcing – Sheet B-61 **(FIGURE 6-5)**
- Post-tensioning – Sheets B-67 and B-69

FIGURE 6-2
North end main span truss dimensions from RFC plan Sheet B-37.

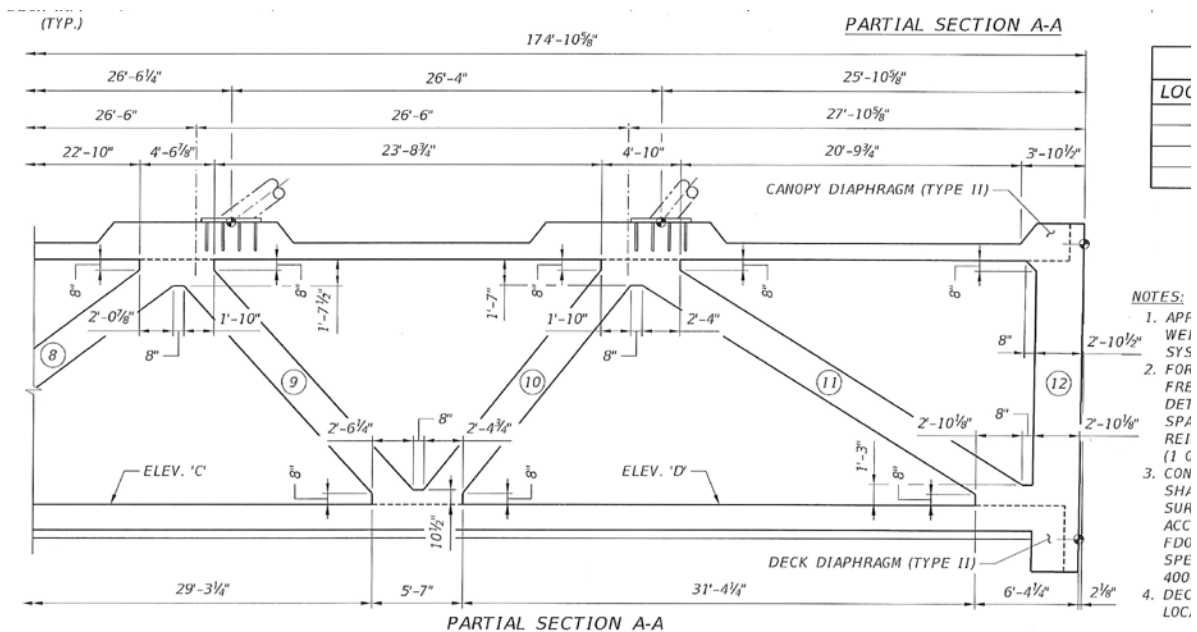


FIGURE 6.3 Truss member reinforcing at north end of span from RFC plan Sheet B-40.

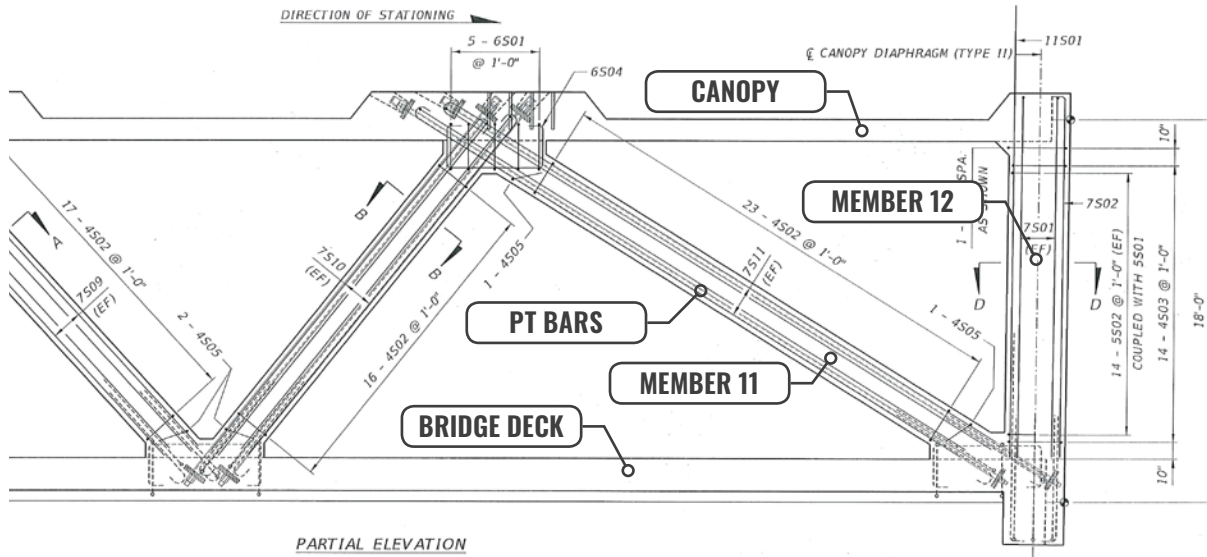


FIGURE 6-4 North end diaphragm reinforcing details from RFC plan Sheet B-47.

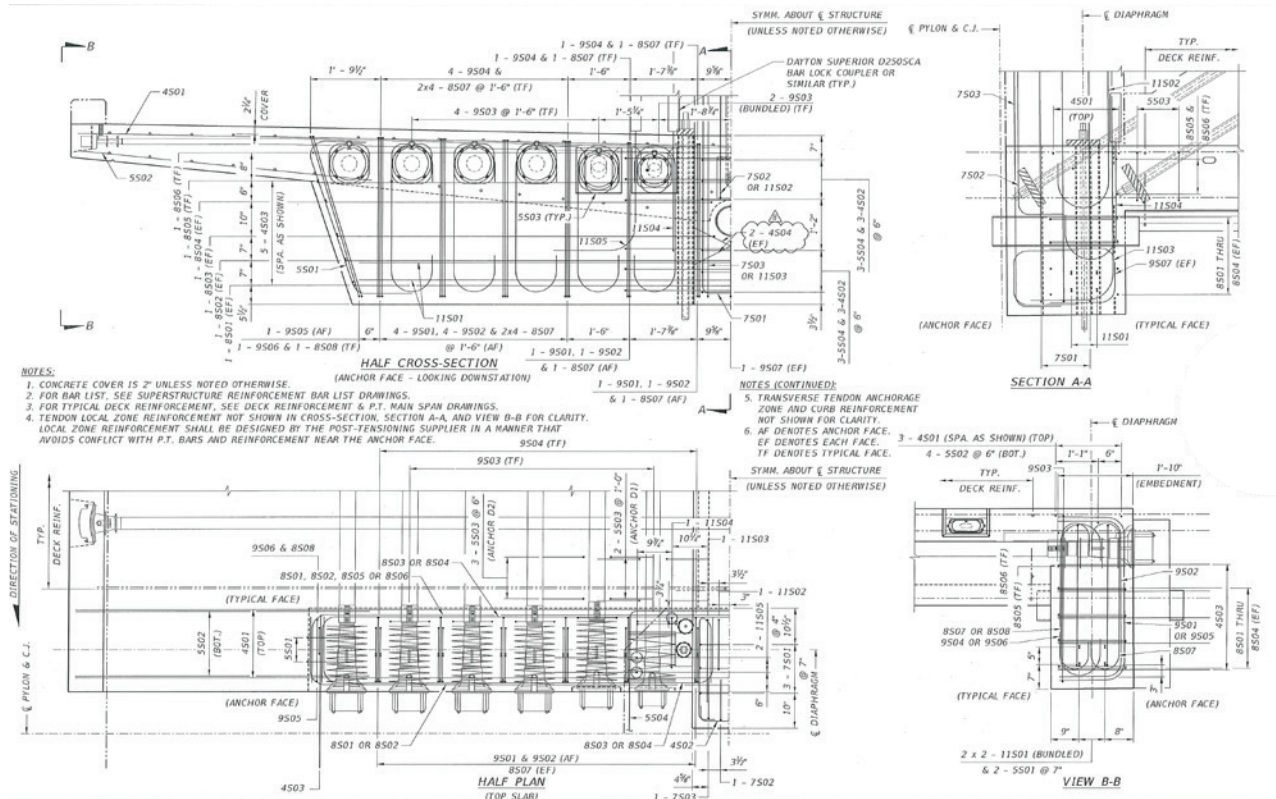
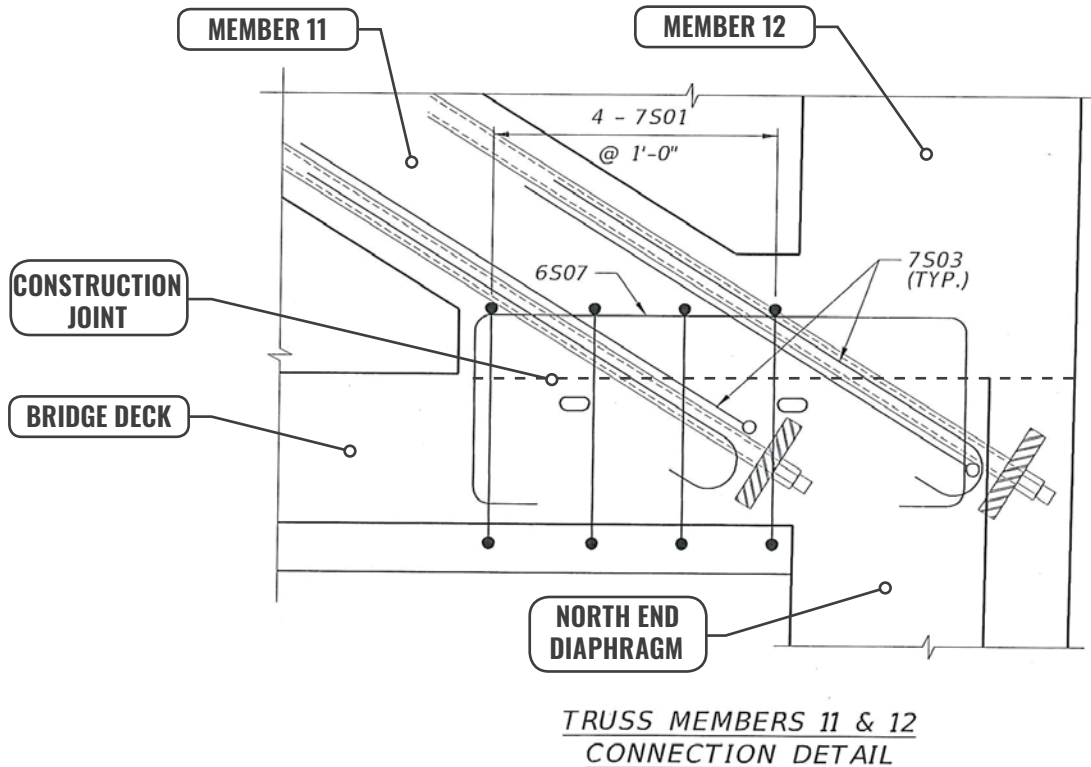


FIGURE 6-5

Truss member 11/12 connection to deck detail from RFC plan Sheet B-61.



Note 8 on Sheet B-38 specifies that the post-tensioning (PT) bars in truss members 2 and 11 are temporary and are to be destressed, but not removed, after the main span construction is complete.

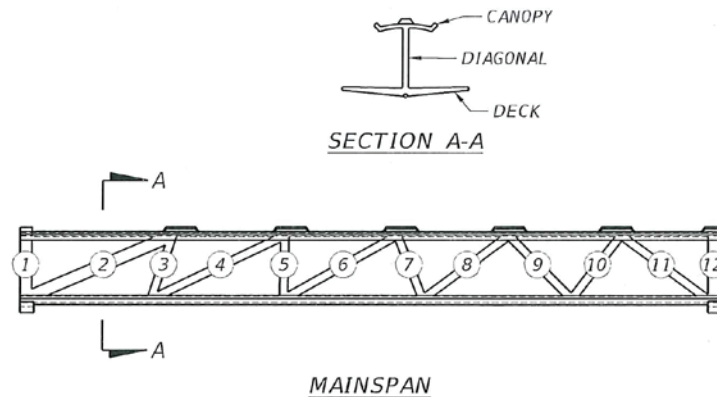
Notable features at the 11/12 nodal zone include longitudinal post-tensioning tendons in the bridge deck anchoring in the diaphragm close to the base of member 12, an 8-inch diameter sleeve through the diaphragm under member 12 for drainage, and two 4-inch diameter vertical sleeves through the diaphragm as part of the connection of the span to the pier.

Sheets B-109 and B-110 of the RFC plans indicates the construction steps that were to be followed. In Stage 2 (superstructure precasting) it is noted that the bridge deck and diaphragms were to be cast first, then the truss members, and finally the canopy and top anchor blocks (**FIGURE 6-6**). At the north end of the bridge, this meant that the deck and north diaphragm would be cast in one pour, and after the concrete cured, truss members 11 and 12 would be cast on top of the deck. The interface between the two pours is a concrete construction joint.

The General Notes on Sheet B-2 of the RFC plans reference the FDOT Standard Specifications for Bridge Construction 2015 as the governing specifications for construction (**FIGURE 6-7**). This important reference is the very first note on the General Notes sheet and applies to all pages of the RFC plans.

FIGURE 6-6

Steps 1 (A) through 1 (C) in Stage 2 of the construction sequence shown on RFP plans Sheet B-109 calls for casting the superstructure in three separate pours.



STAGE 2 - SUPERSTRUCTURE PRE-CASTING

1. CAST MAIN SPAN SUPERSTRUCTURE AS FOLLOWS:
 - A) CAST DECK AND DIAPHRAGMS.
 - B) CAST DIAGONAL AND VERTICAL MEMBERS.
INSTALL PT BARS AS SHOWN IN SHEET B-38.
 - C) CAST CANOPY AND TOP ANCHOR BLOCKS.
2. AFTER CONCRETE COMPRESSIVE STRENGTH HAS REACHED 6000 PSI, STRESS POST-TENSIONING OF THE MAIN SPAN IN THE FOLLOWING SEQUENCE:
 - I. STRESS DECK LONGITUDINAL TENDONS D1.
 - II. STRESS CANOPY LONGITUDINAL TENDONS C2.
 - III. STRESS PT BARS IN DIAGONAL MEMBERS 2 AND 11.
 - IV. STRESS DECK LONGITUDINAL TENDONS IN THE FOLLOWING SEQUENCE: D2, D3, D4, D5 & D6.
 - V. STRESS BOTTOM SLAB TRANSVERSE POST-TENSIONING. ALTERNATED END STRESSING IS REQUIRED FOR THE TRANSVERSE TENDONS.
 - VI. STRESS PT BARS IN DIAGONAL MEMBERS 3 AND 10.
 - VII. STRESS PT BARS IN DIAGONAL MEMBERS 5 AND 8.
 - VIII. STRESS PT BARS IN DIAGONAL MEMBERS 6 AND 7.
 - IX. STRESS CANOPY LONGITUDINAL TENDONS C3.
3. TEMPORARY SUPPORTS OF MAIN SPAN SECTION SHALL STAY IN THE MIDDLE OF THE CROSS SECTION DURING SPMT TRANSPORT.

FIGURE 6-7

FDOT Standard Specifications for Road and Bridge Construction 2015 referenced in the General Notes on Sheet B-2 of the RFC plans. This is the very first note on the General Notes sheet in the front of the plan set.

CONSTRUCTION SPECIFICATIONS:

1. FLORIDA DEPARTMENT OF TRANSPORTATION STANDARD SPECIFICATIONS FOR ROAD AND BRIDGE CONSTRUCTION 2015.
2. AMERICAN ASSOCIATION OF STATE HIGHWAY AND TRANSPORTATION OFFICIALS (AASHTO) LRFD BRIDGE CONSTRUCTION SPECIFICATIONS, SECOND EDITION, 2004 WITH INTERIMS THROUGH 2006.

DESIGN SPECIFICATIONS:

1. AMERICAN ASSOCIATION OF STATE HIGHWAY AND TRANSPORTATION OFFICIALS (AASHTO) LRFD BRIDGE DESIGN SPECIFICATIONS SEVENTH EDITION WITH 2015 INTERIMS.
2. FDOT STRUCTURES DESIGN MANUAL, JANUARY 2015.
3. AASHTO LRFD GUIDE SPECIFICATIONS FOR DESIGN OF PEDESTRIAN BRIDGES, SECOND EDITION (2009).
4. CEB-FIP MODEL CODE, FIRST EDITION, 1990, TIME DEPENDENT BEHAVIOR OF CONCRETE, CREEP AND SHRINKAGE.
5. AASHTO/AMERICAN WELDING SOCIETY (AWS) D1.5 BRIDGE WELDING CODE (2005).
6. 28 CODE OF FEDERAL REGULATIONS PART 36, 2010 AMERICANS WITH DISABILITIES ACT (ADA) STANDARDS FOR ACCESSIBLE DESIGN.
7. AASHTO GUIDE FOR THE DEVELOPMENT OF BICYCLE FACILITIES, 1999.
8. BUILDING CODE REQUIREMENTS FOR STRUCTURAL CONCRETE, ACI 318-14.
9. BUILDING CODE REQUIREMENTS FOR MASONRY STRUCTURES, TMS 402-13 CODE.

6.2.3. Specifications

The design-build contract for the FIU Pedestrian Bridge not only required that the FDOT Standard Specifications for Road and Bridge Construction be used for construction, it also stipulated that "FDOT Specifications may not be modified or revised" (RFP, Section VI.H).

FDOT STANDARD SPECIFICATION SECTION 400-9 STATES:

"400-9 Construction Joints

400-9.3 Preparation of Surfaces: *Before depositing new concrete on or against concrete which has hardened, re-tighten the forms. Roughen the surface of the hardened concrete in a manner that will not leave loosened particles, aggregate, or damaged concrete at the surface. Thoroughly clean the surface of foreign matter and laitance, and saturate it with water."*

These same specifications are used throughout the State of Florida for the preparation of construction joints on all bridge projects that are subject to FDOT oversight. For the FIU Pedestrian Bridge, these requirements were applicable to all concrete construction joints, including the horizontal joints between the deck and truss members.

A plan note on sheets B-24B and B-25 pertaining to vertical construction joints in the pylon with smooth formed surfaces repeats the specification requirement to roughen the concrete surface and includes 1/4 inch amplitude. These two notes were intended to emphasize the need to roughen what would be very smooth formed surfaces after the first concrete element was cast. This was not a standard condition usually seen for horizontal construction joints. Other construction joints on the project were between horizontal layers of concrete and not formed with smooth surfaces.

KEY POINTS

- **Had the surface been roughened as required by FIGG design and Florida regulations, the accident would have never occurred**
- **The failure of the Contractor to roughen the surface was fatal.**

6.2.4. Construction Phasing

As discussed in Section 5 of this report, the design of the FIU Pedestrian Bridge stipulated a construction sequence with a total of eight (8) stages in the Released For Construction (RFC) Superstructure Plans. Stage 1 of the construction was installing the foundations and building the supporting piers. Stage 2 was precasting the main span truss and Stage 3 was moving the truss into position over SW 8th Street and setting it on the permanent piers. The back span over the canal was to be cast during Stage 4 and made into a continuous structure with the main span in Stage 5 when the upper pylon was to be completed. The remaining stages were to install the pipes from the pylon to the bridge spans, the bridge finishes and landings at the bridge ends.

There are two occasions in the plan construction sequence when the main span truss with all post-tensioning stressed was supported only at the end diaphragms, similar to the configuration at the time of the accident. First, when the main span was in the precasting area after shoring removal and prior to the bridge move, and second, after the bridge move until the temporary PT bars in members 2 and 11 were destressed.

Note that in Stage 5 of construction, the member 11/12 nodal area was to become part of the pylon and continuous with the back span over the canal. At that point the capacity of the nodal connection increases further. The rendering in **FIGURE 6-8** shows this area of the bridge after completion with vertical member 12 incorporated into the pylon.

6.2.5. FDOT Reviews

The design submittals were reviewed by a team of 37 individuals representing FIU, FDOT, FHWA and Miami-Dade County. FDOT had 32 reviewers, including a representative from the FDOT Structures Design Office (SDO) in Tallahassee and three outside consultant structural reviewers working for FDOT. FHWA also had a structural reviewer who provided several comments on the final superstructure plans.

KEY POINTS

- Every comment or question regarding the design was fully and completely resolved before construction ever started.
- The collapse was solely a result of failures by the contractors to comply with the design and good practice.
- Dozens of people reviewed FIGG's design
- Not a single person - all experts - raised a single issue regarding the final RFC design

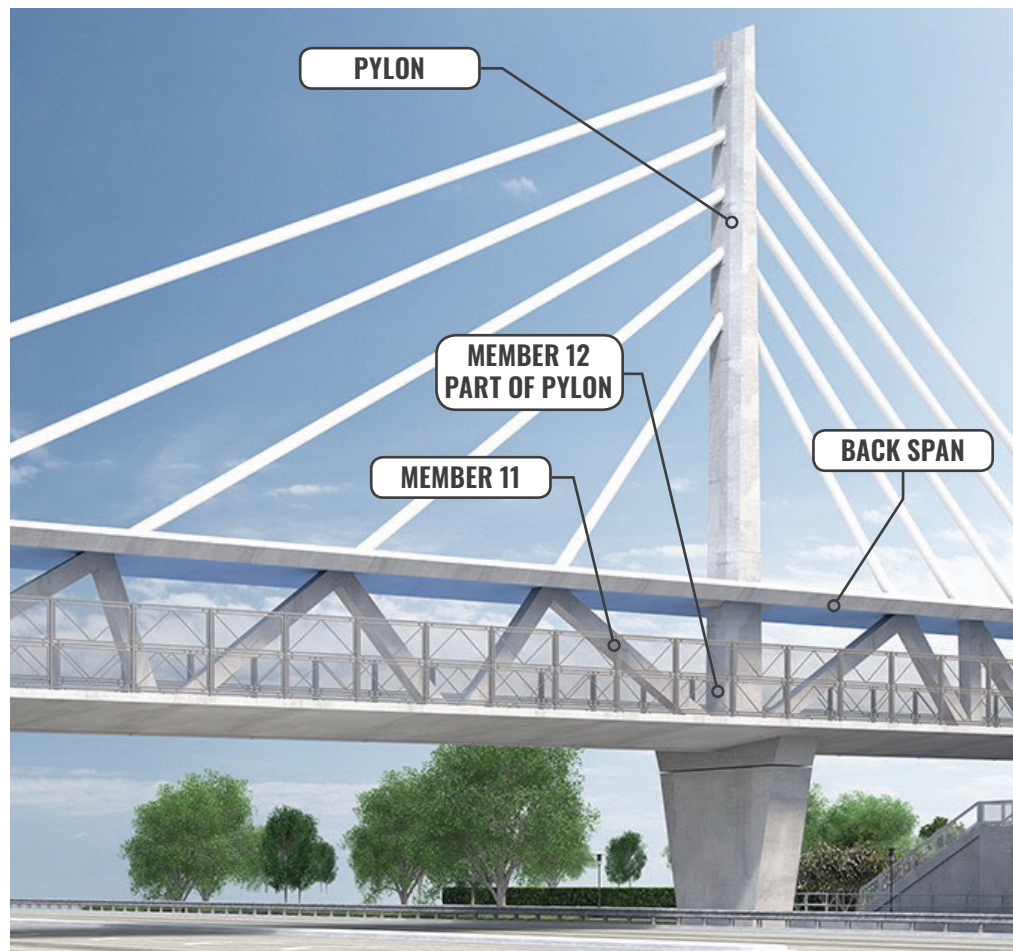


FIGURE 6-8 Rendering of completed bridge. In the finished structure, truss member 12 is incorporated into the pylon and member 11 forces are resisted by the pylon and the back span.

The design review process utilized FDOT's Electronic Review Comments (ERC) system website. All comments, responses and comment close-outs were tracked by the system, and all comments had to be resolved to the reviewer's satisfaction before the plans and specifications were Released For Construction. Plans were submitted at the 30%, 90%, Final and RFC stages of development and calculations were submitted with the Final stage submittal. Over 340 comments were made by reviewers and all of them were resolved before the plans and specifications were issued RFC. These include several comments related to the member 11/12 nodal area from FDOT SDO that were addressed to the satisfaction of FDOT SDO. There were no documented comments related to the subject of redundancy.

6.3. REDUNDANCY

Redundancy is defined in the commentary to The Manual for Bridge Evaluation (AASHTO, 2013) as: "...the capability of a bridge structural system to carry loads after damage to or the failure of one or more of its members". Structural redundancy can be provided in any of three ways (FHWA Technical Memorandum "Clarification of Requirements for Fracture Critical Members", June 20, 2012):

- ⊕ Internal redundancy, where a member is composed of multiple parallel elements
- ⊕ Structural redundancy due to static indeterminacy such as structures continuous over supports
- ⊕ Load path redundancy, where there are more than two primary load-carrying members in a span

The FHWA Memorandum notes that redundancy can be provided in one or more of these ways.

Reinforced and prestressed concrete structures provide a measure of internal redundancy by the fact that members are composed of multiple parallel steel reinforcing bars and/or prestressing tendons surrounded by a concrete matrix composed of aggregates and cement paste. This contrasts with typical steel structure members, which are a single steel element where cracking due to metal fatigue or other effects can propagate through the entire member resulting in a sudden complete failure of the member or connection.

While there are numerous provisions related to redundancy in the AASHTO LRFD design code for steel bridges (Section 6), there are no provisions related to redundancy specifically for concrete bridges (Section 5). Similarly, FDOT SDG provides increased load factors related to redundancy for certain configurations of steel bridges. However, the only redundancy load factors for concrete bridges are for types of support piers that cantilever or span over roadways, none of which apply to the FIU Pedestrian Bridge.

The FIU Pedestrian Bridge superstructure was designed as a single concrete prestressed and reinforced truss. Since the members all have multiple parallel reinforcing bars and/or prestressing tendons, the bridge possesses internal redundancy. The design featured a continuous superstructure once the bridge construction was complete, with the main span over SW 8th Street fully connected at the pylon to the back span over the canal. It also included steel pipes from the pylon to the superstructure that primarily reduced vibrations, but also were capable of supporting some of the pedestrian load. These two features provided structural redundancy in the completed structure. Because the superstructure was composed of a single truss, the bridge did not have the third type of redundancy (load path). In summary, the FIU pedestrian bridge design has several redundant features, including internal redundancy, static indeterminacy and structural continuity of the completed bridge.

The AASHTO LRFD design code permits the use of nonredundant concrete bridge structures and members. If a structure or member is determined to have less than “conventional levels of redundancy”, the acting loads are to be increased by 5% in the design calculations (AASHTO LRFD Section 1.3.4). AASHTO LRFD does not provide specific guidance on what constitutes “conventional levels of redundancy”, leaving it to the discretion of the designer.

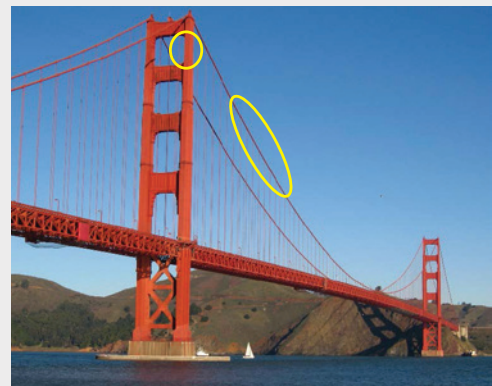
Bridges without load path redundancy (more than two primary load-carrying members) are very common. Some common examples are one or two column piers, bridges with a two-arch superstructure, suspension bridges with two main cables and many cable-stayed bridge pylons. **FIGURE 6-9** is examples of bridges without load path redundancy.

KEY POINTS

- Contrary to the OSHA document, the design was redundant
- The use of guidelines or standards for steel structures to judge redundancy in a concrete bridge is simply stated, wrong.

FIGURE 6-9

Examples of bridges without load path redundancy. Elements circled in yellow are non-redundant for load path.



6.4. INDEPENDENT PEER REVIEW

The MCM design-build proposal accepted by FIU provided for an independent design review of the pedestrian bridge performed by a FIGG office not involved in the original design. Later in the project, FDOT required that the design peer review be performed by an independent engineering firm not involved with the original design. The peer review firm had to be prequalified by FDOT for the type of work they would be performing. By Florida Administrative Code Rule Chapter 14-75, prequalification for Work Type 4.3.1, Complex Bridge Design - Concrete, was required for the peer review firm to review this design.

LOUIS BERGER PREQUALIFICATION

FIGG entered into a contract with Louis Berger, a well-respected engineering firm (now part of WSP, a global engineering firm with 49,000 employees), to perform the peer review services. Louis Berger stated to FIGG in writing that it held the FDOT Work Type 4.3.1 prequalification and provided resumes of engineers with complex concrete bridge design experience. FIGG verified on the FDOT website that Louis Berger was indeed listed by FDOT as having the Work Type 4.3.1 prequalification. The NTSB Factual Report Section 21 contains statements from FDOT that although Louis Berger was listed on the FDOT website as having the Work Type 4.3.1 prequalification, they were not actually prequalified for this, and that the FDOT website should not be relied upon for engineering consultant teaming. However, the FDOT consultant prequalification website page contains no such disclaimer of the information provided, and it is typical practice for engineering firms to rely on the information posted on FDOT's website to confirm consultants' FDOT prequalification status.

PEER REVIEW SCOPE OF WORK

The FIGG/Louis Berger contract Scope of Work stipulated that Louis Berger was to "...perform Independent Peer Review for the concrete pedestrian bridge plans in accordance with the project and RFP requirements and FDOT Plans Preparation Manual (Chapter 26)." The review was for the final foundation, substructure and superstructure submittals for the pedestrian bridge only (excluding the stairways and landings).

Louis Berger was obligated to check constructability considerations of the bridge by FDOT Plans Preparation Manual (Chapter 26), AASHTO LRFD Bridge Design Specifications, Section 2.5.3, and by FDOT Structures Design Guidelines, Sections 2.13, 4.58, 4.59 and 6.10. All of these documents were requirements of Louis Berger's Scope of Work and required investigations of the structure during various construction phases. Louis Berger's scope also included reviewing connections since the reference documents in the scope were comprehensive and did not exclude any of the bridge structural elements.

LOUIS BERGER CERTIFICATION LETTERS

After reviewing each of the submittals, Louis Berger provided certification letters for the foundations, substructure and superstructure final plans. These certifications were in accordance with the FDOT Plans Preparation Manual (Chapter 26) requirements for format and content, and were signed/sealed by Louis Berger’s review engineer. The letters each state in part:

“Pursuant to the requirements of the Contract Documents, Louis Berger hereby certifies that an independent peer review of the above-referenced submittal has been conducted in accordance with Chapter 26 of the Plans Preparation Manual and all other governing regulations.”

And,

“I certify that the component plans listed in this letter have been verified by independent review, that all review comments have been adequately resolved, and that the plans are in compliance with Department and FHWA requirements presented in the Contract Documents.”

FDOT later performed an audit of the peer review performed by Louis Berger and had no comments.

INDEPENDENT REVIEW OF LOUIS BERGER PERFORMANCE

Forensic consultant Wiss, Janney, Elstner Associates (WJE) conducted an independent review of the services provided by Louis Berger after the construction accident (see Exhibit A to this report). It found numerous deficiencies with the peer review, including:

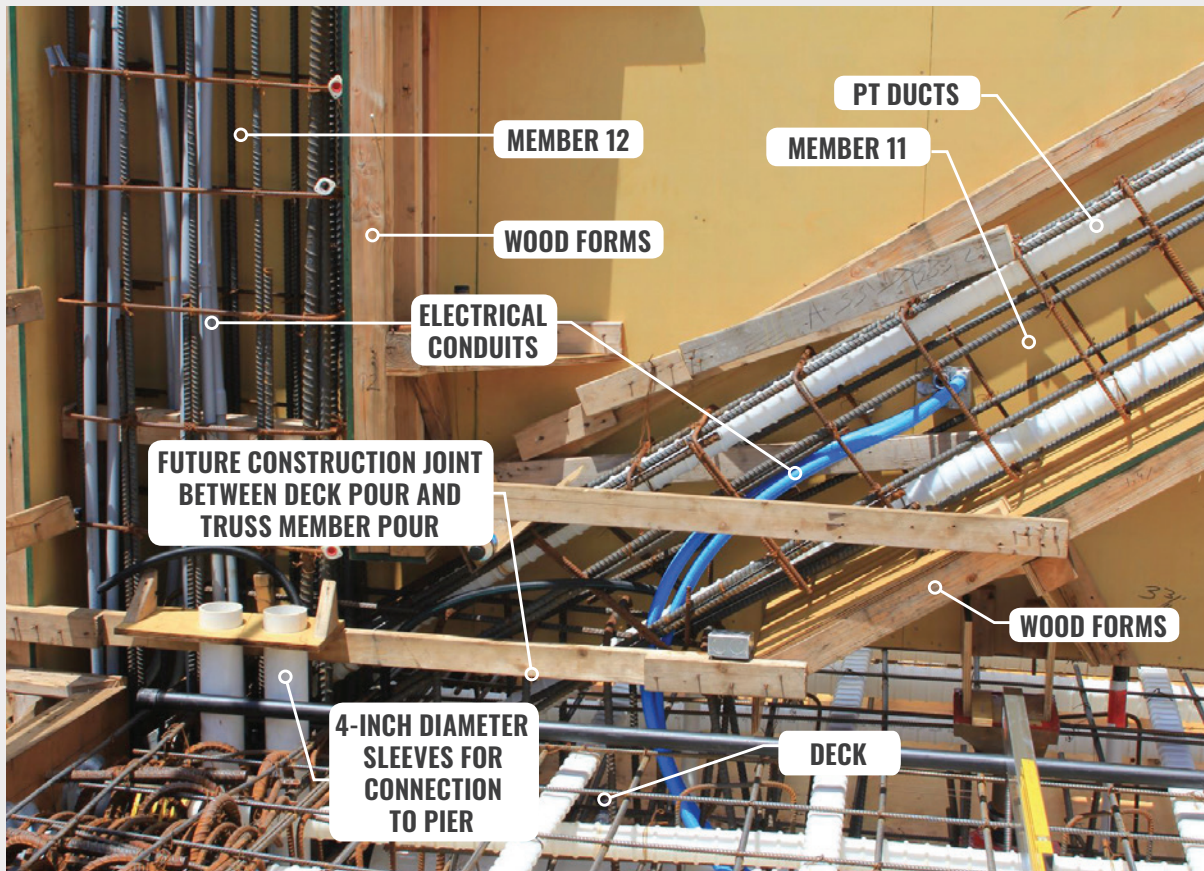
- The computer model incorrectly assumed that the steel pipes connecting the pylon to the truss span carry self-weight of the bridge
- No investigation was made of the various stages of construction
- The truss connections were not reviewed
- Documentation of the independent peer review is lacking and indicates that the complete scope of services was not performed

KEY POINTS

- Louis Berger unbeknownst to FIGG completely failed in their role as an independent peer reviewer.
- Despite being listed as pre-qualified on FDOT’s website, Louis Berger was not pre-qualified by FDOT to act in the the role of an independent peer reviewer.

FIGURE 6-10

Reinforcing and post-tensioning ducts placed in forms for bridge deck and truss members 11 & 12 prior to the deck concrete pour (looking at what would be the west face after the span is moved).



6.5. CONSTRUCTION

6.5.1. Main Span Fabrication

As noted in Section 5.1 above, the precast truss main span was cast in three pours: first the bottom slab (bridge deck), then the truss members and finally the canopy. Between each of the pours, the lower portion of concrete was allowed to cure before wet concrete was cast for the next pour above it. The interfaces between the prior pour and the subsequent pour are concrete construction joints which must transfer forces between the two concrete pours so that the span behaves as a continuous structure when completed. As discussed in Section 6.2.3 above, the construction specifications required that all construction joints be roughened and cleaned after the first concrete pour has hardened. **FIGURE 6-10** shows the north end of the main span prior to casting the deck concrete.

E-MAILS REGARDING CONSTRUCTION JOINT REQUIREMENTS

The construction specification requirements for roughening construction joints were confirmed and emphasized in an e-mail exchange between MCM (the

contractor), BPA (the independent construction quality inspector) and FIGG (designer) starting on June 10, 2017 and continuing through June 13, 2017.

June 10 at 9:20 a.m. – MCM’s Superintendent to BPA:

“We are scheduled to pour the first bottom 3.5 ft. of the South column on Foundation Type 3 this coming Monday morning – June 12, 2017 at 8:00 a.m. ... should you have any questions or concerns feel free to contact me.”

June 10 at 10:44 a.m. – BPA’s Project Administrator to MCM’s Superintendent and others at BPA and MCM:

“Every cold joint generated on structural elements will require a treatment with a APL [Approved Products List] list product. Please ask FIGG their opinion and suggestion.”

June 10 at 10:48 a.m. – MCM’s Superintendent to BPA’s Project Administrator and others at BPA and MCM:

“The question will be asked.”

June 12 at 9:18 a.m. - BPA’s Project Administrator to MCM’s Superintendent and others at BPA and MCM:

“...any response from Figg regarding potential cold joints? Please advise.”

June 12 at 10:06 a.m. – MCM’s Project Engineer to BPA’s Project Administrator and others at BPA and MCM:

“Please clarify if you are referring to construction joints or cold joints. For construction joints we will roughen the surface of the hardened concrete and remove loose particles prior to placing new concrete.”

June 12 at 10:10 a.m. - BPA’s Project Administrator to MCM’s Project Engineer and others at BPA and MCM:

“Yes, I am referring to construction cold joints on structural elements, please get an answer from FIGG of the appropriate treatment.”

June 12 at 10:15 a.m. – MCM’s Project Engineer to BPA’s Project Administrator, FIGG’s Project Manager and others at BPA and MCM:

“I spoke with FIGG and they advised us to follow FDOT specs which is as follows:

400-9.3 Preparations of Surfaces: Before depositing new concrete on or against concrete which has hardened, re-tighten the forms, roughen the surface of the hardened concrete in a manner that will not leave loosened particles, aggregate, or damaged concrete at the surface. Thoroughly clean the surface of foreign matter and laitance, and saturate it with water.

The plan notes do not mention the use of a bonding agent so it is not required."

June 12 at 10:37 a.m. - BPA's Senior Project Engineer to MCM's Project Engineer, FIGG's Project Manager and others at BPA and MCM:

"Lets make sure we keep FIGG informed about the location of the all future construction joints and represent them accurately in the final as-built."

The e-mail included an image from the bridge plans showing the south landing bent (also referred to as the south abutment) with an arrow pointing to a construction joint at the top of one of the columns.

June 13 at 7:48 a.m. - BPA's Project Administrator to FIGG's Project Manager and MCM's Project manager with copy to BPA's Senior Project Engineer:

"Please make sure we have FIGG blessing for the construction cold joints treatment, my personal experience is that a bonding agent will be a reliable way to good because proposed method is not easy to do (column with steel) and achieve good results."

400-9.3 Preparations of Surfaces: Before depositing new concrete on or against concrete which has hardened, re-tighten the forms. Roughen the surface of the hardened concrete in a manner that will not leave loosened particles, aggregate, or damaged concrete at the surface. Thoroughly clean the surface of foreign matter and laitance, and saturate it with water."

June 13 at 7:56 a.m. - FIGG's Project Manager to BPA's Project Administrator and MCM's Project Manager with copies to BPA's Sr. Project Engineer and others at FIGG:

"We have had previous communications with MCM regarding this topic and the FDOT specification referenced below was to be followed. Let us know if you have any further questions."

June 13 at 8:04 a.m. - BPA's Project Administrator to FIGG's Project Manager:

"Thank you."

The NTSB Factual Report in Section 20 incorrectly states that the above e-mail chain was strictly limited to a discussion of construction joints at the columns on the south abutment (south landing bent). A review of the e-mail text shows that this is clearly not the case and that the discussion was regarding the treatment of all concrete construction joints. MCM's June 12 e-mail at 10:15 a.m. transmitting FIGG's instructions to follow FDOT Specification 400-9.3 was prior to BPA's e-mail at 10:37 a.m. that included a sketch of the south landing bent and did not mention the south landing bent in the text.

KEY POINTS

- FIGG made it clear both in the design drawings and subsequently that roughening of the concrete construction joints was required.
- If the concrete joints had been roughened, this incident would not have happened.

WITNESS STATEMENTS CONCERNING CONSTRUCTION JOINT TREATMENT

Despite the FDOT construction specification adherence required by the design-build contract and RFC plans, and the e-mails on the subject of roughening construction joints, the concrete construction crews responsible for placing the concrete apparently were not aware that construction joints were to be roughened in accordance with the FDOT standard construction specifications. In witness interviews with NTSB, MCM and their concrete construction subcontractor, Structural Group of South Florida, it is apparent that the construction crews left the construction joint surfaces as-cast and not intentionally roughened. Also, a large number of concrete vibrator tools, which help to liquify the concrete during placement and result in smooth surfaces, were used to pour the deck.

NTSB Interview with MCM QC Technician (April 11, 2018):

Page 23 of 37

- 1 Q. Can you speak to especially the deck area, were there any
- 2 issues or difficulties placing the concrete?
- 3 A. Not really. Since we have two firms, one crew on each side,
- 4 because we have our (indiscernible) in the middle because you have
- 5 to support the trusses. So it was, I mean, a very new way to go
- 6 uniformly. So in this one and the – not to put so much concrete
- 7 at a time. So we were very, very slow.
- 8 Q. How about as far as vibration of the concrete and placement?
- 9 Was it, was it normal? Required more, less, especially –
- 10 A. More than enough. We have like 16 vibrators. Had a lot of
- 11 Vibrators, four of each on each side, plus the one on the finisher
- 12 in the middle, so it was pretty good.

13 Q. Can you say that number again? How many –

14 A. Eight on – say four, three – probably seven on each side.

Page 24 and 25 of 37

25 Q. Was any special treatment made to the finish at the, at the
1 deck surface where the diagonals came in and connected to the –

2 A. No, just to cover where instead of using the special
3 products, like compounds or anything, for curing, we used curing
4 blankets. Yeah. And then protect it with plywood, which – yes.

5 Q. Was that, was that surfaced roughened in any way or prepped
6 in any way?

7 A. No. After the finish, that was it.

8 Q. So it wasn't finished. It was just covered and –

9 A. Just covered. Yes.

14 Q. Were the surfaces of the diagonals cleaned and prepped prior
15 to placement? Was any kind of prep done to those surfaces?

16 A. You have to understand that the – in order to lift it
17 better, those PT bars has to be placed before we pour. So all the
18 forms was pretty much done with the rebar, and the PT was in
19 place. So practically those was a second pour, the trusses.

20 Q. Were all four sides of the formwork in place of the –

21 A. No.

22 Q. -- diagonal when you placed the soffit?

23 A. Three sides.

24 Q. Three sides.

25 A. Yeah.

Page 26 of 37

1 Q. So there was one face –

2 A. One side open.

3 Q. -- to give you access to cure it.

4 A. Right. Right. Cure and clean it after – to do the second

5 pour.

**NTSB Interview with Owner of Structural Group of South Florida
(March 22, 2018):**

Page 24 of 38

19 Q. Was any surface prep required for the interface for the
20 diagonal hit, the bottom slide?

21 A. Yes. It had to be roughened up.

22 Q. So, each one had a roughened surface?

23 A. Yes.

24 Q. And how did you – just try all buffing or –

25 A. Yeah, we just left it like it was. I mean we just roughed

Page 25 of 38

1 boomed it and, you know, how you just mix it up with a trowel.

2 You just don't – you don't do a nice finish on it. You just

3 leave it roughened up.

4 Q. So, it's just as it settles.

5 A. Yes. Then before we pour it, obviously, we had one side up.

6 We had everything in, everything inspected –

7 Q. Right.

8 A. -- and then we closed it up. Left the bottoms all open so

9 they could be washed out and cleaned out and put a – whatever

10 they call for – I don't know it was a bonding agent. But there

11 was something that was called for there or just roughened up the

12 surface. I'm not sure.

13 Q. So, it wasn't prescribed – sometimes you get surface

14 (Indiscernible) so they kind of ask you to roughen it to a certain

15 but it was just don't finish it.

16 A. Don't finish it, yeah.

Page 28 of 38

8 Q. So, you had the diaphragm area where you were casting it.

9 So, you had the truck ready to go and you just went back and forth

10 and you brought it up, brought it up, brought it up.

11 A. Four very small vibrators.

- 12 Q. Four small vibrators.
- 13 A. And then once we got past the rebar then we went to the
- 14 bigger vibrators.
- 15 Q. There was no disruption in that pour?
- 16 A. No, when we stripped it it looked like glass. It was
- 17 beautiful...

6.5.2. Bridge Move

As discussed in Section 5.1 of this report, the main span truss was moved from the precast area on the south side of SW 8th Street and set on the permanent piers on March 10, 2018 using self-propelled modular transporters (SPMTs) as shown in **FIGURE 6-11**.

KEY POINTS

- ▶ Looking like “glass” is wholly inconsistent with the requirement of roughening.
- ▶ The construction contractor completely failed to follow the design, industry standards or code requirements.

As part of the move planning, FIGG provided a maximum limit for twist in the bridge span of 0.5 degrees between the truss supports during the move. The bridge move subcontractor, Barnhart, contracted with Bridge Diagnostics, Inc. (BDI) to perform electronic monitoring of the span using highly sensitive sensors. BDI installed their monitoring system on the main span in the precast area prior to the SPMT’s lifting of the span from its end supports.

Data from the electronic sensors was recorded by BDI during the move. Select data, principally span twist, was actively monitored by BDI relative to defined

FIGURE 6-11

Precast main span truss move by self-propelled modular transporters (SPMTs) on March 10, 2018 from precast area to permanent piers.



limits of permissible twist. There were multiple occurrences during the move when communication between the remote wireless sensors and the data acquisition/recorder unit were lost. Each time this happened, Barnhart stopped the SPMT movement until communications were restored. However, a complete set of data was not continuously reported during each of these events, between the time when communications were lost and the SPMT were fully stopped.

Upon completion of the move, the span was lowered on to bearings on each end of the span: temporary bearings on the North end of the span and permanent bearings on the South end of the span. Representatives of FIGG were on-site at the time to observe the span move. FIGG was not informed either during or after the move that there were any recorded instances of span twist exceeding the established limits.

BDI prepared a report on the results of the bridge monitoring during the span move approximately twenty days after the construction accident, dated April 4, 2018 (see Exhibit D). Figure 32 of the report is represented as the actual recorded instrumentation readings of twist between the SPMT supports.

KEY POINTS

- Twisting the structure during the move beyond allowable limits and then failing to tell anyone that it had occurred is inexplicable.
- Such action has the practical effect of weakening a structure already weakened by a lack of roughening.
- FIGG was never made aware of any of these failures.

FIGURE 6-12

Figure 32 from BDI monitoring report on twist of the main span during the bridge move (as modified in WJE report). Twist limit of 0.5 degrees was substantially exceeded on multiple occasions.

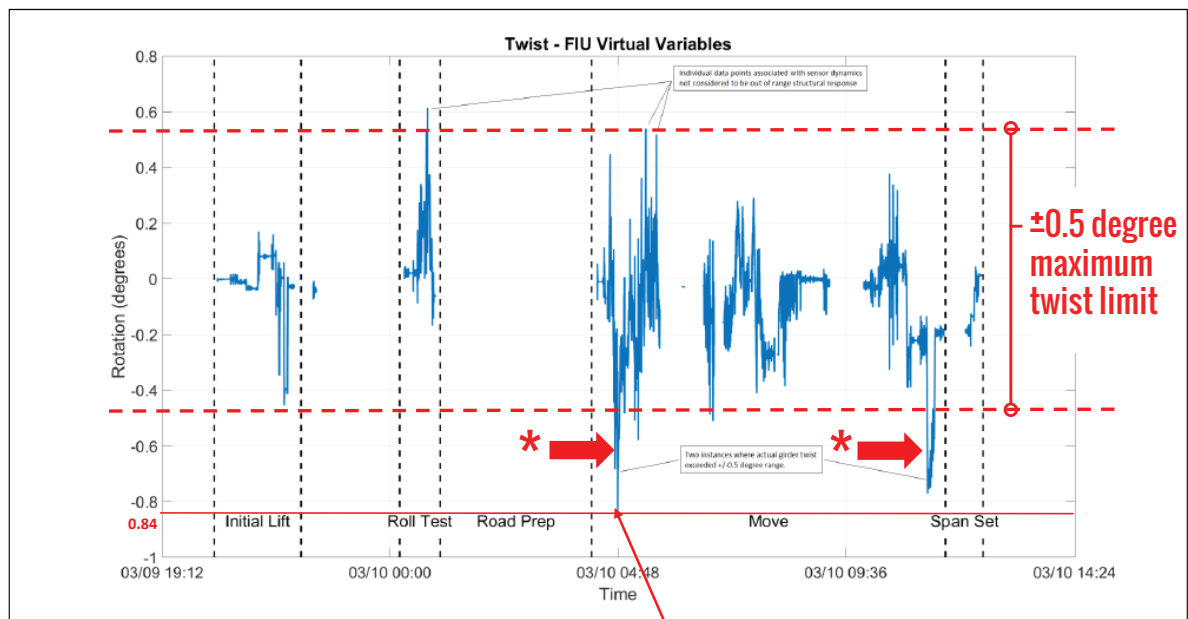


Figure 32 – Girder Twist – Difference in angle between Sections J & L

***Instances where twist substantially exceeded limits**

Difference in rotation between north and south supports: 0.84°

FIGURE 6-13

Cracking at the base of member 11 before versus after the span move.
(Source: BPA February photos; Corradino March photos)



February 28, 2018

March 10, 2018 at 3:07 p.m.

The graph shows the twist was exceeded on at least three occasions, with a maximum twist of over 0.84 degrees (see **FIGURE 6-12**). In their report, BDI asserts that some of this is due to “sensor dynamics” and “based on visual interpretation of data plot” they conclude that the maximum twist was exceeded in two instances with values of 0.65 and 0.75 degrees. Assuming that this is the case, the actual twist was still 150% of the maximum limit for twist in the bridge span of 0.5 degrees. If the raw data is used, the actual twist would be 168% of the maximum limit.

FIGURE 6-13 is a series of photographs illustrating the change in the observed cracking at the truss member 11/12 connection to the deck prior to the move on February 28, and about three hours after the move on March 10, 2018. Cracking in the area is noticeably more significant. Other photos showed that the top outside edge of the diaphragm on the north end near member 12 had spalled off.

6.5.3. Restressing Member #11

As discussed in Section 5.3 of this report, two days after the post-tensioning (PT) bars in truss members 2 and 11 were destressed in the late afternoon after the moving of the span, MCM’s Project Manager sent FIGG’s Project Manager 16 photographs, mostly of new cracking that was observed at the north diaphragm. No crack inspection report was provided. MCM reported to FIGG during a subsequent phone call at approximately 9:30 a.m. on March 13 that the cracking had gotten slightly worse after the PT bars were destressed and that the cracks had not increased in size since the afternoon of March 10.

Later that day, FIGG recommended placing shims between the pier and the bridge deck at the north end and restressing the PT bars in member 11 while further evaluation was performed. This recommendation to restress the PT bars was based on the observation relayed by MCM that the cracking worsened when the PT bars had been destressed, so the intent was to revert back to the prior state of the structure. The more significant cracking reported to FIGG at the time was at the member 11 chamfer and at the end diaphragm (**FIGURE 6-14**). These were outside of the area that would be compressed by restressing the PT bars, so it was anticipated that the bars could be restressed to restore the same forces in the structure as before destressing the bars on Saturday, March 10, and potentially reduce the diaphragm crack size.

FIGURE 6-14

Member 11 crack photo attached to March 12, 2018 e-mail sent to FIGG by MCM. The larger crack in chamfer (“wedge crack”) is outside of region compressed by member 11 PT bars. (Source: Attachment 24 to Factual Report)



FIGG provided instructions in an e-mail to MCM on March 13 for restressing the member 11 PT bars. This was to be performed in 12 incremental steps while the cracks were being closely monitored. Stressing a PT bar is normally done in one step in a short amount of time. The 12-step stressing sequence required about two hours. If the cracking worsened, the restressing was to immediately stop and notify FIGG.

Structural Technologies (VSL) produced shop drawings for the post-tensioning on the FIU Bridge project. The General Notes sheet includes the following:

“Stressing Safety Guidelines

5. Immediately cease stressing and remove all personnel from the area if any existing crack widening, new concrete cracking, bearing plane movement, or unusual sounds are observed.

6. Work zones shall be defined by the placer and only essential personnel shall occupy the work zones during stressing operations.”

Monitoring cracks to determine changes in width requires some type of measurement tools. The most common tools used for this purpose are shown in **FIGURE 6-15**.

Forensic consultant WJE analyzed a time-lapse video from a FIU construction web cam and concluded that, contrary to FIGG’s instructions, cracks in member 11 and in the north-end diaphragm during re-stressing of member 11 were not closely monitored (see Exhibit A). While wood blocks were in place on the north face of the north diaphragm, there was no access for personnel to view them. Other types of crack monitoring tools do not appear to have been in use and are not referenced in the NTSB interview transcript with BPA’s Sr. Project Engineer,

FIGURE 6-15

Different types of industry-accepted concrete crack measuring devices: 1) Displacement transducer, 2) Humboldt crack gauge, 3) Dial caliper and measurement points, 4) Wood block crack gauge (similar to that used at the site on the north diaphragm), and 5) Crack width ruler (crack comparator). (Source: WJE)



FIGURE 6-16

Post-tensioning subcontractor Structural Technologies defined the work zone on SW 8th Street as only the area occupied by the crane during restressing member 11 PT bars on the afternoon of the accident, March 15, 2018. (Source: Bridge Factors Photographs - FIGG, FCA 10-23)



who stated that he was the only person consistently on the north end of the bridge deck during the PT bar restressing.

The video from the FIU construction web cam also shows that the two north lanes of SW 8th Street were closed during the PT bar restressing, but that all other lanes were open to traffic (**FIGURE 6-16**). This infers that Structural Technologies defined the work zone on SW 8th street as only the area occupied by the crane below the bridge assisting the stressing operation.

6.5.4. Communication With EOR

The Engineer of Record (EOR), FIGG, was not contracted to have a full time representative at the project site. FDOT rules also do not permit the design engineer to have a role in the construction engineering inspection (CEI) of the project, which was performed by BPA in this case. Located approximately 500 miles from the project in Tallahassee, Florida, FIGG relied on communication with the construction contractor (MCM) for information on construction processes and results. The NTSB Factual Report includes observations and information collected at the project site regarding cracking at the north end of the bridge from the time the bridge was moved to the day of the construction accident. It is apparent that incomplete and inaccurate information was provided to FIGG by those at the project site during this time, as illustrated in **TABLE 6-1**.

Note: Redaction in photograph "Bridge Factors Photographs - FIGG, FCA 10-23" as per NTSB Operations Bulletin CIO-GEN-016.

TABLE 6-1: Observations made by on-site personnel versus information provided to Engineer of Record, FIGG, located in Tallahassee.

DATE	ON-SITE OBSERVATIONS	INFORMATION PROVIDED TO FIGG
Saturday (*) 3/10/18	<p>MCM, BPA and Corradino note increased cracking of member 11/12 nodal area, cracking of the north diaphragm north face and spalling of the north deck edge around 3:00 p.m. Documented with series of photographs by MCM and BPA.</p> <p>Structural Technologies completes destressing member 11 PT bars and sends text to co-worker at about 6:00 p.m. stating "It cracked like hell".</p>	None.
Sunday 3/11/18	None.	None.
Monday 3/12/18	Ongoing crack monitoring, measurements and photos by BPA and MCM in the morning of members 11/12 and diaphragm. Cracks larger than on Saturday.	E-mail at 4:51 p.m. from MCM to FIGG with 16 photos, almost all of north diaphragm. Two photos of member 11/12 node. No information on crack size or growth provided to FIGG (other than tape measure in some photos). No phone calls to FIGG expressing any concern.
Tuesday 3/13/18	Ongoing crack monitoring, measurements and photos by BPA and MCM of members 11/12 and diaphragm. Cracks larger than on Monday.	Phone call between MCM and FIGG at approximately 9:30 a.m. MCM states cracks in photos were observed Saturday afternoon before destressing PT bars, grew slightly when the bars were destressed, and have not grown in size since. No photos or other information on crack size, location or growth provided to FIGG.
Wednesday 3/14/18	Ongoing crack monitoring, measurements and photos by BPA and MCM of members 11/12 and diaphragm. Cracks larger than on Tuesday.	E-mail at 1:38 p.m. from MCM to FIGG with photos without commentary. No information on crack size or growth provided to FIGG.

(*) After FIGG left the site at approximately 12:30 p.m. following completion of the bridge move.

The information provided to FIGG by site personnel starting late Monday, March 12, pertained almost exclusively to the north diaphragm region. FIGG was not provided with a crack inspection report or told of any growth in cracks. FIGG's analyses performed prior to the Thursday meeting consequently focused on the north diaphragm and assumed that the bridge had been constructed in accordance with the RFC plans and specifications. **FIGURE 6-17** shows example of photographs that were provided to FIGG to perform its analysis versus those taken at the site.

KEY POINT

- Had FIGG known about the lack of roughening the excessive twisting during movement of bridge, the "cracked like hell" comment, smooth as "glass" comment and the locations involved, they would have raised alarm bells.

6.6. ROAD CLOSURES

Section 25 of the NTSB Factual Report discusses the authority to close a bridge or road to protect the public. For the FIU Pedestrian Bridge project, the Florida Department of Transportation (FDOT) had authority over the SW 8th Street right-of-way since it is a State facility. FDOT delegated authority to the Owner, FIU, per procedures for a Local Agency Project (LAP). FIU contracted with Bolton Perez & Associates (BPA) for Construction Engineering Inspection (CEI) services on the project, which includes oversight of the construction contractor's maintenance of traffic (MOT). MCM, the construction contractor, was responsible for creating and properly implementing a MOT plan. These four entities, FDOT, FIU, MCM and BPA had the authority, acting alone or collectively, to close or restrict traffic on SW 8th Street. Only MCM and BPA had personnel assigned to the project site full-time. Other project participants had the ability to recommend or request traffic closures or restrictions if required.

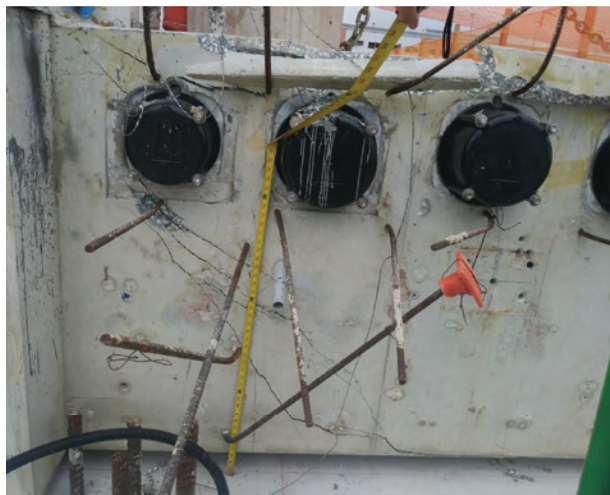
At 9:00 p.m. on Friday, March 9, 2018, SW 8th Street was closed to all traffic in preparation for moving the main span truss from the casting area to the permanent location. MCM had a permit from FDOT allowing this closure over a weekend from Friday at 9:00 a.m. to Monday at 5:00 a.m. The bridge move was performed by Barnhart Crane and Rigging starting around 4:30 a.m. on Saturday, March 10, and finishing around 12:30 p.m. that day.

A FIGG representative reviewed the truss members at approximately 12:30 p.m. on March 10 prior to leaving the site after the move. Photographs taken by him show that cracking was similar to that documented on February 28 before the move.

An inspector for Corradino (subcontractor to BPA) and a representative from MCM observed more significant cracking later that afternoon prior to when Structural Technologies destressed the member 11 PT bars. This included significantly wider cracks at the member 11 chamfer and at the deck surface adjacent to member 12, a new crack in the west face of member 11, and a spall at the top edge of the diaphragm on the north end.

FIGURE 6-17

Photos of the member 11/12 node provided to FIGG are shown on the left side of this figure. There were 13 photos of the north diaphragm provided. Many other photos of the member 11/12 node were taken during the time between the bridge move on March 10, 2018, and the accident on March 15, but not provided to FIGG in a timely manner. Some examples of these are shown on the right side of this figure. (Source: NTSB Factual Report Attachment #24 and Bridge Factors Photographs #'s 90, 83 and 76)



Photos provided to FIGG

Sample of photos taken over the March 13-14 period

Nevertheless, with full knowledge of the worsened cracking, destressing of truss members 11 and 2 was carried out by Structural Technologies. At approximately 6:00 p.m. on Saturday March 10, SW 8th Street was re-opened to traffic. At 7:08 p.m., the Structural technician who had been working on the PT bar destressing texted another person within Structural stating "It cracked like hell". At that time, the permit to close SW 8th Street was still valid for approximately another 34 hours. Also, the SPMTs and equipment used to move the span were still at the project site and conceivably could have been used to support the span temporarily or move the span back to the casting area.

From Monday, March 12 through Wednesday, March 14, MCM and BPA had a full-time presence at the project site and were monitoring the cracking. Neither MCM or BPA acted or recommended to close SW 8th Street to traffic. The March 15, 9:00 a.m. meeting at the project site to discuss the cracking was attended by representatives of FDOT, FIU, BPA, MCM and FIGG. No one at the meeting suggested that SW 8th Street should be closed until the situation was resolved. At the time of the accident later that afternoon, two lanes of westbound traffic were closed for the member 11 restressing operations, with six lanes of traffic open.

6.7. CONSTRUCTION QC/QA

On the FIU Pedestrian Bridge design-build project, the construction contractor, MCM, was responsible for providing construction Quality Control, which is the first check that the materials, construction processes and final product conform to the Released For Construction (RFC) plans and specifications. The Owner's CEI consultant, BPA, was responsible for providing construction Quality Assurance, which is verification that Quality Control is being performed adequately and that the materials, construction processes and final product conform to the RFC plans and specifications.

Both MCM and BPA were responsible for verifying, among many other items, that the concrete construction joints between the deck and the truss members were prepared in accordance with FDOT Standard Specification 400-9.3, which requires roughening the surface of the hardened concrete prior to pouring the next layer of concrete. As presented in Section 6.5.1 above, both MCM and BPA, including MCM's Quality Control Technician, were included in the series of e-mails confirming these requirements prior to precasting the main span truss.

In an interview with the NTSB after the accident, however, MCM's Quality Control Technician stated that he understood the construction joints between the deck and truss members were to be left as-cast and "just covered" (see Section 6.5.1). In contrast, BPA's Project Administrator told the NTSB in an interview after the accident that the construction joints were to be roughened:

NTSB Interview with BPA Project Administrator (March 20, 2018):

Pages 108 and 109 of 127

- 24 Q. ...But did they
25 prescribe any particular surface prep between the pours? Usually
1 a hand trowel, a roughened surface between –
4 The construction joint between – especially the
5 diagonal and the bottom slab?
6 A. They rough it.
7 Q. Huh?
8 A. Rough it. Rough it.
9 Q. It called for a roughened surface?
10 A. Yes.
11 Q. Okay.
12 A. If I recall correctly. Remember, I'm not
13 inspecting it, okay.
20 A. But between them – and I know because I asked
21 the question, not because I inspect it. But I asked the question
22 how are we treating between surface? And they said rough it.
23 That's the way it was designed.

KEY POINT

Despite knowing that the FIGG design, code and industry requirements, required roughening the concrete construction joint was not roughened.

6.8. NTSB TESTING

As presented in Section 30 of the NTSB Factual Report, material samples were taken from the north end of the bridge after the accident to determine if they conform to the project requirements. These were tested by the NTSB Materials Laboratory and the FHWA Turner-Fairbank Highway Research Center (TFHRC).

6.8.1. Post-Tensioning Jack

The post-tensioning jack and hydraulic system that was being used by Structural Technologies to restress the member 11 PT bars at the time of the accident was recovered and tested in the laboratory. NTSB Materials Laboratory Factual Report No. 18-081 describes the equipment and the testing. There was damage to the jacking system tested, presumably from the accident, but no evidence that the system was malfunctioning prior to the accident.

6.8.2. Concrete and Reinforcing / Post-Tensioning Steel

NTSB Materials Laboratory Factual Report No. 18-082 documents sampling and testing of concrete and steel specimens. The specimens were taken from the north end of the bridge. These included concrete cores from the bridge deck and canopy, post-tensioning rods from truss member 11 and from a stockpile at the site, and mild reinforcing steel from the deck and truss members 11/12. The materials were tested at TFHRC in Virginia and found to meet the minimum requirements specified for the FIU Pedestrian Bridge project.

6.8.3. Deck and Truss Members 11 & 12 Construction Joint

The TFHRC Factual Report "Concrete Interface Under Members 11 and 12" is an evaluation of the horizontal construction joint (also referred to as "cold joint") between the bridge deck and truss members 11 and 12 at the north end of the bridge (See Exhibit B for the FHWA Turner -Fairbanks lab report, TFHRC).

TFHRC found that the construction joint between the deck and truss members 11/12 was smooth and covered in concrete paste (FIGURES 6-18 AND 6-19). The report concludes "that the failure interface coincides with the original cold joint and that the cold joint was not intentionally roughened".

FIGURE 6-18

Interface under member 11 showing smooth construction joint surface (Source: TFHRC Report "Concrete Interface under members 11 and 12")

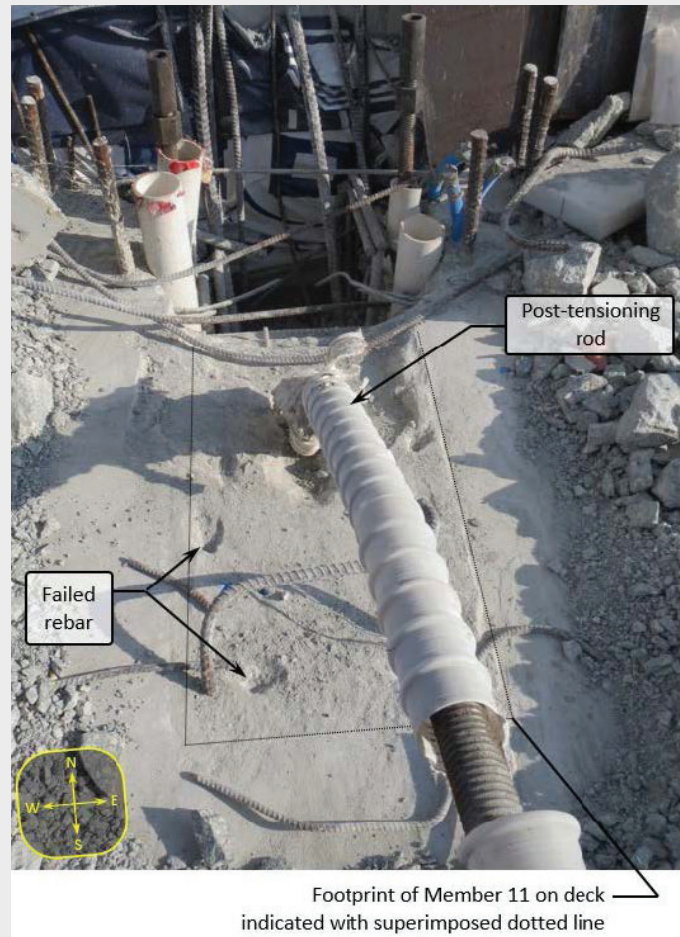
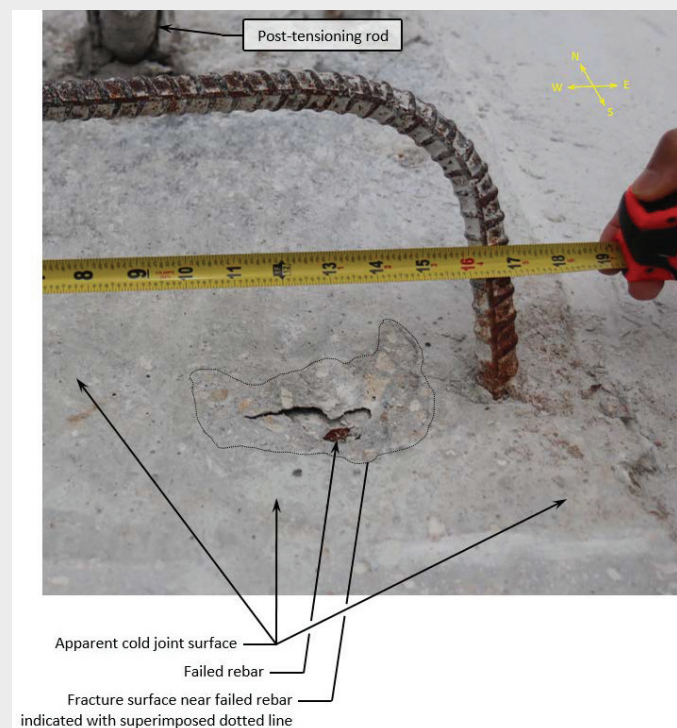


FIGURE 6-19

Interface under southeast corner of member 11 showing smooth construction joint surface (Source: TFHRC Report "Concrete Interface under members 11 and 12")



Had the construction joint been prepared in accordance with FDOT Construction Specification 400-9.3 the surface would have been rough, with cement paste removed and aggregate exposed. Therefore, the joint was not constructed in accordance with the Released For Construction (RFC) project specifications.

KEY POINT

The failure to intentionally roughen the concrete caused this tragedy

6.8.4. Roughness Measurements of Member 11/12 Construction Joint

The construction joint surfaces between the bridge deck and truss members 11 and 12 were further studied as reported in NTSB Materials Laboratory Study Report No. 19-043 (Exhibit C). Samples of the actual surfaces were scanned using a short-range laser scanner to determine relative variations in surface height across the interface. The report notes that “there is no industry standard that specifies a direct method for quantitatively measuring the surface roughness of concrete”. The report concludes that “The average Sa [“arithmetic mean roughness value”] for the flat areas evaluated on both the Member 11 pieces as well as the Member 12 surface was approximately 1 mm (0.04 in) as measured in the partially damage post-collapse condition.”

This conclusion is consistent with the TFHRC report, that the construction joint between the deck and truss members 11/12 was not roughened as required by Florida Department of Transportation standard construction specifications.

6.9. CONSTRUCTION JOINT SLIDING TESTS BY WJE

To study the effect of intentional roughening on the capacity of the concrete construction joint between the deck and truss member 11, an experimental

FIGURE 6-20

Full-sized test specimens were designed to replicate the truss member 11 connection to the bridge deck. (Source: WJE)

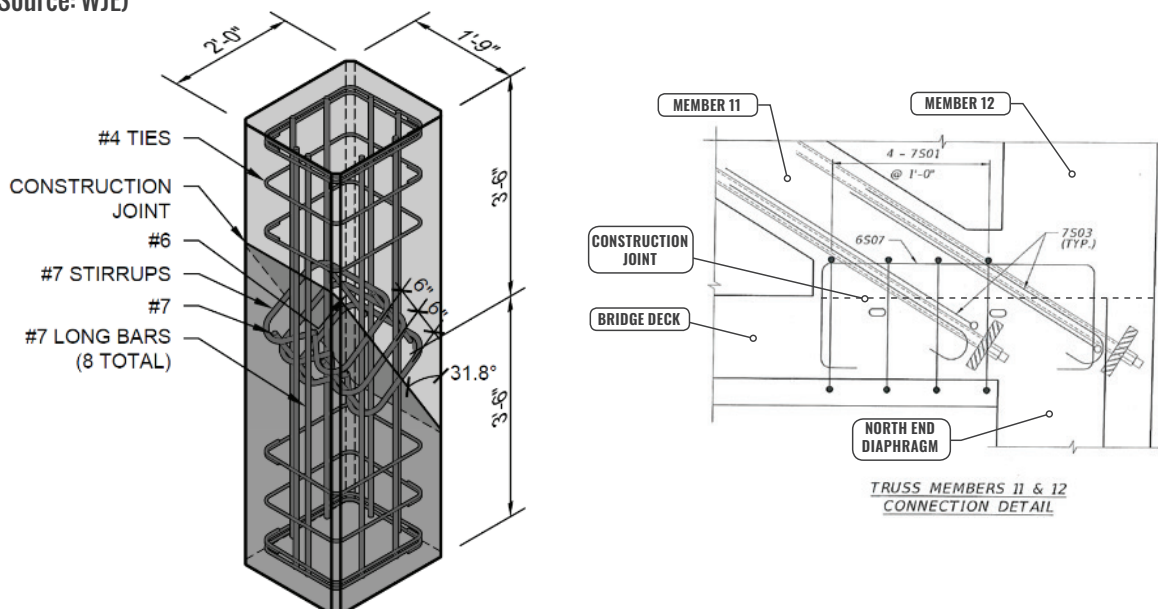




FIGURE 6-21
Lower half of test specimens cast at same angle as member 11 connection to the bridge deck. The lower half is analogous to the bridge deck. Note the electric chipping hammer used to roughen the surface of the roughened joint specimens. (Source: WJE)



FIGURE 6-22
Electric chipping hammer and tool bit used to roughen specimen joint surface in accordance with FDOT Standard Specifications. (Source: WJE)

program was developed and carried out by forensic engineers Wiss, Janney, Elstner Associates (WJE). The full report of this test program is included in Exhibit A.

TEST SPECIMENS

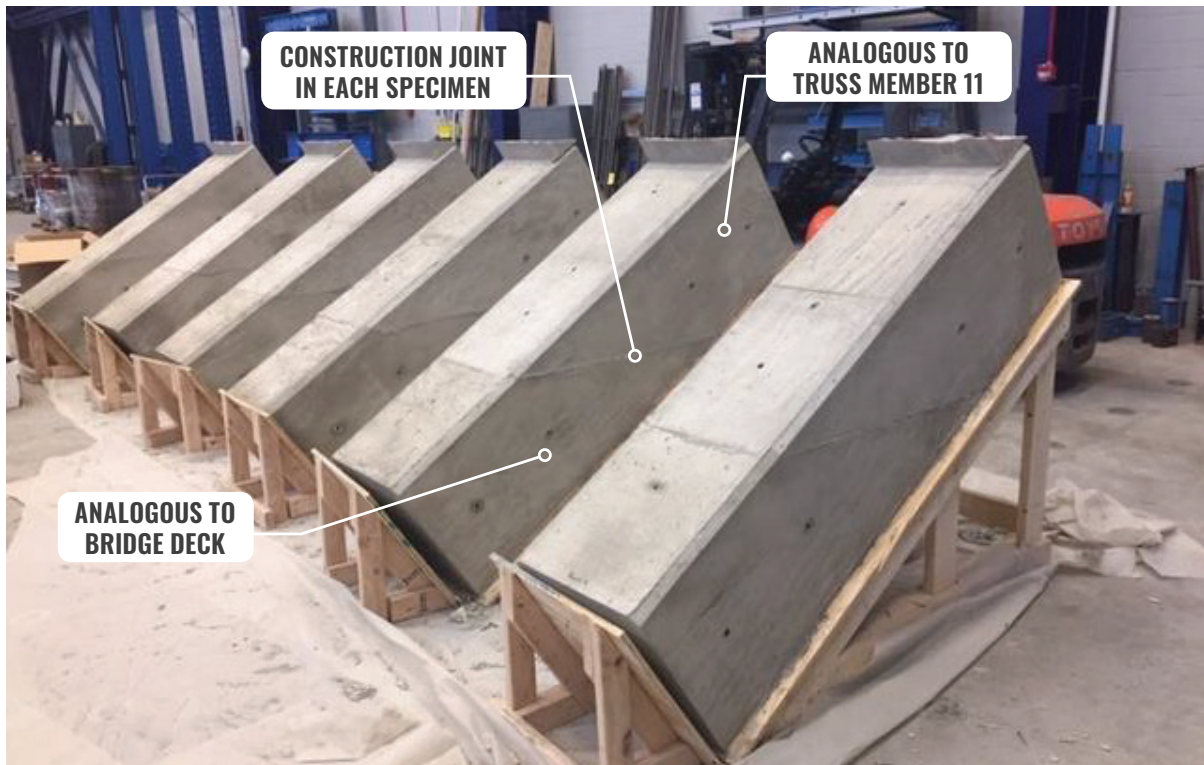
The experimental program consisted primarily of testing six (6) full-sized specimens designed to replicate the truss member 11 connection to the bridge deck. Each seven-foot long specimen had the same cross-section dimensions as truss member 11 and was cast with concrete made from the same mix design as the FIU Pedestrian Bridge (**FIGURE 6-20**). A sloped construction joint was created in each specimen at the same angle (31.8 degrees) that member 11 framed into the bridge deck.

The longitudinal reinforcing bars in the test specimens were identical to those of member 11, although the section did not include post-tensioning bars or ducts. The #4 size reinforcing ties above and below the construction joint were similar to the ties in member 11. Three #7 stirrup bars were provided across the construction joint to replicate the effect of the three northernmost shear friction reinforcement stirrups (identified as 7S01 bars in **FIGURE 6-20**). The southernmost stirrup was not included because it did not contribute to the shear resistance of the connection.

The specimens were cast in two lifts. The lower lift was cast with the forms on an angle of 31.8 degrees up to the level of the construction joint (**FIGURE 6-21**). Concrete vibrators, similar to those used in casting the actual bridge deck, were used to consolidate the concrete, but no finishing or other treatment of the

FIGURE 6-23

Completed full-sized test specimens of truss member 11 connection to bridge deck. (Source: WJE)



concrete surface was done at that time. Three of the specimens were left with the construction joint in the as-placed condition, also referred to in this report as “non-roughened”.

The other three specimens had the construction joint intentionally roughened one day after casting using an electric chipping hammer with amoil bit, a rectangular bit tapered to a sharp point (FIGURE 6-22). The intent was to meet FDOT Standard Specification 400-9.3 to “roughen the surface of the hardened concrete in a manner that will not leave loosened particles, aggregate, or damaged concrete at the surface” using practical methodology and common construction tools.

A week after the lower half of the test specimens were cast, the upper halves were cast, again using the same concrete mix design as the FIU bridge (FIGURE 6-23). Testing was performed on the specimens once the concrete reached a compressive strength of approximately 8,500 psi. Note that the concrete from the north end of the bridge deck tested by TFHRC after the accident had an average strength of approximately 9,800 psi, so the specimen tests were conservative.

CONSTRUCTION JOINT ROUGHNESS MEASUREMENTS

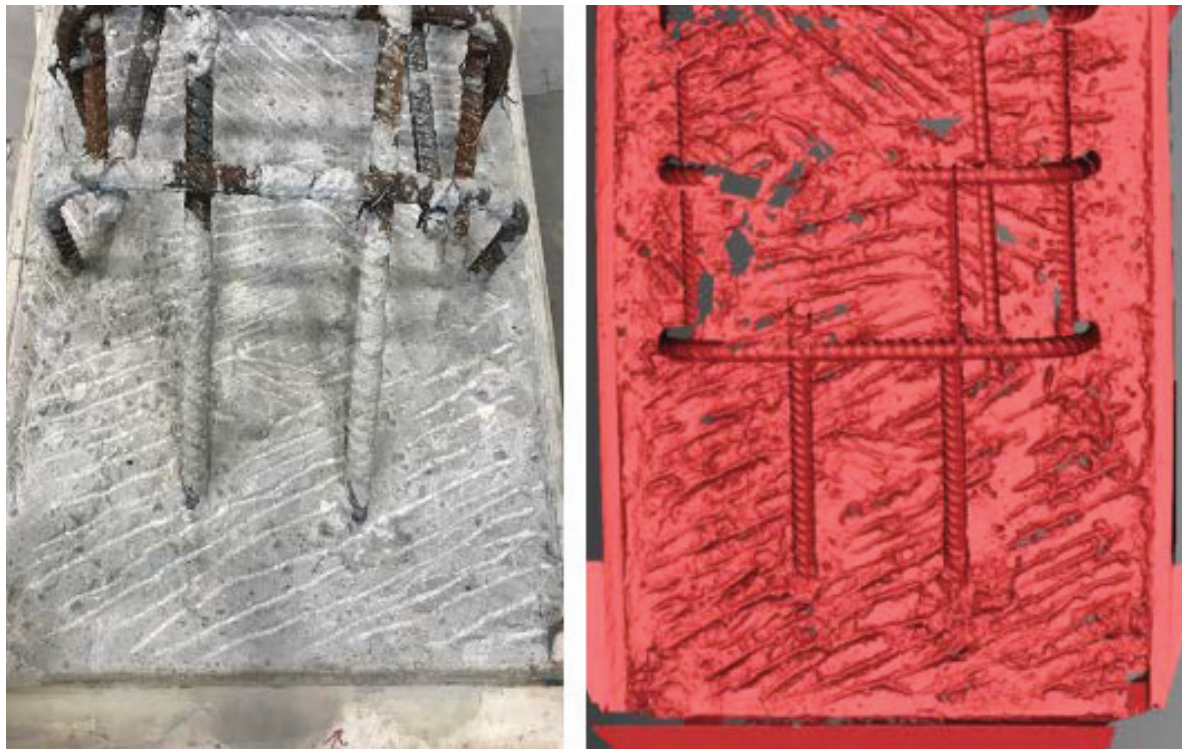
To establish the degree of surface roughening, laser scans were performed on one non-roughened joint surface and one roughened joint surface, similar to the scans performed as part of NTSB Materials Laboratory Study Report No. 19-043 discussed in Section 6.8.4 above. FIGURE 6-24 shows a comparison of the two specimens and laser scans.

FIGURE 6-24

As-placed (non-roughened) and roughened test specimen construction joints and laser scans. (Source: WJE)



(a) As-placed (non-roughened) specimen construction joint (left) and laser scan of surface (right)



(b) Roughened specimen construction joint (left) and laser scan of surface (right)

The scan data was analyzed by defining a “mean plane” such that the area above the mean plane is equal to that below the plane. Deviations are measured relative to the mean plane. For comparison purposes, laser scan data provided by NTSB for Sample 1 of the member 11 interface was analyzed using the same methodology as for the WJE laboratory specimens. Since amplitude of roughness is normally considered as the distance between high and low points, the amplitude of the roughening can be estimated as twice the standard deviation of distances from the scanned points to the mean plane. The resulting roughness measurements are shown in **TABLE 6-2** on page 6-35.

TABLE 6-2: Laser scan measurements of non-roughened and roughened test specimen construction joints and comparison to actual sample from member 11.

JOINT SAMPLE	STANDARD DEVIATION		AMPLITUDE = 2 X STD. DEVIATION	
	MM	INCHES	MM	INCHES
WJE Non-roughened	0.94	0.04	1.88	0.07
WJE Roughened	2.03	0.08	4.06	0.16
Member 11 NTSB Sample 1	0.76	0.03	1.52	0.06

Comparing the WJE non-roughened surface to the actual joint under truss member 11 obtained by NTSB, the WJE specimen is 24 percent rougher. The WJE roughened surface is more than twice as rough as the WJE non-roughened surface.

Note that the scanned amplitude of the WJE roughened surface is 0.16 inches. This is approximately 2/3 of the 0.25 inch amplitude referenced in the AASHTO LRFD design specifications for shear friction that the design calculations for the truss connections used (see Section 6.2.1 above). However as a practical matter, contractors are not known to measure the roughening amplitudes so the idea was to test a typical scenario of intentional roughing.

LOAD TEST SET-UP AND PROTOCOL

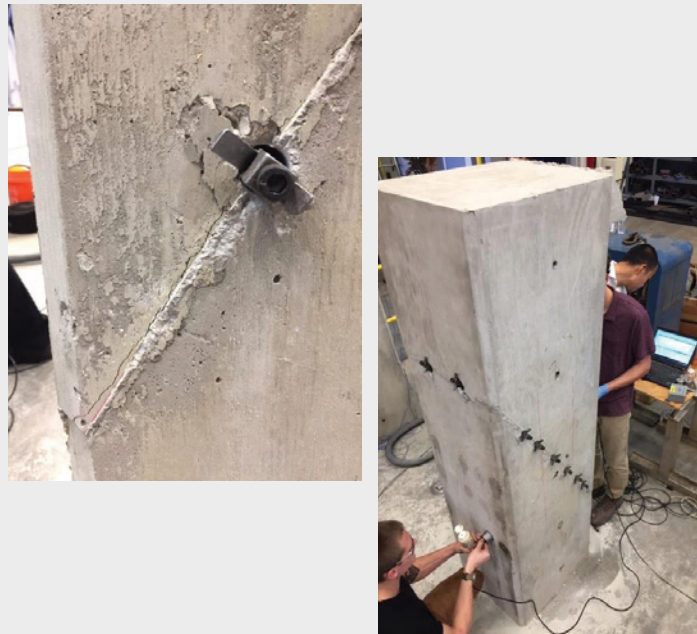
To simulate a cracked condition of the construction joint between member 11 and the bridge deck, two of the non-roughened and two of the roughened specimens were intentionally cracked at the construction joint using stone-splitting wedge sets in drilled holes along the joint (**FIGURE 6-25**). The third roughened specimen was also pre-cracked after the testing machine reached maximum capacity without failure. Note that pre-cracked and unbonded specimens were also typically used in shear friction research that the AASHTO design code was based on.

The loading protocol for testing the specimens was developed to simulate the axial force in truss member 11 from the time the shoring was removed in the casting area, to restressing the member 11 PT bars when the span was on the permanent piers. The forces used for each loading condition were based on a finite element structural analysis by WJE of as-built conditions to determine the member 11 axial forces. The resulting test load sequence is shown below in **TABLE 6-3**:

Table 6-3: Test load sequence simulated the actual forces in truss member 11 from the time the shoring was removed in the casting area to restressing the member 11 PT bars.

FIGURE 6-25

Five of the six test specimens were pre-cracked with stone splitting wedges along the construction joint prior to testing to simulate actual conditions of the member 11 connection with the bridge deck. (Source: WJE)



TEST STAGE	FIELD CONDITION	LOADING	MEMBER 11 FORCE (KIPS)	
			START	FINISH
1	Shoring removal in casting yard	Self-weight and PT	0	1680
2	<i>Lifting by transporter</i>	<i>Self-weight and PT</i>	1680	0
3	Placement on permanent piers	Self-weight and PT	0	1680
4	<i>Destress member 11 PT bars</i>	<i>Self-weight</i>	1680	1227
5	Restress member 11 PT bars	Self-weight, PT & construction Live load	1230	1743
6	N/A		1743	3000 or failure

Notes: 1) 1 kip = 1,000 lbs.

2) *Italic type indicates unloading stage*

Testing of specimens was performed at the structural laboratory at the University of Illinois Urbana-Champaign using a testing machine with a 3000 kip (3 million pound) capacity (**FIGURE 6-26**). Instrumentation to measure displacements was mounted across the construction joints of each specimen (**FIGURE 6-27**).

TEST RESULTS

Most specimens failed suddenly at peak load. **FIGURE 6-28** shows specimens at the moment of failure and **FIGURE 6-29** shows a typical specimen after failure. **TABLE 6-4** on page 6-39 shows the peak loads achieved for each of the six specimens. Note that the capacity of the member 11 and 12 connection to the deck was provided by a combination of the construction joint under member 11 and under member 12. These tests are for the member 11 connection portion only.

FIGURE 6-26

Testing machine at the University of Illinois Urbana-Champaign structural laboratory with 3 million pound capacity used to test the specimens. (Source: WJE)



FIGURE 6-27

Test specimen setup and displacement instrumentation to measure cracking. (Source: WJE)

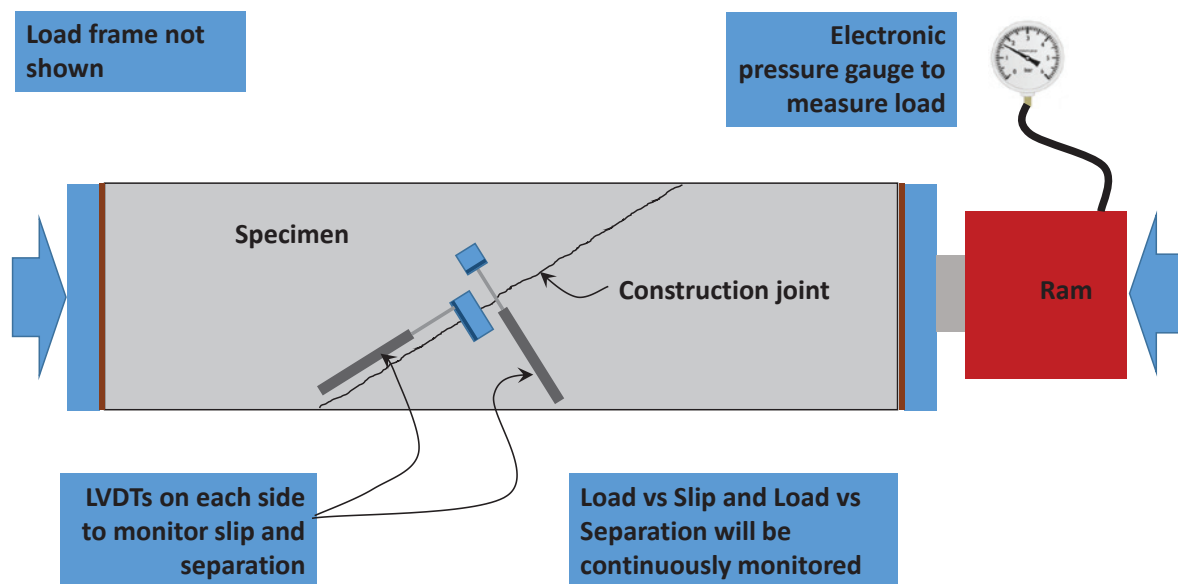


FIGURE 6-28
The moment of failure
for two specimens
captured from video of
the tests. (Source: WJE)

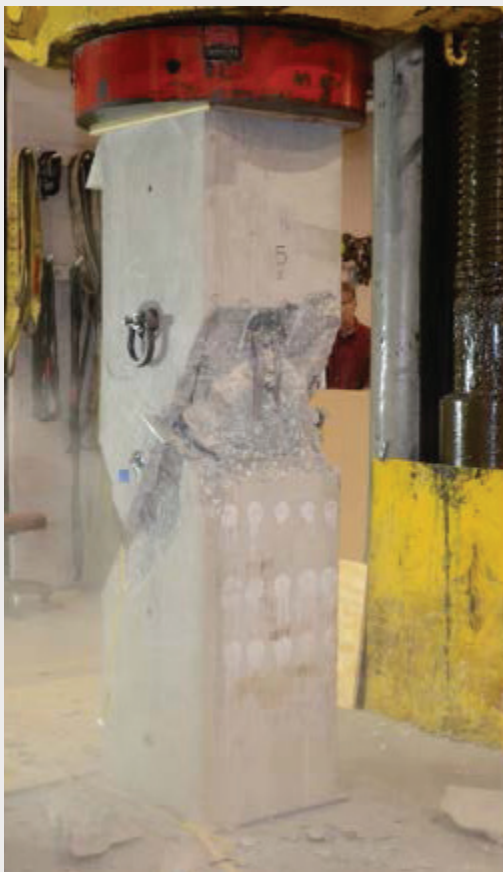


FIGURE 6-29
Specimen after failure along the construction joint.
Detail shows close-up of sliding along the joint
surface. This specimen had a roughened pre-cracked
construction joint surface. (Source: WJE)



TABLE 6-4: Results from load tests showing that the capacity of specimens with non-roughened construction joint surfaces is substantially less than the capacity of specimens with roughened surfaces.

SPECIMEN #	CONSTRUCTION JOINT CONDITION	PEAK LOAD (KIPS)	NOTES
1	Non-roughened Cracked	1296	
2	Non-roughened Cracked	1614	
3	Non-roughened Uncracked	2775	
4	Roughened Cracked	2516	
5	Roughened Cracked	2551	
6	Roughened Uncracked	3000	Did not fail. Specimen was pre-cracked and retested (see below).
6	Roughened Cracked	2714	
Average	Non-roughened Cracked	1455	Peak axial load in truss member 11 at end of restressing the PT bars was approximately 1743 kips.
Average	Roughened Cracked	2594	

FIGURE 6-30 shows the construction joint surface after failure from a roughened pre-cracked specimen. **FIGURE 6-31** shows the construction joint surface after failure from a non-roughened specimen, which appears similar to the observed post-failure construction joint surfaces of the member 11/12 node.

KEY POINT

If the concrete construction joint had been roughened, as the design called out and required, and is the FDOT standard construction specifications, the accident would not have happened.

CONCLUSIONS

Roughening the hardened concrete at the construction joint in accordance with FDOT Standard Construction Specification 400-9.3 increased shear capacity of the joint by an average of 78%. The average capacity of the modeled roughened joint between member 11 and the deck alone (conservatively excluding the capacity



FIGURE 6-30
Construction joint interface surface after failure for a roughened specimen. Circled areas show corresponding fractured aggregate on each side of the joint interface. (Source: WJE)

FIGURE 6-31
Construction joint interface surface after failure for an as-placed (non-roughened) specimen on the top, compared to the actual interface under member 12 on the bottom. (Source: WJE and NTSB Material Laboratory Study Report 19-043)



of the member 12 connection to the deck) was almost 50% greater than the calculated force applied at the time of the accident. This capacity was obtained following construction joint preparation methods in accordance with FDOT specifications, resulting in a surface roughness amplitude of approximately 0.16 inches, which is less than the 0.25 inch amplitude referenced in the AASHTO LRFD design code for intentionally roughened surfaces. This means that if the joint had been roughened as required by the FDOT standard construction specifications applicable to the project, the accident would not have happened.

In the next section, Section 7, the factual information is analyzed to develop conclusions.

7. ANALYSIS

7. ANALYSIS

7.1. COLLAPSE SEQUENCE

Forensic engineer WJE analyzed available photographs and video from when the main span truss was in the precasting area, through the time of the accident and post-accident (SEE **WJE'S FULL 132 PAGE REPORT IN EXHIBIT A**). Frames extracted from a dashboard video in a vehicle headed east on SW 8th Street are shown in **FIGURE 7-1**. From the photos and videos, they concluded that the collapse sequence developed at the north end of the main span truss where truss members 11 and 12 connect to the bridge deck and north diaphragm (SEE **FIGURES 7-2 AND 7-3**).

Prior to the bridge move, cracking in the chamfer between member 11 and the deck was documented by BPA on February 28, 2018 (also referred to as "wedge cracks"). A photo taken March 8 shows a crack in the top side of the deck adjacent to member 12. It is now considered that these cracks were the result of debonding of the construction joint between the deck and member 11, and northward sliding of member 11 (SEE **FIGURES 7-4 AND 7-5**).

Photographs taken immediately after the move on March 10 at 12:30 p.m. show that the cracks had not noticeably changed (**FIGURE 7-6**). However, photos taken after 3:00 that afternoon before the member 11 post-tensioning (PT) bars were destressed show a widening of the previous cracks in the member 11/12

FIGURE 7-1

Sequential video frames of the accident taken by a dashboard camera showing collapse initiating on the north end (left side) of the span.



Note: Redaction in photograph "Figure 7-1" as per NTSB Operations Bulletin CIO-GEN-016.

FIGURE 7-2

North end of main span after collapse (looking west). (Source: NTSB)

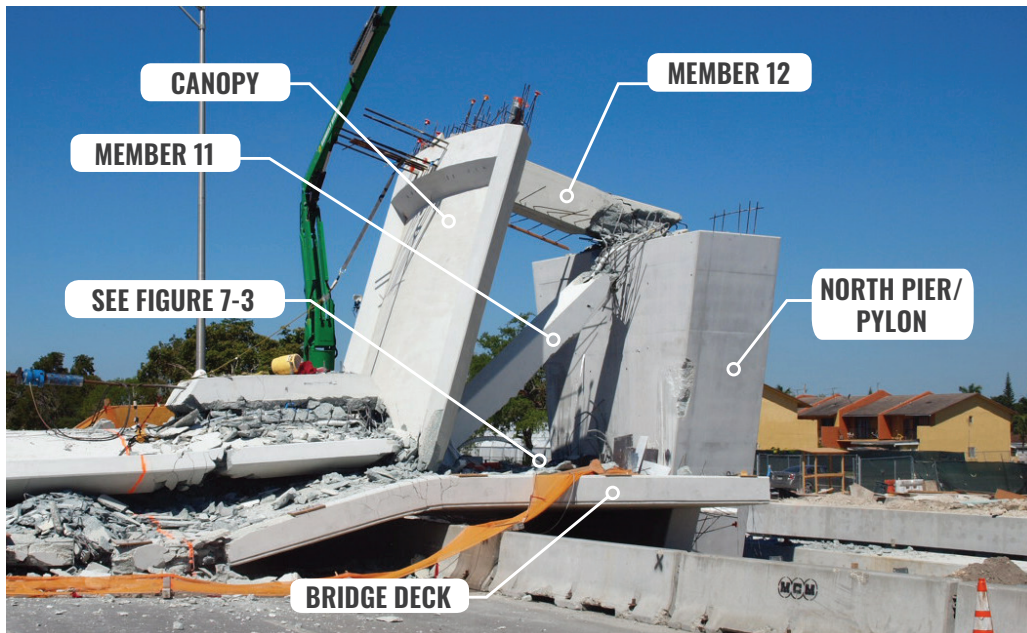


FIGURE 7-3

North end of main span bridge deck after collapse resting on the ground adjacent to the north pier / pylon (looking north). (Source: NTSB)

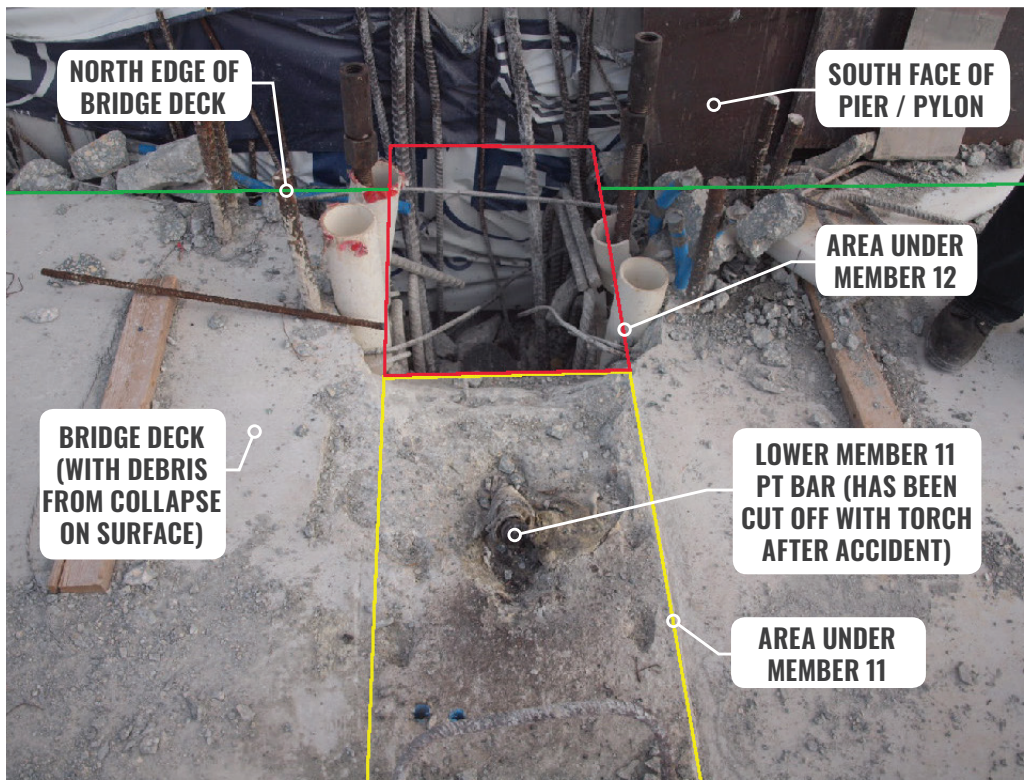


FIGURE 7-4

East side of member 11 at the chamfer with the bridge deck after falsework removal in the casting area as reported by BPA on February 28, 2018. (Source: BPA)



FIGURE 7-5

Crack in deck on the west side of member 12 before the span move on March 8, 2019. (Source: Barnhart)

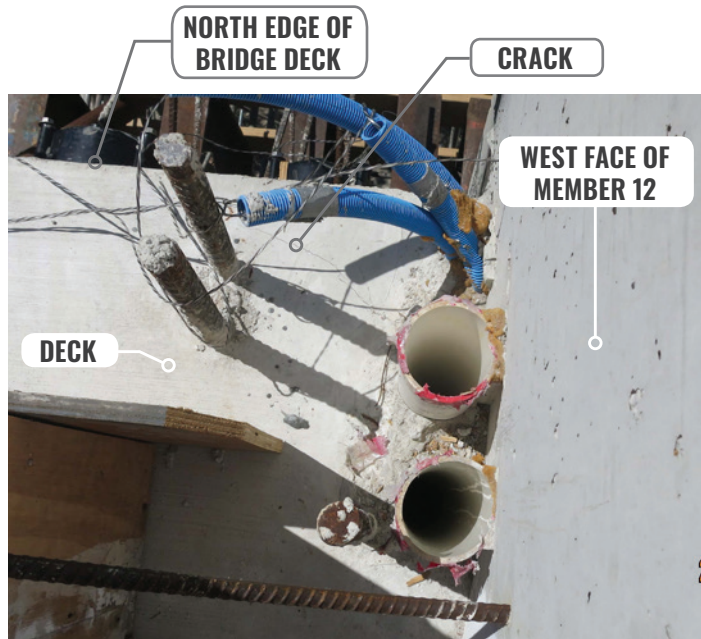


FIGURE 7-6

Cracks in member 11 chamfer with deck on March 10, 2018 at approximately 12:30 p.m. (Source: FIGG)



East face of member 11 chamfer.



West face of member 11 chamfer.

nodal area, and spalling developing at the north outside edge of the deck. This now suggests that member 11 slid northwards while the chamfer (“wedge”) stayed attached to the deck (**SEE FIGURE 7-7**).

On March 12, photographs indicate that the cracking had slightly widened. In addition, cracking and faulting of the north face of the north diaphragm was apparent, transverse cracks on the north face of member 12 appeared, and an additional longitudinal crack developed near the base of member 11. These changes indicate that member 11 experienced additional sliding (**SEE FIGURE 7-8**).

Photos from March 14, the day before the collapse, show continued widening and progression of the cracks. At the base of member 11, the cracks divided the concrete member into smaller individual pieces such that the element no longer acted as a composite member. The individual pieces were subject to bending stresses due to member 11 sliding northward (**SEE FIGURES 7-9**).

Damage after the collapse at the north end of the bridge at the member 11/12 node is illustrated in **FIGURES 7-10 AND 7-11**. WJE concluded the following:

- Cracking initiated in the member 11/12 region after the shoring was removed due to loss of bond and sliding at the construction joint below member 11 (because it was not roughened, See Section 7.2 and 7.3).
- Cracking substantially worsened after the bridge was placed on the

FIGURE 7-7

Cracking observed at north end of bridge at 3:16 p.m. on March 10, 2018 after bridge move and before member 11 PT bar destressing. (Source: Bridge Factors Photos 62 - 66)



FIGURE 7-7A

East side of member 11 at base near deck.



FIGURE 7-7B

West side of member 11 at base near deck.



FIGURE 7-7C

North edge of diaphragm west of member 12.



FIGURE 7-7D

North edge of diaphragm east of member 12.

FIGURE 7-8

Cracking observed on March 12 had slightly widened from that observed on March 10, 2018. (Source: MCM)



FIGURE 7-9

Member 11 crack progression on March 14, 2018. Per WJE in Appendix A, at the time of the accident the next day, the cracks divided the base of member 11 into smaller individual pieces such that the element no longer acted as a composite member. (Source: Bridge Factors Photograph #s 90 and 83)



East face of member 11

West face of member 11

FIGURE 7-10
 Damage to member 11/12 connection to bridge deck from the collapse looking west. (Source: WJE modified)

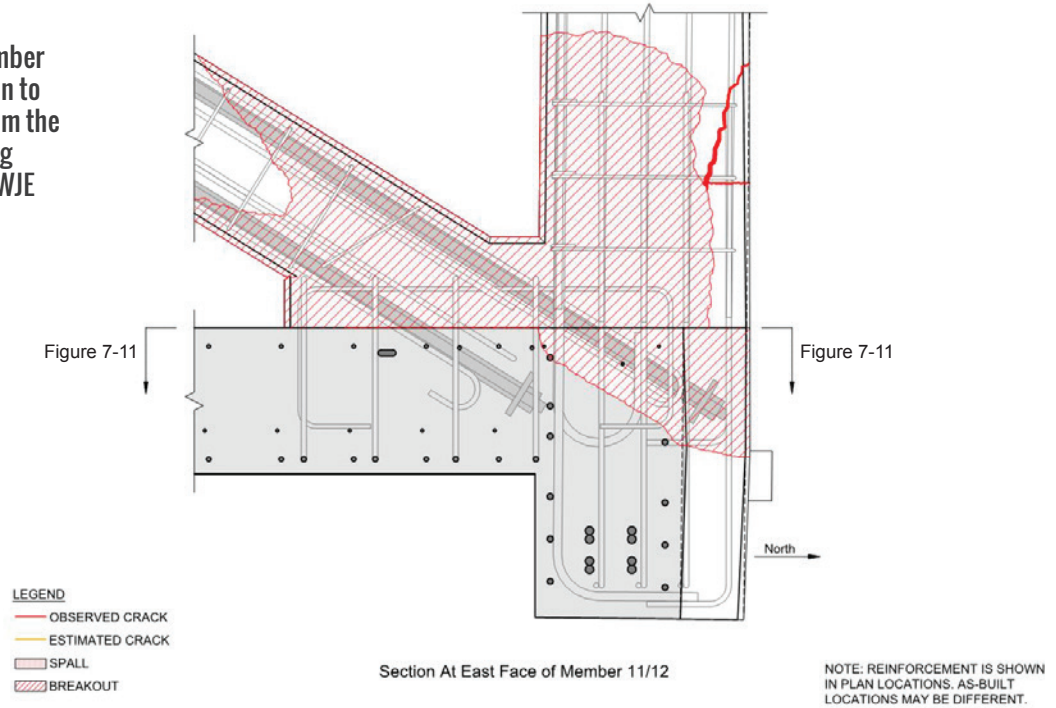
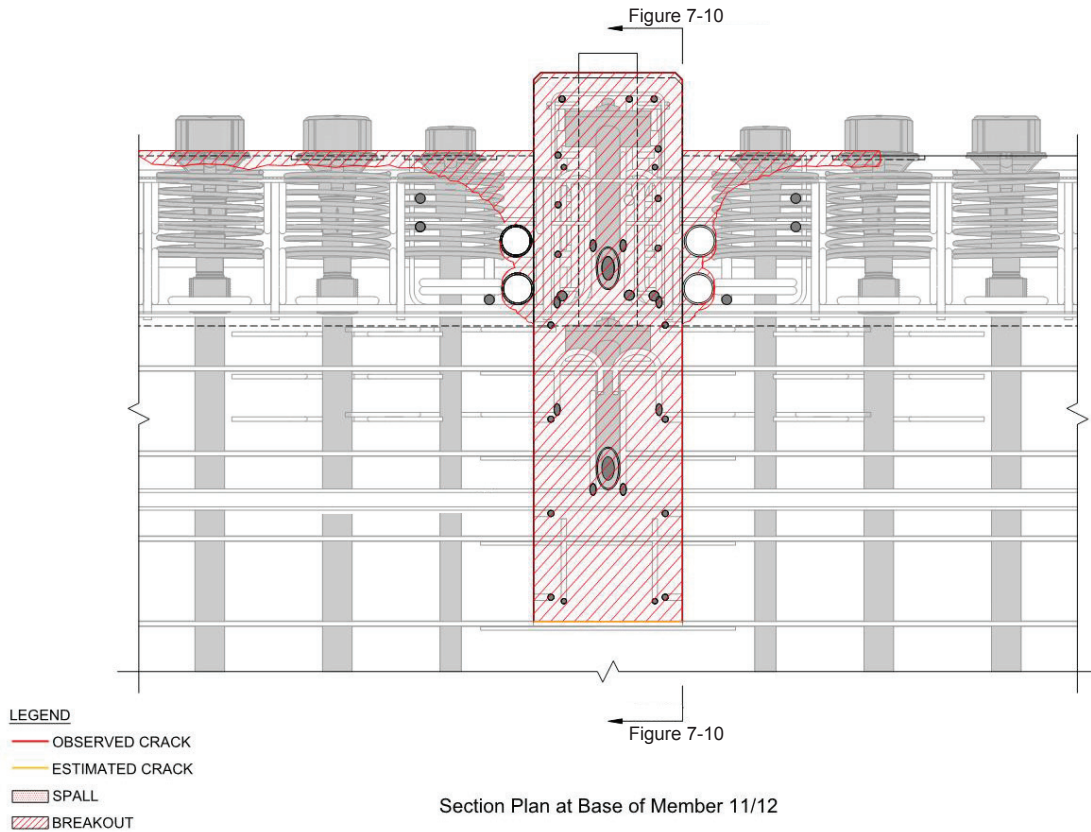


FIGURE 7-11
 Damage to member 11/12 connection to bridge deck from the collapse looking down (plan view). (Source: WJE modified)



permanent piers before member 11 was de-tensioned. Northward sliding of member 11 led to breakout failure of the north end diaphragm below member 12 while existing cracks continued to widen. New cracks developed at the base of member 11 as it separated into smaller individual sections.

- Cracking continued to worsen until the bridge collapsed. The collapse was triggered by sudden crushing of member 11 near its base. After the base of member 11 was lost, a hinge in the truss developed near the top of member 11. Additional damage developed in the member 11/12 nodal region as the collapse progressed, including severe damage to the base of member 12 and the north end diaphragm.

KEY POINTS

- Lack of roughening, aggravated by excessive twisting during the move caused the collapse when the post-tensioning stressing was performed.
- FIGG was never aware, before the collapse, of any of these issues.

In summary, a loss of bond and sliding failure at the construction joint below member 11 led to a breakout failure of the north end diaphragm and ultimately to the collapse, triggered by sudden crushing of member 11 near its base.

7.2. EVALUATION OF JOINT BELOW MEMBERS 11/12

Section 400-9.3 of the FDOT Standard Construction Specifications requires roughening of the hardened concrete at construction joints by mechanical means. Roughening the hardened concrete is preferable to creating a rough surface texture during finishing because roughening the hardened concrete also removes the surface laitance, which improves bond. The following facts were presented in Section 6 of this report:

The FHWA Turner-Fairbanks Research Center (TFHRC) Factual Report “Concrete Interface Under Members 11 and 12” dated October 19, 2018 (Exhibit B) found that the construction joint between the deck and truss members 11/12 was smooth and covered in concrete paste. It concluded “that the failure interface coincides with the original cold joint and that the cold joint was not intentionally roughened” (Section 6.8.3).

NTSB Materials Laboratory Study Report No. 19-043 on laser scans of the actual member 11/12 construction joint surfaces found that “The average Sa [“arithmetic mean roughness value”] for the flat areas evaluated on both the Member 11 pieces as well as the Member 12 surface was approximately 1 mm (0.04 in) as measured in the partially damage post-collapse condition” (Section 6.8.4 and Exhibit C).

A separate analysis of the NTSB scan data for Sample 1 of the member 11 construction joint estimated a roughness amplitude of 0.06 inches, similar to that determined by NTSB. This was similar to the 0.07 inch roughness amplitude

measured by laser scan for a laboratory specimen prepared by placing concrete with a vibrator similar to the FIU Pedestrian Bridge deck and leaving the surface as-placed, also referred to as “non-roughened” (Section 6.9).

NTSB interviews with the Contractor’s (MCM) Quality Control Technician and concrete placement subcontractor (Structural Group of South Florida) indicate that the construction joint beneath members 11/12 was left as-placed and not roughened after it had hardened (Section 6.5.1).

It is clear from these investigated facts that the construction joint surface below members 11/12 was left in an as-placed, relatively smooth condition and not intentionally roughened.

7.3. STRUCTURAL ANALYSIS

Additional structural analyses were performed to compare the loads applied to the member 11/12 nodal joint with the estimated capacities for both roughened and non-roughened construction joint surfaces.

7.3.1. Factor of Safety

Factor of Safety is the ratio of calculated capacity divided by the calculated load:

$$\text{Factor of Safety} = \text{Capacity} / \text{Load}$$

A Factor of Safety greater than 1.0 indicates that the element strength is greater than the applied load. A Factor of Safety less than 1.0 indicates that the element strength is less than the applied load and a failure would be expected.

For the purposes of determining the Factor of Safety, the member capacities and loads are calculated using the AASHTO LRFD design code provisions without applying any factors. The loads reported in this section are for the case with member 11 post-tensioning (PT) bars stressed with the main span truss on the permanent piers, similar to when the accident took place.

The Engineer of Record, FIGG, performed an independent analysis of the member 11/12 loads and capacities post-accident. The information was presented to NTSB at a meeting on March 13, 2019. FIGG’s analysis considered shear capacity of the construction joint between the deck and members 11/12. For the non-roughened case, the area under member 11 was considered non-roughened, while the area under member 12 was considered roughened (since evidence indicates that the deck concrete under member 12 did not remain intact during the accident).

Forensic engineers WJE also determined the un-factored loads and capacities for the member 11/12 connection with the deck for both roughened and non-

roughened construction joint surfaces. WJE considered shear strength of the connection under member 11, and breakout strength of the member 12 connection to calculate capacity.

The AASHTO LRFD design code equations for member capacity are necessarily a lower bound estimate of strength to provide conservatism in design. Therefore, WJE also utilized the results from the full-sized specimen construction joint load tests described in Section 6.9 of this report to estimate the actual strength for the member 11/12 connection to the bridge deck.

Details of the FIGG Factor of Safety calculations can be found in the presentation “Factual Information From Released for Construction (RFC) Plans” and supporting calculations presented to NTSB on March 13, 2019 and included in the NTSB docket material. Details on WJE’s load and resistance calculations are in Exhibit A to this report. The resulting loads, capacities and Factors of Safety are shown in **TABLE 7-1** below.

TABLE 7-1: Horizontal shear capacities versus loads at member 11/12 connection to bridge deck calculated per AASHTO and from specimen test program.

METHOD OF DETERMINING CAPACITY	CONSTRUCTION JOINT SURFACE	MEMBER 11/12 CONNECTION SHEAR CAPACITY (KIPS) ①	SHEAR LOAD ON MEMBER 11/12 CONNECTION (KIPS) ①	FACTOR OF SAFETY ②
AASHTO	Roughened	2084	1661	1.25
(FIGG)	Non-roughened	1374	1661	0.83
AASHTO	Roughened	2389	1677	1.42
(WJE)	Non-roughened	1285	1677	0.77
Test Results	Roughened ③	2485 ④	1677	1.48
(WJE)	Non-roughened	1677	1677	1.00

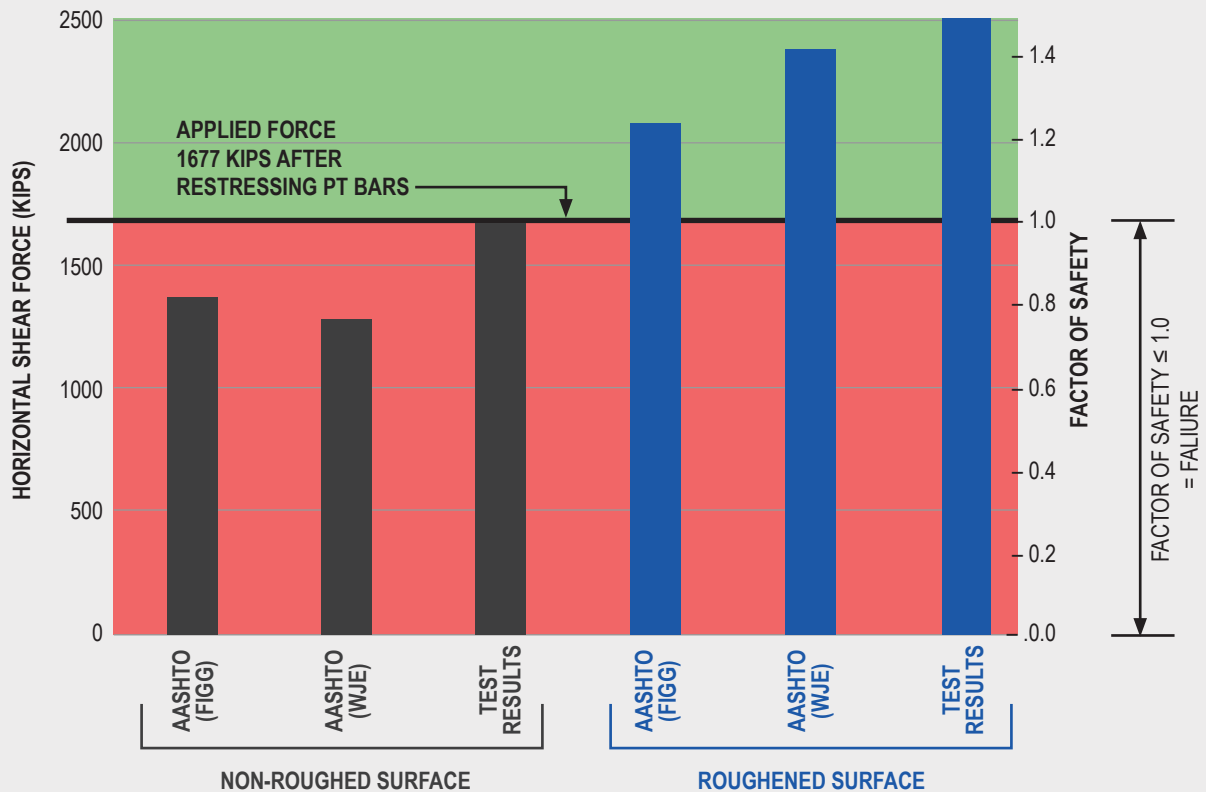
Notes: ① 1 kip = 1,000 lbs.

② Factor of safety less than 1.0 means failure expected

③ Roughened per FDOT Construction Specifications, measured roughness amplitude of 0.16 inches

④ Value shown has been reduced by 6% for Florida aggregate (does not affect non-roughened)

FIGURE 7-12
Member 11/12 connection capacity (kips) for non-rough versus roughened joint



The graph in **FIGURE 7-12** provides a comparison of these capacities to the applied force along with the respective Factors of Safety. As noted in **TABLE 7-1** and **FIGURE 7-12**, all three methods of calculating the Factor of Safety for the roughened joint result in a factor greater than 1.0, with the minimum being 1.25. This indicates that the capacity of the member 11/12 nodal connection if roughened would be 25% higher than the applied load.

Conversely, all the calculated Factors of Safety for the non-roughened construction joint at member 11/12 are less than or equal to 1.0, ranging from 0.77 to 1.00. This indicates that the capacity of the connection if the concrete was left as-placed and not roughened would be less than or equal to the applied load, and a failure of the connection would be anticipated.

KEY POINT

The lack of roughening, contrary to the FIGG design and FDOT Standard Construction Specification requirements, set the stage for the construction accident.

7.3.2. Compliance with Design Requirements

WJE performed an independent structural analysis of the superstructure to evaluate adequacy of the member 11/12 deck connection design with respect

to the AASHTO LRFD bridge design code applicable to this Project. A computer model was created to analyze the main span member forces during construction Phase 3 (when the accident occurred). Load factors and resistance factors were applied per AASHTO. Details of the WJE analyses are found in Section 5 of Exhibit A.

MEMBER 11/12 DECK CONNECTION DURING CONSTRUCTION

WJE evaluated the adequacy of the truss member 11/12 connection to the deck main span design when the main span was supported on the permanent piers during Phase 3 of construction, which includes the member 11 PT bars being stressed.

Section 1.3.2.1 of the AASHTO Code requires increasing the factored loads by 5% for non-ductile members and 5% for non-redundant members. However, the code is silent on whether or not these factors would apply during temporary conditions during construction. Note that even highly-redundant common multi-girder bridges are often non-redundant during certain construction phases. WJE evaluated the member 11/12 connection both with and without applying these load modifiers.

The resulting factored horizontal shear force (demand) at the member 11/12 connection to the deck during Phase 3 of construction with the PT bars stressed is

1979 kips without the load modifiers

2182 kips with the load modifiers

The factored horizontal shear resistance (capacity) of the member 11/12 connection to the deck during Phase 3 of construction with the PT bars stressed is:

2150 kips

The capacity-demand ratio (CDR) is the factored capacity of the member divided by the factored demand. This ratio should be equal to or greater than 1.0 to comply with the AASHTO design code. The CDRs for the member 11/12 connection are:

1.09 without the load modifiers

0.99 with the load modifiers

Since the CDR without the modifiers is greater than 1.0 and the CDR with both modifiers is within a percent of 1.0, WJE independent analysis concludes that the member 11/12 connection to the deck met the AASHTO LRFD design code requirements for the construction load case when the main span was supported

on the permanent piers with the PT bars stressed in member 11 (the phase of construction when the accident occurred).

7.4. BRIDGE MOVE

As discussed in Sections 5.1 and 6.5.2 of this report, the precast main span truss was moved from the precast area on the south side of SW 8th Street and set on the permanent piers on March 10, 2018 using self-propelled modular transporters (SPMTs). Forensic engineer WJE analyzed the bridge move, the exceedance of the maximum twist limit that occurred during the move, and the cracking in the north end of the main span before and after the move. A summary of their findings is provided below. The full report is provided in Exhibit A.

Cracking at the north end in member 11 and at the top of the end diaphragm was noted prior to the move. After the move, the cracks significantly widened as shown in **FIGURE 7-7**. There are four possible contributors to widening of the cracks:

A 0.5-degree twist limit was established prior to the move, and this limit was exceeded on several occasions during the move. The degree of the exceedance is somewhat uncertain due to “spikes” in the rotation and twist readings. As shown through a detailed finite element analysis (**SEE FIGURE 7-13**), the rotation associated with the twist exceedances caused high transverse bending stress near the base of

FIGURE 7-13
WJE analysis model of main span twist during span move on March 10 (deformations shown with increased scale by a factor of 20 for illustration). (Source: WJE)

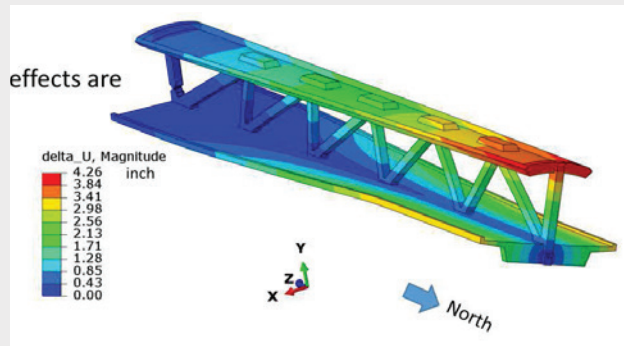
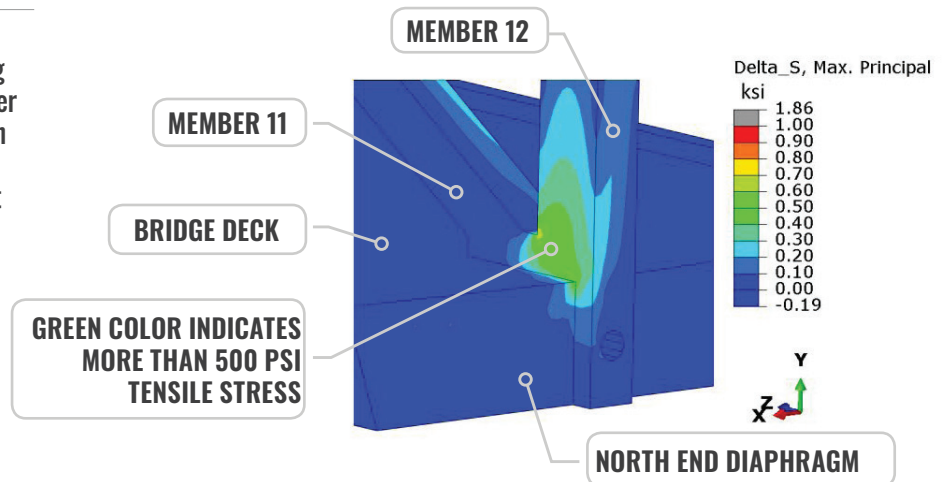


FIGURE 7-14
WJE analysis results showing maximum stresses in member 11/12 node from twist of main span during bridge move on March 10 (looking southwest at the north end of the main span). (Source: WJE)



member 12, the northernmost vertical. Although the calculated stress is somewhat less than that needed to initiate cracking, the stress from the tilt would tend to exacerbate cracking in the region **(FIGURE 7-14)**.

Prior to the move, the north end diaphragm was supported on shoring at close intervals. After the move, the diaphragm was supported on temporary shims that were nearly continuous except for a gap at the centerline. The truss reaction at the center of the north end diaphragm spanned the gap, increasing shear and bending stresses in the north end diaphragm relative to the diaphragm stresses in the casting yard.

The north end diaphragm and member 11 exhibited distress prior to the move related to the northward sliding of Diagonal 11. Before the bridge was lifted by the transporter, the force in member 11 would have been approximately equal to the force at the time of the accident. The horizontal force at the member 11/12 connection to the deck was temporarily relieved when the transporter lifted the main span from the end supports in the casting yard and was then reapplied when the span was set in its final location. Thus, the move applied an additional load cycle to a connection that was near its strength limit. Damage can increase significantly due to even one additional load cycle when the load is near the strength limit.

After the move, the north diagonal connection was near its strength limit. Cracks can widen over time due to sustained load near the strength limit.

Although there is not enough information to assess the degree to which each of these factors contributed to the increase in distress after the bridge move, it is likely that all of these factors contributed to the damage at the north end and ultimately the collapse.

WJE's analysis concluded that cracks in the region of the member 11/12 connection to the deck increased dramatically in the afternoon after the move from the casting area to the final location. The twist associated with exceeding the established twist limits during the span move caused high stresses in the connection region. Along with other factors, this stress contributed to damage in the region and ultimately the collapse.

KEY POINT

- **The contractor handling the move clearly exceeded the twist limits by a large amount which contributed to damage of the member 11/12 connection.**

7.5. RESTRESSING MEMBER #11

The construction accident occurred near the completion of the restressing operation for the PT bars in member 11. According to WJE's analysis referred to in Section 7.3.1 above, the horizontal shear load at the member 11/12 connection to the bridge deck was approximately:

- 1148 kips prior to restressing the PT bars
- 1677 kips after completion of the PT bar restressing

As presented in **TABLE 7-1** above, the capacity of the joint would have been at least 2084 kips had the surface been roughened, but no more than 1677 kips if the deck surface had been left in an as-cast (non-roughened) condition when the truss members were cast above.

This is consistent with the evidence presented in Section 7.2 above that the construction joint between truss members 11/12 and the bridge deck was not roughened as required by the project specifications. The joint was already compromised by the factors discussed in Section 7.4 above. The failure occurred when the shear force at the member 11/12 nodal area increased beyond the joint capacity during restressing the member 11 PT bars.

Restressing the member 11 PT bars included requirements to closely monitor the cracking and to immediately stop restressing and notify FIGG if the cracks worsened. Structural Technologies (VSL) shop drawings for the post-tensioning also contained safety guidelines requiring that stressing cease if any existing crack widening or new cracking is observed. An analysis from a FIU construction web cam shows that the cracks were not closely monitored during restressing of member 11 and proper crack monitoring tools do not appear to have been in use. Had proper crack monitoring been performed, it is possible that a worsening condition could have been detected and the restressing operation halted.

8. CONCLUSIONS

8. CONCLUSIONS

8.1. PROBABLE CAUSE

The FIU UniversityCity Prosperity Pedestrian Bridge construction accident occurred because the construction joint between main span truss members 11/12 and the bridge deck was not roughened as required by the Florida Department of Transportation (FDOT) Standard Specifications for Road and Bridge Construction.

- Analysis of accident video, photographs and as-built bridge elements indicates that a debonding and sliding failure at the construction joint below member 11 led to a breakout failure of the north end diaphragm and ultimately collapse, triggered by sudden crushing of member 11 near its base. (Section 7.1 and WJE Report Sections 2 and 9).
- The contract for the FIU Pedestrian Bridge required that the FDOT Standard Specifications be used for construction. The requirement to adhere to these specifications was also the first note on the General Notes sheet at the front of the Released For Construction plans (Sections 6.2.2 and 6.2.3).
- FDOT Standard Specification Section 400-9.3, Construction Joints / Preparation of Surfaces, states: "Roughen the surface of the hardened concrete in a manner that will not leave loosened particles, aggregates or damaged concrete at the surface." (Section 6.2.3).
- The requirement to roughen construction joints in accordance with FDOT construction specifications was reiterated by the designer (FIGG) in an e-mail exchange between the contractor (MCM), the independent construction quality inspector (BPA) and FIGG in June 2017 (Section 6.5.1) prior to precasting the bridge span.
- Examination and testing of the as-built bridge, as well as worker interviews, indicate that the concrete construction joint under members 11 and 12 was left in an as-placed condition and not roughened per the FDOT specification requirements (Section 7.2).
- ⊗ The FHWA Turner-Fairbank (TFHRC) Factual Report "Concrete Interface Under Members 11 and 12" concluded "that the failure interface coincides with the original cold joint and that the cold joint was not intentionally roughened" (Section 6.8.3).
- ⊗ NTSB Materials Laboratory Study Report No. 19-043 on laser scans of the actual member 11/12 construction joint surfaces found that the mean roughness value was approximately 0.04 inches (Section 6.8.4). This correlates with the roughness of a laboratory test specimen prepared by placing concrete with a vibrator similar to the actual construction techniques used and leaving

the surface as-placed and non-roughened (Section 6.9).

- ⊙ NTSB interviews with the Contractor's Quality Control Technician and concrete placement subcontractor indicate that the construction joint was left as-place and not roughened (Section 6.5.1).
- Analysis of the member 11/12 connection to the bridge deck, based on both AASHTO LRFD Design code capacity estimates and independent laboratory tests show that the capacity of the non-roughened connection is less than the load applied to the connection at the time of the accident, resulting in a failure (Section 7.3 and WJE Report Sections 5.3 and 9).
- Conversely, analysis of the member 11/12 connection to the bridge deck, based on both AASHTO LRFD Design code capacity estimates and independent laboratory tests show that the capacity of the construction joint with the surface prepared in accordance with FDOT Standard Specification 400-9.3 is at least 125% of the maximum load on the connection at the time of the accident, and no failure would occur (Section 7.3).
- Adequate capacity of the member 11 connection to the bridge deck would have been achieved if the joint surface had complied with FDOT Specification 400-9.3 for roughening the hardened concrete surface without necessarily roughening the surface to the 0.25 inch (1/4 inch) amplitude referenced in the AASHTO LRFD

Bridge Design Specifications (Section 6.9 and WJE Report Sections 4 and 9).

- ⊙ Laboratory test results of full-sized specimens replicating the connection of member 11 to the bridge deck indicate that roughening the construction joint surface in accordance with FDOT Specification 400-9.3 increases the shear capacity of the joint by an average of 78% over the as-placed, non-roughened joint surface.
- ⊙ The average roughness amplitude of the roughened test specimen joint surface as measured by laser scanner was 0.16 inches (5/32 inch) compared to the AASHTO LRFD value of 0.25 inches (1/4 inch), which is 64% of the AASHTO value. The measured amplitude of the NTSB member 11 Sample 1 from the as-built structure was approximately 0.06 inches (1/16 inch), which is just 37% of the surface roughened per FDOT specifications and 24% of the AASHTO value.
- ⊙ Roughening of the hardened concrete surface regardless of specific amplitude is important for achieving joint capacity since it removes the surface laitance, which improves bond (WJE report, Exhibit A).
- ⊙ The FDOT Standard Specifications, as proven by the project testing, achieves the requirements of the AASHTO Code.

8.2. CONTRIBUTING CAUSES

The following were contributory factors leading to the accident:

➤ Damage from bridge move

Sensors indicated that twist in the main span was as much as 168% of the maximum allowable twist during the move from the casting area to the final location (Section 6.5.2). Cracks in the member 11/12 connection to the bridge deck increased dramatically in the afternoon after the move (Section 5.2). WJE's analysis shows that the twist associated with exceeding the established limits during the move caused high stresses in the connection region. Along with other factors, this stress contributed to damage in the region and ultimately the collapse (Section 7.4).

➤ Miscommunication between Contractor and Engineer of Record concerning cracking

The design Engineer of Record, FIGG, did not have a person on-site during construction other than occasional site visits and thus relied on communications with the construction contractor, MCM, for information on construction processes and results. No information was provided to FIGG concerning the increased cracking noticed the afternoon of the move on Saturday March 10 until late Monday, March 12. The information sent then pertained almost exclusively to the north diaphragm region. Despite on-going photography and evaluation

of the cracking by BPA and MCM at the site, limited information was conveyed to FIGG. No crack reports or reports of crack growth were provided to FIGG for its evaluation, and some of the information that was provided was inaccurate. FIGG's analyses performed prior to the Thursday meeting consequently focused on the north diaphragm and assumed that the bridge had been constructed in accordance with the RFC plans and specifications (Section 6.5).

➤ Failure to close SW 8th Street while investigating (Section 6.6)

FDOT, FIU, MCM and BPA had the authority, acting alone or collectively, to close or restrict traffic on SW 8th Street. Only MCM and BPA had personnel assigned to the project site full-time. At approximately 6:00 p.m. on Saturday March 10, SW 8th Street was re-opened to traffic, despite significantly wider cracking being observed that afternoon. At 7:08 p.m., the Structural Technologies technician who had been working on the PT bar destressing texted another person within Structural stating "It cracked like hell". At that time, the permit to close SW 8th Street was still valid for approximately another 34 hours and the equipment used to move the span was still at the project site.

From Monday, March 12 through Wednesday, March 14, MCM and BPA had a full-time presence at the project site and were monitoring the cracking. Neither MCM or BPA acted or recommended to close SW 8th

Street to traffic. The March 15, 9:00 a.m. meeting at the project site to discuss the cracking was attended by representatives of FDOT, FIU, BPA, MCM and FIGG. No one at the meeting suggested that SW 8th Street should be closed until the situation was resolved.

➤ Failure to monitor cracks while restressing member 11

FIGG provided instructions to MCM for restressing the member 11 PT bars. These included closely monitoring the cracking and to immediately stop restressing and notify FIGG if the cracks worsened. Structural Technologies (VSL) shop drawings for the post-tensioning also contained safety guidelines requiring that stressing cease if any existing crack widening or new cracking is observed. An analysis from a FIU construction web cam shows that the cracks were not closely monitored during restressing of member 11 and proper crack monitoring tools do not appear to have been in use. Had proper crack monitoring been performed, it is possible that a worsening condition could have been detected and the restressing operation halted before any structural failure (Section 6.5.3).

➤ Failure to clear work zone while restressing member 11

Structural Technologies (VSL) shop drawings for the post-tensioning on the FIU Bridge project contain safety guidelines requiring appropriate work zones to be

established and that only essential personnel shall occupy the work zones during stressing operations. The video from the FIU construction web cam also shows that the two north lanes of SW 8th Street were closed during the PT bar restressing, but that all other lanes were open to traffic (Section 6.5.3). Had the work zone been defined to include the entire width of the roadway that was under the span that was being post-tensioned, the collapse would not have impacted vehicles on the roadway.

8.3. EXCLUDED CAUSES

The design of the FIU Pedestrian Bridge was neither causal nor contributory to the construction accident.

The design of the member 11/12 connection as shown in the Released For Construction plans complied with the applicable AASHTO LRFD Bridge Design Specifications, the Florida DOT Structure Design Guidelines and the contract design criteria for this project. If the construction joint between member 11/12 and the bridge deck had been roughened in accordance with FDOT Standard Construction Specifications as required by the construction documents, the connection would have functioned properly without failure (Section 7.3 and WJE Report Sections 5.2 and 9).

Adequate capacity of the member 11/12 connection to the deck would have been achieved if the joint surface had complied with FDOT Specification 400-9.3 for roughening the hardened

concrete surface without achieving the 1/4 inch amplitude referenced in the AASHTO LRFD Bridge Design Specifications. This is demonstrated by the laboratory test results of full-sized specimens where a 78% increase in shear capacity was achieved with joint surfaces with an average roughness of 0.16 inches (5/32 inch), which is 64% of the AASHTO LRFD value of 0.25 inches (1/4 inch) (Section 6.9).

Although the breakout failure surface in the north deck / diaphragm area was near the 4-inch vertical sleeves adjacent to truss member 12 and the 8-inch diameter drain pipe through the diaphragm, this did not contribute to the accident since the member 11/12 connection to the deck would have had sufficient strength to resist the applied loads had the construction joint surface been roughened, and thus the breakout failure in the north diaphragm would not have occurred.

The tests performed for this investigation shows that the Florida Department of Transportation Standard Construction Specification for concrete construction joints meets the AASHTO LRFD Code. The test results indicate that this FDOT specification is excellent.

9. SAFETY RECOMMENDATIONS

9. SAFETY RECOMMENDATIONS

9.1 ROLE OF ENGINEER OF RECORD (EOR) DURING CONSTRUCTION

Recommendation to Support Transportation Safety Improvements

Require bridge owners to create requirements for implementing major bridge construction with full time, on-site roles and responsibilities of the Engineer of Record. With the Engineer of Record's meaningful involvement as part of the Construction Engineering and Inspection, and Quality Assurance oversight the Owner receives the benefits of the most project design knowledge in successfully achieving all requirements.

The FIU Pedestrian Bridge is an example of a major bridge where a full time, on-site construction engineering and inspection (CEI) role for the Engineer of Record (EOR), working in partnership with the primary CEI consultant, contractor, subcontractors and others on-site, would have benefited the Project. This would have resulted in additional oversight to the Released For Construction plans and support of decisions in the field with -

- Real-time communication
- Real-time verification of information
- Quality Assurance sign-offs by EOR
- Participation in weekly construction discussions
- Plus more

Currently, the Florida Department of Transportation and a few other Departments of Transportation have policies that do not support the active oversight role of the EOR during construction. FIGG believes that this is never beneficial to the success of building a major bridge.

When a Construction Engineering & Inspection Team, Contractor, Subcontractors, and everyone building and inspecting the bridge are on-site, and the EOR is off site and not involved in the official inspection, there are more chances for problems and challenges to arise that do not get solved in the best way possible.

The EOR is the guardian of the design given in the Released For Construction plans and is always interested in seeing that the design is successfully built for the Owner.

The lessons learned here should create new thinking around this policy and introduce change to require the EOR's role on-site throughout construction with some inspection authority and functioning as part of a unified site team with all interests aligned for the Owner.

Some successful case studies are beneficial to the discussion of this recommendation, as given below.

Supporting Case Studies

There are a number of major bridge case studies that demonstrate the benefits of the Engineer of Record having a significant role in construction engineering inspection during construction.

Four (4) examples are given in this discussion for major bridges in the United States involving federal funding. These examples include:

1. **Design-Bid-Build Bridge Contracts** - where the Engineer of Record is accomplishing the design for the Owner and then represents the Owner with CEI services
2. **Design-Build Bridge Contracts**- where the Engineer of Record is accomplishing the design for the Contractor in a turnkey for the Owner, and supports both the Contractor and Owner in the field full-time

Two major bridges that FIGG designed working directly for the Federal Highway Administration (FHWA) involved contracts where the Engineer of Record was required to have Construction Engineering Inspection responsibilities during construction of the bridge, while teaming with FHWA on-site. These two examples with photographs are given on the following two pages.

The next example is a design-build bridge interstate involving accelerated bridge construction.

The fourth example is a design-bid-build bridge that the FHWA used as an example in their "Highways for Life" Program.

THESE TWO DESIGN-BID-BUILD BRIDGE EXAMPLES ARE:

1) Natchez Trace Parkway Arches, Tennessee

The EOR (FIGG) accomplished the design and oversaw the construction inspection and erection geometry of the precast arch and precast bridge deck.



NATCHEZ TRACE PARKWAY ARCHES, IN FRANKLIN, TENNESSEE

FIGG designed for FHWA and the National Park Service

Winner of 16 Awards, including Presidential Award for Design Excellence in 1995 from the National Endowment for the Arts

2) Blue Ridge Parkway, North Carolina

The EOR (FIGG) was required to support the Construction Engineering Inspection activities including inspection and checking the erection geometry of every precast segment.



BLUE RIDGE PARKWAY, GRANDFATHER MOUNTAIN, NORTH CAROLINA

FIGG designed for FHWA and the National Park Service

Winner of 13 Awards, including the Presidential Award for Design Excellence in 1984 from the National Endowment for the Arts

A DESIGN-BUILD BRIDGE EXAMPLE WITH ACCELERATED BRIDGE CONSTRUCTION (ABC) IS:

3) New I-35W Bridge across the Mississippi River, Minnesota

During the construction of this fast-paced interstate bridge replacement, the Minnesota Department of Transportation had the EOR (FIGG) responsible for final sign-off on construction quality assurance prior to a construction activity taking place. There were other construction engineering inspection companies on site as well with sign-off responsibilities and everyone worked as a team with the common interest of achieving the Minnesota DOT's requirements for the Project.



NEW I-35W BRIDGE, MINNEAPOLIS, MINNESOTA

FIGG designed for Minnesota Department of Transportation

Winner of 25 Awards, 10-lane interstate bridge designed and built in 11 months, 3 months early, opening in 2008

The reason this successful example is important is because the process was design-build and the Minnesota Department of Transportation wanted the EOR's on-site presence sign-off on the construction and documentation, for additional confidence that everything was being reviewed from the design side during construction as another check.

DESIGN-BID-BUILD BRIDGE – ANOTHER INTERESTING MAJOR BRIDGE EXAMPLE IS:

4) Victory Bridge, New Jersey

During the construction of the Victory Bridge in Perth Amboy, New Jersey, the New Jersey DOT hired the EOR (FIGG) for the design-bid-build contract to lead both the design and after the design asked the EOR to lead the Construction Engineering Inspection team providing the Resident Engineer, Project Engineer, inspectors and integrating the NJDOT field team participants.



VICTORY BRIDGE, PERTH AMBOY, NEW JERSEY

**FIGG designed for New Jersey Department of Transportation
Winner of 14 Awards, EOR accomplished design and led the CEI during construction for the New Jersey DOT**

This all precast segmental bridge was a first for the state of New Jersey and the contractor who won the bid to build the bridge. The FHWA made this bridge an example of excellence representing the “Highways for Life Program” on their website.

9.2 TRAINING FOR CONTRACTORS AND INSPECTORS OF CONCRETE CONSTRUCTION JOINTS

Recommendation to Support Transportation Safety Improvements

Encourage more training and certifications for both inspectors and construction quality managers on concrete construction joints.

The Florida Department of Transportation's (FDOT's) Construction Training and Qualification Program (CTQP) is an outstanding model for construction training for concrete construction joints nationally. Enhancing this program even more could broaden the scope of knowledge in the field with hands-on visual learning experiences, situational training, and lessons learned. Construction quality control personnel could be required to receive this same training and certification to ensure broader experience in the construction market place.

States have different requirements for contractors and inspectors who build or inspect concrete construction joints. The FDOT, as one of the leaders in the requirements for concrete construction inspections, has developed a Construction Training and Qualification Manual (CTQM) and training program with certification for inspectors, Construction Training and Qualification Program (CTQP). This is an outstanding program of training.

The FDOT program instructors will have better ideas on how to broaden and enhance the certification program than the ideas presented in this discuss. FDOT's ideas may be continually on-going. The main thought here was to recommend the possibility of including construction personnel and construction quality personnel in the program and include such resources as:

1. Hands-on training and photographic examples
2. Physical specimen examples for visual inspection. Create testing on which samples meet the Standard Construction Specifications.
3. Hands on practice sessions with various on-site tools.
4. Industry presentations on lessons learned.
5. Share the program with other states nationally including benefits to the training and certifications.

**EXAMPLE OF
INTENTIONALLY
ROUGHENED
CONCRETE SURFACE
(ROUGHENED JOINT)**

per Florida Department
of Transportation's
Standard Construction
Specifications



How construction joints are built on any construction project are important to how an overall structural system works, and engineering designers always expect that the Standard Construction Specifications will be followed. On the FIU Pedestrian Bridge construction accident, there were people with different understandings of what the Standard Construction Specifications required. Maybe requiring a small mock-up of how to prepare a construction joint with a concrete sample at the beginning of concrete pouring activities would be beneficial. A video training guide for viewing before the work is done could also be helpful.

Many states' specifications treat concrete construction joints in the same manner and require surface cleaning and roughening of the existing surface prior to placement of the new concrete against it. Some state's specifications require use of a bonding agent. Testing has demonstrated that the FDOT Standard Construction Specifications, without a bonding agent, meets the AASHTO LRFD requirement.

FDOT has very thorough construction specifications and an extensive certification training program for inspectors. This program includes the Construction Training and Qualification Manual (CTQM) and Construction Training and Qualification Program (CTQP) training to ensure that personnel responsible for providing inspection services obtain a specific minimum level of training to perform their quality function. The FDOT requires inspection personnel that are providing quality checks on concrete work to hold either a Level I or Level II certification as a Concrete Field Inspector. This is an advanced program and each class lasts several days followed by a written test. The classes are usually conducted in a classroom or training facility (but may be taken via their web-based training) and consist of presentations by an instructor.



Construction

Office of Construction / Training

Construction Learning Portal



The Computer Based Training (CBT) course shown below are available on the RedVector website. The links below will take you the FDOT Construction learning portal hosted by Red Vector (Opens a New Window).

Topics

[Asphalt Paving Level 1](#)

[Asphalt Paving Level 2](#)

[Concrete Field Inspector Specifications](#)

[Concrete Lab Technician Specifications](#)

[Earthwork Construction Inspection Level 1](#)

[Earthwork Construction Inspection Level 2](#)

[Final Estimate Level 1](#)

[Quality Control Manager](#)

FDOT's Construction Learning Portal

<https://www.fdot.gov/construction/training/cbt/cbt-courses.shtm>

While most states require inspectors to hold applicable certifications, they usually do not require any special training or certification for construction workers performing concrete work or the contractor's quality control personnel. Expanding this training could include such goals as:

- Review the current presentations to include more images of roughened and non-roughened concrete so that the attendees can more easily identify what roughened concrete needs to look like and the steps in preparing and cleaning the construction joint.
- Develop physical mock-up displays of roughened and non-roughened concrete and have these at each training session so that the attendees can get hands on with the material (and show the displays on web-based training). This will allow them to better understand what will be required in the field.
- Develop a list of construction tools typically used to roughen hardened concrete along with short videos of the tools in action.
- Require contractors to have their quality control personnel receive the training and certification that is currently only provided to inspectors.

Training is a continual learning experience that advances, expands and imparts knowledge and know how on all those who participate. There can never be enough training. The FDOT already knows the importance of this and has this in practice. Perhaps there is a way to include a broader participation for those in the industry on construction sites. Maybe even a comprehensive refresher course before a construction project starts that is carried out at the job site in a kick-off, partnering type session with the team doing the work before it starts. There are many ideas to explore for true effectiveness in making this recommendation.

9.3 PERSONAL SAFETY EQUIPMENT

Recommendation to Support Transportation Safety Improvements

Support, encourage, and require construction industry change to improve protective helmets, or hard hats, for construction workforce to enhance head protection in falls and to protect the wearer from rotational injuries from an impact.

Better hard hats could possibly have prevented the fatality and severe injuries of two workers on the bridge at the time of the construction accident. The leader of Structural Group shared this information at an industry meeting and was discussing the need for committed change in construction hard hat safety equipment. This would include chin straps to enable hard hats to stay on in a fall, to protect against head injuries. There are construction leaders who are moving in this direction, such as Clark Construction (see Attachment A at the end of this section) and Structural Group, forging an interest to make a difference in this area. Clark Construction's leadership on this and Structural Group's passion for better hard hats can be an important catalyst for the industry.

NTSB could enhance the momentum for state-of-the-art personal safety equipment through collaboration with industry leaders and initiatives that advance technologies to protect against head injuries.

There are many activities today that people enjoy while wearing head protection, such as biking, roller blading, mountain climbing, hockey, skiing and similar sports – and these all have protective head gear with chin straps. A minimum of the same type of protection seems logical for construction field work. Included in this discussion is some background information, requirements, research and ideas for incorporation into the design of hard hats. This information shows that work is being done in this area in various ways. With a strong voice such as NTSB behind a national initiative, more can be done to save workers from future injuries involving construction accidents.

Background:

Since the Hoover Dam construction in the US, some contractors and Owners have required the workforce to wear hard hats as part of a personal protection program. The hard hats have evolved from glued canvas, to aluminum to high density plastics. They have also evolved to provide greater protection for the wearer from objects falling onto the wearer and from electrical conductivity hazard.

In the US, OSHA regulation 1910.135 states that the employer shall ensure that each affected employee wears a protective helmet when working in areas where there is a potential for injury to the head from falling objects. Additionally, the employer shall ensure that a protective helmet designed to reduce electrical shock hazard is worn by each such affected employee when near exposed electrical conductors that could contact the head.

When Does OSHA Require Hard Hats?

OSHA has two standards that govern hard hat requirements:

- **29 CFR 1910.135 governs hard hat requirements for general industry workers**
- **29 CFR 1926.100 refers to head protection requirements for construction, demolition, and renovation workers**

Both standards require workers to wear hard hats when there is a potential for head injury from “impacts, falling or flying objects, or electrical shock.”



This means that employers must provide hard hats and ensure that employees wear protective coverings in the following situations:

- When objects or debris might fall from above and strike workers on the head
- When employees may strike their heads against fixed objects, like supports, beams, or other equipment
- When there is the possibility that workers' heads will make contact with electrical hazards

In all cases, hard hats must meet OSHA head protection requirements.

The OSHA regulation does not specifically cover any criteria for the protective helmets, instead OSHA requires that protective helmets comply with ANSI/ISEA Z89.1-2014 – American National Standard for Industrial Head Protection.

Each hard hat is specified by both Type and Class. Types include:

- ANSI Type I / CSA Type 1 hard hats meet stringent vertical impact and penetration requirements.
- ANSI Type II / CSA Type 2 hard hats meet both vertical and lateral impact and penetration requirements and have a foam inner liner made of expanded polystyrene (EPS).

Classes:

- Class E (Electrical) provides dielectric protection up to 20,000 volts.
- Class G (General) provides dielectric protection up to 2,200 volts.
- Class C (Conductive) provides no dielectric protection.

A hard hat is specified by both Type and Class; for example: Type I Class G.

ANSI standards for hard hats set combustibility or flammability criteria. ANSI Z89 standard was significantly revised in 1986, 1997 and 2003. The current American standard for hard hats is ISEA Z89.1-2009, by the International Safety Equipment Association that took over publication of the Z89 standard from ANSI. The ISO standard for industrial protective headgear is ISO 3873, first published in 1977.

Areas for Improvement

While these hard hats do protect workers from falling objects, there are two key areas that could benefit from improvement:

1. If a worker falls, most hard hats are not connected by any chin strap and can become loose or even fall off before the worker lands. Effectively, the worker's head can hit the ground or other objects without any protection coming from the hard hat.



HARD HATS WITHOUT CHIN STRAP CAN DISLODGE AND FAIL TO PROTECT DURING FALLS



Example of Hard Hat
with no Chin Strap



Example of Hard Hat
with Chin Strap

CG SCHMIDT EMBRACES SAFETY FIRST: TRANSITIONING FROM HARDHATS TO SAFETY HELMETS

By CG Schmidt Posted June 28, 2019 In Industry, Insights, Safety



This week, our jobsites will become even safer and our employees will be even better protected due to our new safety helmet initiative. Every CG Schmidt employee on a jobsite will receive a safety helmet that will take the place of their existing hard hats.

CG Schmidt is the first Wisconsin-based firm to embrace the transition from the traditional hardhat to the safety helmet. Why change now? One of the most visible and critical forms of Personal Protective Equipment (PPE) on a jobsite is the hardhat, yet it is also one of the least evolved. Many hardhats used today are the same that have been used for decades.

As the design and technology of construction evolve, so should the protective equipment we provide. A traditional hardhat is designed for impact protection at the top of the head and has little effectiveness protecting against impacts to the front, back or sides of the head. A sudden movement, tilt of the head, or fall, typically leads to the hardhat falling off, leaving the worker unprotected.

The Bureau of Labor Statistics stated that brain injuries led to the deaths of at least 992 construction workers from 2011 through 2015. In 2016, there were nearly 400 fall fatalities. The National Institute for Occupational Safety and Health (NIOSH) found that 25% of deaths in 2016 resulted from Traumatic Brain Injuries (TBIs), most of which occurred from a fall. NIOSH has been studying and working on a change for the past 5 years to help save lives.

The traditional hardhat has evolved and the transformation is not only keeping our crews safer, but also more comfortable. An addition of the chin strap keeps the safety helmet in place, while also offering additional protection from front, rear and side impacts.

Through research and discussion, CG Schmidt has selected the 3M SecureFit Safety Helmet. 3M has a patented pressure diffusion technology that reduces the force on the forehead up to 20% compared to the traditional hardhat, making the new safety helmets more comfortable for daily wear. Furthermore, the new helmets have an eight-year lifespan and 10-year shelf life with a UV indicator on the back. Once the red UV indicator reaches its shelf life, it will turn white, indicating the helmet is no longer safe to use. However, the true comfort comes in knowing that in the event of a fall, your safety helmet will stay on your head and protect against severe injury and death.

**US MANUFACTURER OF SAFETY HELMETS
DESIGNED TO KEEP THE HELMET IN PLACE EVEN DURING A FALL**

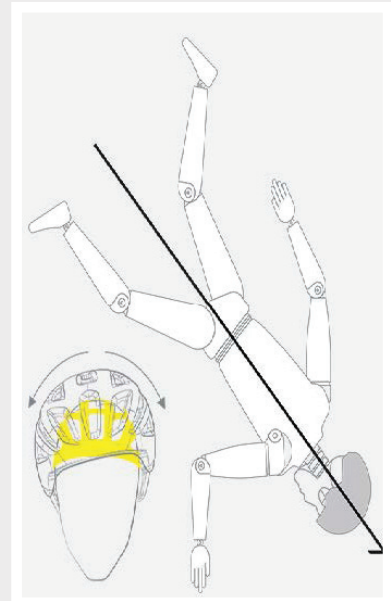
The recommended solution is to require that all construction hard hats include a mandatory chin strap device that will securely hold the hard hat in place.

2. If a worker's hard hat is hit by a force that imparts a rotational impact, current hard hat design can allow a portion of the rotational impact to be transferred to the brain, potentially causing a Traumatic Brain Injury (TBI). A large percentage of construction fatalities result from TBIs

In Sweden, a partnership between MIPS Corp., a company that specializes in helmet-liner systems for protecting the brain, and Guardio Safety AB, a Swedish industrial safety firm, has led to the release in June of a construction hard hat, or helmet, designed to mitigate brain-damaging forces that often are suffered in construction falls.

A low-friction layer in the liner allows a sliding movement of 10 millimeters (mm) to 15 mm in all directions upon impact, reducing rotational forces on the brain.

NOTE THAT THE IMPACT IMPARTS AN AXIAL FORCE AND A ROTATIONAL FORCE TO THE WEARER THROUGH THE HELMET.



Guardio says the ARMET helmet is the first construction helmet to be equipped with the MIPS brain protection system, which is used in some specialized helmets for other activities, including skiing, bicycling and hockey. The company cites data from the U.S. Centers for Disease Control and Prevention that asserts that **“the construction industry has the greatest number of both fatal and nonfatal traumatic brain injuries (TBIs) among U.S. workplaces,”** and which further states that from 2003 to 2010, **25% of all construction fatalities were caused by a TBI.**

NEW!

Guardio ARMET

World's first safety helmet for industrial use (EN397) with MIPS!

We are proud to launch the first safety helmet in the world with the patented brain protection system from MIPS. The Guardio ARMET helmet have a low-friction layer designed to reduce rotational motion transferred to the brain from angle impacts to the head. MIPS adds a low friction layer that enables a relative movement of 10-15mm between the head and the helmet in any direction at the brief moment of an angled impact.



SWISS VERSION OF IMPROVED SAFETY HELMET

[The recommended solution is to require that all construction hard hats include a mandatory low friction layer in the liner that allows for a sliding movement of 15 mm.]

ATTACHMENT A

May 11, 2018 [Press Releases & News](#)

MAKING A SAFER CHOICE: CLARK DRIVES CHANGE FOR ENHANCED HEAD PROTECTION

Bethesda, MD— One year ago, Clark Construction Group became the first general contractor in the United States to implement the company-wide adoption of safety helmets with chin straps for all employees. Since then, the company has witnessed improvement in the prevention of head injuries on its projects.

Why did Clark make the decision to adopt the new helmets?

In 2016, there were nearly 400 fall fatalities in the construction industry. That year, the National Institute for Occupational Safety and Health (NIOSH) found that 25% of all construction fatalities result from Traumatic Brain Injuries (TBIs), most of which occurred from a fall.

With this alarming data in hand, Clark's safety team began to search for ways to improve the protective gear utilized by employees. The traditional hard hat, a 60-year staple in the industry, provides protection from falling objects. But if a person falls, the standard hard hat falls off, and falls short.

After more than a year of testing and research and development, Clark determined that safety helmets with chin straps were a prudent solution to preventing TBIs as the result of a fall. In 2017, Clark made the decision to adopt the use helmets with chinstraps. Today, all 3,000+ employees wear the safety helmet. In the year since its adoption, the helmet has already made a big impact in preventing TBIs.

Division Safety Manager Seth Randall was a leader in Clark's safety helmet initiative. "The industry didn't have much consensus on head protection during a fall, so we wanted to find a better solution," says Seth. "We saw that there was a need, and an opportunity to change for the better. Since adopting the helmet, we've already seen positive results from a couple of incidents where head injuries have been avoided because of the helmet."

As just one example, in February 2018, Marvin Taylor was cleaning stairs on a jobsite when a guardrail on a stair mid-landing gave out, and he fell seven feet onto a concrete slab below. "At the hospital, the doctor confirmed that I didn't have a concussion or anything," remarked Marvin. "I didn't even realize that I had hit my head. Then I was shown the helmet I was wearing. There was a three-inch crack in the helmet. My old hard hat... it would have fallen off my head. That would have been a three-inch crack in my skull. It could have been so much worse." Shortly after the incident, Marvin was able to return to work on site.

Clark is proud to be at the helm of an industry movement to push for safer head protection. Vice President of Safety Kris Manning commented, "We recognize that PPE should be the last line of worker safety, but as responsible leaders within the industry we truly believe the adoption of these helmets with chin straps is the right thing to do. Internal and third-party research supports enhanced worker protection, and the most powerful confirmation for me is speaking to a worker who fell and was able to walk away to spend time with his family again."

The theme of Safety Week 2018 is "The Power of Choice." Two years ago, Clark chose to find better head protection. One year ago, Clark chose to make it company policy. Every day, Clark chooses to provide the safest possible work environment for each and every person on its jobsites.

10. OTHER REPORTS

10. OTHER REPORTS

10.1 NTSB FACTUAL REPORT DISCUSSION

NTSB Factual Report shared with party members on March 21, 2019 as final stated no additional comments allowed. Party members were notified of changes that NTSB was making to the Factual Report after this date but an updated Report has not been posted as of the time of this submission. There are a number of inaccuracies in the current Report. Eight (8) examples of inaccuracies are described in this section with explanations on importance for an accurate Factual Record.

As a party member to the National Transportation Safety Board (NTSB) investigative process on the FIU Pedestrian Bridge Construction Accident, FIGG Bridge Engineers (FIGG) participated in researching facts, reviewing available information, and providing comments in order to fully support the NTSB values of integrity, transparency, independence, and excellence. As the draft Factual Report was prepared by the NTSB with the combined party member information, it went out to the parties to verify, comment, and determine if important factual information was missing, along with the accuracy of that information.

The “Bridge Factors Group Chairman’s Factual Report” (Factual Report) was issued to party members on March 21, 2019 following a round of comments on the Factual Report and two rounds of comments on other party members’ comments and on resolution language by the NTSB (a full version of the Factual Report was not recirculated for comment). This Factual Report included highlighted text and stated that no further comments would be accepted. Later, NTSB advised of updates to the Report, and distributed corrected tables. Party members were not asked to confirm their agreement with this Factual Report or provide an objection. Since it was important to FIGG to adhere to the rules outlined by the NTSB, and it was stated that “NTSB will not be taking any additional comments”, we believed that the only choice was to share these comments concerning accuracy here in our party submission. Based on the last Factual Report available to the party members, there are a number of factual inaccuracies that remain in the document, resulting in incomplete and misleading information. Therefore, this discussion shares eight (8) facts as examples that are important for an accurate factual record.

This is the first time FIGG has participated in an NTSB process, but we understand that this process was different from aviation investigations. The initial organization meeting with party members was cancelled. Interviews commenced. Party members were first invited to participate by observing a site destructive testing on 6/12/2018. Party members did not participate in interviews of other party members in order to ask questions and find out more information. This would have been helpful to finding all the facts. There were no meetings of the parties other than a half of a day to go through NTSB's resolution of one set of member comments and a meeting FIGG requested with NTSB and FHWA to share information. Party Meetings would have helped with discussion and discovery of information. Party members were not asked to confirm their agreement with the Factual Report. This kind of feedback would seem helpful to the process

As a result of the current status of the Factual Report and the reasons presented in this discussion, FIGG cannot agree with the Factual Report. Should the Factual Report be updated to correct and complete the record, FIGG could consider withdrawing any objection.

EXAMPLES OF INACCURACIES

1. Section 30 - Large Sample Examinations (Pages 190-191)

FHWA's Turner-Fairbank Highway Research Center (TFHRC) 15-page Factual Report on materials testing of the "Concrete Interface Under Members 11 and 12" is an important material fact that is inaccurately represented in the Factual Report.

Section 30 in the Factual Report fails to highlight a key finding of the material testing conducted during the investigation. The **TURNER-FAIRBANK HIGHWAY RESEARCH CENTER (TFHRC) REPORT** (referenced at the bottom of page 191) concluded that the surface under the failed connection was "not intentionally roughened" as required by the Standard Specifications of the Florida Department of Transportation, which was required in the Released For Construction plans. The lack of intentional roughening would result in a reduction in the capacity of the connection that failed. The conclusions in this FHWA Materials Lab report

TURNER-FAIRBANK HIGHWAY RESEARCH CENTER
FACTUAL REPORT
Concrete Interface Under Members 11 and 12

Prepared For:
National Transportation Safety Board
NTSB Accident ID: HWY18MH009

Prepared by:
Benjamin Graybeal, Ph.D., P.E.
Zachary Haber, Ph.D.

Federal Highway Administration
Turner-Fairbank Highway Research Center
6300 Georgetown Pike, McLean, VA 22101

October 19, 2018

clearly indicate that the material preparation of the construction joint was not in compliance with the required Project specifications.

Instead, this section of the Factual Report includes several statements that: “No significant abnormalities were noted...”. Where the material testing reports prepared by TFHRC are listed, there is no discussion on the report conclusions. This TFHRC report that determined that there was a failure to roughen was also not properly addressed in the NTSB Investigative Update released on November 15, 2018, which stated concerning these same reports that “the concrete and steel specimens tested by TFHRC personnel met the minimum requirements specified in the project’s build plans”. This is simply not accurate because the Florida Department of Transportation’s Standard Specifications, which are given in the Project build plans (Released For Construction plans), required intentional roughening of hardened concrete joints. This is an important material fact that cannot be dismissed.

The factual information from the TFHRC report “Concrete Interface Under Members 11 and 12” is critical to the investigation and should be summarized in the body of the main report rather than be restricted to the docket materials. Additionally, the recently produced (August 2, 2019) NTSB Report 19-043 “Materials Lab Study Report - Member 11-12 Surface Roughness” is also an examination further showing the lack of roughening at the failed connection and should be discussed in this section as well.

See Party Submission, Section 7.2 for more information.

2. Section 22 - Redundancy (Pages 148-151)

Information on “Redundancy” in the Factual Report includes code information for “steel” bridges and this is a “concrete” bridge. This is inaccurate.

Section 22 describing Redundancy in the NTSB Factual Report is misleading. Most of the materials in this section of the report are requirements for bridges constructed of steel, which behave differently than concrete bridges such as this structure. The inclusion of this material in the NTSB Factual Report gives the false impression that the FIU Pedestrian Bridge was a steel bridge subject to these requirements, when different requirements apply to a concrete bridge.

See Party Submission, Section 6.3 for more information.

3. Section 16 - Move of Main Span by Barnhart Crane and Rigging on March 10, 3. 2018 (Pages 112-115)

During the investigation, it was discovered that during the moving of the span, the boundaries for twist were exceeded at least twice, up to 168% of the allowable boundary value. These significant violations of the agreed-to boundaries are dismissed inappropriately, and party member comments ignored.



Precast main span truss move by transporters on March 10, 2018 from casting area to permanent piers.
(Source: FIGG)

Section 16 contains primarily an after-the-fact narrative of the main span bridge move provided by Barnhart Crane, who was responsible for the bridge move. It is presented in such a way as to give the impression that the narrative is completely factual. Adjectives such as “immediately” describing what cannot be substantiated are included in the text, and Barnhart’s interpretation of the reported measurements is presented as factual without the complete picture of what happened in the move of the main span.

The firm responsible for monitoring the structure during the move, Bridge Diagnostics, Inc. (BDI), produced a report of the move dated April 4, 2018 (20 days after the construction accident) that included detailed information on the measured displacements and strains during the move, that show the boundaries

for allowable twist was exceeded during the move at least twice, up to 168% of the allowable value. It was a surprise for FIGG to learn during the investigation that the boundaries for twist during the move had been exceeded so significantly. FIGG had been told at the time of the move that the boundaries were never exceeded. This deformation of the bridge added stress to the bridge member connections that should not have happened. Neither Barnhart nor BDI nor anyone else informed FIGG during or following the move that this had occurred. This information and the BDI report were excluded from the Factual Report and the BDI report does not appear to be included in the NTSB's docket on the investigation.

Additionally, when this information was learned, it would have been appropriate to interview key people from Barnhart, BDI, and others, as this was significant information and a violation of the Project requirements that required further investigation.

See Party Submission, Section 6.5.2 for more information.

4. Section 20 - Specific Information taken from FDOT's Standard Specifications for Road and Bridge Construction related to the Signature Pedestrian Bridge (Page 142)

The Factual Report should include the e-mails between MCM, BPA, and FIGG that occurred prior to the main span construction where confirmation was asked and given to follow FDOT Standard Specifications for all construction joints, as given in the Released For Construction (RFC) plans. These e-mails should be reported factually as they were written and included in their own attachment.

The discussion on page 142 references a series of e-mails between MCM, BPA and FIGG concerning treatment of construction joints in the concrete (the interface between two concrete pours). The treatment used for the construction joints is a key fact in the investigation, since improper preparation of the joint between the truss members and the deck would affect capacity of the connection. One of the e-mails in the referenced series mentions a particular construction joint in an abutment column. The other e-mails contain a broader discussion of the requirements for joint construction.

However, the Factual Report text provides an interpretation of the e-mails in multiple places that the discussion only applies to one construction joint on the Project. This interpretation is not factual, and the e-mails should be reported as they were written.

See Party Submission, Section 6.5.1 for more information.

5. Section 14 Restressing post tensioning bars in diagonal support # 11 on March 15, 2018 (Pages 101-106)

The Factual Report contains inaccurate and incomplete information on the restressing operation at the time of the construction accident.

Section 14 describes the restressing of post tensioning bars in diagonal support #11, including the restressing operations, and the requirement to monitor. The Factual Report includes an explanation that BPA, the construction engineering inspection company representing the Project Owner, was not aware of the restressing operation until shortly before concluding the morning meeting and not aware of the requirement to monitor during the restressing operation. However, BPA requested the partial road closure in connection with the restressing operation in an e-mail on that same morning of March 15, 2018 at 9:10 am (meeting commenced at 9:00 am). BPA's role was to make certain that qualified personnel with proper certification were available for inspection of operations, which requires coordination with the Contractor and, absent availability, delay of operations. Personnel from Corradino, the certified post-tensioning inspector that was a subconsultant to BPA, were not available at that time but work was allowed to take place anyway.

Post-tensioning operations typically involve all tension being placed on each bar in a single application of tension. However, this restressing operation took more than two hours, due to the small application of tension placed on each bar with proper monitoring required. Structural, who was performing the post-tensioning operation, is required by its own signed and sealed plan to establish the work zone of safety (i.e., whatever is needed in closing the road, etc.) and to monitor the operation and, if cracking worsens, to stop operations immediately. BPA was responsible for inspecting Structural's work.

See Party Submission, Section 6.5.3 for more information.

6. Section 10.0 - Timeline of Construction (Page 90-91) and Section 23 - Meeting on March 15, 2018 Before the Collapse (Page 151)

Meeting minutes distributed five days after the accident are incorrectly assumed to be endorsed by all the attendees and inaccurately taken as factual.

Sections 10.0 and 23 describe the two sets of meeting minutes that document the March 15, 2018 meeting at the Project site, the morning of the construction accident. One set was prepared by BPA, the on-site construction engineering inspection company, and the other by FIGG. Both sets of minutes were prepared after the construction accident.

The Factual Report gives preference to the document prepared by BPA by stating that BPA “circulated the typed document for comment on March 20, 2018, five days after the collapse. Having received no comments from any of the parties present at the meeting, the meeting minutes were incorporated in the Project documentation.” After the collapse, the normal administration and communications on the Project were no longer functioning. A lack of comments or response to the BPA post-accident document was certainly not a sign of endorsement and should not be presented as such in the Factual Report. These meeting minutes were prepared in a different format to all other meeting minutes during the history of the meetings on the Project.

An engineer with FIGG, who participated in the March 15, 2018, morning meeting and who was interviewed by NTSB, was asked if FIGG agreed with the BPA minutes and he stated disagreement. It was agreed that FIGG would prepare a set of meeting minutes for NTSB. This is the reason FIGG prepared meeting minutes - to provide NTSB with more information. As a minimum, both sets of meeting minutes should be treated equally in the Factual Report.

7. Section 21 - Prequalification of Louis Berger to Conduct an Independent Peer Review (Pages 145-146)

Misleading statement in the Factual Report concerning Louis Berger’s prequalification should be corrected.

Louis Berger was the Independent Peer Review Consultant for the design and was required to be prequalified with FDOT for Work Type 4.3.1 Complex Bridge Design - Concrete. Prior to being subcontracted by FIGG to perform the review work,

Louis Berger stated in writing that they held the required prequalification, and FIGG verified on the FDOT website that FDOT listed Louis Berger as having the 4.3.1 prequalification. FIGG took a screenshot of the FDOT website and a Senior Executive of Louis Berger verified the prequalification. After the construction accident, it was learned that, in fact, Louis Berger did not have the required FDOT prequalification.

This section of the Factual Report uses a description provided by FDOT stating that FDOT's website should not be relied on to verify a consultant's prequalification status and inferring that FIGG improperly selected Louis Berger to perform the review work. While this may be FDOT's position, it should be clearly presented as such and not as factual.

It should be noted that FDOT accepted Louis Berger's independent peer review certifications that were signed and sealed by their Engineer and FDOT performed an audit of the Louis Berger work. At no time during the Project did FDOT or anyone else ever tell FIGG that Louis Berger did not meet the FDOT prequalification for these services before the construction accident.

See Party Submission, Section 6.4 for more information.

8. Sections 29.1 - AASHTO LRFD Bridge Design Specifications Provisions (Page 180)

Section 29 of the Factual Report characterizes the design calculations in a negative light rather than a neutral fashion since the Released For Construction final plans and Specifications represent the actual final design.

The discussion at the bottom of page 180 is another example of inaccurate language in the Factual Report. The description "...these design decisions restricted the area of the interface providing resistance to interface shear forces and caused the resistance calculation to rely on the second term..." gives the impression that the design somehow reduced the strength of the connection. In fact, the opposite is true in that these were conservative design assumptions that resulted in the calculated capacities being less than what the design code allowed to be used as the assumed capacity of the connection.

Additionally, the design of the bridge is reflected in the official, approved Released For Construction (RFC) plans, which incorporate review comments during the phases of design development and formal submittal reviews prior to construction starting.

See Party Submission, Section 6.2.1 for more information.

10.2 NTSB INVESTIGATIVE UPDATE 2 (RELEASED NOVEMBER 15, 2018)

Investigative Update No. 2 contained inaccurate information on two key points, one from NTSB's own investigation. These were pointed out for correction; however, NTSB chose to disregard these important inaccuracies and the public record was not corrected. This section provides a discussion of this process, the factual information, and the results.

There have been four public statements made by the National Transportation Safety Board (NTSB) concerning the March 15, 2018 FIU Pedestrian Bridge construction accident. In each NTSB Report or Update, the following statement is at the top:

"The information in this report is preliminary and will be supplemented or corrected during the course of the investigation."

This statement is beneficial because, as an investigation takes place and additional facts are learned, the information can be supplemented and corrected during the process, as NTSB did on several occasions.

The first statement was titled "Preliminary Report" on March 21, 2018. During an NTSB interview, it was pointed out that certain information was incorrect. NTSB appreciated the information and made the corrections.

The second statement was an update on May 23, 2018 of the "Preliminary Report".

The third statement was the first "Investigative Update" on August 9, 2018, discussing information on:

"...various tests and examinations to evaluate multiple concrete core and steel samples taken from the bridge following the collapse."

The tests were conducted by the Federal Highway Administration's (FHWA) Turner-Fairbank Highway Research Center. The update also included interview updates, photographs, and more. This update was sent to party members before publishing and comments were received to assist with correctness and appreciated.

The fourth statement was the second “Investigative Update” on November 15, 2018. On November 9, 2018, the first draft of the NTSB Factual Report was sent to party members asking for comments by November 30, 2018.

This Investigative Update No. 2 included information from the draft NTSB Factual Report, which was in the process of being reviewed and the NTSB had not received party member comments yet to ensure accuracy. The party members were not invited to review the Update before it was made public and there was information in the Update that was incorrect and conclusionary with the factual record still being determined. The analysis part of the investigation had not started, and the facts were incomplete.

Based on the incomplete information and language included, the Update misled the public regarding conclusions of the investigation and created premature determinations. There are two key points that were incorrect:

1 - The Update did not include complete and available testing results from FHWA’s Turner-Fairbank Highway Research Center (TFHRC), which was available a month before the Update. The Update incorrectly stated that all of the concrete tests met the Florida Department of Transportation specifications, when in fact certain tests from the TFHRC proved otherwise. These research reports were as follows:

- Material Testing Reports by Turner-Fairbank, dated October 24, 2018, were included. These reports concluded that the concrete and steel specimens met the minimum requirements.
- Concrete Interface Under Members 11 and 12 Report by Turner-Fairbank, dated October 19, 2018, was **not** included. This 15-page report concluded that the concrete interface did **not** meet the Florida Department of Transportation’s Standard Specifications, which was a Project requirement.

Despite the fact that the Concrete Interface Report was available on October 19, 2018 (before the other material tests on October 24, 2018) and this report concluded that the concrete did not meet requirements, the Update only included results from one of the Reports and provided the statement below, which implied that all the tests achieved specified requirements, even though the concrete interface specimens did not meet the Project’s build plans:

“In summary, the concrete and steel specimens tested by TFHRC personnel met the minimum requirements specified in the project’s build plans.”

There is high regard for the FHWA’s Turner-Fairbank Highway Research Center and the excellent concrete testing and research that is accomplished at this center. Unfortunately, this significant report was ignored, and results misrepresented in the Investigative Update.

2 - The Update contained an evaluation of partial information with a conclusionary statement that there were design errors without complete information on the design. This determination was viewed by the public as a probable cause determination by the NTSB while party members were in the factual investigation period.

The statement from the Update read:

“Although the evaluation is ongoing, the assessment has determined that errors were made in design of the northernmost nodal region of the 174-foot-long span, where two truss members were connected to the bridge deck. These design errors resulted in (1) overestimation of the capacity (resistance) of a critical section through the node comprised of diagonal member 11 and vertical member 12; and (2) apparent underestimation of the demand (load) on that same critical section. Additionally, the FHWA evaluation determined that the cracking observed in the node prior to the collapse is consistent with the identified errors.” (note: underlining added to highlight points)

Unfortunately, this was based on incomplete information on how the bridge system worked and was later addressed in the Factual Report. The actual final design of the bridge is reflected in the Released For Construction (RFC) plans, which incorporated comments from the design review process.

In the interest of integrity and transparency, and reflecting NTSB’s previous efforts to have information “corrected during the course of the investigation”, it was expected that corrections would be made to the Investigative Update for accuracy. A request was made to the NTSB to correct the public record during the investigative process that was not addressed.

In conclusion, the analysis of the factual record includes the following determinations, as well as others:

- The bridge construction accident occurred because the construction joint between main span truss members 11/12 and the bridge deck was not roughened as required by the Florida Department of Transportation (FDOT) Standard Specification for Road and Bridge Construction, as required by the Released For Construction (RFC) plans.
- The FDOT Standard Specifications, as proven by laboratory testing, achieves the requirements of the AASHTO Code.
- The design of the member 11/12 connection as shown in the Released For Construction plans complied with the applicable AASHTO LRFD Bridge Design Specifications, the Florida DOT Structure Design Guidelines, and the contract design criteria for this Project.

For other conclusions, see Section 8 of this Party Submission. See Section 7.3.2 for supporting information, along with Exhibit A, Report from Wiss, Janney, Elstner Associates, Inc. (WJE), Forensic Engineering Specialists, titled “Research and Analysis Related to Collapse during Construction”, a 132-page report that includes testing and analysis.

10.3 OSHA DOCUMENT DISCUSSION

This discussion explains that OSHA violated the NTSB party rules and was removed from the investigation by the NTSB following their surprise public document of June, 2019. This document was never reviewed by party members to the investigation and there are many inaccuracies throughout the document. This discussion begins to correct some of these inaccuracies and relates detailed factual information given in this Party Submission.

On June 11, 2019, the Occupational Safety and Health Administration (OSHA) Directorate of Construction issued an independent document of their view concerning the March 15, 2018 pedestrian bridge construction accident at Florida International University (FIU) in Miami, Florida. This came as a surprise to the National Transportation Safety Board (NTSB) and the party members to the investigation because OSHA was a party member and the investigative process was still taking place. OSHA's document had not been commented on by the NTSB and the party members. OSHA's public issuance of this document was in violation of the NTSB process and as a result, NTSB Chairman Robert L. Sumwalt, III, sent a letter on June 20, 2019 to OSHA revoking their party member status for "...breach of NTSB party participation rules." Party members were "...directed to cease contact with any and all representatives from OSHA regarding the NTSB's on-going investigation..."

As a party member, Figg Bridge Engineers, Inc. (FIGG) was instructed by NTSB that any public responses regarding specifics to the OSHA document could not be released without NTSB approval. FIGG issued the following NTSB approved press release:

"The OSHA FIU Pedestrian Bridge report is factually inaccurate and incomplete and includes errors and flawed analyses. It does not include an evaluation of many important factors pertinent to the construction process leading up to the accident. Additionally, it has not been reviewed by any other entities involved in the accident investigation. FIGG disagrees with the conclusions in the OSHA report. At this juncture, as a party member to the NTSB process, we are not able to elaborate further, but at the appropriate time the facts and the truth will be released to the public."

The purpose of the discussion in this section is to highlight some of the many inaccuracies of the OSHA document to begin the process of setting the record straight.

1. OSHA incorrectly identifies roles of the project participants. For example, BPA, the on-site inspector in the Construction Engineering and Inspection role, representing the owner, was responsible for construction inspection and MCM, the Project's contractor, had quality management personnel with inspection roles and responsibilities. Both of these Project participants had contractual oversight roles to ensure that the approved Released For Construction (RFC) plans and contract documents were built in compliance with the requirements. See Party Submission to the NTSB by FIGG, Section 4. Project Participants.
2. OSHA incorrectly states that the bridge had structural design deficiencies. As demonstrated in the Party Submission to the NTSB by FIGG, Section 7.3, the bridge design met design requirements and had an adequate factor of safety. Forensic Engineers, Wiss, Janney, Elstner Associates, Inc. (WJE), independently determined that FIGG met the AASHTO design code for members 11/12 and the connection for both staged construction and final construction. See the Exhibit A of this Party Submission with WJE's report titled "Research and Analysis related to Collapse During Construction."
3. OSHA incorrectly states that the cracks on the bridge occurred due to deficient structural design. As explained in this Party Submission to the NTSB by FIGG, Section 7.3, the failure in construction to comply with the Florida Department of Transportation Standard Specifications for routine preparation of concrete construction cold joints, including intentionally roughening the concrete surface, under member 11/12, together with other construction activities in the movement of the span and monitoring of post-tensioning resulted in a failure in the connection. Further information is contained in the WJE Report in the Exhibit A, and Section 7.
4. OSHA has incomplete and misleading facts in its report. For example, the Engineer of Record (EOR), by contract, did not have a role on-site and relied on those building and inspecting the bridge onsite to provide accurate and timely information. The EOR was not kept updated and advised of accurate information over the course of the period between March 10 and March 15. Information concerning various inspections prior to this time, which became important to the investigation, were not known to the EOR. See Party Submission to the NTSB by FIGG, Section 6.5.4.
5. OSHA inaccurately stated that the restressing was not in the original design. Based on information provided by the contractor after a detensioning operation, the Engineer of Record (EOR) determined to step back in the original design plan to when the tensioning was in place. These steps were outlined in

the Released For Construction (RFC) plans. A previous step of tensioning was being reestablished. See Party Submission to the NTSB by FIGG, Section 6.5.3.

6. OSHA inaccurately stated information regarding the independent peer review. See Party Submission to the NTSB by FIGG, Section 6.4 and WJE Report in **EXHIBIT A**.
7. OSHA inaccurately describes redundancy and its application to the bridge. See Party Submission to the NTSB by FIGG, Section 6.3.

EXHIBITS

A. WJE Reports



FIU UNIVERSITY CITY PROSPERITY PEDESTRIAN BRIDGE PROJECT

Research and Analysis Related to Collapse during Construction

Miami and Sweetwater, Florida



Final Report

September 18, 2019

WJE No. 2018.1774

Prepared for:

FIGG Bridge Engineers, Inc.

Prepared by:

Wiss, Janney, Elstner Associates, Inc.



FIU UNIVERSITY CITY PROSPERITY PEDESTRIAN BRIDGE PROJECT

Research and Analysis Related to Collapse during Construction

Miami and Sweetwater, Florida

A blue ink signature of Gary J. Klein, which has been redacted with a black rectangular box.

Gary J. Klein
Licensed Professional Engineer
Florida 86154



Final Report

September 18, 2019

WJE No. 2018.1774

Prepared for:

FIGG Bridge Engineers, Inc.

Prepared by:

Wiss, Janney, Elstner Associates, Inc.

TABLE OF CONTENTS

1	Introduction and Background	1
1.1	Introduction	1
1.2	Project Background	1
1.3	Structure Description.....	2
1.4	Collapse Background	3
2	Evaluation of Failure Pattern	5
2.1	Document Review	5
2.1.1	Photographs	5
2.1.2	Video	5
2.1.3	OSHA Report	6
2.2	Analysis of Photos and Videos.....	6
2.2.1	Pre-Move (Before March 9, 2018): Exhibits 2.1.1 to 2.1.3.....	6
2.2.2	Post-Move and before De-tensioning (March 10, 2018): Exhibits 2.2.1 to 2.2.3	7
2.2.3	Two Days after Move (March 12, 2018): Exhibits 2.3.1 to 2.3.3	7
2.2.4	One Day before Collapse (March 14, 2018): Exhibits 2.4.1 to 2.4.3	7
2.2.5	Post Collapse: Exhibits 2.5.1 to 2.5.4.....	7
2.3	Findings	8
3	Evaluation of Construction Joint Conditions.....	25
3.1	Document Review	25
3.1.1	Construction Documents	25
3.1.2	Pre-Construction Email Correspondence	26
3.1.3	Concrete Placement Video	26
3.1.4	OSHA Report	27
3.1.5	WJE Interface Shear Transfer Specimens	28
3.2	Discussion	29
3.2.1	Project Records	29
3.2.2	Photographs and Laser Scans	30
3.3	Findings	30
4	Interface Shear Transfer Testing	31
4.1	Experimental Program.....	31
4.1.1	Introduction and Specimen Description	31
4.1.2	Specimen Reinforcement	31
4.1.3	Concrete Mixture Proportions	33
4.1.4	Concrete Placement.....	35
4.1.5	Construction Joint Interface	37
4.1.6	Test Set-up and Instrumentation.....	41
4.1.7	Loading Protocol	43
4.1.8	Interface Shear Transfer Results	44
4.1.9	Slant Shear Tests	48
4.2	Discussion	50
4.2.1	Results Relative to AASHTO Code	50
4.2.2	Florida Krome vs Chicago Limestone.....	51
4.2.3	Roughened vs As-Placed (Non-Roughened) Interface.....	52
4.3	Findings	52
5	Structural Analyses.....	62
5.1	Finite Element Analysis	62

5.1.1	Model Description and Assumptions	62
5.1.2	Loading	63
5.1.3	Post-Tensioning Force in Member 11	63
5.1.4	Results	64
5.2	Code Evaluation of Member 11/12 Deck Connection (As-built Condition).....	64
5.2.1	Limit State	64
5.2.2	Demand	65
5.2.3	Capacity.....	66
5.2.4	Findings: Design Conditions	68
5.2.5	Findings: Design Conditions (Non-Roughened Surface).....	69
5.3	Test-based Evaluation of Member 11/12 Deck Connection for As-built conditions	69
5.3.1	Failure Sequence and Pattern	69
5.3.2	Calculated Forces at Time of Collapse.....	69
5.3.3	Connection Strength (As-Built).....	70
5.3.4	Discussion	72
5.3.5	Findings.....	73
6	Evaluation of Peer Review	74
6.1	Document Review	74
6.1.1	Request for Proposals (RFP)	74
6.1.2	Berger Agreement with FIGG	74
6.1.3	FDOT Plans Preparation Manual: Chapter 26	75
6.1.4	Released for Construction (RFC) Plans	76
6.1.5	Berger Peer Review Comments	76
6.1.6	Email Correspondence	77
6.1.7	Berger Analytical Model.....	77
6.1.8	Berger Web Member Checks	79
6.1.9	Certification Letters.....	79
6.2	Expected and Provided Peer Review Documents	79
6.3	Discussion	79
6.3.1	Quality and Completeness of Berger Peer Review.	79
6.4	Findings.....	80
7	Evaluation of Tilt Exceedances During Main Span Transport	87
7.1	Background on Transport of Main Span	87
7.2	Document Review	87
7.2.1	Photos of North-End Distress before and After Move	87
7.2.2	SPMT Bridge Movement Monitoring Plan	87
7.2.3	BDI Monitoring Report.....	88
7.3	Structural Analyses.....	89
7.4	Discussion	90
7.5	Findings.....	91
8	Re-Stressing of Member 11	102
8.1	Timeline and History of Cracking near the North End	102
8.2	Re-Stressing of Member 11.....	103
8.3	Actual Crack Monitoring.....	103
8.4	Possible Crack Monitoring.....	105
8.5	Discussion and Findings.....	107
9	Summary of Findings and Conclusion	127

1 INTRODUCTION AND BACKGROUND

1.1 Introduction

Wiss, Janney, Elstner Associates, Inc. (WJE) has carried out research and analysis related to collapse of main span of the FIU UniversityCity Prosperity Pedestrian Bridge during construction. Studies were carried out in the areas listed in the table shown below. The corresponding sections of the report are indicated.

Area of Research and Analysis	Report Section
Evaluation of failure pattern	2
Evaluation of construction joint conditions	3
Interface shear transfer testing	4
Structural analyses: <ul style="list-style-type: none"> ▪ Finite element analysis ▪ Code evaluation of Member 11/12 deck connection (construction condition) ▪ Test-based Evaluation of Member 11/12 Deck Connection (construction condition) 	5
Evaluation of peer review	6
Evaluation of tilt exceedances during main span transport	7
Re-stressing of Member 11	8

WJE's studies were led by Gary J. Klein (Florida PE 85164), Senior Principal and Executive Vice President of WJE. Mr. Klein's resume is provided in Exhibit 1.1.

1.2 Project Background

The UniversityCity Prosperity Project was created by Florida International University (FIU) to connect the university campus in Miami with the City of Sweetwater. The centerpiece of the project was a pedestrian bridge over SW Eighth Street west of SW 109th Avenue. FIU awarded the design-build contract to Munilla Construction Management, Inc. (MCM). The designer, who was a consultant to MCM, was Figg Bridge Engineers, Inc. (FIGG).

Funding sources included federal, state, local and University contributions. The project was administered by FIU with support from the Florida Department of Transportation (FDOT). The primary parties involved in design and construction of the bridge are listed in Table 1.1.

Table 1.1. Involved Parties

Organization	Role
Florida International University (FIU)	Owner
Florida Department of Transportation (FDOT)	Project oversight and administration
Bolton Perez and Associates, Inc. (BPA)	Certified Engineering Inspector (CEI) for FIU
The Corradino Group (Corradino)	CEI Post-tensioning inspector for BPA
Munilla Construction Management, Inc. (MCM)	General contractor (design-build team leader)
The Structural Group of South Florida (Structural)	Concrete subcontractor to MCM
Structural Technologies /VSL, LLC (Structural/VSL)	Post-tensioning subcontractor to MCM
RC Group, LLC (RC Group)	Formwork and scaffold subcontractor to MCM
Barnhart Crane & Rigging Company (Barnhart)	Precast bridge transporter to MCM
Georges Crane Service, Inc. (Georges)	Crane supplier to MCM
Cemex (Cemex)	Concrete supplier to MCM
FIGG Bridge Engineers, Inc. (FIGG)	Lead structural designer to MCM
The Louis Berger Group, Inc. (Berger)	Independent peer review to FIGG

1.3 Structure Description

The pedestrian bridge design employed a post-tensioned concrete deck and canopy connected by structural concrete columns and diagonals along the centerline to form a two-span continuous truss. The design also featured a tapered pylon extending from the center support with stay pipes connected to the canopy that were intended to increase bridge stiffness and mitigate vibration from pedestrian loading. See cover photo for a rendering of the completed bridge.

Figure 1.1 is a photo of the main (south) span being moved to its final position on the south pier and central pier.

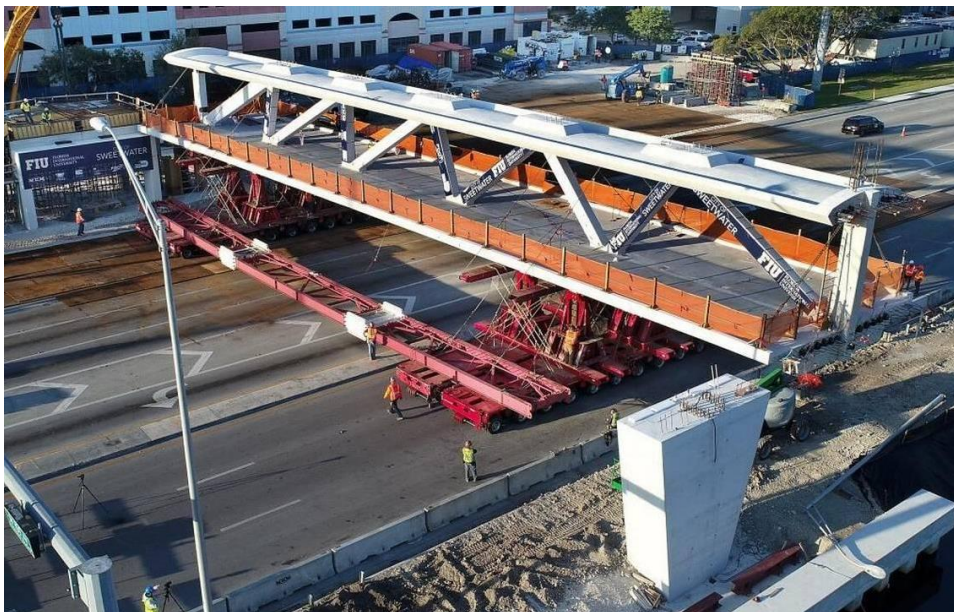


Figure 1.1. Main span being moved into its final position (Barnhart photo, March 10, 2018)

Figure 1.2 shows the key members at the north end of the main span. Member 11 is the northernmost diagonal framing between the canopy and deck. Member 12 supports the north end of the canopy in the main span. A 2-foot-wide diaphragm extends about 4 feet below the deck at the north end.

In the casting yard, the main span was oriented such that Members 11 and 12 were at the west end; however, cardinal directions referred to in this report are relative to the final position of the main span (Members 11 and 12 at the north end).

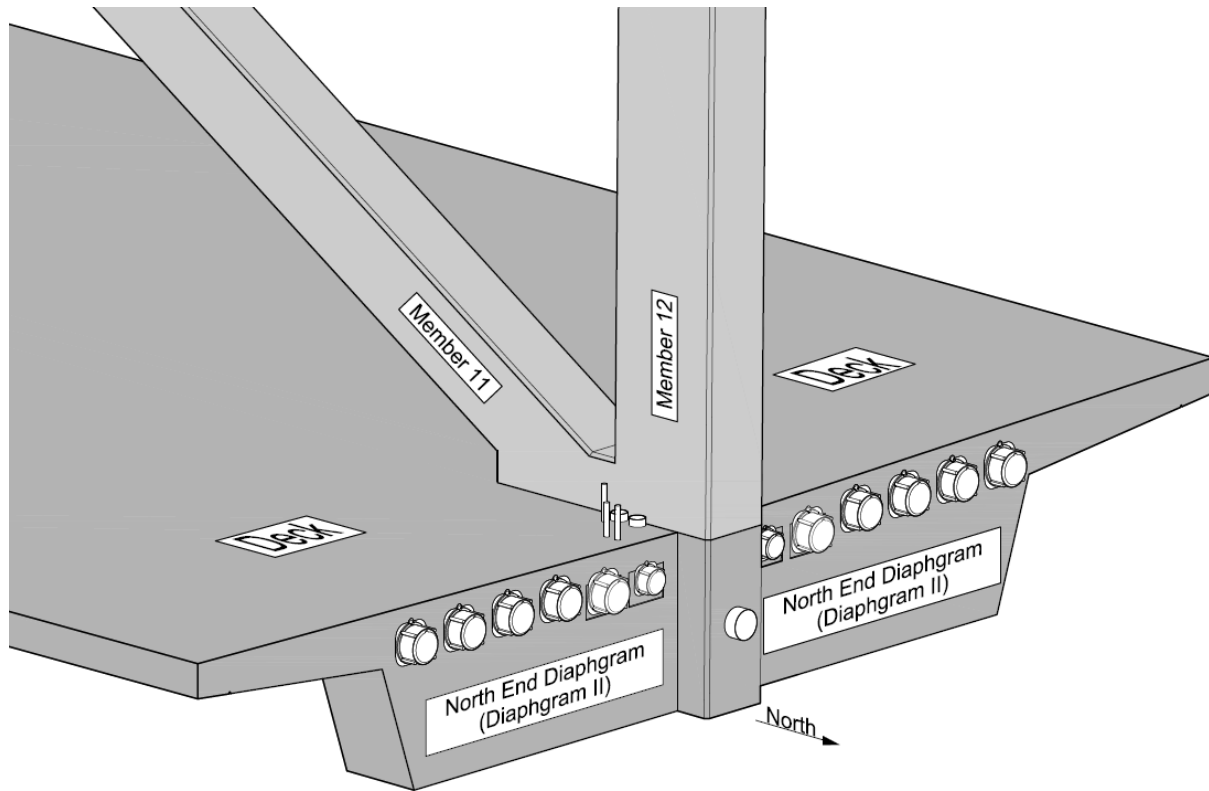


Figure 1.2. Key members at north end

1.4 Collapse Background

On March 15, 2018, at approximately 1:45 p.m., the main span collapsed as post-tensioning bars in the northernmost diagonal (Member 11) were being re-stressed. The collapse was triggered by failure of the connection between the Members 11 and 12 and the deck.

Exhibit 1.1



PERSONNEL QUALIFICATIONS

Gary J. Klein, P.E., S.E. | Executive Vice President and Senior Principal



EXPERIENCE

Gary Klein joined WJE in 1979 and has since investigated hundreds of concrete, steel, and wood structures. Most assignments have involved deterioration, distress, or failure of buildings and bridges. Mr. Klein's experience also includes the investigation of parking structures, tunnels, transit structures, stadiums, piers, environmental facilities, and wind turbines. Many of these studies have included repair design and construction observation services. He also has experience in vibration studies, nondestructive testing, load testing of structures and components, computer modeling of structures, and underwater inspection.

From 1973 to 1979, Mr. Klein worked at the Chicago firms of McDonough Engineering, Inc. (formerly Murphy Engineering, Inc.) and Howard Needles Tammen and Bergendoff (HNTB). While with these firms, he was responsible for structural design and plan preparation for new construction as well as investigation and rehabilitation of existing structures.

REPRESENTATIVE PROJECTS

Bridge Engineering

- Loop Road Bridge - VA: Structural investigation, repair design, and expert testimony
- Wacker Drive Viaduct - Chicago, IL: Durability research, prototype testing, and health monitoring
- Ford Parkway Bridge - Minneapolis, MN: Structural investigation and preservation recommendations
- Venetian Causeway - Miami, FL: Historic preservation study
- Hamakua Coast Steel Trestle Bridges - Hilo, HI: Structural investigation and load testing
- Illinois River Bridge - IL: Design of a twin segmental box-girder bridge (with HNTB)

Collapse Investigation

- I-35W Mississippi River Bridge - Minneapolis, MN: Participated in collapse investigation for MnDOT in cooperation with NTSB
- Kansas City Hyatt Regency Hotel - Kansas City, MO: Suspended walkway collapse
- I-80/94/294 Interchange at IL 394 - Lansing, IL: Collapse of Ramp J framing during erection
- Koror-Babeldaob Bridge - Republic of Palau: 790-foot concrete box-girder span over the Toegel Channel
- Los Angeles Metro Red Line - Los Angeles, CA: Subway tunnel collapse during re-mining
- Central Artery /Tunnel Project (The Big Dig) - Boston MA: Safety audit of tunnel and bridge structures following ceiling collapse

Repair and Rehabilitation Design

- Chicago and Northwestern Trainshed - Chicago, IL: Structural rehabilitation
- Grant Park North Garage - Chicago, IL: Structural rehabilitation
- Soldier Field - Chicago, IL: Structural rehabilitation

Research and Testing

- Dapped Ends Prestressed Concrete Thin-Stemmed Members , PCI 2016
- Development of a Rational Design Methodology for Precast Concrete Slender Spandrel Beams, PCI 2011
- Predicting Volume Change Movements and Forces in Buildings, PCI 2002

TECHNICAL COMMITTEES

- ACI 318 - Standard Building Code
- ACI 318J - Joints and Connections
- ACI 318E - Section and Member Strength
- ACI 378 - Wind Turbines
- ACI 445 - Shear and Torsion
- ACI 445A - Strut-and-Tie Method
- National Construction Safety Team Advisory Committee

EDUCATION

- University of Illinois at Urbana-Champaign
- Bachelor of Science, Civil Engineering, 1973
- Master of Science, Civil Engineering, 1975

PRACTICE AREAS

- Bridge Engineering
- Collapse Investigation
- Historic Preservation
- Repair and Rehabilitation Design
- Structural Research and Testing
- Structural Analysis/Computer Modeling
- Structural Investigation
- Underwater Inspection

REGISTRATIONS

- Professional Engineer in AZ, FL, IL, KY, and MI
- Structural Engineer in IL and MA

PROFESSIONAL AFFILIATIONS

- National Academy of Engineering
- American Concrete Institute
- American Society of Civil Engineers
- Precast/Prestressed Concrete Institute
- Structural Engineers Association of Illinois

2 EVALUATION OF FAILURE PATTERN

The objective of this evaluation is to assess the sequence of distress and failure in vicinity of the Member 11/12 deck connection that led to the collapse of the bridge. Evaluation of the failure sequence is based on photographs taken before and after the collapse.

2.1 Document Review

Assessment of the progression of the cracking at the Member 11/12 region was mainly based on available photographs. Explanation of the sources and observation of key documents pertaining to the cracking are provided in the following sections.

2.1.1 Photographs

Assessment of the failure sequence was dependent on photographs from various sources. A list of sources of photographs used in this report are included in Table 2.1.

Table 2.1. Source of Figures

Source	Dates	Notes
OSHA Report: <i>“Investigation of March 15, 2018 Pedestrian Bridge Collapse at Florida International University, Miami, FL”</i>	Photos: Feb 24, 2018-Apr 2019 Report: June 2019	Pre-collapse and post-collapse photos credited to BPA
Corradino	Mar 10, 2018	
MCM	Mar 12, 2018	Email from MCM to FIGG
WJE	Mar 19, 2018	

2.1.2 Video

Several videos of the collapse were reviewed by WJE. The only non-time-lapse video available to WJE was taken from a vehicle’s dashboard camera as the vehicle headed east on SW Eighth Street. Frames extracted from the video at the time of the collapse are shown in Figure 2.1 to Figure 2.4. Note the frames have been cropped from the original video.



Figure 2.1. Video frame at start of collapse



Figure 2.2. Video frame during collapse

Note: Redaction in "Figures 2.1 and 2.2" as per NTSB Operations Bulletin CIO-GEN-016.



Figure 2.3. Video frame during collapse



Figure 2.4 Video frame during collapse

2.1.3 OSHA Report

OSHA produced a report summarizing its investigation into the cause of the collapse. OSHA collected photographs of the cracking in Member 11/12 region. The majority of photos in the report were taken by BPA. WJE utilized the photos taken by BPA to develop a crack sequence. WJE also used the post-collapse photographs from the OSHA report for evaluation of post-collapse conditions and the construction joint below Member 11. The OSHA report was used as a source of photographs only; WJE did not rely on or necessarily agree with findings in the OSHA report.

2.2 Analysis of Photos and Videos

WJE produced a series of images showing the sequence of cracking and the condition of the bridge after the collapse. WJE created both 2D and 3D images to assist in locating reinforcing steel, post-tensioning, deck penetrations, and crack locations.

2.2.1 Pre-Move (Before March 9, 2018): Exhibits 2.1.1 to 2.1.3

The span was precast on falsework and shoring in a staging area on the south side of SW Eighth St. Falsework and shoring removal started on February 23, 2018. Shoring at the midspan was removed first and continued outwards towards the deck-end diaphragms. All shoring was removed by February 25, 2018. The bracing for the deck-end diaphragms remained in place until the bridge was ready to be lifted by Barnhart.

The Construction Engineering Inspector for the project, BPA, completed a truss crack inspection on February 6, 2018. Minor cracks in several truss members were noted, but no cracking or distress was reported at or near the connection of Members 11 and 12 to the deck. It should be noted that debonding of the construction joint below Members 11 and 12 may have occurred before February 6 due to post-tensioning and thermal stresses, but it is highly unlikely that the crack inspection would have detected it.

The first known indication of distress in the Member 11/12 region was documented in a crack report prepared by BPA on February 28, 2018. The observed crack occurred between Member 11 and the deck chamfer or “wedge.” Although difficult to see, debonding and northward sliding of Member 11 is also evident in the photograph. BPA did not measure the crack; however, a vertical marking, consistent with techniques used to visually track crack growth, is drawn across the crack.

Note: Redaction in "Figures 2.3 and 2.4" as per NTSB Operations Bulletin CIO-GEN-016.

On March 8, a Barnhart photo documented a crack on the topside of the deck, west of Member 12. Crack width was not measured. No photograph was taken on the east side of Member 12; however, WJE assumes that a matching crack likely occurred on the east side, based upon the symmetry shown by future cracking.

2.2.2 Post-Move and before De-tensioning (March 10, 2018): Exhibits 2.2.1 to 2.2.3

The bridge was placed on its final supports at approximately 12:30 p.m. on March 10, 2018. The bridge remained in this state until approximately 4:30 p.m. when VSL de-tensioned Member 11. During this time frame, at approximately 3:07 p.m., the on-site post-tensioning inspector, Corradino, took photos of the deck near Members 11 and 12. These photos show widening of the cracks documented in Exhibits 2.2.1 to 2.2.3.

These photos show widening of the “wedge” crack. Analysis of this crack profile suggests that Member 11 slid northwards while the “wedge” stayed attached to the deck. This is evident from post-collapse photographs to be discussed later. Some of the cracking on the topside of the deck, adjacent to Member 12, developed into spalls and detached from the deck. Member 11 also developed longitudinal cracks generally in line with the longitudinal PT bars.

2.2.3 Two Days after Move (March 12, 2018): Exhibits 2.3.1 to 2.3.3

Two days after the move, MCM documented the cracks and sent an email to FIGG asking for a review. Conditions generally appear similar to those shown in Exhibits 2.2.1 to 2.2.3 but with several of the cracks appearing to have slightly widened.

Several new crack patterns developed as well. It is not known if these existed on March 10 and were not documented, or if they initiated after March 10. Notably, a photograph east of Member 12, looking down on the deck, shows northward faulting of the deck-end diaphragm closest to Member 12. As the deck-end diaphragm displaces north, the base of Member 12 goes into curvature inducing flexural cracks on the north face (the tension face).

An additional longitudinal crack developed near the base of Member 11. WJE believes the development and widening of this crack is a result of additional sliding.

2.2.4 One Day before Collapse (March 14, 2018): Exhibits 2.4.1 to 2.4.3

One day before the collapse, conditions appear generally similar to those shown in Exhibits 2.3.1 to 2.3.3 with several of the cracks appearing to have widened further. Longitudinal cracking and spalling along the east and west faces at the base of Member 11 appears to have progressed. These longitudinal cracks divide Member 11 into individual laminar sections or “teeth.” As the cracks widen, Member 11 no longer acts as a fully composite member. Instead, the laminar planes begin to behave independently and each tooth is subject to flexural stress.

2.2.5 Post Collapse: Exhibits 2.5.1 to 2.5.4

In the following ways, the video and photographic evidence indicates the collapse was triggered by sudden columnar crushing of the teeth at the base of Member 11:

- Post-collapse photos show the laminar fragments or “teeth” at the base of Member 11 have completely failed and separated from Member 11 indicating a sudden failure. Photographs taken before the collapse shows progressive growth of these cracks.
- Video of the collapse shows hinging of the truss at the top of Member 11, which is consistent with shortening of Member 11 due to sudden failure near the deck. Furthermore, the video evidence does

not indicate northward movement at the base of Member 12, which would be expected if the collapse was triggered by sudden and extreme northward sliding and breakout.

- Member 12 was relatively undamaged compared to Member 11. Small portions of the deck stayed intact with Member 12. The observed damage to the lower end of Member 12 is consistent with secondary damage due to the collapse and does not coincide with the cracking observed before the collapse.
- The breakout of the deck-end diaphragm is consistent with the cracking seen in previous days. Concrete damage on areas adjacent to the breakout are shallow and consist mostly of spalling of the concrete cover.
- The construction joint between Member 11 and the deck is relatively unscathed, indicating extreme sliding of Member 11 was not part of the ultimate collapse sequence. Further assessment of the construction joint and sliding resistance is evaluated in Sections 3 and 4.
- Although the collapse was triggered by sudden failure at the base of Member 11, the underlying cause was northward movement of Members 11 and 12 relative to the deck. As described above, the northward movement started with a shear-friction failure below Member 11 that, in turn, led to breakout failure of the north-end diaphragm below Member 12.

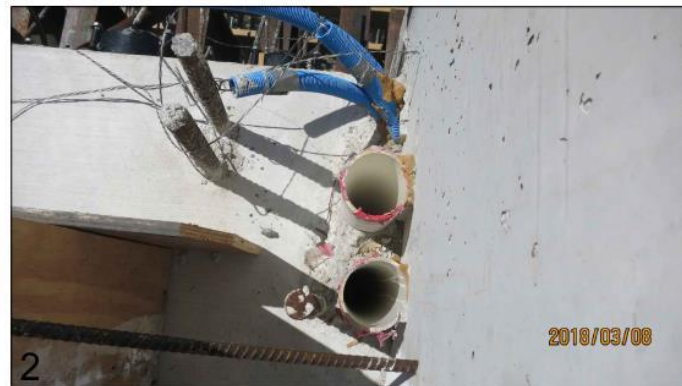
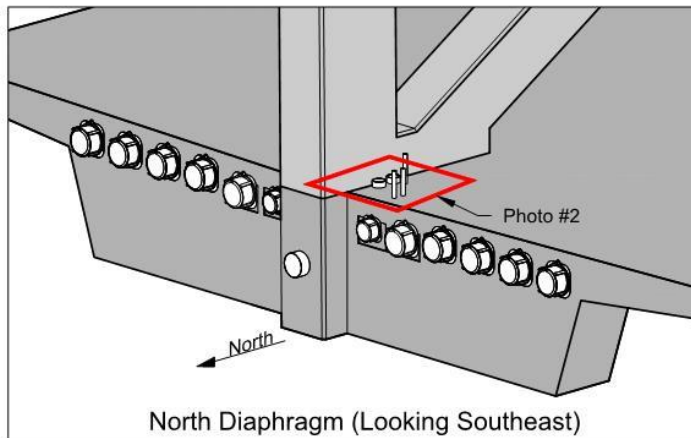
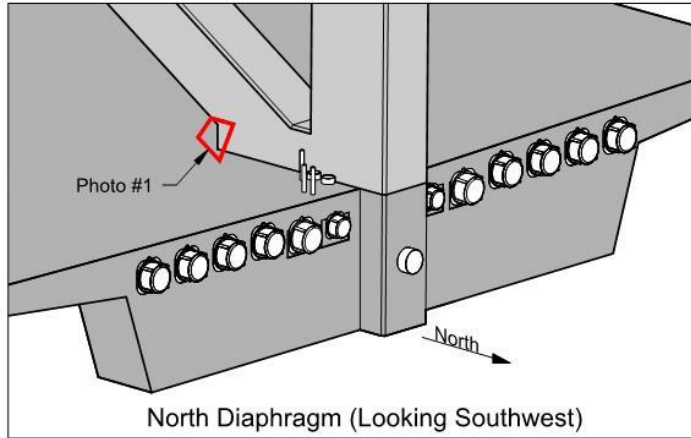
2.3 Findings

The following findings are based on the review and analysis described above:

- Cracking initiated in the Member 11/12 region after shoring was removed due to loss of bond and sliding at the construction joint below Member 11. This type of interface shear transfer failure is also referred to as a shear-friction failure.
- Cracking substantially worsened *after* the bridge was placed in its final location on south pier (End Bent 1) and central pier, *before* Member 11 was de-tensioned. Northward sliding of Member 11 led to breakout failure of the north-end diaphragm below Member 12, while existing cracks continued to widen. New cracks developed as the base of Member 11 as it separated into laminar sections or “teeth.”
- Cracking continued to worsen until the bridge collapsed. The collapse was triggered by sudden crushing of Member 11 near its base. After the base of Member 11 was lost, a hinge in the truss developed near the top of Member 11. Additional damage developed in the connection region as the collapse progressed, including severe damage to the base of Member 12 and the north-end diaphragm.

In summary, a debonding and sliding failure at the construction joint below Member 11 led to breakout failure of the north-end diaphragm and ultimately collapse, triggered by sudden crushing of Member 11 near its base. The reasons for the connection failure are addressed in subsequent sections of this report.

Exhibit 2.1.1
OBSERVED AND ESTIMATED CRACKS AT MEMBER 11/12 DECK CONNECTION
Shoring Removal to Pre-Move (Before March 9, 2018)



Photos

1. East side of Member 11. Included in crack report email on February 28, 2018 from Jose Morales (BPA) to Rodrigo Isaza (MCM).
2. Topside of deck end diaphragm II, west of Member 11. Produced by Barnhart. Photo dated March 8, 2018.

Exhibit 2.1.2
OBSERVED AND ESTIMATED CRACKS AT MEMBER 11/12 DECK CONNECTION
Shoring Removal to Pre-Move (Before March 9, 2018)

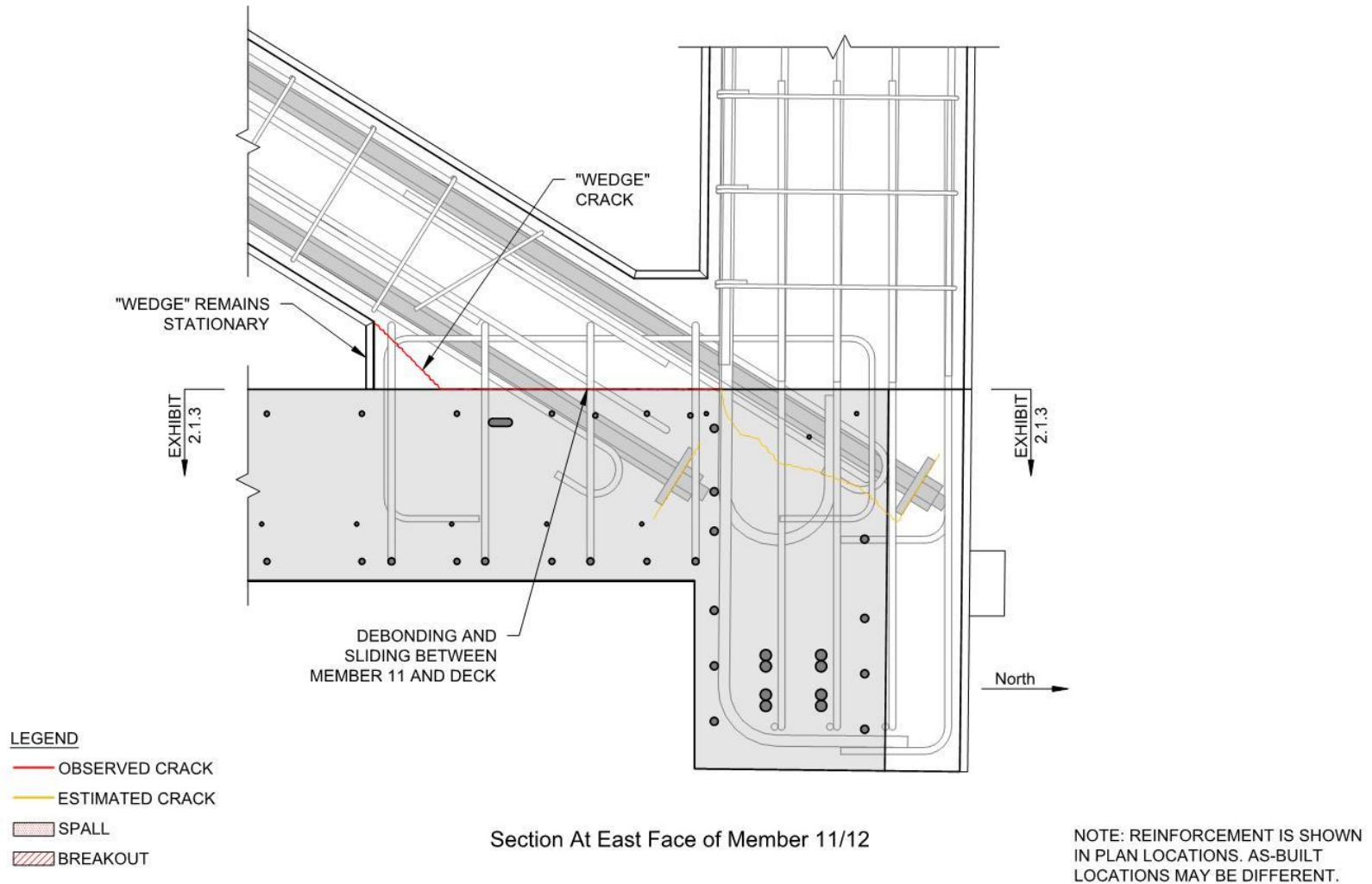


Exhibit 2.1.3
OBSERVED AND ESTIMATED CRACKS AT MEMBER 11/12 DECK CONNECTION
Shoring Removal to Pre-Move (Before March 9, 2018)

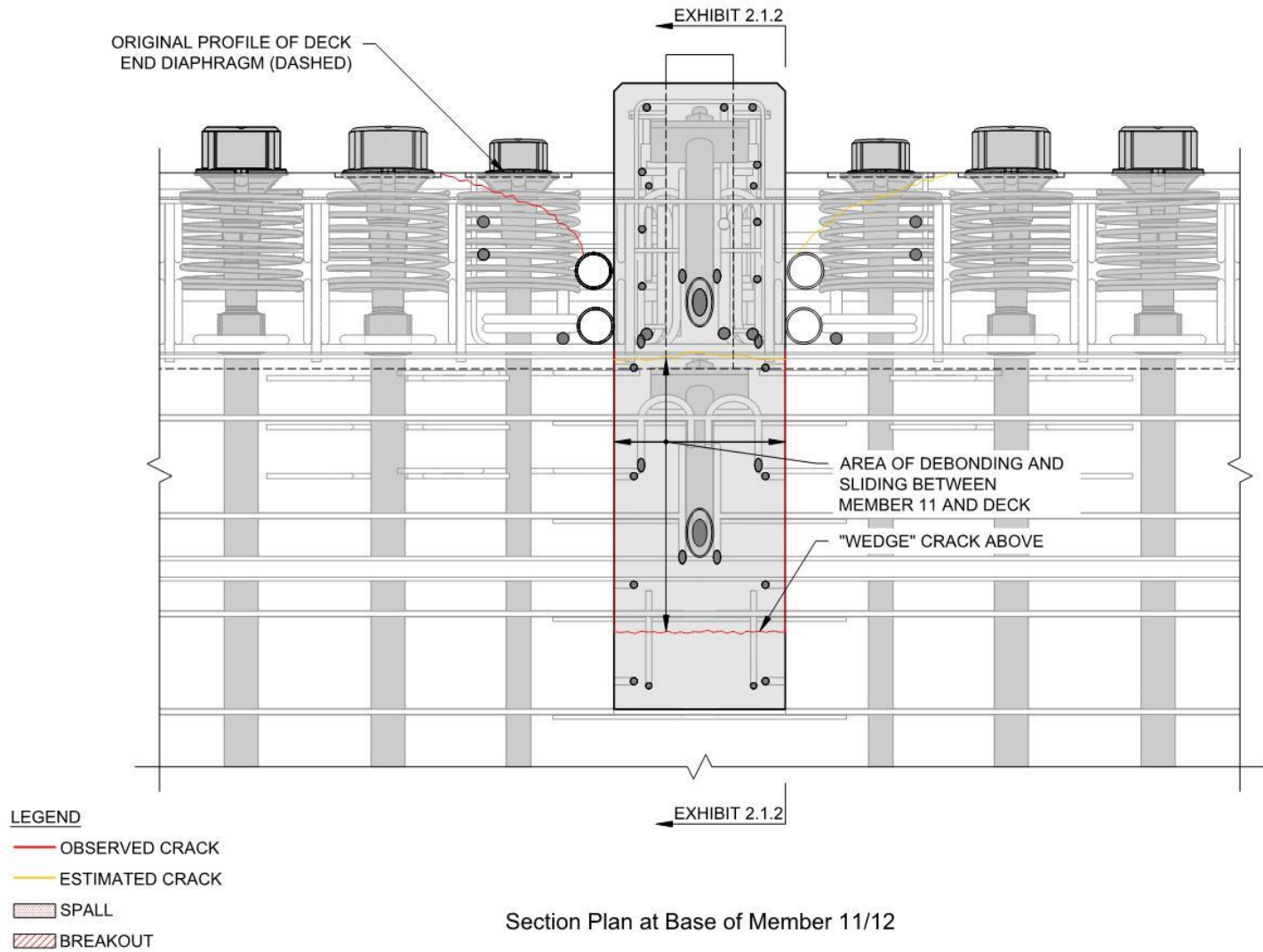
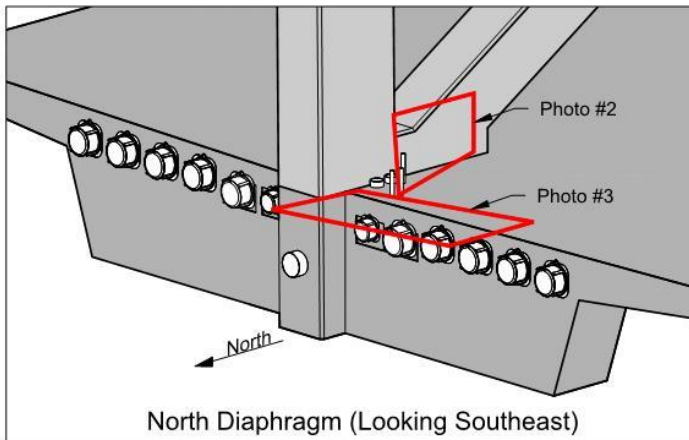
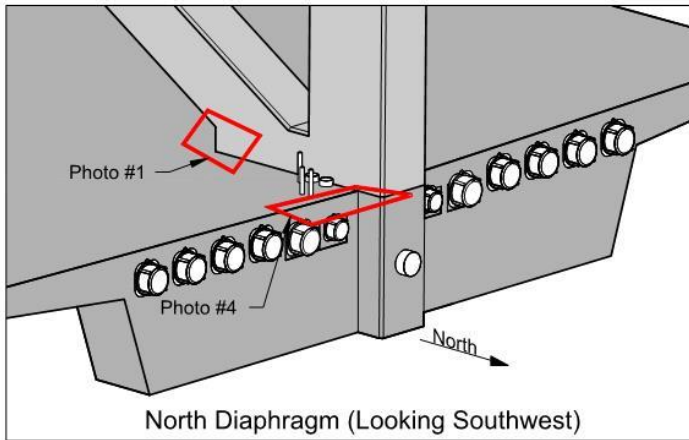


Exhibit 2.2.1
OBSERVED AND ESTIMATED CRACKS AT MEMBER 11/12 DECK CONNECTION
Post-Move (March 10, 2018)



Photos

1. East side of Member 11. Photo taken by Coradino. Photo metadata is time stamped 3:07 PM on March 10, 2018.
2. West side of Member 11. Photo taken by Coradino. Photo metadata is time stamped 3:07 PM on March 10, 2018.
3. Topside of deck end diaphragm II, west of Member 12. Photo taken by Coradino. Photo metadata is time stamped 3:14 PM on March 10, 2018.
4. Topside of deck end diaphragm II, west of Member 12. Photo taken by Coradino. Photo metadata is time stamped 3:14 PM on March 10, 2018.

Exhibit 2.2.2
OBSERVED AND ESTIMATED CRACKS AT MEMBER 11/12 DECK CONNECTION
Post-Move (March 10, 2018)

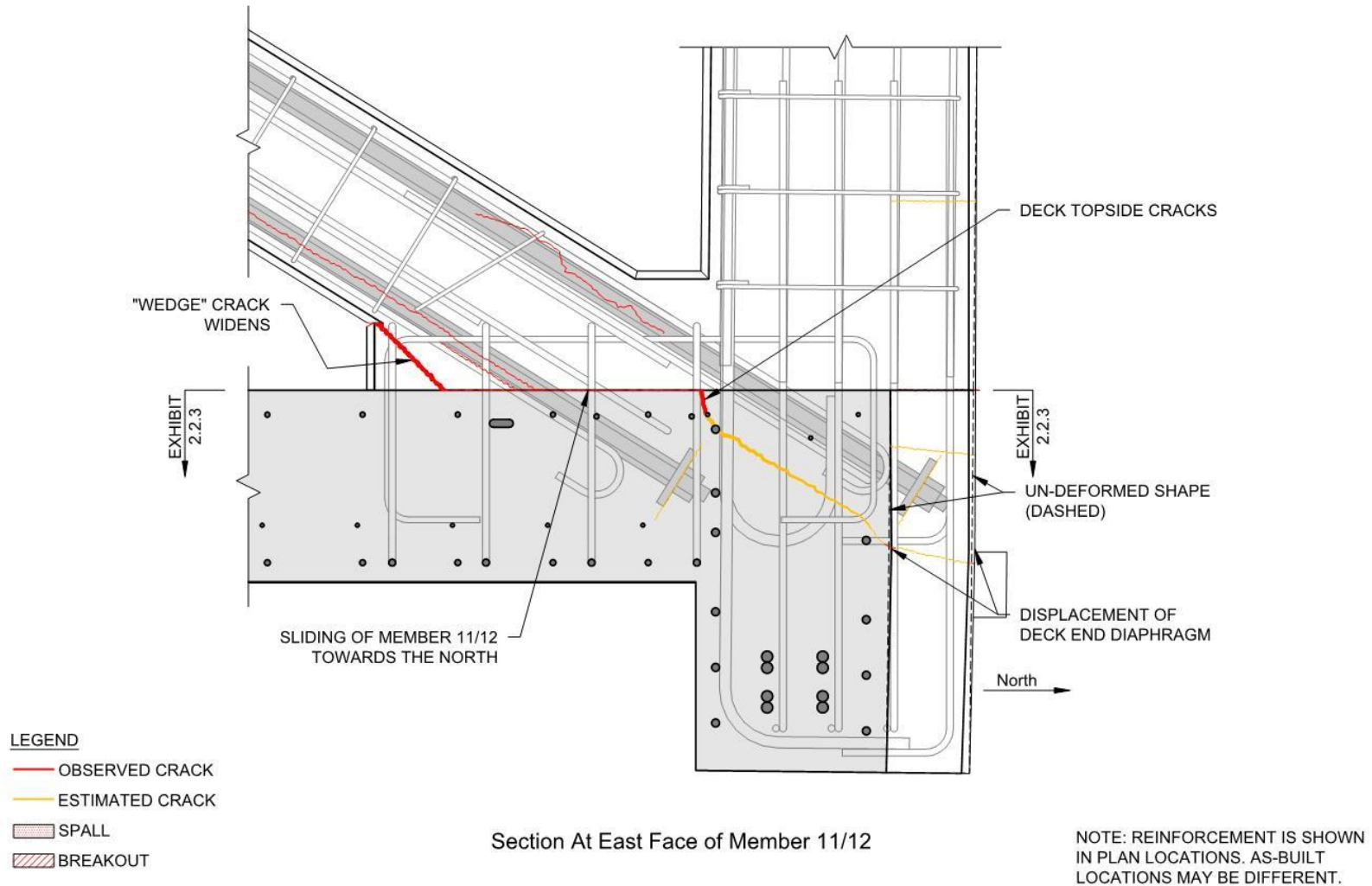


Exhibit 2.2.3
OBSERVED AND ESTIMATED CRACKS AT MEMBER 11/12 DECK CONNECTION
Post-Move (March 10, 2018)

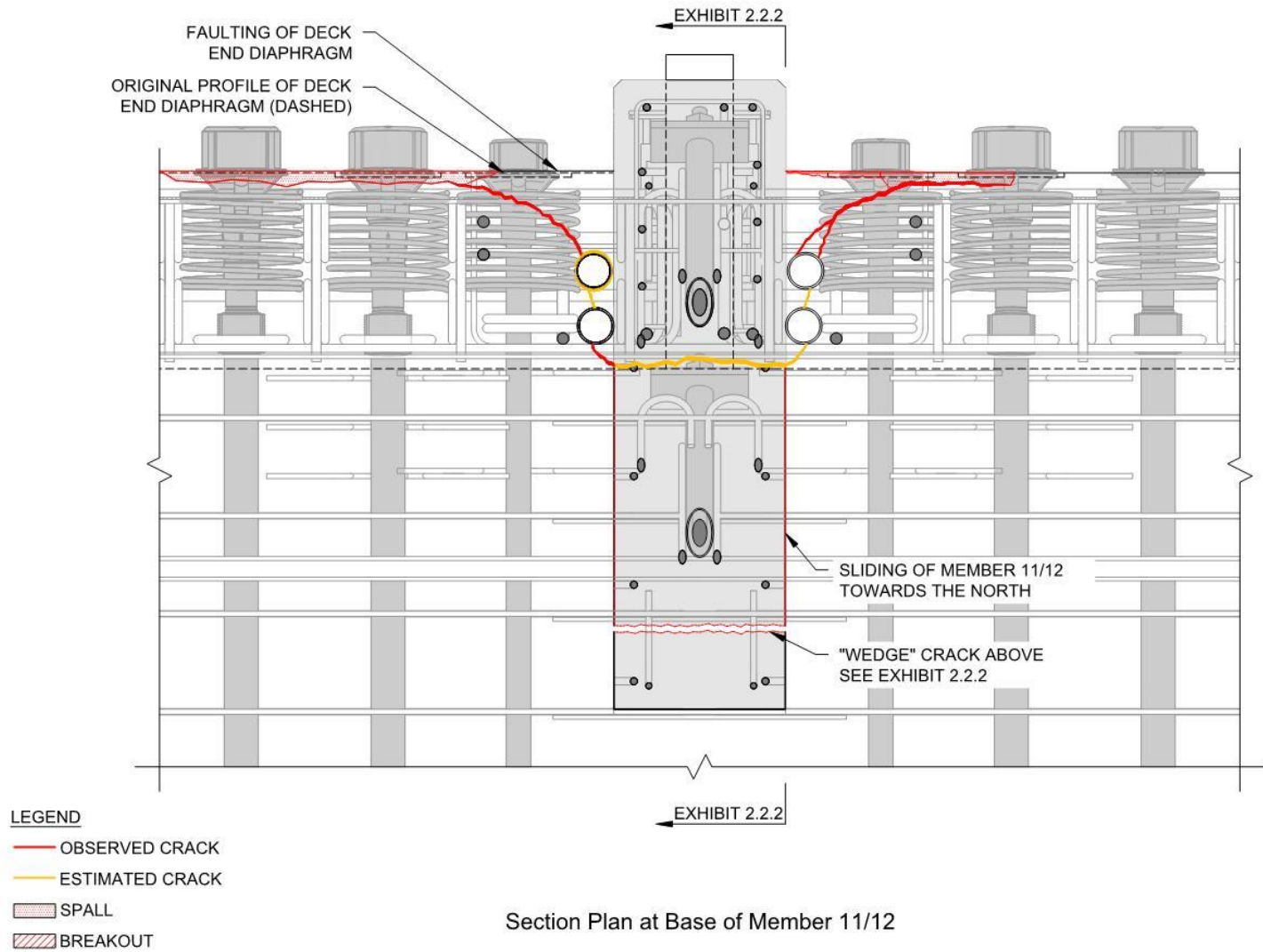
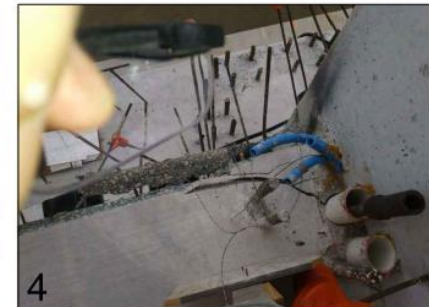
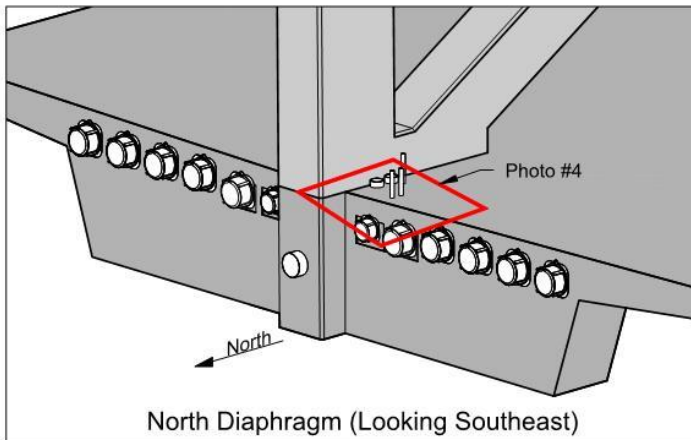
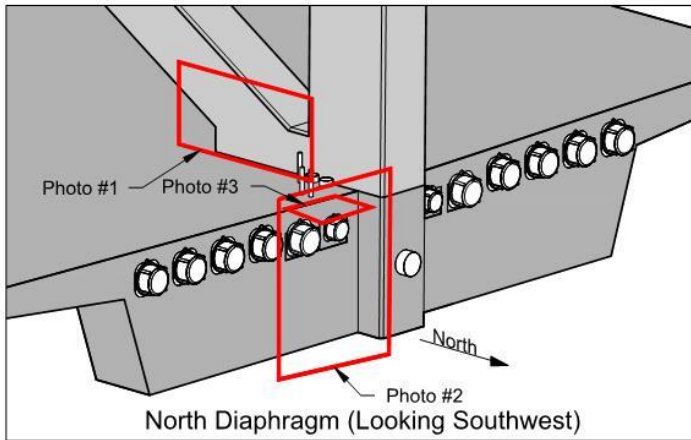


Exhibit 2.3.1
OBSERVED AND ESTIMATED CRACKS AT MEMBER 11/12 DECK CONNECTION
Two Days After Move (March 12, 2018)



Photos

1. East of member 11, looking west. Photo included in email from MCM to FIGG on March 12, 2018.
2. North end of deck end diaphragm II, east of Member 12, looking south west. Photo included in email from MCM to FIGG on March 12, 2018.
3. North end of deck end diaphragm, east of Member 12, looking down. Photo included in email from MCM to FIGG on March 12, 2018.
4. Topside of deck end diaphragm II, west of Member 12. Photo included in email from MCM to FIGG on March 12, 2018.

Exhibit 2.3.2
OBSERVED AND ESTIMATED CRACKS AT MEMBER 11/12 DECK CONNECTION
Two Days After Move (March 12, 2018)

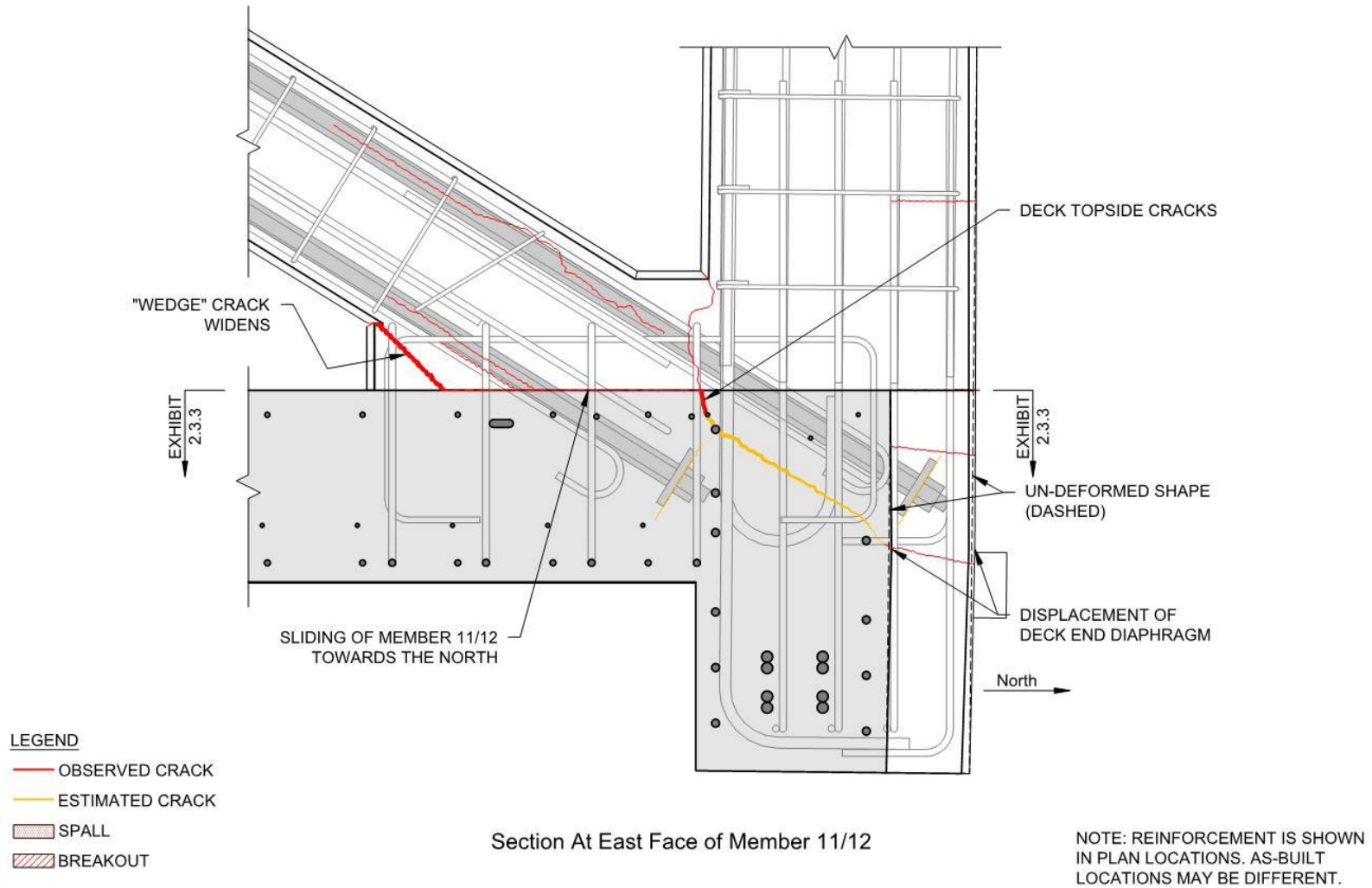


Exhibit 2.3.3
OBSERVED AND ESTIMATED CRACKS AT MEMBER 11/12 DECK CONNECTION
Two Days After Move (March 12, 2018)

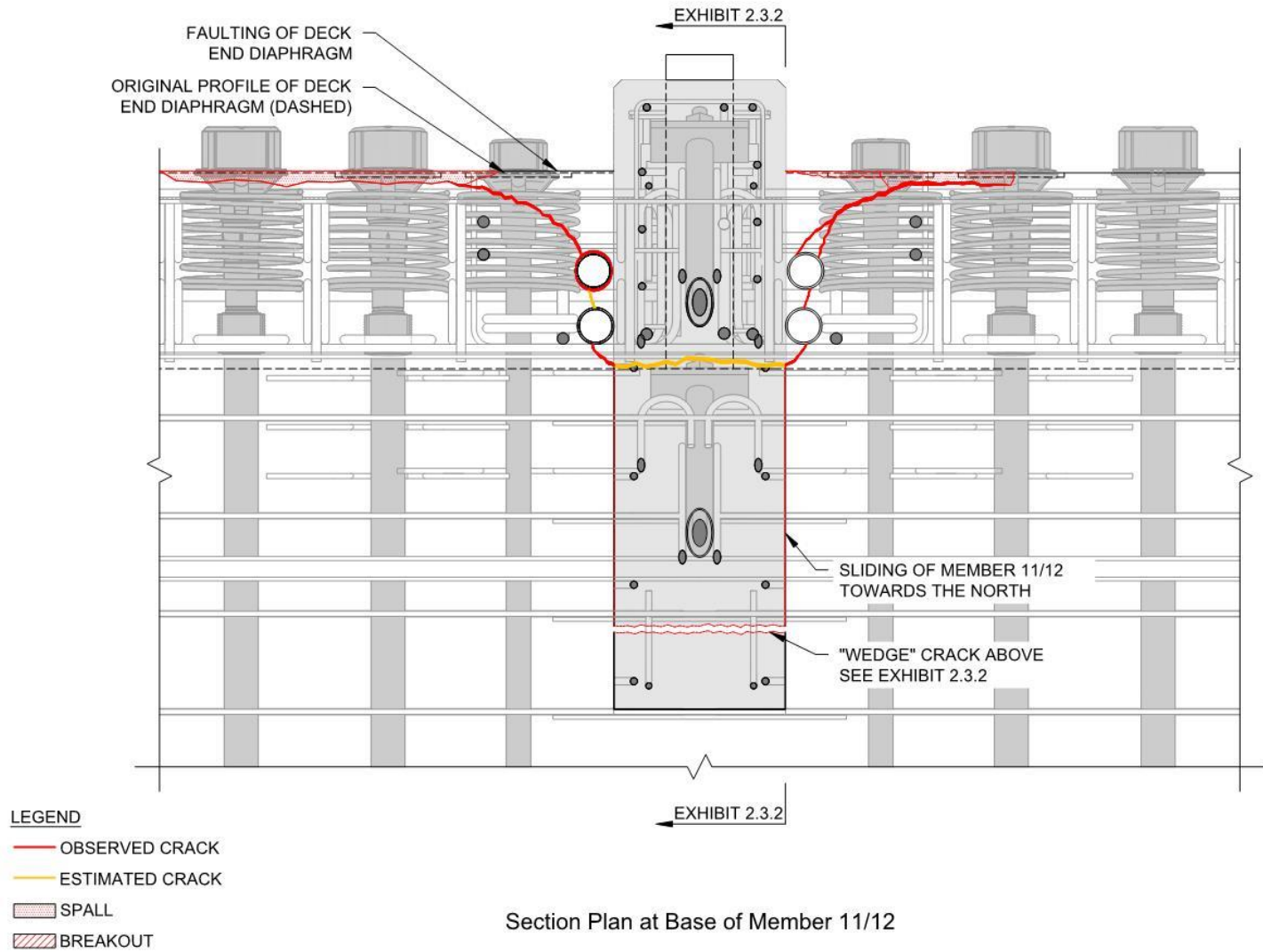
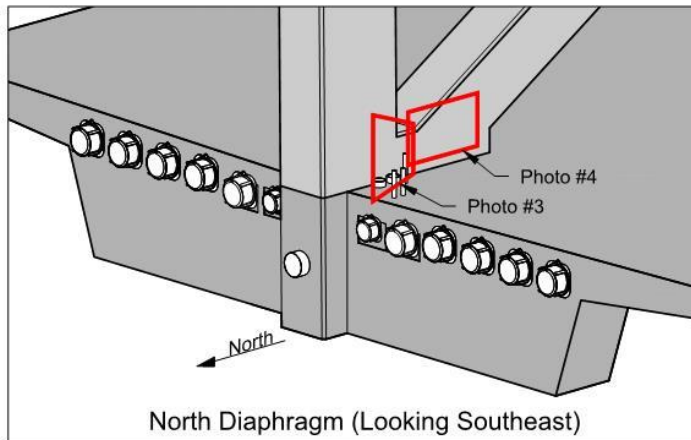
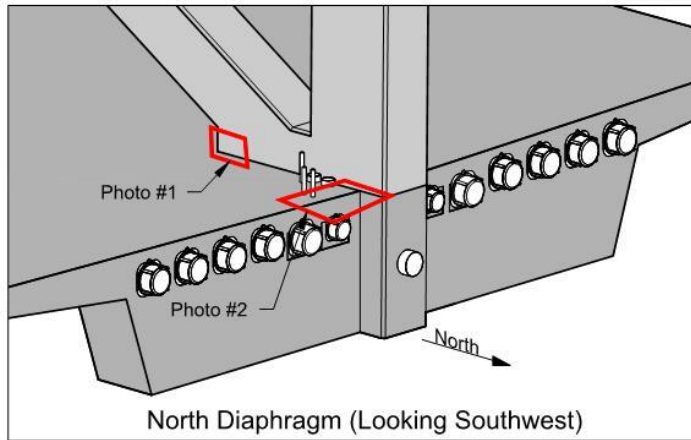


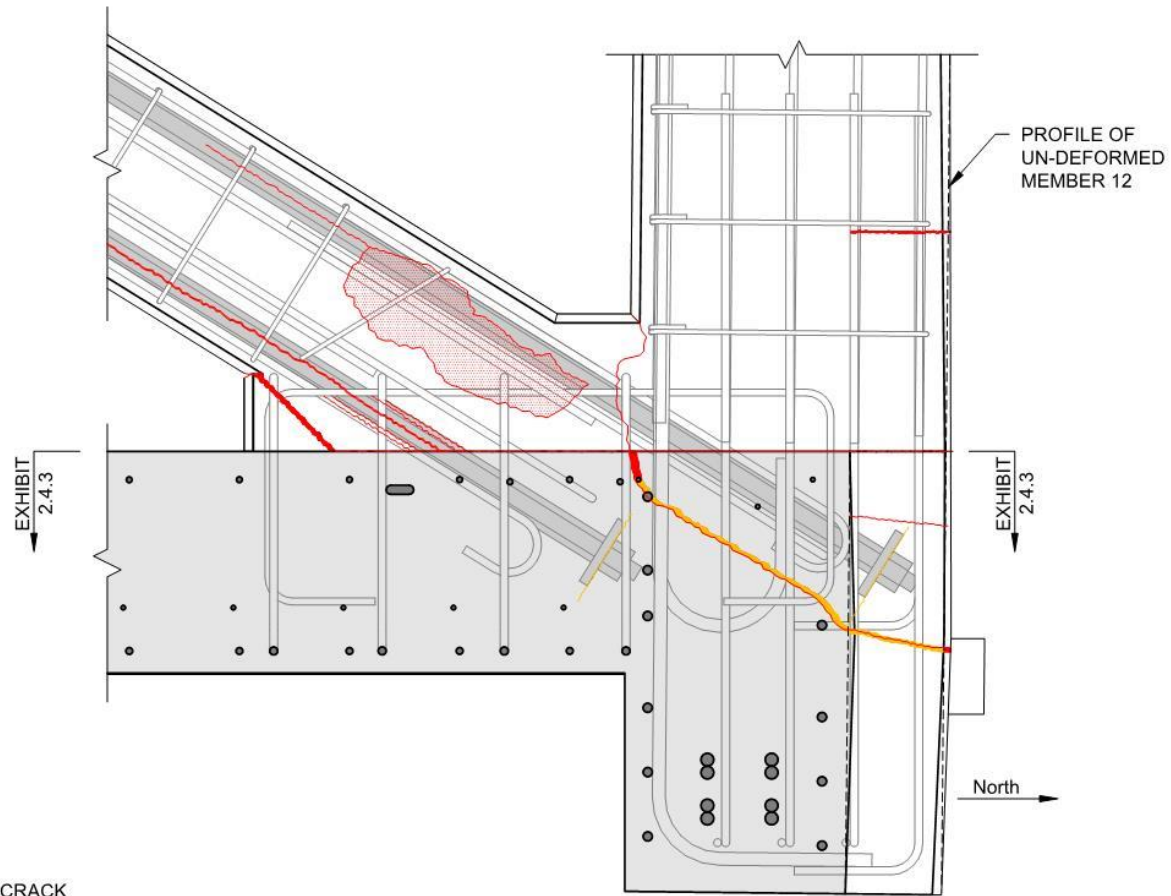
Exhibit 2.4.1
OBSERVED AND ESTIMATED CRACKS AT MEMBER 11/12 DECK CONNECTION
One Day Before Collapse (March 14, 2018)



Photos

1. East side of Member 11. Photo taken on March 14, 2018 by BPA.
2. Topside of deck end diaphragm II and east side of Member 11/12, looking northeast. Photo taken on March 14, 2018 by BPA.
3. Topside of deck end diaphragm II, east of Member 12, looking down. Photo taken on March 14, 2018 by BPA.
4. West side of Member 11. Photo taken on March 14, 2018 by BPA.

Exhibit 2.4.2
OBSERVED AND ESTIMATED CRACKS AT MEMBER 11/12 DECK CONNECTION
One Day Before Collapse (March 14, 2018)



LEGEND

- OBSERVED CRACK
- ESTIMATED CRACK
- SPALL
- BREAKOUT

Section At East Face of Member 11/12

NOTE: REINFORCEMENT IS SHOWN
IN PLAN LOCATIONS. AS-BUILT
LOCATIONS MAY BE DIFFERENT.

Exhibit 2.4.3
OBSERVED AND ESTIMATED CRACKS AT MEMBER 11/12 DECK CONNECTION
One Day Before Collapse (March 14, 2018)

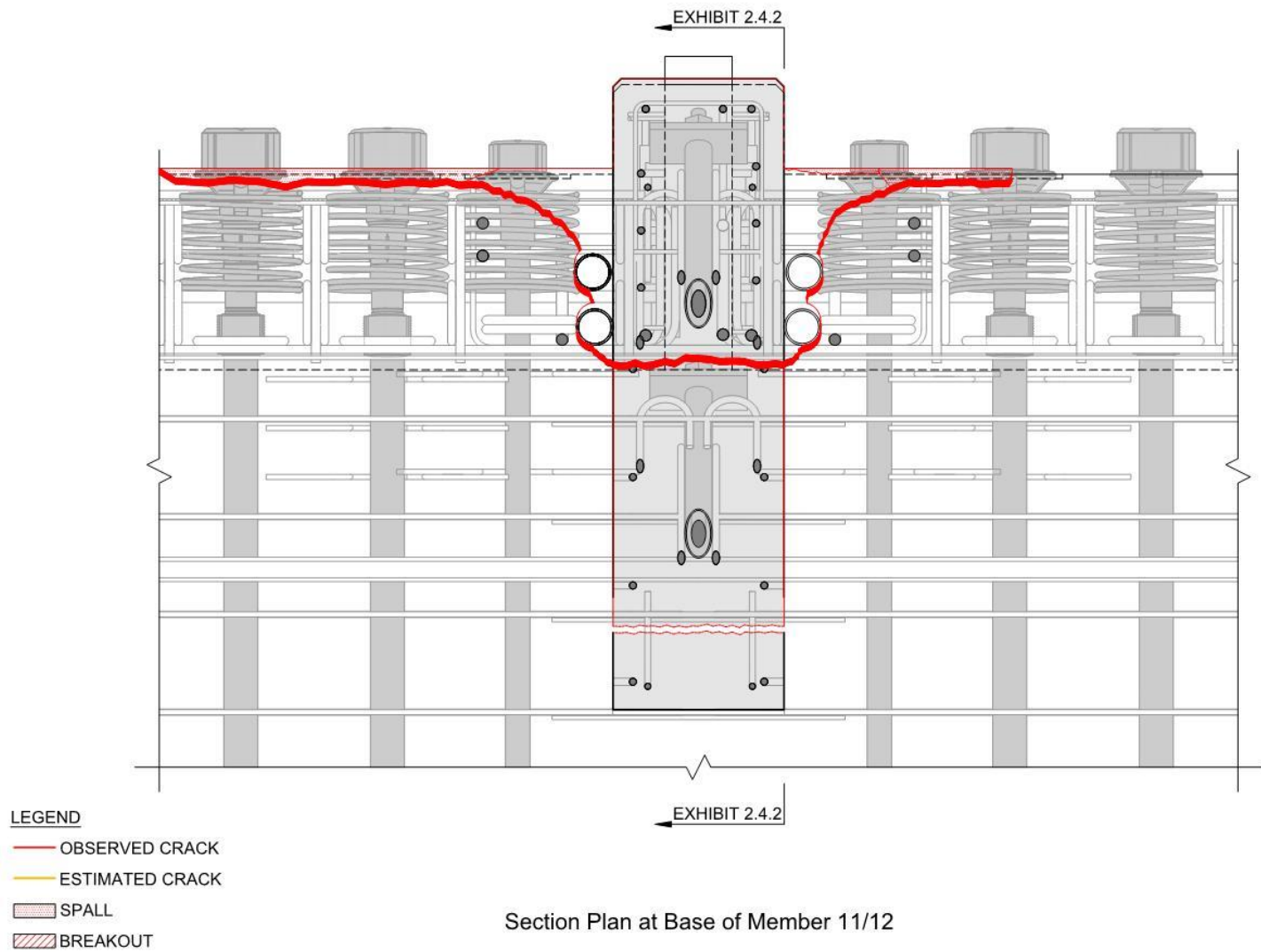
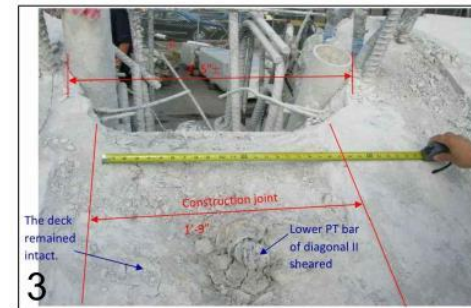
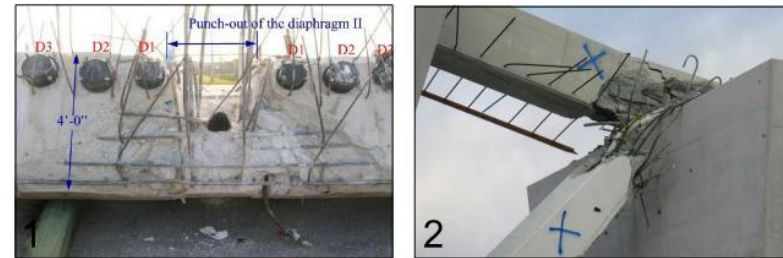
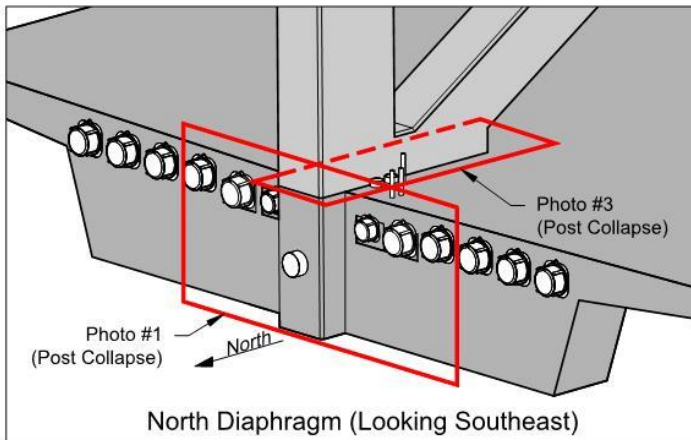
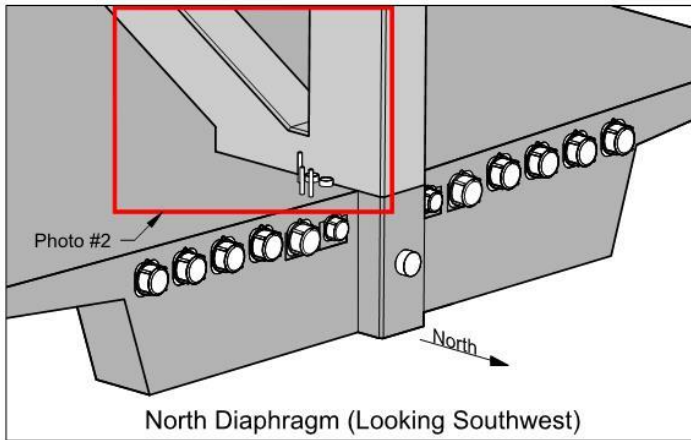


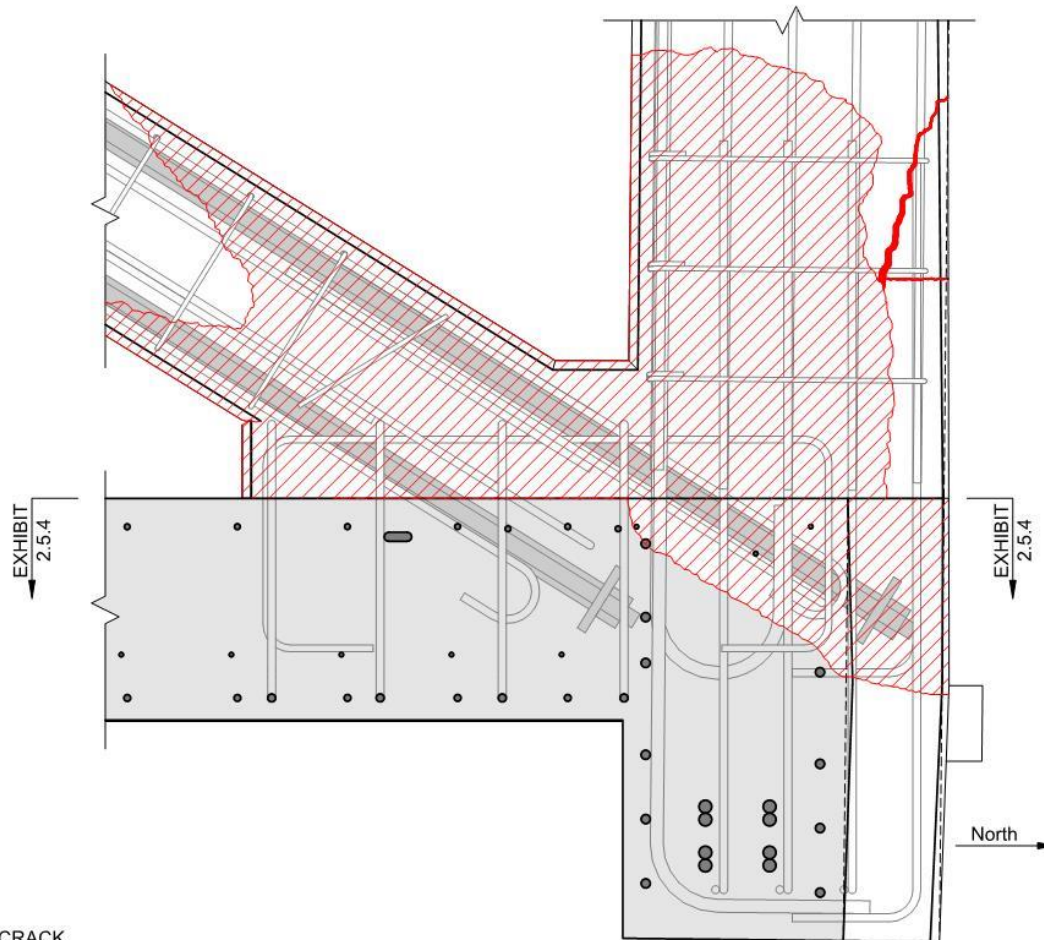
Exhibit 2.5.1
OBSERVED AND ESTIMATED CRACKS AT MEMBER 11/12 DECK CONNECTION
After Collapse (March and April, 2018)



Photos

1. North end of deck end diaphragm II, post collapse. OSHA report figure 62, dated April 8, 2018.
2. East side of Member 11&12. Taken by WJE on March 19, 2018.
3. Topside of north deck under Member 11&12, post collapse. OSHA report figure 63, dated April 8, 2018.

Exhibit 2.5.2
OBSERVED AND ESTIMATED CRACKS AT MEMBER 11/12 DECK CONNECTION
After Collapse (March and April, 2018)

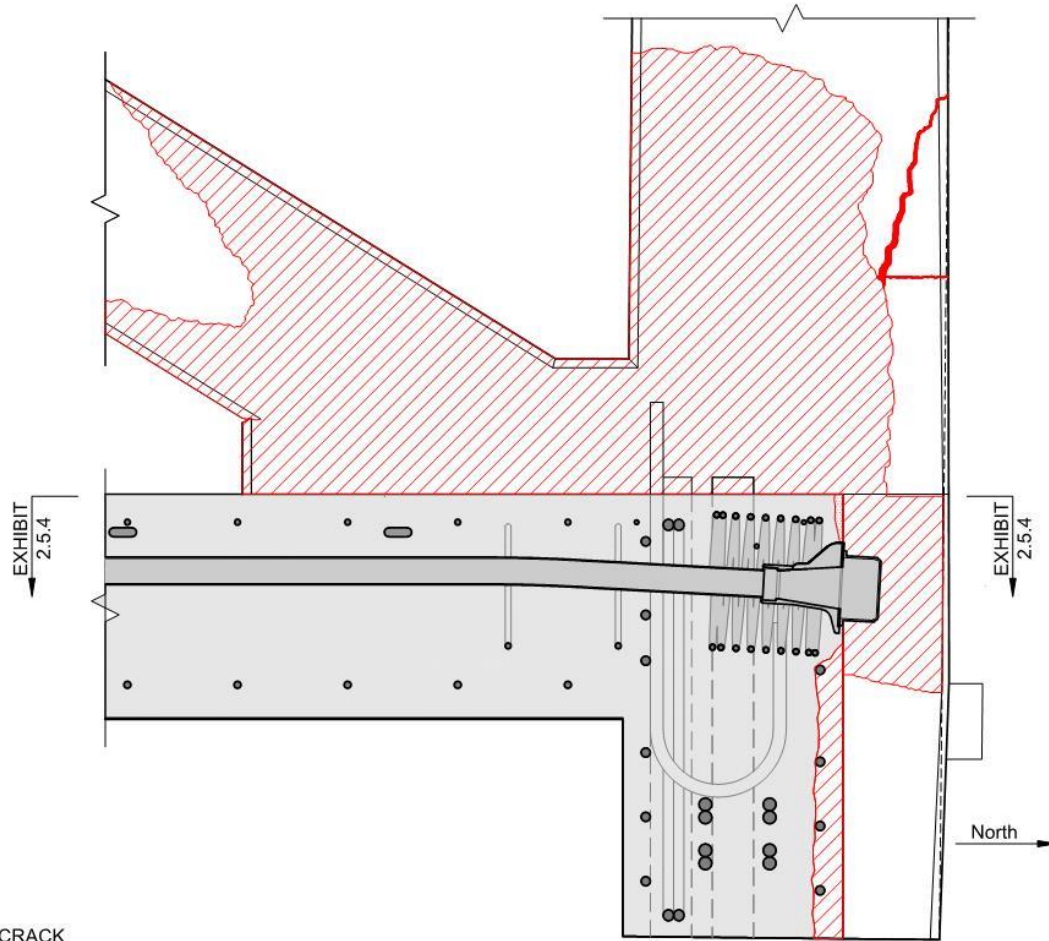


- LEGEND**
- OBSERVED CRACK
 - ESTIMATED CRACK
 - ▨ SPALL
 - ▨ BREAKOUT

Section At East Face of Member 11/12

NOTE: REINFORCEMENT IS SHOWN
IN PLAN LOCATIONS. AS-BUILT
LOCATIONS MAY BE DIFFERENT.

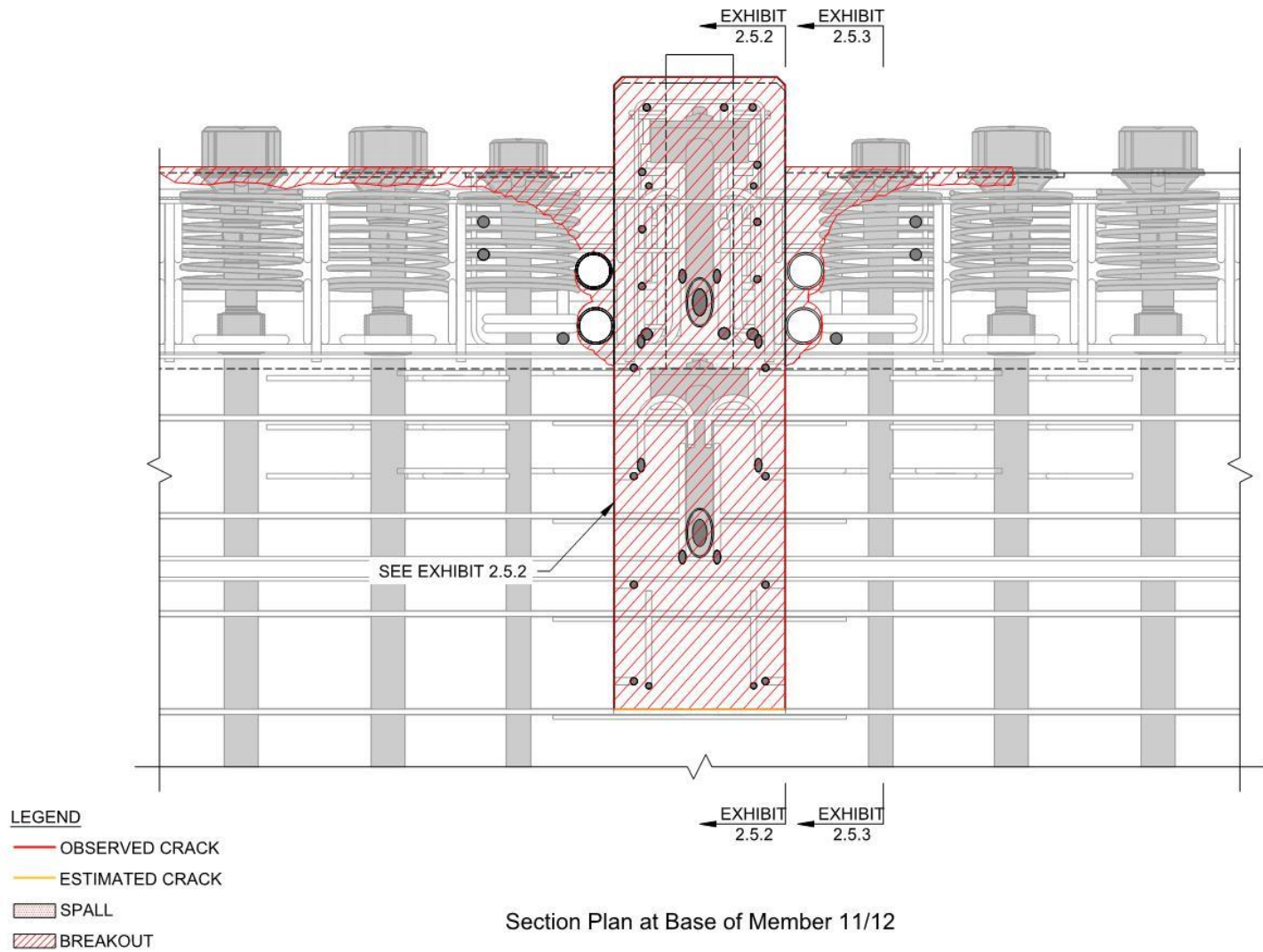
Exhibit 2.5.3
OBSERVED AND ESTIMATED CRACKS AT MEMBER 11/12 DECK CONNECTION
After Collapse (March and April, 2018)



- LEGEND**
- OBSERVED CRACK
 - ESTIMATED CRACK
 - SPALL
 - BREAKOUT

Section 12" East of Member 11/12
(Member 11 and 12 shown in background for reference)

Exhibit 2.5.4
OBSERVED AND ESTIMATED CRACKS AT MEMBER 11/12 DECK CONNECTION
After Collapse (March and April, 2018)



3 EVALUATION OF CONSTRUCTION JOINT CONDITIONS

The objective of this study is to assess the condition of the construction joint between the deck and Members 11 and 12 relative to the project specifications. The assessment of the construction joint condition is primarily based on review of relevant and publicly available documents, including email correspondence, photos, videos, and photos in the OSHA report. The evaluation also includes comparisons to the construction joint condition of WJE’s interface shear transfer test specimens, which are described in Section 4.

3.1 Document Review

Observations from review of key documents pertaining to the construction joint are provided in the following sections.

3.1.1 Construction Documents

The released-for-construction structural drawings comprise three subsets of drawings labeled *Foundation Plans*, *Substructure Plans*, and *Superstructure Plans*. Sheet No. 1 of the contract drawings cites FDOT standards as governance for the bridge. An extract from the cover page citing the FDOT specifications is shown in Figure 3.1.

GOVERNING STANDARDS AND SPECIFICATIONS: FLORIDA DEPARTMENT OF TRANSPORTATION, DESIGN STANDARDS DATED 2015, AND STANDARD SPECIFICATIONS FOR ROAD AND BRIDGE CONSTRUCTION DATED 2015, AS AMENDED BY CONTRACT DOCUMENTS.

APPLICABLE DESIGN STANDARDS MODIFICATIONS: 01-01-15

Figure 3.1. Text from Sheet No. 1

The general notes for the project, provided on Sheet B-2 (which was issued with the Foundation Plans subset), indicate additional specifications. The “CONSTRUCTION SPECIFICATIONS” in the general notes specify FDOT Standard Specifications. An excerpt from the general notes citing the FDOT specifications is shown in Figure 3.2. The FDOT specifications are considered to govern.

CONSTRUCTION SPECIFICATIONS:

1. FLORIDA DEPARTMENT OF TRANSPORTATION STANDARD SPECIFICATIONS FOR ROAD AND BRIDGE CONSTRUCTION 2015.

Figure 3.2. Text from Sheet B-2

FDOT requirements for construction joints are addressed in Article 400-9 of the FDOT Standard Specifications. Preparations of surfaces is covered in Article 400-9.3:

400-9.3 Preparations of Surfaces: Before depositing new concrete on or against concrete which has hardened, re-tighten the forms. Roughen the surface of the hardened concrete in a manner that will not leave loosened particles, aggregate, or damaged concrete at the surface. Thoroughly clean the surface of foreign matter and laitance, and saturate it with water.

3.1.2 Pre-Construction Email Correspondence

WJE reviewed available emails produced before and during construction. Several emails between MCM, BPA, and FIGG discuss construction joint preparation. One email, sent on June 12, 2017, by Alan Ruiz (MCM) to entities of MCM, BPA, and FIGG, confirms that he spoke with FIGG regarding construction joint treatment, as shown in Figure 3.3.

From: Alan Ruiz, P.E. [REDACTED]
Sent: Monday, June 12, 2017 10:15 AM
To: Rafael Urdaneta [REDACTED]; Jose Morales [REDACTED]; Carlos Chapman [REDACTED]; Pedro Cortes [REDACTED]; Pedro Gomez, P.E. [REDACTED]; Ernie Hernandez [REDACTED]; Dwight Dempsey [REDACTED]
Cc: FIU-Field-Office [REDACTED]; Rodrigo Isaza (MCM) [REDACTED]
Subject: RE: Concrete Pour

Rafael,

FCA 19-1

I spoke with FIGG and they advised us to follow FDOT Specs which is as follows:

400-9.3 Preparations of Surfaces: Before depositing new concrete on or against concrete which has hardened, re-tighten the forms. Roughen the surface of the hardened concrete in a manner that will not leave loosened particles, aggregate, or damaged concrete at the surface. Thoroughly clean the surface of foreign matter and laitance, and saturate it with water.

The plan notes do not mention the use of a bonding agent so it is not required.

Thanks,

Figure 3.3. June 12th, 2017 email regarding surface preparation from MCM's project engineer to members of the construction and design teams

3.1.3 Concrete Placement Video

An initial attempt to place the concrete deck was made on September 1, 2017. The placement was aborted when it was learned that concrete could not be continuously supplied due to a problem at the ready-mix plant. Nevertheless, the video from this first placement attempt shows the placement methods, consistency of the concrete, and surface texture. Figure 3.4 is a screenshot from one of the videos showing concrete placement and internal vibration. At the time the video was taken, the concrete level had not yet reached the top reinforcing bar mat. Note that the surface texture is relatively smooth, especially in the vicinity of the vibrator, although the coarse aggregate occasionally protrudes above the surface. The surface texture appears comparable to the as-placed (non-roughened) surface texture of the WJE interface shear transfer Specimen 3 (Figure 3.4).



Figure 3.4. Screenshot of video of first deck concrete placement attempt.

3.1.4 OSHA Report

In their June 2019 report on the collapse, which was publicly released, OSHA included an annotated photograph of a portion of the construction joint below Member 11. This photograph is shown below in Figure 3.5. The area around and to the north of the lower PT bar was damaged due to the collapse. Elsewhere, within the limits of the construction joint shown, the deck remained intact and appears to be smooth, especially on the right hand (east) side of the joint where the deck has been cleared of debris.

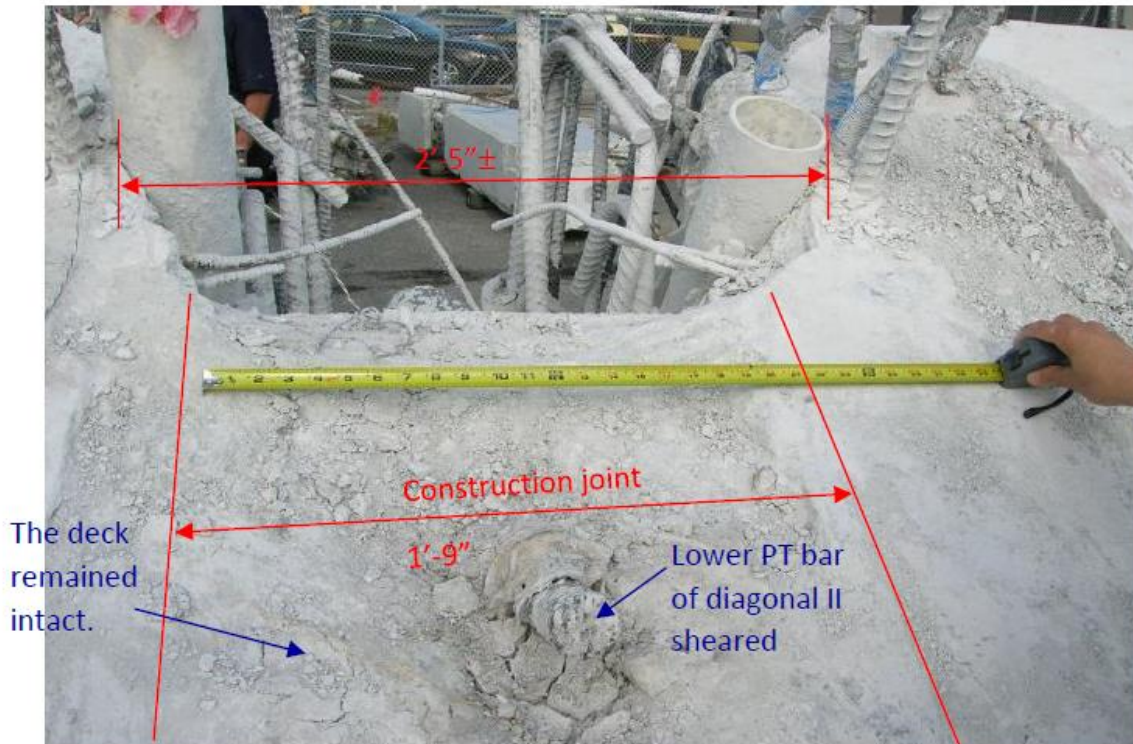


Figure 3.5. Construction joint below Member 11. (North is upward in the photograph.)

3.1.5 WJE Interface Shear Transfer Specimens

WJE conducted compression testing of column-like specimens with inclined construction joints to evaluate interface shear transfer at construction joints in the main span. The tests are described in Section 4. The mix design and slump of the specimen concrete was designed to match the concrete in the deck and diagonal members. Laser scan measurements of an as-placed (non-roughened) and roughened construction joint were made.

Figure 3.6 shows a photograph of the as-placed (non-roughened) surface of the Specimen 3 construction joint, and a laser scan of the same surface. The as-placed surface was created by internally vibrating the concrete during placement without further treatment. Note that the surface texture is similar to that shown in Figure 3.4, which is a screenshot of the first deck placement attempt.



Figure 3.6. Photograph and laser scan of Specimen 3 (as-placed). (Note: the mortar adhering to the reinforcing bars in the left photo was removed before scanning and placement of the upper lift.)

Table 3.1 provides the surface roughness parameters for Specimen 3.

Table 3.1. Surface Roughness Parameters (mm)

Parameter	Specimen 3 (as-placed)
Maximum Positive Deviation	5.29
Maximum Negative Deviation	-4.48
Average Positive Deviation	0.82
Average Negative Deviation	-0.64
Standard Deviation	0.94
RMS Estimate	0.94
Segment Length	775
Segment Width	320

3.2 Discussion

3.2.1 Project Records

Construction drawings by FIGG cite FDOT as the governing construction specifications. As indicated by the email correspondence, the FDOT specifications were considered to govern. The FDOT specifications include the following explicit instructions on the preparation of construction joints: “Roughen the surface of the hardened concrete in a manner that will not leave loosened particles, aggregate, or damaged concrete at the surface.” Furthermore, these specifications were re-iterated by MCM in an email to members of the design and construction team before the concrete for the main span of the superstructure was cast.

About half of the state DOT standard specifications require roughening of the hardened concrete at construction joints by mechanical means. Roughening the hardened concrete is preferable to creating a rough surface texture during finishing because roughening the hardened concrete also removes the surface laitance, which improves bond.

3.2.2 Photographs and Laser Scans

Comparison of the OSHA photograph to the WJE test specimens indicates that the construction joint below Members 11 and 12 was most likely left as-placed (non-roughened) after internal vibration; that is, the condition shown in the video of the first deck placement attempt (Figure 3.4). This observation is contrary to the project specifications, which were reconfirmed before the deck concrete was placed.

3.3 Findings

The following findings as to the construction joint below Members 11 and 12 are based on the reviews described above:

- Construction documents cite FDOT specifications. The FDOT specifications governed and required the contractor to “roughen the surface of the hardened concrete in a manner that will not leave loosened particles, aggregate, or damaged concrete at the surface.”
- In response to a question by MCM before the placement of the deck, FIGG confirmed that the FDOT construction joint requirements were to be followed. MCM reiterated these instructions by email correspondence to BPA and the MCM construction team, which included the relevant excerpt from the FDOT specifications.
- Photographic evidence indicates the construction joint below Members 11 and 12 was not intentionally roughened and appeared to be in an as-placed, relatively smooth condition.

In summary, despite FIGG’s confirmation to MCM that the FDOT specifications requiring roughening of the *hardened* concrete must be followed, the construction joint surface below Members 11 and 12 appeared to have been left in an as-placed, relatively smooth condition.

4 INTERFACE SHEAR TRANSFER TESTING

WJE has carried out independent testing to evaluate interface shear transfer at construction joints in the main span of the FIU UniversityCity Prosperity Pedestrian Bridge. The objective of the testing program was to assess the effect of surface condition on interface shear transfer at construction joints between the northernmost diagonal and deck.

4.1 Experimental Program

4.1.1 Introduction and Specimen Description

The experimental program features slant shear tests of column-like specimens with a diagonal construction joint. The specimens were designed to reasonably replicate shear transfer between Member 11 and the deck. Two construction joint interface conditions were tested: as-placed (non-roughened) and roughened.

In total, six specimens were fabricated and tested: three with an as-placed construction joint and three with a roughened construction joint in accordance with FDOT Standard Specifications. Additional details on the reinforcement, concrete mix design, placement methods, and construction joint treatment are provided in subsequent sections of this report.

4.1.2 Specimen Reinforcement

Figure 4.1 is an isometric view of a typical specimen showing the internal reinforcement. The detail of the connection of Members 11 and 12 to the deck taken from Sheet B-61 of the FIGG superstructure drawings is provided in Figure 4.2. The cross-sectional dimensions and longitudinal reinforcing bars in the test specimens are identical to those of Member 11, although the section does not include post-tensioning bars or ducts. The #4 ties above and below the construction joint are similar to the ties in Member 11. Three #7 stirrups are provided across the construction joint to replicate the effect of the three northernmost shear-friction reinforcement stirrups (identified as 7S01 bars in Figure 4.2). The southernmost #7 stirrup is not included because it did not contribute to shear-friction resistance. As explained in a Section 2, the concrete “wedge” between the deck and Member 11 remained attached to the deck when Member 11 slid to the north. Also, consistent with the design plans, #6 and #7 bars are provided across the top and bottom legs of the #7 stirrups, respectively.

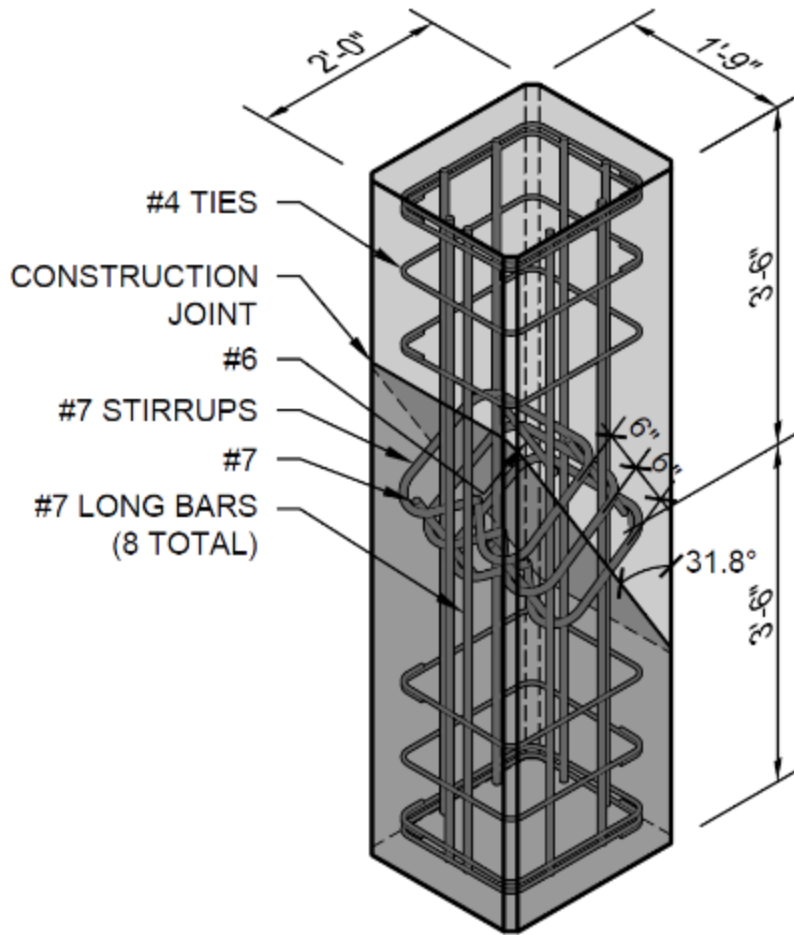


Figure 4.1. Isometric view of specimens

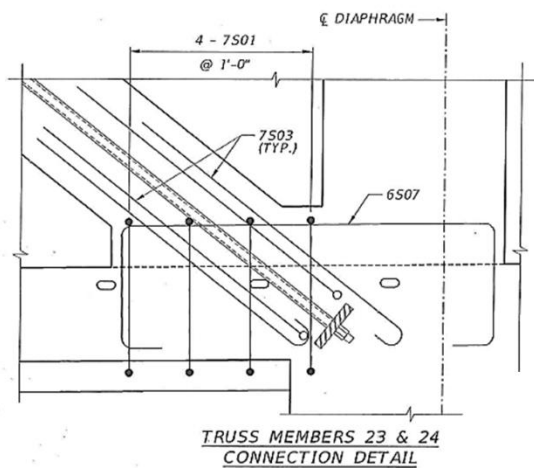


Figure 4.2. Detail of connection between deck and Members 11 & 12 from FIGG drawings

4.1.3 Concrete Mixture Proportions

For the fabrication of laboratory test specimens, WJE developed a mix to closely match the original mixture proportions (Class VI 8,500 psi) using materials available in the Chicago area¹. The original Class VI 8,500 psi mix had a target slump of 7 to 9 inches, an air content of 0 to 6.0 percent, and a 28-day design compressive strength of 8,500 psi. WJE developed a mix to closely match these properties, which is provided in Table 4.1. The following describes the developed mix as it relates to the original:

- The water to cementitious ratio was kept at 0.33.
- The total cementitious materials (cement, slag cement, fly ash, and metakaolin) was kept at 800 pounds per cubic yard (lb./yd³)
- The portland cement to slag cement ratio was increased in order to facilitate early strength development. The original mix had a portland cement to slag cement ratio of 0.76, and the mix developed had a ratio of 2.45.
- A different source of portland cement was used but of the same type (Type I). Gray portland cement was used and not white.
- A different source of fly ash was used but at the same dosage rate.
- A different source of slag cement was used but the same grade.
- A different source of metakaolin was used but at the same dosage rate.
- The same source of Titanium dioxide² was used at the same dosage rate.
- Chicago area coarse and fine aggregates were used in lieu of original Florida coarse (Cemex - Krome) and fine (CEMEX Krome and Palmdale) aggregates. Like the Krome coarse aggregates, the Chicago aggregates were crushed limestone.
- The combined aggregate gradations were designed to closely match the original.
- A high range water reducer (HRWR - Sika ViscoCrete 2100) and hydration stabilizer (SikaTard 440) were used to establish the target slump and setting properties of the original mix. The original mix used W.R. Grace chemical admixtures as opposed to the Sika products.

Table 4.1. Concrete Mixture Proportions

Constituent	Source	Quantity (lb./yd ³)
Cement	Type I-II, St. Mary's - Charlevoix	500
Slag Cement	Grade 100, Skyway Cement - Chicago	204
Fly Ash	Class C, LaFarge - Elm Road Unit 2	80
Metakolin	Burgess Optipozz	16
Titanium Dioxide	Ti-Pure R-103	5
Fine Aggregate	Hanson Materials - Romeoville	1400
3/4 Coarse Aggregate	Hanson Materials - Romeoville	1310
1/2" Coarse Aggregate	Hanson Materials - Thornton	303
Water		264
High Range Water Reducer (HRWR)	Sika ViscoCrete 2100	As Needed
Hydration Stabilizer	SikaTard 440	As Needed
W/cm		0.33
Target Slump		8-in.
Target Air Content		0 to 6 %

¹ Concrete mixes using locally available materials are routinely used in research and testing to replicate concrete mixes from other locales.

² Titanium dioxide was used in the original mix design for aesthetic purposes

A trial batch of this mix was performed on July 2, 2019, with ready mix concrete supplied by Prairie Material (Votorantim Cimentos). The metakaolin and titanium dioxide were added by WJE once the concrete was delivered to the laboratory. The concrete slump and air content of this trial batch were measured to be 9.0 inches and 1.8 percent, respectively. Both are consistent with the original mix. Compressive strength cylinders were fabricated and tested (ASTM C39) at 1, 3, 6, 7, 14, 17, and 28 days, and the results are presented in Table 4.2 and plotted in Figure 4.3. The measured 28-day compressive strength of 9,270 psi exceeded the design compressive strength of 8,500 psi and is consistent with measured 28-day strengths for the project. A Universal Engineering Sciences concrete testing report provided in the OSHA Report indicate 28-day strengths ranging from 8890 to 9380 psi.

Table 4.2. Compressive Strength Results*

Test Age (days)	July 2 - Trial Batch (psi)
1	2,850
3	4,770
6	6,710
7	7,300
14	8,780
17	8,850
28	9,270

*Each entry represents an average of two compressive strength cylinders (6 x 12-in.)

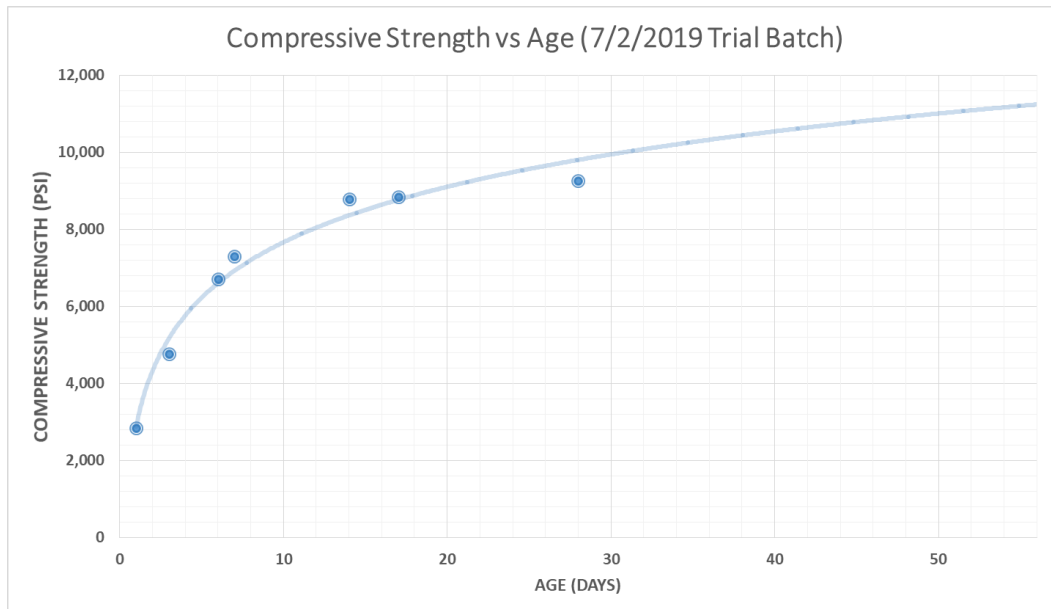


Figure 4.3. Concrete strength development of trial batched concrete, 7/2/2019

4.1.4 Concrete Placement

As illustrated in Figure 4.1, the specimens were cast in two lifts with a sloped construction joint at mid-height. The angle of the construction joint relative to the longitudinal axis of the specimens, 31.8 degrees, matched the angle between Member 11 and the concrete deck.

The lower lift was placed on July 9, 2019, and the upper lift was placed on July 16, 2019, using the mixture proportions in Table 4.1 supplied by ready mix concrete from Prairie Material (Votorantim Cimentos). Similar to the trial batch, the met kaolin and titanium dioxide were added by WJE once the concrete was delivered to the laboratory. Concrete slump, air content, unit weight, and temperature were measured on each of these placements and are summarized in Table 4.3. The concrete slump and air content of the two placements were both consistent with the original mix design. Compressive strength cylinders (6 x 12-in.) were fabricated from each placement and cured under standard conditions (ASTM C31) and match cured (cured alongside the replicate construction joint specimens). In addition to the 1, 7, and 14-day compressive strength testing (ASTM C39), strength testing was performed during the first replicate construction joint test and after completion of all joint tests. The testing of the replicated construction joints were started when the lower and upper lift were at an age of 27 and 20 days, respectively, with the completion of the testing at 28 and 21 days, respectively. The compressive strength results are presented in Table 4.4 and plotted in Figure 4.4 and Figure 4.5.

Table 4.3. Plastic Concrete Properties

Concrete Property	Lower Lift	Upper Lift
Slump (in.) - ASTM C143	8.5	8.5
Air Content (%) - ASTM C231	2.2	1.7
Unit Weight (lb./ft ³) - ASTM C138	148.0	149.4
Temperature (F) - ASTM C1064	87.0	84.0

Table 4.4. Compressive Strength Results (psi)*

Test Age (days)	Lower Lift		Upper Lift	
	Standard Cure ³	Match Cure ⁴	Standard Cure ³	Match Cure ⁴
1		2,860		2,760
7	7,080	7,090	6,640	6,860
14		8,020		8,260
During First Joint Test	9,410	8,680	8,930	8,360
After Testing	9,550	8,870	8,990	8,500

*Each entry represents the average compressive strength of two cylinders

³ Standard-cured cylinders are cured at specified temperature and humidity conditions in accordance with ASTM C511

⁴ Match-cured cylinders are cured in the same environment as the structure or specimen

Compressive Strength vs Age (7/9/2019 Placement)

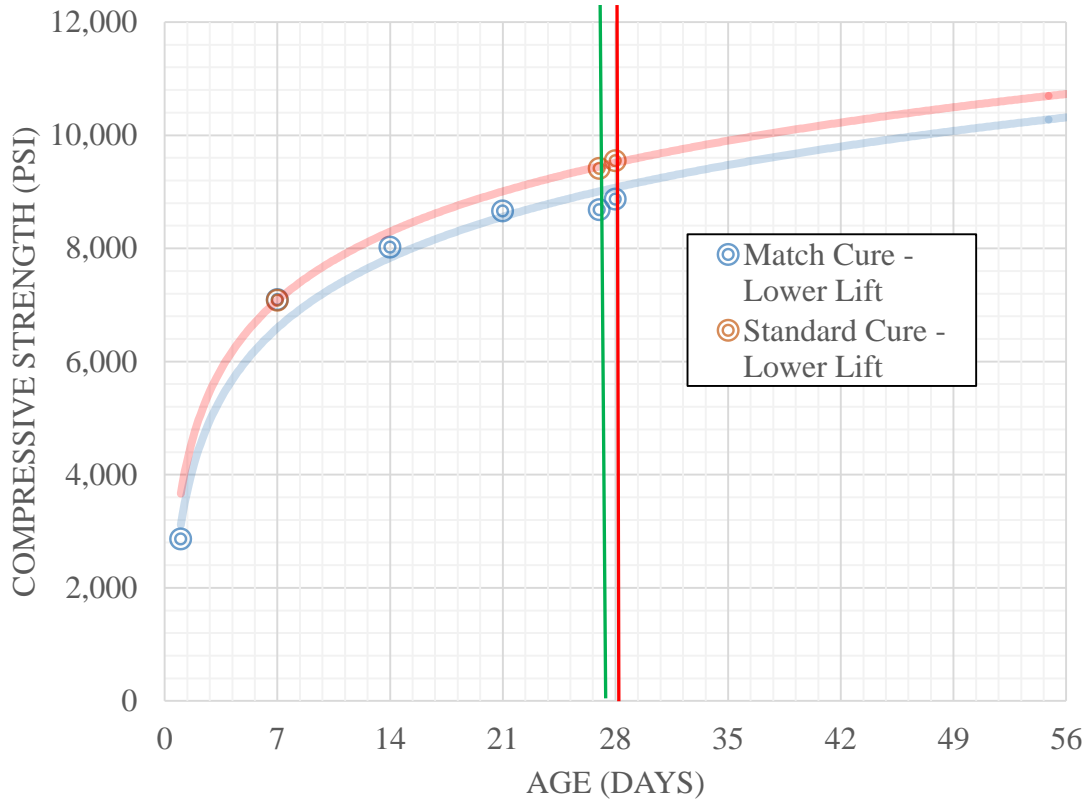


Figure 4.4. Strength development of lower lift fabricated on 7/9/2019. The vertical green and red lines represent the start and completion dates of the replicate construction joint tests, respectively.

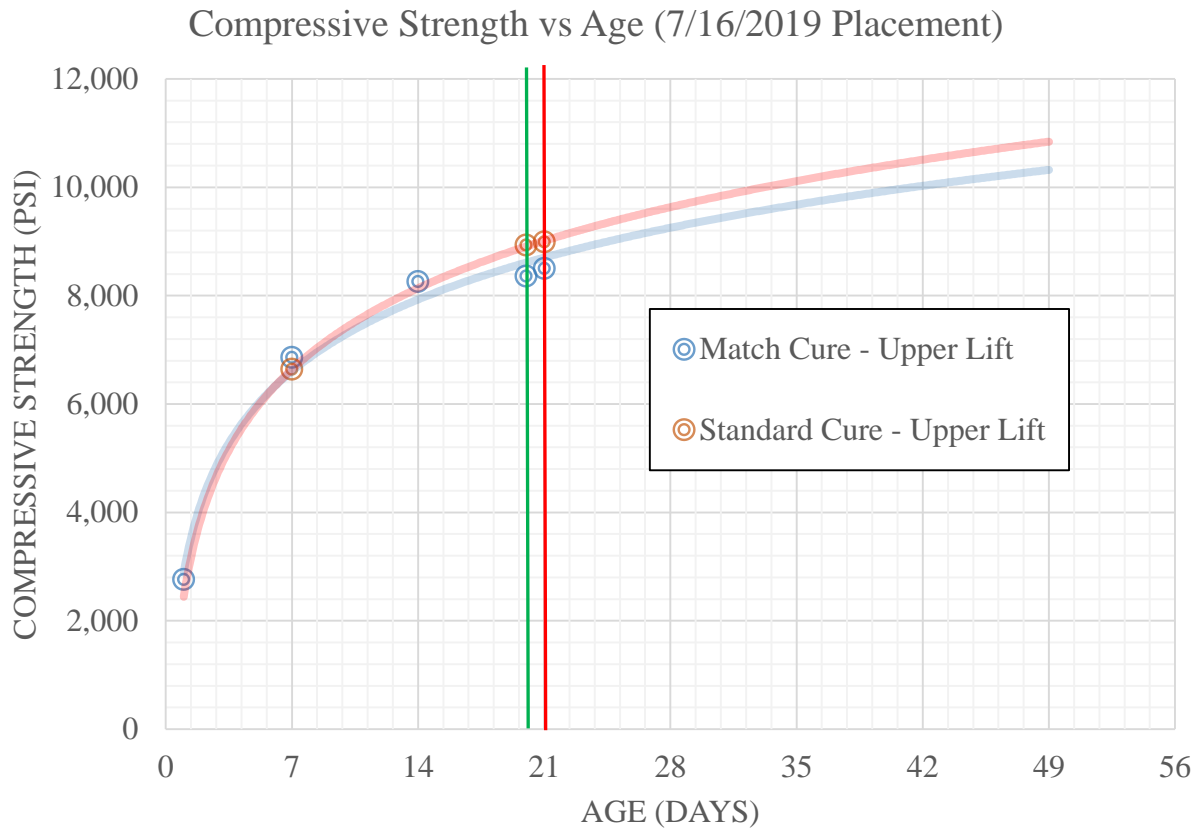


Figure 4.5. Strength development of upper lift fabricated on 7/16/2019. The vertical green and red lines represent the start and completion dates of the replicate construction joint tests, respectively.

4.1.5 Construction Joint Interface

To create the *as-placed* (non-roughened) condition, the concrete was placed using internal vibration without further treatment of the construction joint surface. Based on WJE’s review of the construction records and available photographs and videos, it appears the deck concrete below Members 11 and 12 was vibrated and left as-placed.

For the *roughened* condition, the hardened concrete was roughened one day after placement using an electric chipping hammer with amoil bit (a rectangular bit tapered to a sharp point). The roughening operation is shown in Figure 4.6.

This roughening method was considered the most practical means to meet the requirements of the FDOT Standard Specifications⁵. Article 400-9.3 on preparation of construction joint surfaces requires: “roughen the surface of the hardened concrete in a manner that will not leave loosened particles, aggregate, or damage concrete at the surface.” Note that this requirement does not permit roughening the concrete before

⁵ Florida Department of Transportation, *Standard Specifications for Road and Bridge Construction*, 2015.

hardening, while it is still in a plastic state. Removing the hardened concrete removes the surface laitance, which is also required by FDOT Standard Specifications. Use of a chipping hammer with amoil point was selected because this equipment is readily available and commonly used at construction sites. Also, themoil point can work around most interferences from reinforcement.



Figure 4.6. Roughening operation using an electric chipping hammer with amoil point (trial slab shown)

To determine the surface roughness, the surface of one as-placed (non-roughened) and one roughened construction joint surface was measured using a laser scanner. The laser scans were conducted by WJE's scanning consultant, Khan Consultants. The Khan report is provided in Exhibit 4.1.

Figure 4.7 compares a photograph of the Specimen 3 construction joint surface (as-placed) to a laser scan of the same surface. Figure 4.8 provides a similar comparison for Specimen 4 (roughened).



Figure 4.7. Photograph and laser scan of Specimen 3 (as-placed). (Note: the mortar adhering to the reinforcing bars in the left photo was removed before scanning and placement of the upper lift.)



Figure 4.8. Photograph and laser scan of Specimen 4 (roughened in accordance with FDOT Standard Specifications). (Note: the mortar adhering to the reinforcing bars in the left photo was removed before scanning and placement of the upper lift.)

Table 4.5 compares the surface roughness parameters for the as-placed (non-roughened) and roughened test specimens. Using the standard deviation for comparison purposes, Specimen 4 (roughened) is more than twice as rough as Specimen 3 (as-placed). Comparison using the sum of average positive and negative deviations indicates that the roughened surface is about 2.2 times as rough as the as-placed surface.

Table 4.5. Surface Roughness Parameters (mm)

Parameter	Specimen 3 (as-placed)	Specimen 4 (roughened)	Specimen 4 Specimen 3
Maximum Positive Deviation	5.29	6.72	1.27
Maximum Negative Deviation	-4.48	-10.03	2.24
Average Positive Deviation	0.82	1.31	1.60
Average Negative Deviation	-0.64	-1.91	2.98
Standard Deviation	0.94	2.03	2.16
RMS Estimate	0.94	2.04	2.17
Segment Length	775	778	1.00
Segment Width	320	321	1.00

To simulate the condition of the construction joint between Member 11 and the deck prior to moving the main span, two as-placed specimens (Specimens 1 and 2) and two roughened specimens (Specimens 4 and 5) were intentionally cracked at the construction joint. Unbonded and initially cracked specimens are primarily used in shear-friction research because a crack at the interface between concrete cast at different times should be assumed.

The construction joints at the remaining two specimens (Specimens 3 and 6) remained bonded. However, after Specimen 6 (roughened) sustained the maximum test load of 3 million pounds, the interface was then cracked, and the specimen was re-tested.

Stone-splitting wedge sets in drilled holes were used to create the cracks at the construction joint. Figure 4.9 is a photograph of the cracking operation at Specimen 6. Machined measurement points and a digital caliper were used to detect and monitor the width of the crack at the surface. The wedge sets were driven until the surface crack width was approximately 0.012 to 0.014 inches. In WJE’s laboratory, an ultrasonic pulse velocity meter was used to verify that this surface crack width was sufficient for propagation of the crack across the width of the specimen. The wedge sets were removed after cracking.



Figure 4.9. Stone-splitting wedge sets being used to create a crack across the construction joint of Specimen 6

4.1.6 Test Set-up and Instrumentation

Testing of specimens was performed at the University of Illinois at Urbana-Champaign in the Talbot Laboratory using the Southwark-Emery universal test machine. The test machine uses manually controlled hydraulics and has a load capacity of 3,000,000 lbs. (Figure 4.10).



Figure 4.10. University of Illinois Southwark-Emery test machine

Linear variable displacement transducers (LVDT) were attached on either side of each test specimen and positioned to measure sliding and separation of the interface shear joint (Figure 4.11) during testing. The transducers have a maximum displacement range of 0.5-in.

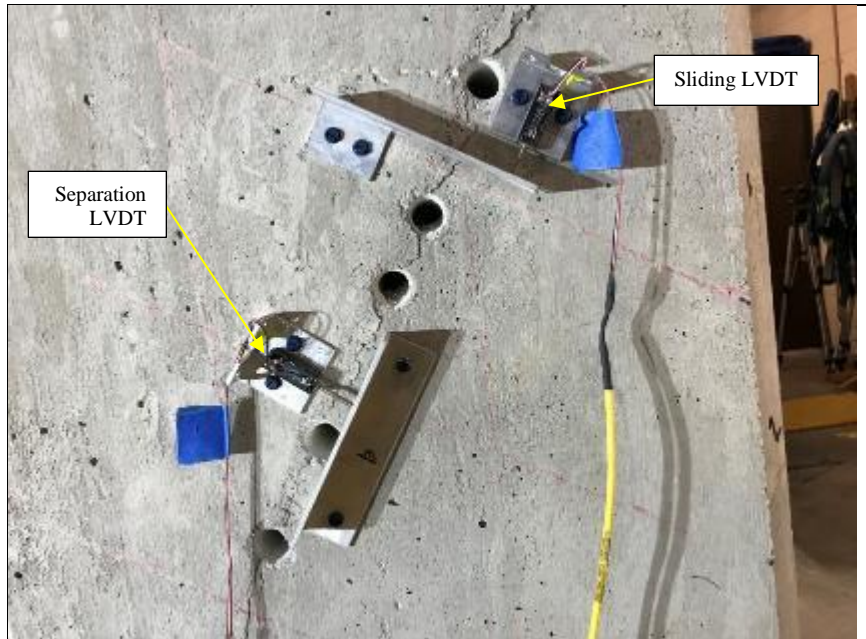


Figure 4.11. Linear displacement transducers across interface shear joint

Load and displacement data were continuously collected using a computer controlled data acquisition system to capture load and corresponding sliding and separation values.

4.1.7 Loading Protocol

A loading protocol was developed to simulate the axial force in Member 11 from shoring removal in the casting yard through re-stressing. The loading protocol is presented in Table 4.6⁶.

Table 4.6. Loading Protocol

Stage	Field Condition	Loading	Force (kips)	
			Start	Final
1	Shoring removal in casting yard	Dead + PT	0	1680
2	<i>Lifting by transporter</i>	<i>Dead + PT</i>	<i>1680</i>	<i>0</i>
3	Placement on piers	Dead + PT	0	1680
4	<i>De-stressing Member 11</i>	<i>Dead</i>	<i>1680</i>	<i>1227</i>
5	Re-stressing Member 11	Dead + PT + CLL	1230	1743
6	NA	To 3000 kips or failure	1743	3000 or Failure

Note: *Italic* type indicates unloading stage

⁶ Forces are based on finite element model of main span. See Section 5.1.1.

4.1.8 Interface Shear Transfer Results

The interface shear transfer results are summarized in Table 4.7. Both axial load and shear stress along the construction joint are reported. Sliding and separation at peak load are also reported.

Table 4.7. Summary of Shear Transfer Test Results

Specimen	Construction Joint Condition	Peak Load (kip)	Maximum Shear Force (kip)	Sliding at Peak Load (in.)	Separation at Peak Load (in.)	Failure Mode
1	As-placed cracked	1296*	1101	0.0023	None measured	Shear-friction
2	As-placed cracked	1614	1372	0.0070	None measured	Shear-friction
3	As-placed bonded	2775	2358	0.0024	0.0006	Shear-friction
4	Roughened cracked	2516	2138	0.0120	None measured	Shear-friction
5	Roughened cracked	2551	2168	0.0145	-0.0008	Shear-friction
6	Roughened bonded	3000	2550	0.0025	0.0014	Did not fail; specimen retested
6	Roughened cracked	2714	2307	0.0120	None measured	Shear-friction
Average	Roughened cracked	2594	2204	0.0128		
Average	As-placed cracked	1455	1237	0.0047		

*Because Specimen 1 was not severely damaged in the initial test, the specimen was reloaded after the first failure. The peak load in the retest was 737 kips.

Most failures were similar. Except for Specimen 1, the specimens failed suddenly at peak load. A typical specimen after failure is shown in Figure 4.12. The wedges of concrete at the top and bottom of the construction joint broke away and the underlying #7 longitudinal reinforcement bars buckled. Also, the side faces typically delaminated or spalled along the joint, apparently due to deformation of the #7 stirrups at the side faces.

Although measured sliding at peak load is very small (0.0025 inches or less), the specimens continued to slide along the construction joint after failure due to strain energy in the sample and testing machine. The crack specimens began sliding early, usually after a load of a few hundred kips. The residual sliding after failure was typically about 0.5 inches, as can be seen in Figure 4.12.



Figure 4.12. Specimen 5 after failure: overall view looking southwest (left); close-up of sliding on east side (right)



Figure 4.13. Screenshots from slow-motion video showing instant of failure: Specimen 3 (left) and Specimen 6 (right)

The images in Figure 4.13 are screenshots from slow-motion video recordings and show Specimen 3 (as placed, bonded) and 6 (roughened, cracked) at the instant of failure. As can be seen, both specimens slid suddenly along the construction joint with a concentration of damage near the top and bottom of the joint. The spalling and delamination described above is secondary damage, which occurred with continued sliding.

The behavior of Specimen 1 was atypical. At an axial load of 1296 kips, the specimen slid along the construction joint without spalling or delamination, which is similar to the sliding failure observed in the actual structure. Because Specimen 1 was not severely damaged, the specimen was reloaded after the initial failure. The peak load in the retest was 737 kips.

Figure 4.14 is a close-up of the interface of Specimen 5 (roughened, cracked) after failure. Numerous fractured aggregate are evident, but these fractures may have occurred when the specimen was intentionally cracked. The circled areas show corresponding fractured aggregate on each side of interface. Figure 4.15 is

a similar photo from Specimen 1 (as-placed, cracked). Relatively few fractured aggregate are evident at the construction joint.



Figure 4.14. Construction joint interface of Specimen 5 (roughened, cracked) after failure. Circled areas show corresponding fractured aggregate on each side of interface.



Figure 4.15. Construction joint interface of Specimen 1 (as-placed, cracked) after failure.

4.1.9 Slant Shear Tests

The Chicago coarse aggregates used in the testing of the replicate construction joints were of higher specific gravity than the Florida (Krome) aggregate used in the actual construction, with the specific gravity of the Chicago aggregates equal to 2.69 to 2.71 and the Florida aggregates equal to 2.43. Some research has shown that the interface shear transfer across roughened specimens is affected by the density of the aggregates.^{7, 8} In order to assess this effect, slant shear tests were performed using a modified version of ASTM C882. A total of 20 slant shear specimens, 10 with Chicago aggregates (2 specimens were rejected as outliers) and 10 with the Florida aggregates, were fabricated using the mixture proportions in Table 4.1 and tested with the following modifications to ASTM C882:

- The bottom halves of the slant shear specimens were cast using an angle of incidence of 38.9 degrees in 6 x 12-inch cylinder molds.
- The bottom halves were removed from the cylinder molds and roughened, within 48 hours after fabrication, in the same fashion as the replicated construction joints by use of a chipping hammer. In order to avoid chipping and spalling of the edges of bottom halves of the cylinders, the roughened surface was limited to the inner portion, leaving approximately 1 inch along the perimeter smooth.
- The outside perimeter was coated with form release agent to prevent any bond (for the subsequent top half concrete placement) in the smooth (unroughened) area.

⁷ AlMosawi, F.H., “Effect of Coarse Aggregate Type on Shear Transfer Strength. International Journal of Scientific & Engineering Research”, Volume 8, Issue 3, March 2017.

⁸ Krc, K., “An Investigation of Shear-Friction of Lightweight Aggregate Concretes”, University of Missouri Science and Technology, 2015.

- The prepared bottom halves were placed back into 6 x 12-in. cylinder molds, and the top halves of the cylinders were cast directly onto the bottom halves, with the top and bottom halves having the same aggregate source.
- Similar to the replicated construction joint testing, all slant shear specimens were pre-cracked within 48 hours after fabrication. Cracking along the top and bottom half interface was achieved by cutting an approximately 3/4-inch groove along the interface, inserting a thin steel plate in the groove, and loading the specimen parallel to the interface plane.

Concrete was made and specimens were cast in general accordance with ASTM C192. The compressive strength and slant shear specimens were demolded at 1 day cured in the concrete laboratory until loading, in accordance with ASTM C31 Field Curing, with the following exception. The Florida aggregates specimens were placed in water and cured at 100 °F for 6 days (from 36 to 42 days for the top halves and age of 49 to 55 days for the bottom halves) in order to increase the compressive strength of the top halves to be similar to Chicago aggregate top half concrete. For the bottom and top concrete, compressive strength specimens were fabricated and tested according to ASTM C31 and ASTM C39 (Table 4.8).

Table 4.8. Compressive Strength of Slant Shear Concrete (psi)

Test Age (days)	Chicago Aggregates		Florida Aggregates		
	Bottom Half (CB)	Top Half (CT)	Bottom Half (FB)	Top Half - Batch 1 (FT1)	Top Half - Batch 2 (FT2)
1	4,570	2,610	4,150	1,510	2,050
2		3,960		2,520	2,800
7		6,250		4,740	5,620
14	11,860	7,280	9,290		
15		7,250			
23				5,810	6,640
28	13,260				
35				5,870	6,770
43				5,770	7,340
56			10,150		
Strength at testing	13,260	7,250	10,150	5,770	7,340

The slant shear testing of all specimens were tested per ASTM C882 when the upper halves of both aggregate sources achieved similar compressive strengths. In the case of the Florida aggregate specimens the replicate batches of concrete for the top half of slant shear cylinders had significantly different compressive strengths at the time of the slant shear testing. The replicate batches for the other mixtures (bottom half Chicago aggregate, bottom half Florida aggregate, top half Chicago aggregate) had typical variance between batches and the results shown are the average of the replicate batches. The results for the Chicago and Florida aggregate are summarized in Table 4.9 and Table 4.10, respectively.

Table 4.9. Slant Shear Test Results: Chicago Aggregate

Specimen	Mix	Test Load (lbs)	Shear Stress (psi)	Normalized to Top Compressive Strength	Normalized to Average Compressive Strength
C1	CT/CB	163,700	2,829	0.390	0.276
C2	CT/CB	179,760	3,107	0.429	0.303
C3	CT/CB	150,150	2,595	0.358	0.253
C4	CT/CB	164,330	2,840	0.392	0.277
C5	CT/CB	145,970	2,523	0.348	0.246
C6	CT/CB	174,640	3,019	0.416	0.294
C7	CT/CB	166,260	2,874	0.396	0.280
C8	CT/CB	162,230	2,804	0.387	0.273
Average		163,380	2,824	0.390	0.275
Standard Deviation		9,910	171	0.024	0.017

- Notes
1. Shear stress divided by compressive strength of top half
 2. Shear stress divided by average compressive strength of both halves

Table 4.10. Slant Shear Test Results: Florida Krome Aggregate

Specimen	Mix	Test Load (lbs)	Shear Stress (psi)	Normalized to Top Compressive Strength	Normalized to Average Compressive Strength
F1	FT1/FB	144,810	2,503	0.434	0.314
F2	FT1/FB	96,660	1,671	0.290	0.210
F3	FT1/FB	156,640	2,707	0.469	0.340
F4	FT1/FB	89,980	1,555	0.270	0.195
F5	FT1/FB	91,170	1,576	0.273	0.198
F6	FT1/FB	107,470	1,858	0.322	0.233
F7	FT2/FB	126,550	2,187	0.298	0.250
F8	FT2/FB	134,420	2,323	0.317	0.266
F9	FT2/FB	158,040	2,732	0.372	0.312
F10	FT2/FB	142,800	2,468	0.336	0.282
Average		124,854	2,158	0.338	0.260
Std. Dev.		24,072	416	0.061	0.047

- Notes
1. Shear stress divided by compressive strength of top half
 2. Shear stress divided by average compressive strength of both halves

4.2 Discussion

4.2.1 Results Relative to AASHTO Code

All test specimens exhibited capacities greater than predicted by the AASHTO Code⁹. To at least some degree, these results are expected because the Code equations provide a lower-bound to expected capacity.

⁹ See Section 5.2.3 for discussion of AASHTO Code provisions for interface shear.

For all samples, the peak load was reached when measured sliding was 0.0025 inches or less. The measured separation, if any, was typically much less. This behavior is not indicative of true shear-friction behavior where sliding causes separation that strains the shear-friction reinforcement, increasing the normal force. In this case, most of the normal force resulted from the component of the axial force acting perpendicular to the construction joint. Thus, capacity was apparently limited by shear stress rather than yield strength of the shear-friction reinforcement.

The observed shear stress limit on capacity is consistent with the AASHTO Code prediction. As described in Section 5.2.3, capacity is limited by maximum shear stress: 1.5 ksi for concrete roughened to an amplitude of 0.25 inches and 0.8 ksi for a surface that is not intentionally roughened. However, the observed shear stresses at failure were much higher: 2.30 ksi average for a roughened cracked interface, and 1.29 ksi for the as-placed (non-roughened) cracked interface. The maximum shear stress in the bonded specimens was even greater.

The AASHTO Code specifically calls for a roughness amplitude of 0.25 inches, but this criterion is not included in the FDOT Specifications. The test results indicate that intentionally roughening the *hardened* concrete, as required by FDOT specifications, achieves the roughness required by the AASHTO Code — in effectiveness, if not actual amplitude.¹⁰ Therefore, these calculations use the friction parameters for intentional roughness found in the AASHTO Code.

4.2.2 Florida Krome vs Chicago Limestone

As can be seen in Table 4.9 and Table 4.10, the slant shear test results were normalized by dividing the shear stress by the compressive strength of the top half of the time of testing. Using this method, the average shear stress at failure of the Florida aggregate slant shear specimens was 13.3 percent less than that of the Chicago area specimens. This approach is based on the assumption that shear stress is controlled by the lesser of the two concrete strengths.

The results were also normalized by dividing the shear stress by the average compressive strength of both halves. This approach is based on the assumption that the failure shear stress is influenced by the compressive strength of the bottom half as well as the top half. Normalizing with respect to the average compressive strength, the average failure shear stress Florida aggregate specimens was just 5.5 percent less than that of the Chicago aggregate specimens. The slant shear test results do not apply to the as-placed (non-roughened) specimens because interface shear transfer does not depend on aggregate interlock across the relatively smooth surface.

Arguments for either normalization approach can be made, and there is no available research on interface shear transfer between concretes of significantly different strengths. As such, reductions of both 13.3 percent and 5.5 percent are considered for adjusting the results of the full-sized interface shear strength specimens with roughened, cracked surfaces.

Based on the above, Table 4.11 summarizes the unadjusted and adjusted capacities of the specimens with roughened, cracked surfaces.

¹⁰ Neither the AASHTO Code nor ACI 318-19 provide detailed criteria for measuring amplitude. In WJE's experience, 1/4-inch amplitude is generally taken as the typical peak-to-valley heights over short distances.

Table 4.11. Capacities of Roughened, Cracked Specimens Adjusted for Florida Aggregate

Adjustment for Florida Aggregate Based on Slant Shear Tests	Florida Aggregate Adjustment	Adjusted Average Capacity (kip)	<u>Roughened As-Placed</u>
None	No Adjustment	2594	1.78
Normalized to average compressive strength of both halves	5.5% reduction	2451	1.68
Normalized to lower compressive strength of top half	13.3% reduction	2246	1.54

4.2.3 Roughened vs As-Placed (Non-Roughened) Interface

Roughening the construction joint surface in accordance with FDOT Standard Specifications greatly improved performance. On average, the roughened cracked interface was 1.78 times as strong as the as-placed (non-roughened) cracked interface. The relative difference according to the AASHTO Code is similar: the maximum allowable shear stress for a roughened surface (1.5 ksi) is 1.88 times that for a non-roughened surface (0.8 ksi). However, the observed maximum shear stresses are at least 50 percent greater than the Code values. As previously noted, Code values represent the lower-bound to research data.

The bonded roughened specimen was also stronger than the bonded as-placed (non-roughened) specimen. The actual difference is not known because the bonded roughened specimen did not fail at the maximum testing machine capacity of 3000 kips.

Also, it is noteworthy that the tested capacity of the as-placed (non-roughened) cracked interface (average of 1455 kips) is less than the calculated force in Member 11 after the shoring was removed (1680 kips, see Table 4.6). This result explains the initial cracking and horizontal movement when the shoring was removed and suggests that the construction joint was at least partially debonded when the shoring was removed. It is also possible that the bond between Member 11 and the deck was weaker than that of Specimen 3 (as-placed, bonded), which failed at an axial force of 2775 kips (see Table 4.7).

4.3 Findings

The primary finding from the experimental program described above is that intentional roughening of the construction joint following FDOT Standard Specifications improved the shear capacity of the cracked interface by a factor of 1.78. This factor reduces somewhat if adjustment for Florida aggregate is made. The Florida aggregate reduction does not apply to as-placed (non-roughened) specimens because friction across the relatively smooth surface does not depend on aggregate interlock.

Comparison of observed axial strengths of the as-placed (non-roughened) specimens to the calculated force in Member 11 after the shoring was removed suggests that the construction joint was weakened or at least partially debonded when the shoring was removed.

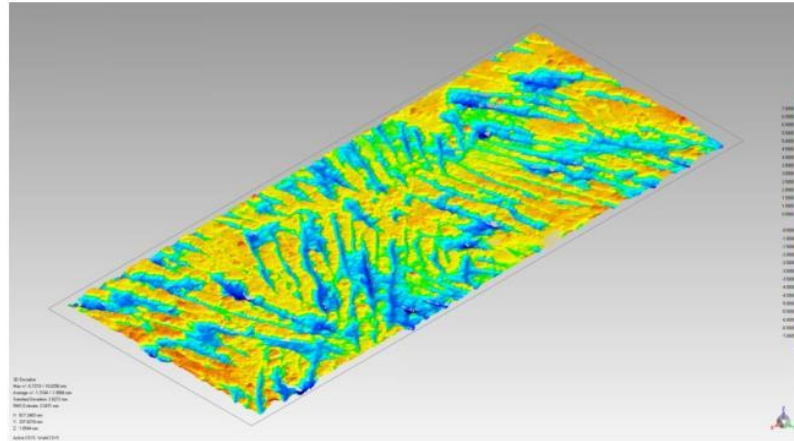
More significantly, the axial capacities of the roughened specimens, before or after adjustment for Florida aggregate, substantially exceed the calculated force in Member 11 at the time of the collapse. As such, if the construction joint were roughened as required by the project specifications, the collapse would not have occurred. See Section 5.3 for evaluation of the observed performance of the Member 11 and 12 deck connection relative to the expected resistance based on test results. Also see Sections 7 and 8 for evaluation of other factors contributing to the collapse.

Exhibit 4.1



WJE As Placed vs Roughened Concrete Blocks Deviations Results Comparison July 22, 2019

KHAN CONSULTANTS



Disclaimer

The following report of data is the result of calculation from data gathered via 3D scanning of physical concrete blocks as provided to Khan Consultants. The analysis of the data in a pre-determined manner to elicit certain mathematical characteristics is submitted purely as a report of mathematical results from the data and is not warranted to be findings or conclusions of any kind or representative of any physical behavior. The accuracy of the scan data is only as defined by the manufacturer of the HDI ADVANCE 3D scanner in publicly available information.

Exhibit 4.1



Summary of Deviations - Numerical

The values calculated by the system for the segments studied from each block are as follows (in millimeters):

	3-As Placed	4-Roughened
Max Pos Deviation	5.29	6.72
Max Neg Deviation	-4.48	-10.03
Avg Pos Deviation	0.82	1.31
Avg Neg Deviation	-0.64	-1.91
Standard Deviation	0.94	2.03
RMS Estimate	0.94	2.04
Segment Length	775.01	778.33
Segment Width	320.57	321.73

Exhibit 4.1



Isometric and Top of view of Full Block - Original Scan Data with Rebar members:

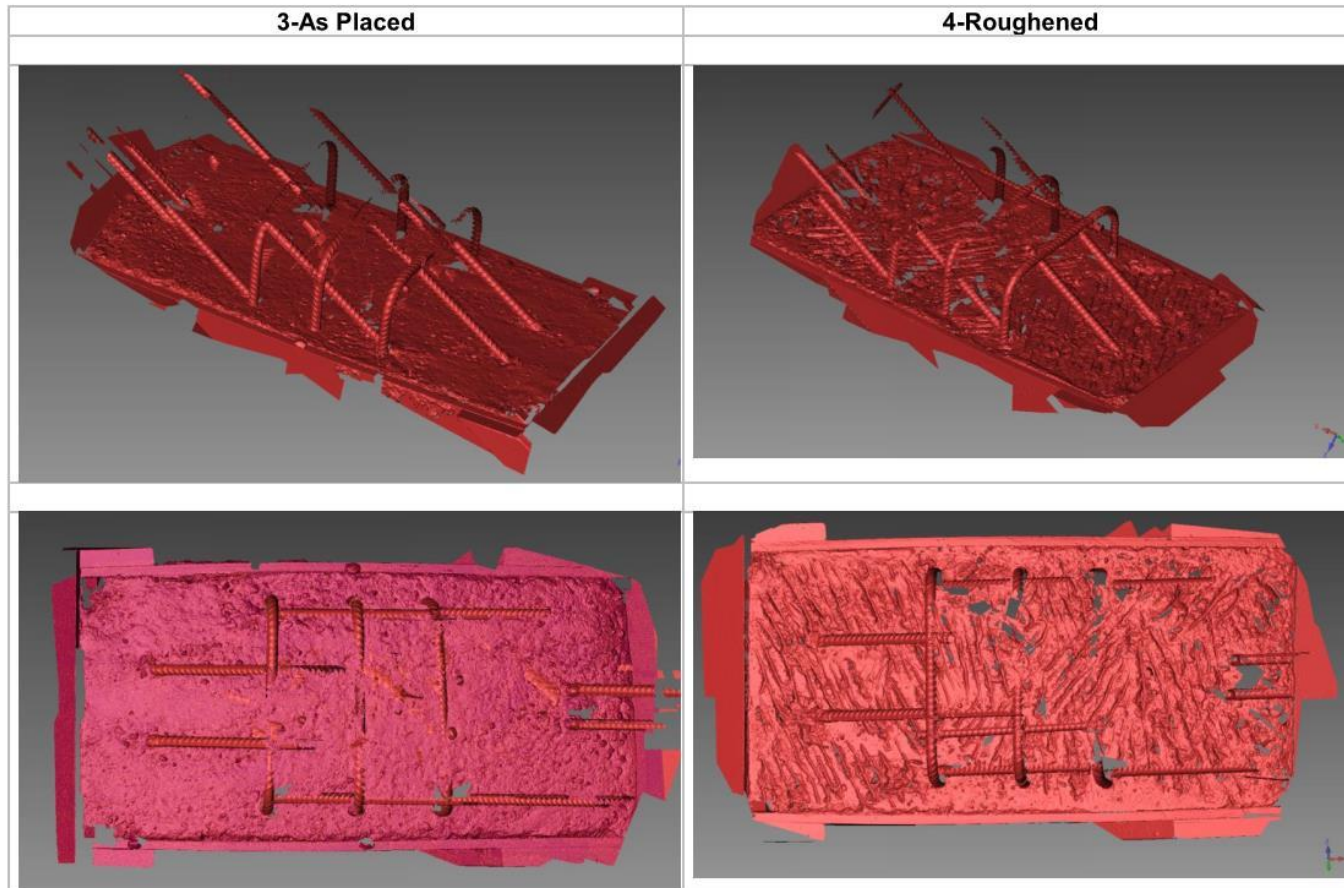


Exhibit 4.1



Isometric view of Scan Data Used (in red) for concrete section:

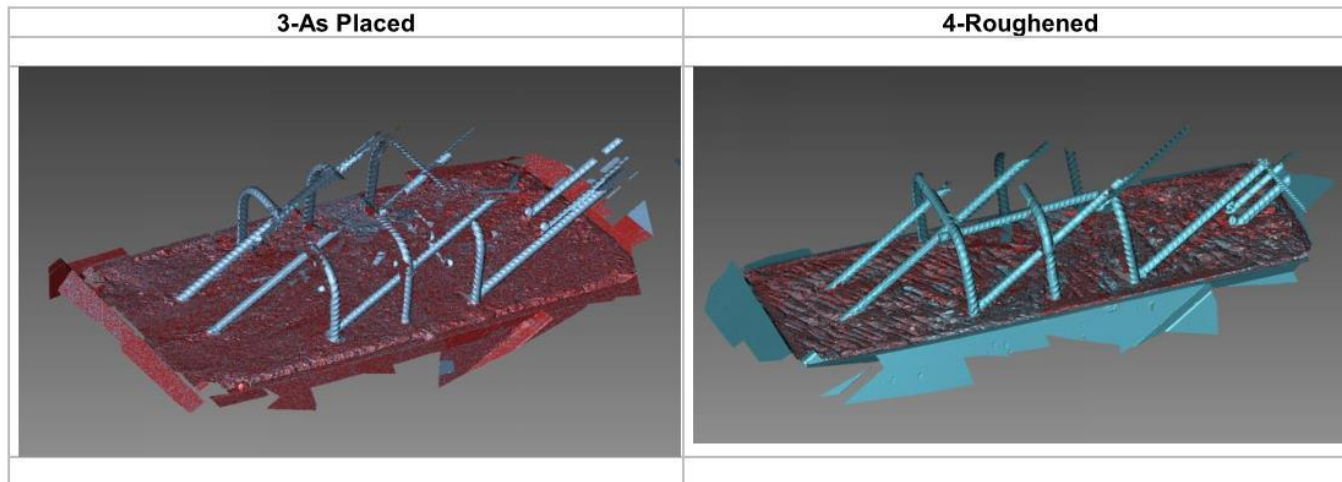


Exhibit 4.1



Top of view of Full Block and Colormap showing deviations to best-fit plane:

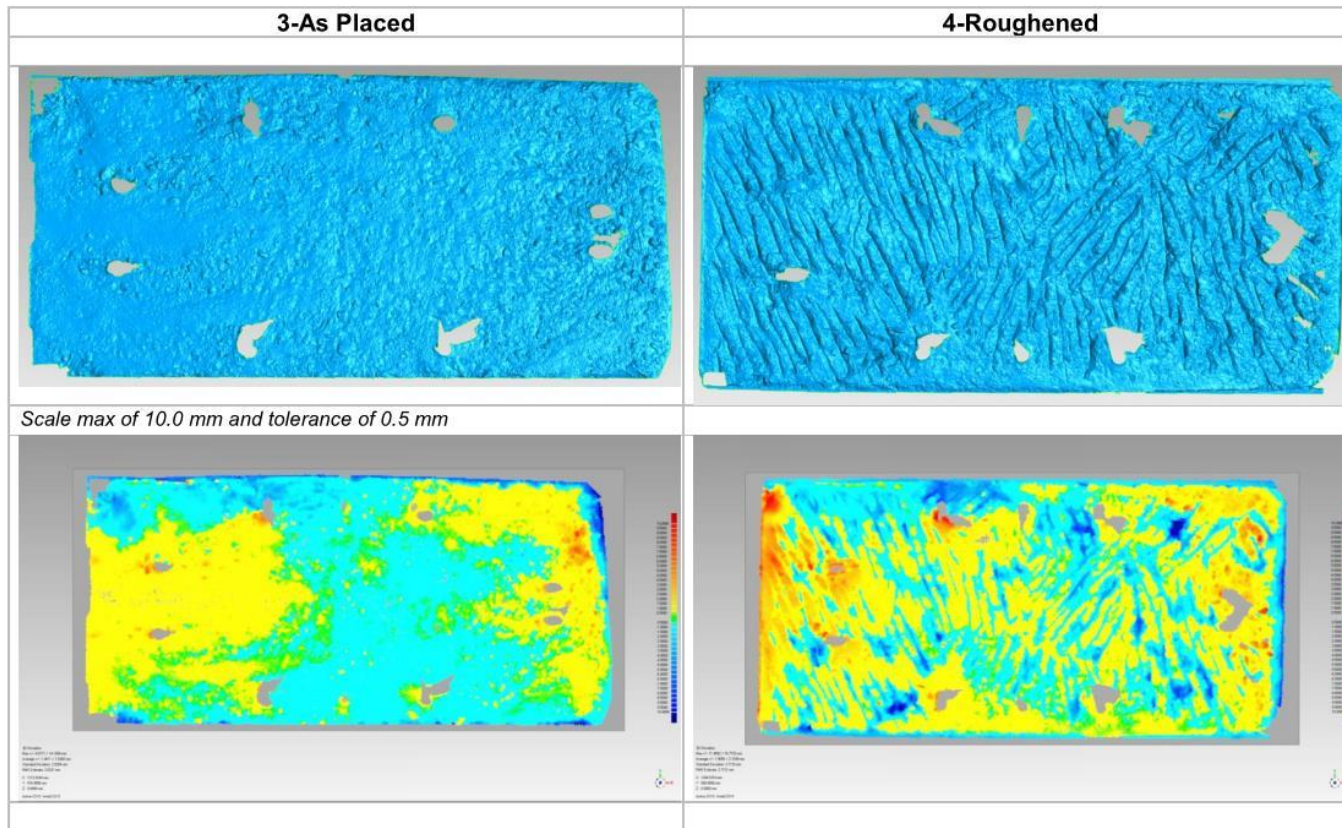


Exhibit 4.1



Top of view of Data Segment and Colormap showing deviations to best-fit plane:

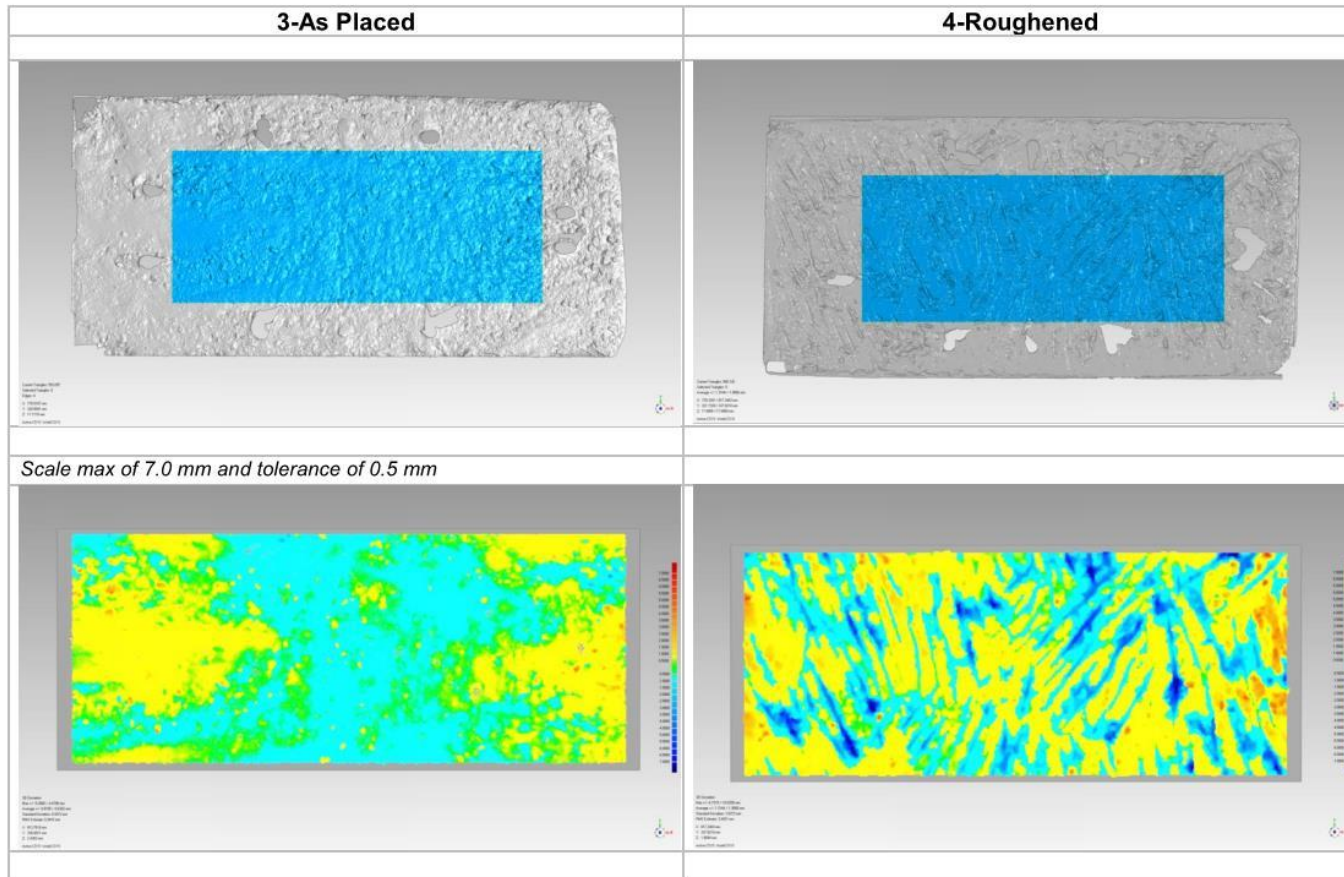


Exhibit 4.1



Isometric view of Data Segment and Colormap showing deviations to best-fit plane:

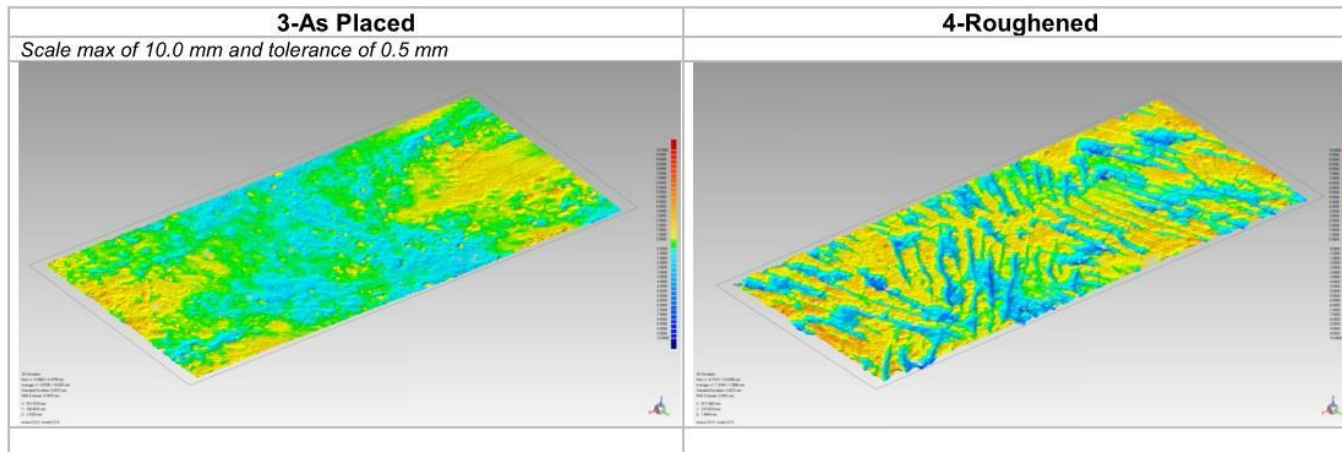


Exhibit 4.1



Isometric view of Colormap showing deviations to best-fit plane (different tolerance thresholds):

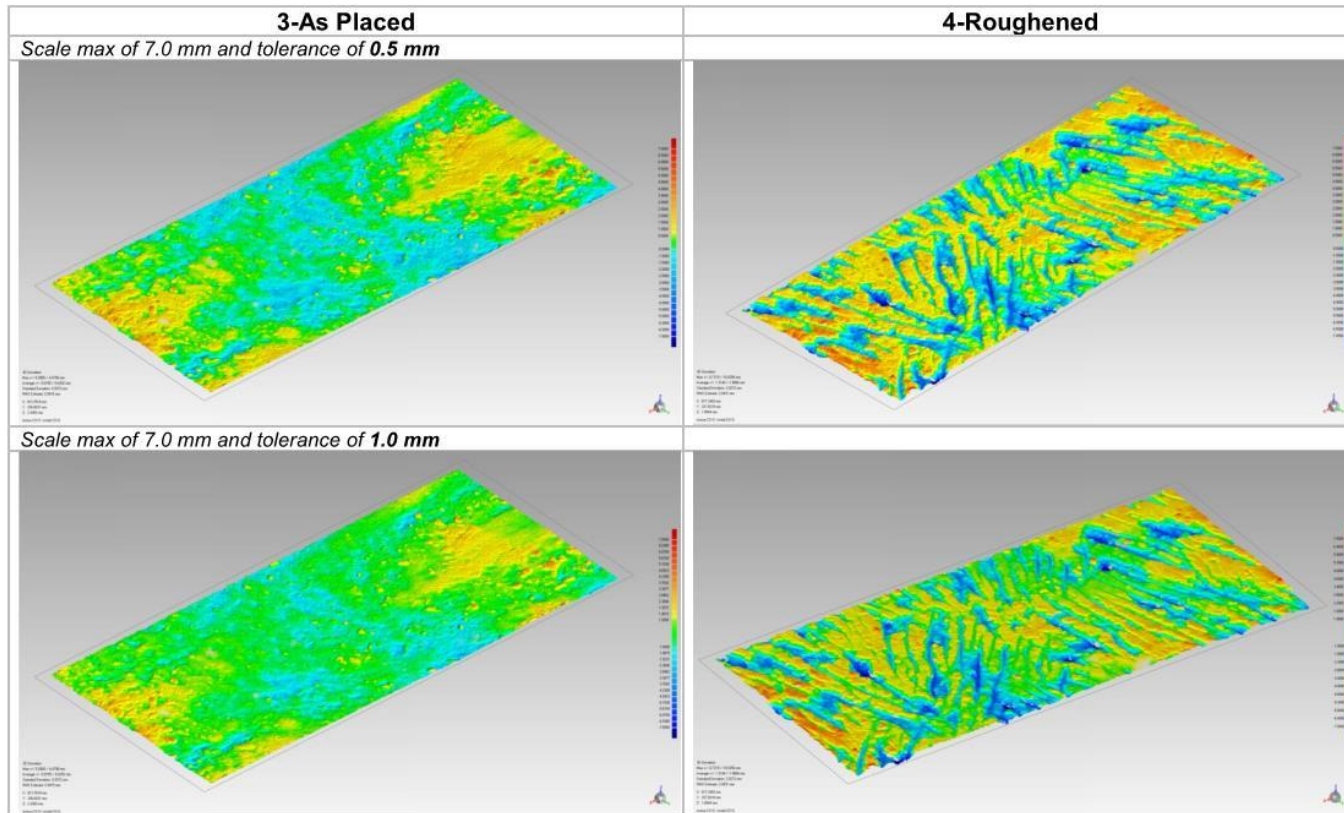
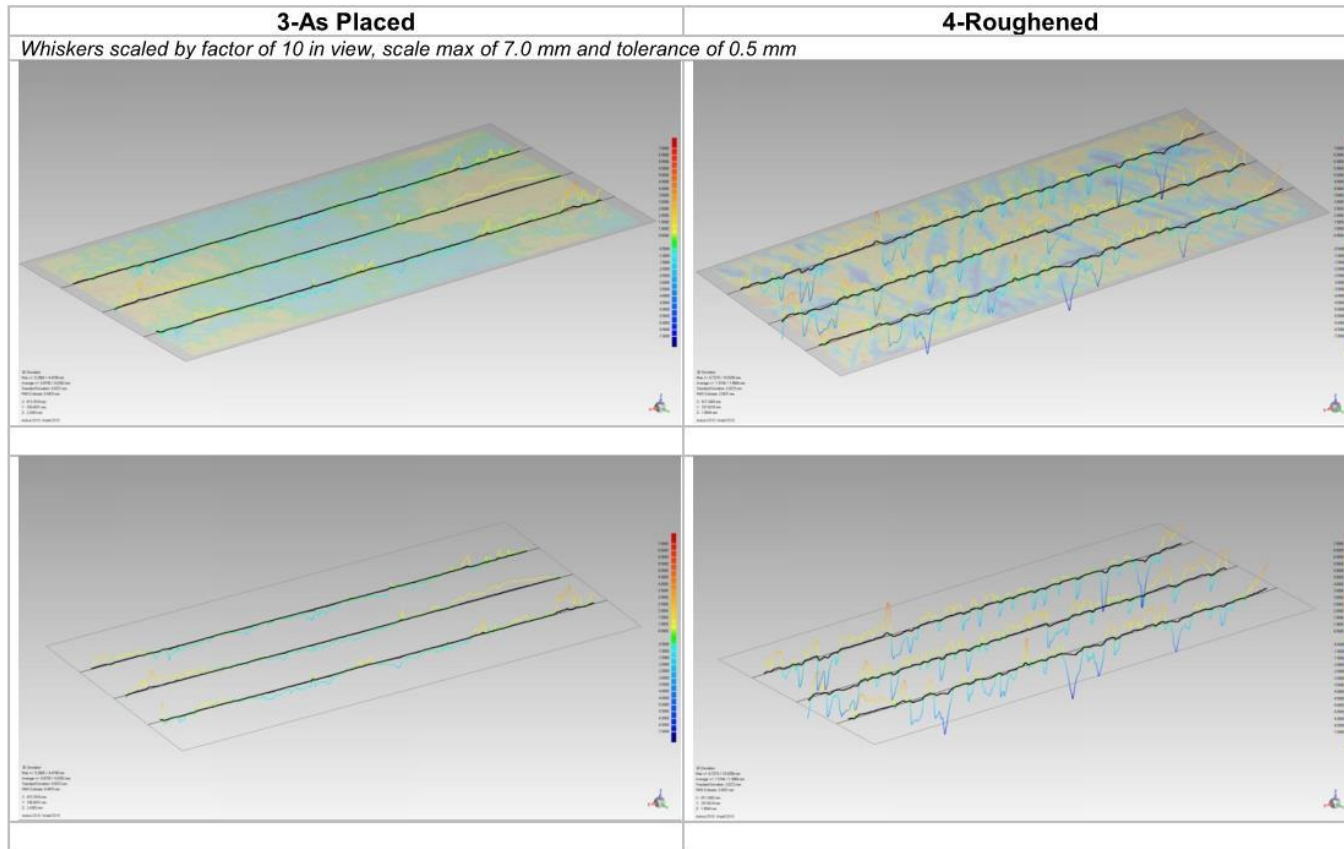


Exhibit 4.1



Sectional Deviations (whiskers scaled by factor of 10 in view, scale max of 7.0 mm and tolerance of 0.5 mm):



5 STRUCTURAL ANALYSES

WJE carried out independent structural analyses of the main span. The analyses included the following:

- Development of a finite element models to independently determine the forces and bending moments in the truss members during construction.
- AASHTO Code evaluation of the Member 11/12 deck connection for loading during construction when the main span was placed on its final supports.
- Evaluation of the Member 11/12 deck connection for the conditions at the time of the collapse based on test results.

5.1 Finite Element Analysis

5.1.1 Model Description and Assumptions

A finite element model of the main span was developed and analyzed using Abaqus, general purpose commercial finite element software for structural analysis of complex systems. The model was used to determine truss forces and bending moments during construction. The concrete elements were modeled using approximately 800,000 solid hexahedral elements. Diagonal and horizontal post-tensioning bars were modeled with beam and truss elements, respectively. An overview of the model is shown in Figure 5.1.

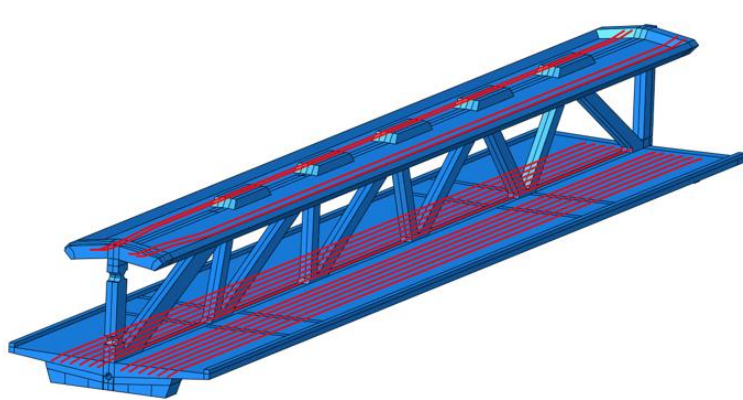


Figure 5.1. Abacus model of main span (Blue elements are concrete; red elements are post-tensioning tendons.)

Two versions of the model were developed:

- *Model 1 – Design Conditions.* A model representing the conditions required for design of the main span after it was placed in its final position between the south pier and central pier.
- *Model 2 – As-Built Conditions.* A model representing as-built conditions at the time of the collapse.

The materials properties for each of these models are summarized in the following table.

Table 5.1. Materials Properties for Finite Element Models

Property	Model	Value	Source
Concrete compressive strength	1	8,500 psi	Project General Notes
	2	10,200 psi	Estimate based on concrete testing information in the OSHA Report
Concrete unit weight	1	148.5 pcf	AASHTO ¹¹ Table 3.5.1-1 based on specified compressive strength. Unit weight was increased 5 pcf to account for mild reinforcement.
	2	138.7 pcf	Estimate from WJE replication of project mix design, not including 5 pcf allowance for weight of mild reinforcement.
Concrete modulus of elasticity	1	5255 ksi	AASHTO Equation 5.4.2.4-1
	2	4584 ksi	Estimate for project mix design
PT modulus of elasticity	1 and 2	29,700 ksi	DSI DYWIDAG Post-tensioning Systems brochure (page 25)

5.1.2 Loading

The loadings for each of these models are summarized in the following table. Load factors are not included. The weight of the concrete curb is not included in the design conditions model because the project drawings show it being constructed after the back span is placed. The weight of the curb is included in the as-built conditions model because it was constructed in the casting yard.

Table 5.2. Loadings for Finite Element Models

Loading	Model	Loading
Dead load	1	Specified dimensions and AASHTO unit weight of 148.5 pcf increased by 5 pcf for mild reinforcement. Concrete curb not included.
	2	Specified dimensions and unit weight of 138.7 pcf increased by 5 pcf for mild reinforcement. Concrete curb included.
Construction load	1	20 psf on deck walking surface, the minimum construction load required by Section 4.10 of the project design criteria (April 2015 revision).
	2	Calculated weight of temporary railing (3 plf) plus the estimated weight of the workers and hydraulic jack on the canopy at the time of the collapse (1.5 kips at blister above Member 11).

5.1.3 Post-Tensioning Force in Member 11

The specified post-tension force of 280 kips in each post-tensioning bar was applied as an imposed strain. The construction sequence was considered. For the design conditions model, the post-tensioning was applied before shoring below the main span was removed. In this way, the post-tensioning force decreased due to shortening of Member 11 as the self-weight was applied in the final, simply-supported condition.

For the as-built conditions model, the specified post-tensioning force was applied when the span was supported in its final position between the south pier and central pier to simulate the re-tensioning. Consistent with review of the time of collapse video, it was assumed that the final post-tensioning step was being applied when the collapse occurred. In this case, the specified post-tensioning force was not reduced

¹¹ AASHTO LRFD Bridge Design Specifications, Seventh Edition

due to elastic shortening of Member 11 due to self-weight. Therefore, the Member 11 post-tensioning force in the as-built conditions model is slightly greater than that in the design conditions model.

5.1.4 Results

The results are summarized in Table 5.3. Finite Element Model Results. These results are considered in the evaluations of the Member 11/12 Deck Connection in Sections 6 and 7.

Table 5.3. Finite Element Model Results

Member	Model	Axial Force (kips)			Bending Moment (kip-ft)		
		DL	CL	PT	D	CL	PT
Member 11	1	-1236	-68	-589	217	9.8	-11
	2	-1166	-3	-574	207	0.4	-9
Member 12	1	-67	-1	-15	57	5	210
	2	-63	0	-14	55	0.2	197

Notes:

DC = Dead load of structural components

CL = Construction live load

PT = Post-tensioning force

Negative axial force indicates compressive force

For design, the forces and bending moments listed in Table 5.3. Finite Element Model Results must be multiplied by the appropriate load factor for the controlling load combination.

5.2 Code Evaluation of Member 11/12 Deck Connection (As-built Condition)

The objective of the evaluation was to independently determine the capacity of the northernmost truss web member's connection to the deck per the governing design code¹² (AASHTO Code). The loading configuration considered was the main span placed in its final position between the south pier and central pier before the post-tensioning in Member 11 was released.

5.2.1 Limit State

The main span was constructed in three primary casting operations: the deck, the diagonal and vertical web members, and the canopy. Figure 5.2 shows an elevation view of the M11/M12 joint and the deck with the construction joint between the deck and web members is highlighted. This evaluation focuses on the horizontal shear transfer across this interface to resist the horizontal component of the compressive axial force in Member 11. The most obvious load transfer mechanism is shear-friction, which uses surface roughness and reinforcement crossing the interface to transfer shear with a combination of dowel action, cohesion, and friction. If the interface is not cracked, shear along an interface is resisted by cohesion from cementitious bond. After cracking, cementitious bond is lost and load is resisted by aggregate interlock, friction, and dowel action.¹³ The friction component relies on the reinforcement and applied loading to develop a normal force.

¹² AASHTO LRFD Bridge Design Specifications, Seventh Edition

¹³ Hofbeck, J. A., Ibrahim, I. O., & Mattock, A. H. (1969, February). Shear transfer in reinforced concrete. In Journal Proceedings (Vol. 66, No. 2, pp. 119-128).

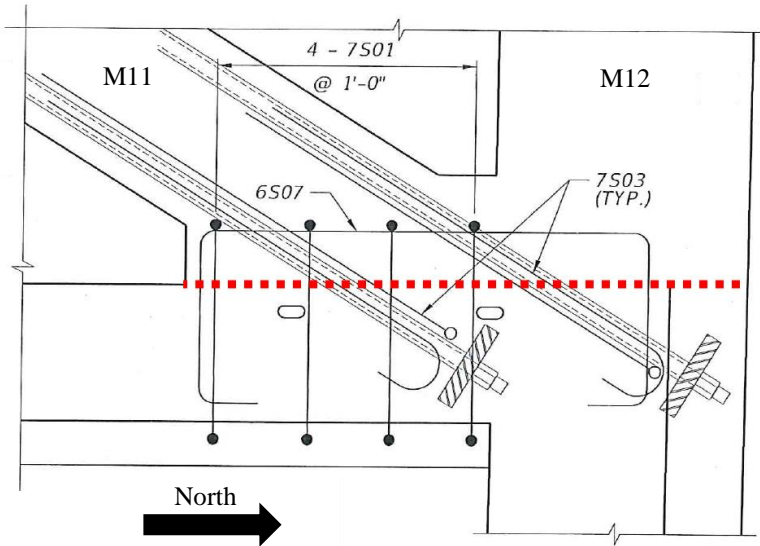


Figure 5.2. Excerpt from Design Drawings showing configuration of joint area. Construction joint indicated by dotted line.

At the time of collapse, the bridge was in a temporary condition with only the main span in place. In the final configuration, Member 12 and the north diaphragm would have been incorporated into the pylon, and Span 2 would have been placed against the north end of the main span. These changes would have made the truss continuous and prevented any horizontal displacement at the joint.

5.2.2 Demand

The structural demands at the joint were due to dead load, construction live load, and post-tensioning force in Members 11 and 12 (see Table 5.3). To determine the factored load effect, the controlling load combination was evaluated. Per the AASHTO Code Strength I load combination, load factors of 1.25, 1.5, and 1.0 apply to the dead load, construction live load, and post-tensioning load, respectively.

Section 1.3.2.1 of the AASHTO Code requires consideration of load modifiers greater than 1.0 for the strength limit state in certain circumstances. Specifically, Section 1.3.3 specifies a load modifier of 1.05 for non-ductile components and connections, and Section 1.3.4 specifies the load modifier of 1.05 for non-redundant members. However, the AASHTO Code lacks specific guidance on when to apply these factors, apparently leaving it to the judgment of the engineer. Also, the AASHTO Code makes no mention of the applicability of these factors to temporary construction stages, nor does it exempt construction activities from their applicability. However, as a practical matter, even highly-redundant multi-girder bridges are often non-redundant when the first beam is erected.

The results are summarized in Table 5.4 in terms of the northward force at the M11/M12 interface with the deck. The northward force includes horizontal force components from both Members 11 and 12.

**Table 5.4. Calculated Horizontal Shear Force at Connection of M11/M12 to Deck
(Finite Element Model 1: Design Conditions)**

Load	Northward Force at M11/M12 (kips)		
	Un-Factored	Factored	Factored with Load Modifiers
Dead Load	1089	1361	1501
Construction Live Load*	59	89	98
Post-tensioning	529	529	583
Total	1677	1979	2182

*20 psf on deck walking surface as required by Section 4.10 the Project Design Criteria

5.2.3 Capacity

The capacity of the connection between Member 11/12 and the deck is shear-friction at the construction joint below Members 11 and 12, the dashed red line in Figure 5.2.

Shear-Friction in AASHTO. A pure shear-friction model assumes interface shear resistance is a product of the net normal clamping force and the friction coefficient. The normal force is usually provided by reinforcement crossing the interface and axial load. The AASHTO Code uses a modified shear-friction model accounting for a contribution from cohesion and/or aggregate interlock, which is evident in the experimental data. In this way, the AASHTO Code shear-friction model is analogous to the vertical shear resistance expression of $V_c + V_s$.¹⁴

The nominal shear resistance of the interface plane is given by AASHTO Code Equation 5.8.4.1-3:

$$V_{ni} = cA_{cv} + \mu(A_{vf}f_y + P_c)$$

where:

- V_{ni} = nominal interface shear resistance (kip)
- c = cohesion coefficient (ksi)
- A_{cv} = area of concrete section resisting shear transfer (in.²)
- μ = coefficient of friction
- A_{vf} = area of shear-friction reinforcement (in.²)
- f_y = yield strength of shear-friction reinforcement (ksi)
- P_c = permanent compressive force (kip)

As can be seen in the above equation, the resistance provided by cohesion is taken as a cohesion factor times the interface area under consideration. For simplicity, a “cohesion factor” is used in the AASHTO Code to capture the effects of cohesion and/or aggregate interlock. However, cohesion provided by cementitious bond and the shear-friction contribution of reinforcement cannot co-exist because the latter requires separation across the interface to develop strain in the shear-friction reinforcement. Thus, when friction from a normal force provided by reinforcement is combined with the “cohesion” contribution, the latter is actually the contribution of aggregate interlock or other effects related to the concrete area. For concrete that is roughened to amplitude of 0.25 inches, the cohesion coefficient is 0.24 ksi and the friction

¹⁴ Commentary to AASHTO Code, Section C5.8.4.1

coefficient is 1.0. For concrete that is not intentionally roughened, the cohesion coefficient is 0.075 ksi and the friction coefficient is 0.6.

In the above resistance equation, P_c is defined as the permanent compressive force. While an argument could be made that this refers to dead load, P_c was interpreted to mean force that is coincident by necessity with the design interface shear; that is, forces that are present by virtue of the presence of the shear demand. Vertical components of truss compressive force meet this criterion.

These shear-friction parameters are based on research in which the interfaces of most specimens were intentionally unbonded or initially cracked.¹⁵ Unbonded and initially cracked specimens were primarily used because a crack at the interface between concrete cast at different times should be assumed.

In addition, the AASHTO Code includes two maximum shear stress limits. The first limit is the concrete compressive strength multiplied by a surface preparation coefficient: 0.25 for concrete roughened to an amplitude of 0.25 inches and 0.2 for a surface that is not intentionally roughened. The second shear stress limit depends only on surface roughness: 1.5 ksi for concrete roughened to an amplitude of 0.25 inches and 0.8 ksi for a surface that is not intentionally roughened.

Construction Joint. One of the primary factors in evaluating the shear-friction capacity is the roughness of the construction joint when the web members were cast against it. In correspondence between FIGG and MCM during construction, FIGG confirmed that the FDOT Standard Specifications¹⁶ were to be followed. These include instructions for preparations of construction joints before casting new concrete against hardened concrete including direction to “roughen the surface of the hardened concrete.” Despite this, the joint appeared to be left in an as-placed (non-roughened) condition, as described in Section 3.

For the assumption of a roughened surface, the AASHTO Code specifically calls for a roughness amplitude of 1/4 inch, but this criterion is not included in the FDOT Specifications. However, AASHTO does not provide specifics on preparation of the construction joint (including intentional roughening of hardened concrete) or how roughness amplitude is measured. The FDOT Standard Specifications, as proven by the tests described in Section 4, achieves the requirements of the AASHTO Code. Therefore, these calculations use the friction parameters for intentional roughness found in the AASHTO Code.

Shear-Friction Assumptions. Although inconsistent with the failure mode described in Section 2, which involved a combination of shear-friction below Member 11 and breakout below Member 12, shear-friction was evaluated across the entire construction joint shown in Figure 5.2. The AASHTO Code does not require or even address evaluation of a combined shear-friction and breakout resistance. As such, the assumption of shear-friction resistance across the entire construction joint is considered to be a likely choice in design.

Section 5.8.4.1 of the AASHTO Code requires reinforcement for interface shear transfer to be developed on both sides of the interface to develop the design yield stress. At mid-length, there are three #11 bars on the south face of Member 12. However, only two of three #11 bars on the north face are fully developed across the construction joint and considered to contribute to shear-friction resistance.

¹⁵ Mattock, A., "Shear Transfer under Monotonic Loading, across an Interface between Concrete Cast at Different Times," Report SM 76-3, University of Washington Department of Civil Engineering, 1976.

¹⁶ Florida Department of Transportation. (July 2015). *Standard Specifications for Road and Bridge Construction, Division II - Construction Details.*

The #6 and #7 stirrups shown in Figure 5.3 were not fully developed above the interface in accordance with the AASHTO Code requirement for development of hooked bars in tension (AASHTO 5.11.2.4). However, the vertical legs of the #6 and #7 stirrups are connected across the top. The vertical legs of these bars are fully developed based on the AASHTO requirements for strut-and-tie models in Section 5.6.3. The strut-and-tie model for the #7 stirrups is shown in Figure 5.3. As such, these bars were considered to contribute to shear-friction resistance.

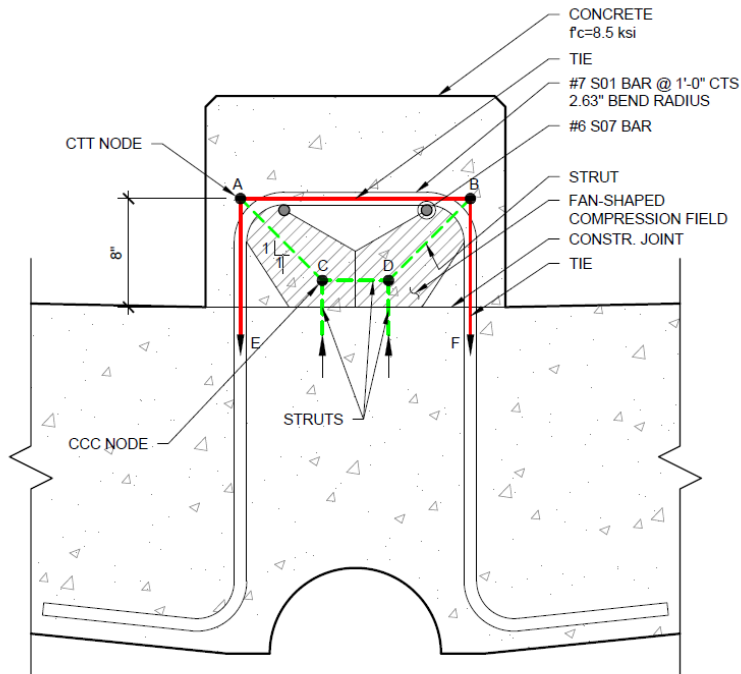


Figure 5.3. Strut-and-tie model of #7 stirrups across construction joint

The inclined #7 bars in Member 11 crossing the interface were not considered to contribute to shear-friction capacity because northward sliding produces compression in the inclined bars, as explained in Section R22.9.4.3 of ACI 318-14.¹⁷

5.2.4 Findings: Design Conditions

The findings with respect to shear-friction design capacity are summarized in Table 5.5, both in terms of factored shear-friction resistance and the ratio factored load effects to factored resistance, capacity-demand ratio (CDR). As described above, a roughened surface is assumed in accordance with the FDOT Standard Specifications. In light of the uncertainty as to their applicability to as-built conditions, Factored resistance and CDRs excluding and including the load modifiers are provided. Design strengths include the strength reduction factor, ϕ , for shear of 0.9.

¹⁷ ACI 318-14. “Building Code Requirements for Structural Concrete and Commentary.” American Concrete Institute.

Table 5.5. Summary of Shear-Friction Resistance and CDRs

Factored Northward Force (kips)		Factored Shear-Friction Resistance, ϕV_n (kips)	CDR	
Load Modifiers			Load Modifiers	
Excluded	Included		Excluded	Included
1979	2182	2150	1.09	0.99

These results indicate compliance with the AASHTO Code for shear-friction along the construction joint below Members 11 and 12.

If a combined shear-friction and breakout failure similar to that observed were to be evaluated assuming a roughened surface, a somewhat lower resistance would be calculated than that assuming resistance by shear friction across the entire construction joint. Such a combined failure is not likely to be envisioned in design and is not addressed by the AASHTO Code. Regardless of which of the two failure mechanisms is assumed, the connection would not have failed if the joint was prepared in accordance with FDOT Standard Specifications.

5.2.5 Findings: Design Conditions (Non-Roughened Surface)

The CDRs for shear-friction are much lower if a non-roughened surface is assumed, as summarized in Table 5.6.

Table 5.6. Summary of Shear-Friction Resistance and CDRs

Factored Northward Force (kips)		Factored Shear-Friction Resistance, ϕV_n (kips)	CDR	
Load Modifiers			Load Modifiers	
Excluded	Included		Excluded	Included
1979	2182	1157	0.58	0.53

5.3 Test-based Evaluation of Member 11/12 Deck Connection for As-built conditions

The objective of this study is to evaluate the observed performance of the connection relative to the expected resistance based on test results and advanced analyses. The determination of loading and resistance is based on actual conditions at the time of the failure, when the main span was supported between the south pier and central pier. The resistance is based on calculations as well as the results of tests of specimens that replicate shear transfer between the northernmost diagonal of the main span (Member 11) and the deck.

5.3.1 Failure Sequence and Pattern

The failure pattern and sequences described in Section 2. The physical evidence indicates extreme northward deformation of the Member 11/12 deck connection due to shear-friction failure at the construction joint below Member 11 in combination with breakout failure of the north end diaphragm below Member 12. The movement caused sudden crushing of Member 11 near its base, which in turn triggered the collapse.

5.3.2 Calculated Forces at Time of Collapse

The structural demands at the joint were due to dead load, construction live load, and post-tensioning. Construction loading included the calculated weight of the temporary railing plus the estimated weight of

the workers and hydraulic jack on the canopy at the time of the collapse. The calculated axial force in Member 11 and the calculated northward force at the M11/M12 interface with the deck are based on the finite element model of the main span and are provided in Table 5.7. Note that the northward force includes force components from both Members 11 and 12.

Table 5.7. Calculated Forces in Member 11 and Connection of M11/M12 to Deck

Load	Axial Force in Member 11 (kips)	Northward Force at M11/M12 (kips)
Dead Load	1166	1028
Construction Live Load*	3	3
Post-tensioning	574	527
Total	1743	1677

5.3.3 Connection Strength (As-Built)

Based on the observed failure pattern, the resistance of the connection to horizontal movement comes primarily from two mechanisms: 1) horizontal shear-friction below Member 11, and 2) horizontal break-out of the north and diaphragm below Member 12. Apparently, the # 11 bars extending from the diaphragm into Member 12 precluded continued sliding; that is, north of the #11 bars, the observed behavior indicates breakout resistance was less than shear-friction resistance.

The following sections discuss these two primary resistance mechanisms as well as other factors affecting resistance of the connection to horizontal force.

Shear-Friction Resistance. Shear-Friction resistance depends on the area and roughness of the interface, the reinforcement crossing the interface, as well as any external normal force across the interface. As described in Section 3, the concrete on the deck surface below Members 11 and 12 was apparently left in an as-placed (non-roughened) condition. Photographs indicate that the surface texture is relatively smooth, although coarse aggregate occasionally protrudes above the surface. Longitudinal reinforcement and stirrups cross the interface. The axial force in Member 11 creates both a normal force and sliding force at the interface.

Given the unique interface conditions, shear-friction resistance was evaluated based on tests of specimens that replicate shear transfer between the Member 11 and the deck. As described in Section 4, six specimens were tested: three with an as-placed (non-roughened) interface and three with a roughened interface. Two of the three as-placed and roughened specimens were cracked at the bond line prior to testing. The specimens with an as-placed, cracked interface (Specimens 1 and 2) best reflect the field conditions at the time of the failure. The results are summarized in Table 4.7.

Because Specimen 1 was not severely damaged in the initial test, the specimen was reloaded after the first failure to get a sense of residual strength. After the initial failure, displacement along the construction joint was about 0.5 inches. The peak axial load in the retest was 737 kips, 43 percent less than the axial load at the initial failure.

The performance of the as-placed (non-roughened) cracked specimens described in Section 4 indicate that the vast majority of the shear force at the connection was resisted through shear-friction below Member 11. Based on results of Specimens 1 and 2, 66 to 82 percent of the calculated horizontal force (1677 kips) is

resisted by shear-friction. The remainder, roughly 400 kips, must be resisted by breakout or other mechanisms.

Breakout Resistance. The physical evidence indicates breakout of the north end diaphragm below Member 12 contributed to resistance to the horizontal force at the Member 11/12 deck connection. The total breakout resistance was calculated to be 440 kips. This calculated resistance was determined by modifying the code-based breakout capacity for breakout angle and the expected difference between experimental results and lower-bound code resistance equations.

To evaluate the breakout capacity of the north end diaphragm, the #11 column bars in the south face of Member 12 were treated as anchors loaded in shear. The AASHTO Code does not include provisions for breakout and instead refers to ACI 318. Section 17.5 of ACI 318-14 was applied to the joint geometry. This approach produced a calculated resistance of 161 kips. Reinforcement crossing the breakout plan, which may enhance breakout resistance, was not considered. Likewise, the vertical PVC pipes and the drainpipe, which may reduce breakout resistance, were also not considered.

However, the interior post-tensioning tendons forced a narrow breakout cone. The angle between the outermost #11 bars and the interior post-tensioning tendons is about 55 degrees relative to an east-west line, as illustrated in Figure 5.4. In contrast, the breakout angle on which the ACI 318 resistance model is based is 35 degrees¹⁸.

Shear resistance increases with increasing crack angle, which is reflected in research¹⁹ as well as ACI 318 provisions for shear in discontinuity regions²⁰. In ACI 318-19 Eq. 23.4.4, which applies to one-way shear in discontinuity regions, shear strength is proportional to the tangent of the crack angle. Applying this rationale to breakout strength, the observed narrow breakout cone would double the breakout resistance ($\tan 55 / \tan 35 = 2.04$).

Furthermore, the basic ACI 318 expression for breakout²¹ is based on the lower-bound of test results. The design equation is partly derived from research by Eligehausen, et al²². The coefficient of variation for the underlying test results is 19 percent. The Eligehausen expression for the mean value of the test data gives results that are 34 percent greater than the ACI 318 expression.

¹⁸ ACI 318-19, Figure R17.5.1.

¹⁹ Zsutty, T. C., 1971, "Shear Strength Prediction for Separate Categories of Simple Beams Tests," ACI Journal, Proceedings V. 68, No. 2, Feb., pp. 138-143

²⁰ ACI 318-19, 23.4.4

²¹ ACI 318-19, Eq. (17.6.2.2.1)

²² Eligehausen, R.; Fuchs, W.; and Mayer, B., 1987, "Load Bearing Behavior of Anchor Fastenings in Tension," Betonwerk + Fertigteiltechnik, V. 12, pp. 826-832, and 1988, V. 1, pp. 29-35.

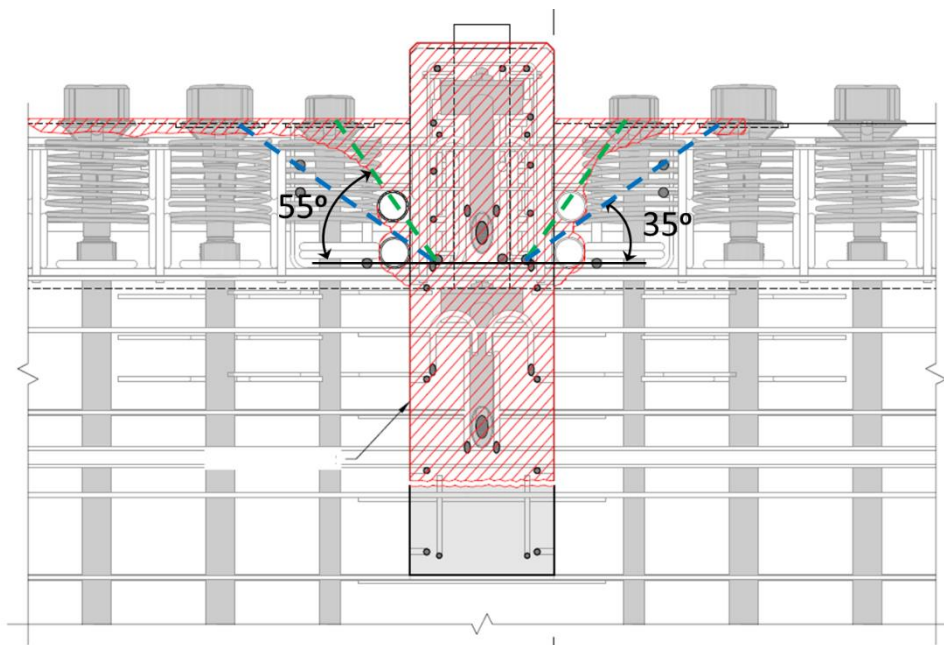


Figure 5.4. Plan view at north end showing breakout angle

Adjusting for both breakout angle and the conservatism of the ACI expression, a breakout resistance of 440 kips would be expected ($161 \times 2.04 \times 1.34 = 440$ kips).

The maximum measured shear forces for the as-placed (non-roughened), cracked specimens were 1101 kips and 1372 kips (see Table 4.7). Thus, the shear-friction resistance from testing plus the adjusted calculation of the breakout resistance (440 kips) ranges from 1541 kips to 1812 kips. The calculated shear force, 1677 kips (see Table 5.7), is in the middle of this range.

5.3.4 Discussion

The test results and calculations described above indicate the potential resistance of shear-friction and breakout is consistent with the calculated horizontal force at the Member 11/12 connection to the deck and the observed cracking and sliding shortly after the shoring was removed.

However, both shear-friction and breakout reach peak resistance with very little deformation. In the case of the interface shear tests, peak shear-friction resistance occurs at a deformation of approximately 0.02 inches. Deformations at breakout failure are about twice this amount, 0.04 inches. Before collapse occurred, the total horizontal deformation exceeded 0.5 inches. Therefore, other mechanisms must have taken over as shear-friction and breakout resistance dropped off. Recall that the shear-friction capacity of Specimen 1 was reduced by more than 40 percent when the specimen was retested after the initial failure and displacement of about 0.5 inches.

In WJE's opinion, the most likely source of supplemental resistance is the numerous reinforcing bars that cross the shear-friction interface and breakout cone. More than 20 square inches of reinforcement with a combined yield strength exceeding 1200 kips cross the perimeter of the shear-friction and breakout planes. With significant north-south movement, this reinforcement would offer resistance that increases with increasing displacement through dowel action as well as the north-south component of tension in the

deformed reinforcement²³. The resistance from shear-friction and breakout together with the resistance from the deformed reinforcement explains why resistance was maintained even though northward displacement exceeded 0.5 inches.

5.3.5 Findings

The studies described in this section indicate that the combined shear-friction and breakout resistance is consistent with the calculated horizontal force at the Member 11/12 deck connection. The estimated actual resistance of the Member 11/12 connection to the as-placed (un-roughened) deck surface is roughly equal to the estimated northward force of 1677 kips at failure.

²³ With large displacement, reinforcement crossing the interface would bend into an S-shaped curve, the north-south component of which would add to shear resistance.

6 EVALUATION OF PEER REVIEW

WJE evaluated the peer review of the structural design Louis Berger²⁴ for FIGG. The objective of the independent evaluation is to assess the quality and completeness of the peer review relative to the requirements of Berger's contract, applicable standards, and the standard of care for peer review services.

6.1 Document Review

Observations from review of key documents pertaining to the Berger peer review are provided in the following sections.

6.1.1 Request for Proposals (RFP)

With respect to the peer review, the Florida Department of Transportation, working through FIU, required the following:

“Prior to submittal to the OWNER, bridge plans shall have a peer review analysis by an independent engineering firm not involved with the production of the design or plans, prequalified in accordance with Chapter 14-75²⁵. The peer review shall consist of an independent design check, a check of the plans, and a verification that the design is in accordance with AASHTO, FDOT, and other criteria as herein referenced. The cost of the peer review shall be incurred by the Design-Build Firm. The independent peer review engineer's comments and comment responses shall be included in the 90% plans submittal. At the final plans submittal, the independent peer review engineer shall sign and seal a cover letter certifying the final design and stating that all comments have been addressed and resolved.”

6.1.2 Berger Agreement with FIGG

An excerpt from the scope of services in Berger's agreement with FIGG is shown below in Figure 6.1. The agreement required an independent peer review of the pedestrian bridge plans (foundation, substructure, and superstructure plans) as well as independent estimation of demands on all elements due to different load combinations based on a finite element model. The peer review was to be carried out in accordance with project and RFP requirements as well as Chapter 26 of the FDOT Plans Preparation Manual.

²⁴ Since conducting the peer review in 2016, Louis Berger has become part of WSP Global Inc. Louis Berger is referred to herein as Berger.

²⁵ Refers to Chapter 14-75 of the Florida Administrative Code

Independent Peer Review Scope

1. Louis Berger will perform Independent Peer Review for the concrete pedestrian bridge plans in accordance with the project and RFP requirements and FDOT Plans Preparation Manual (Chapter 26).
2. The Independent Peer Review will include the following activities:

Item #	Item Description
1	Develop finite element model for the bridge and estimation of demands on all elements due to different load combinations
2	Peer review of foundation plans
3	Peer review of substructure plans
4	Peer review of superstructure plans
3. The Independent Peer Review will be performed for the following submittals:
 - a) Final Foundation and Substructure Plan Submittals
 - b) Final Superstructure Plan Submittals
4. This Independent Peer Review scope of work is for the pedestrian bridge structure components only. The elevator structures and stairways/landings are not included in this scope of work.

Figure 6.1. Excerpt from FIGG agreement with Berger (Scope of Services)

Referring to Figure 6.1, note that the agreement requires peer review of the superstructure plans and references the RFP requirements as well as Chapter 26 of the FDOT Plans Preparation Manual.

6.1.3 FDOT Plans Preparation Manual: Chapter 26

Section 26.12 of the FDOT Plans Preparation Manual²⁶ (2015 Edition) addresses independent peer review of Category 2 bridges. The FIU pedestrian bridge is a Category 2 bridge in accordance with Section 26.3.2 because it includes post-tension components and design concepts, components, details, and construction techniques not normally used by the Florida DOT. Section 26.12 includes the following statements and requirements:

- “An independent peer review ... is an independent verification of the design using different programs and independent processes than what was used by the EOR.”
- “All independent peer review shall include... 4. Compliance with AASHTO, Department and FHWA design requirements... 7. Design results/recommendations (independent verification of design)... 10. Constructibility assessment limited to looking at fatal flaws in design approach.”

²⁶ Excerpts are from the 2015 edition, which is believed to be applicable. However, the quoted requirements are not substantially changed in subsequent editions through 2017.

6.1.4 Released for Construction (RFC) Plans

Sheet B-109 of the Superstructure Plans, which are included within the scope of the peer review, illustrate and describe the construction sequence. Figure 6.2 is an excerpt from Sheet B-109 showing erection of the main span in Stage 3. Step 2 of Stage 3 calls for “move main span from the staging area to final position.” At this stage of construction, the main span functions as a simply supported concrete truss and must carry its own weight plus any construction live load without the benefit of the back span or stay pipes, which are constructed in subsequent stages.

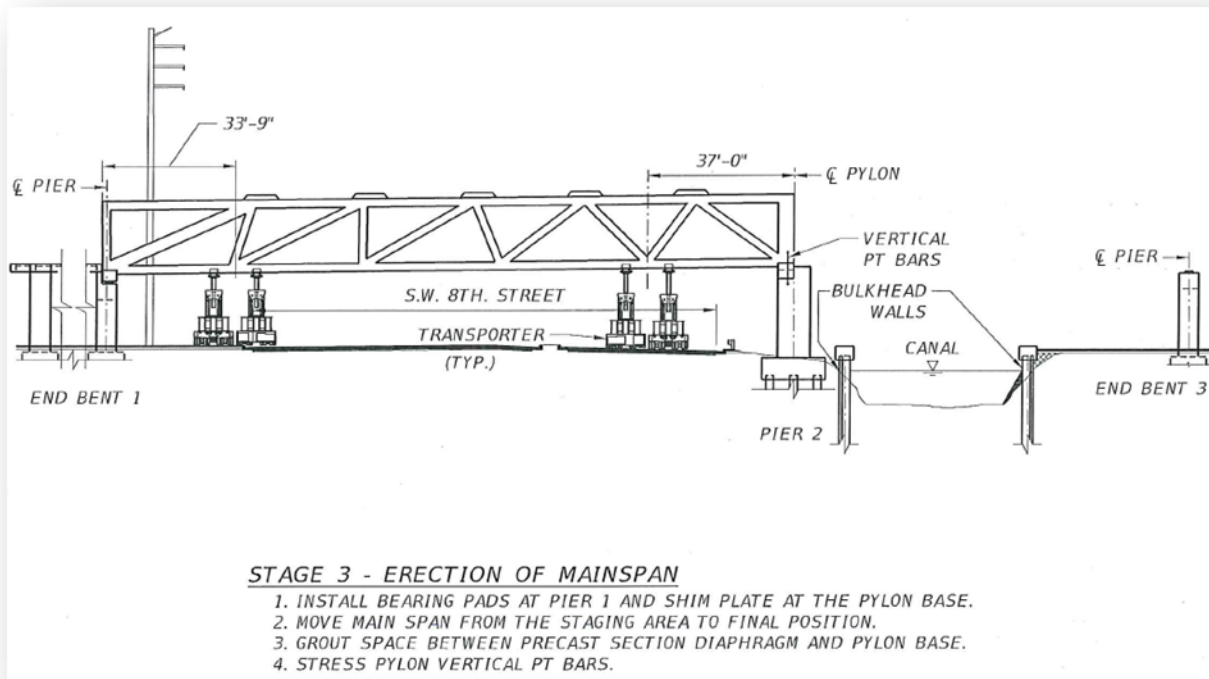


Figure 6.2. Illustration and description of Stage 3 of construction sequence from Superstructure Plan Sheet B-109

6.1.5 Berger Peer Review Comments

Under the Design Quality Management Plan for the project, review comments from all parties were submitted using the Review Comment Form, which included numbered comments and responses. Based on WJE’s review of documents produced by Berger, Berger submitted only one Review Comment Form, which pertained to the Foundation Plans (attached hereto as Exhibit 6.1.1 and 6.1.2). All but one comment pertained to foundation issues. The exception is Comment 2, which expresses concern that the first vertical vibration frequency calculated by Berger was just under the AASHTO minimum of 3 Hertz. FIGG responded that their calculations indicate a natural frequency of 3.1 Hertz. Accordingly, the comment was closed.

6.1.6 Email Correspondence

Only a few email messages were found in the Berger file. Two emails are considered noteworthy:

1. Ayman Shama, the lead peer reviewer for Berger, emailed Jamey Barbas, Berger Senior VP, on July 25, 2016. The email is provided in Figure 6.3. The message describes Mr. Shama’s understanding of the bridge’s structural behavior, indicating that “While the bridge is not a cable stayed bridge, but all the steps followed in analyzing and reviewing a cable stayed bridge will be followed.”
2. Nick Ivanoff, Berger Executive VP, emailed Jeff D’Agosta, also with Berger, on March 15, 2018, at 3:38 p.m., less than two hours after the collapse. The email states that “Louis Berger had provided a review of the design but had nothing to do with the constructibility review or issues.”

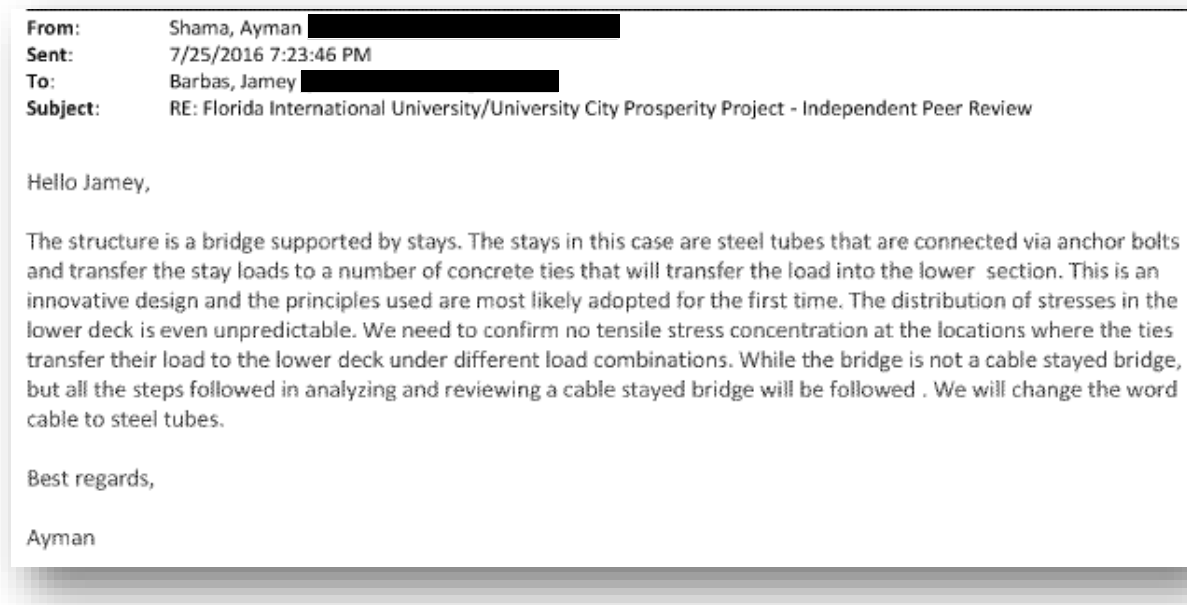


Figure 6.3. July 25, 2016, email from Ayman Shama, lead peer reviewer for Berger, to Jamey Barbas, Berger Senior VP

6.1.7 Berger Analytical Model

Berger developed an analytical model of the bridge using Adina, a finite element analysis program for linear and nonlinear analysis of solids and structures in statics and dynamics. Berger’s input and output files were provided after the collapse and reviewed by WJE. WJE re-created the model using Berger’s input file. Figure 6.4 shows Berger’s model of the bridge.

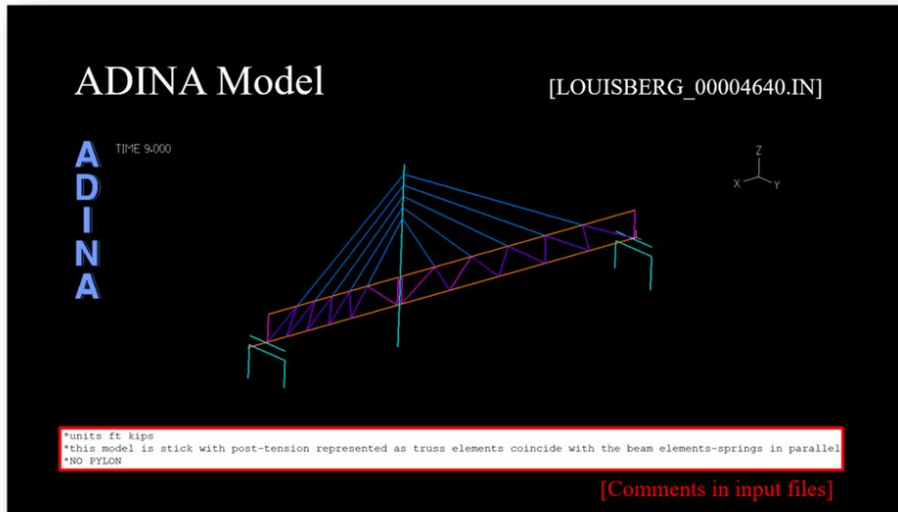


Figure 6.4. Adina finite element model of the bridge re-created from the Berger input file

As can be seen in Figure 6.4, the model includes the stay pipes as well as the concrete truss members in the main span and back span. Figure 6.5 shows the deformed shape under dead load according to Berger's model. In this model, the stay pipes work with the truss members to resist dead load from the concrete structure. However, according to the construction sequence, the concrete structure must support itself before the stay pipes are installed. As previously noted, the stay pipes are intended only to increase bridge stiffness and mitigate vibration. As such, the Berger model could not have been used to reasonably estimate the forces in the concrete truss members, which was required by their peer review contract.

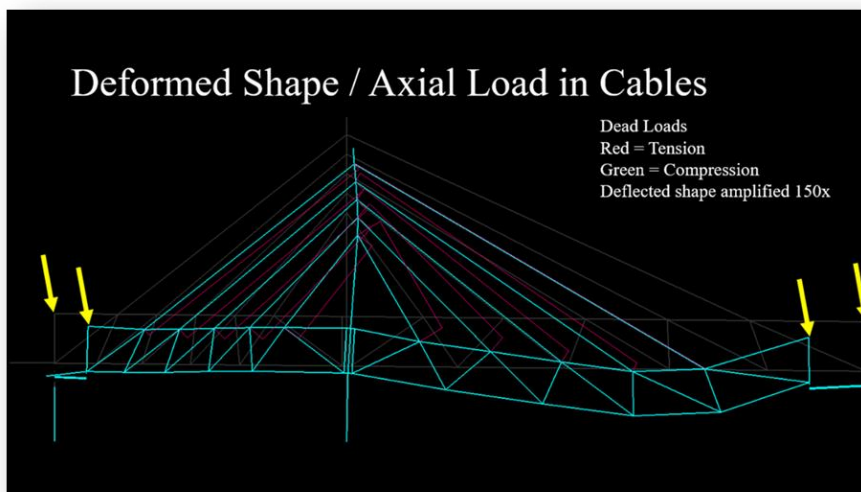


Figure 6.5. Deformed shape according to Berger model

6.1.8 Berger Web Member Checks

Although no comprehensive calculation package was found in the file, it was apparent that Berger analyzed the capacity of the web members. The web members were evaluated by Berger using *pcaColumn*, software for design and investigation of reinforced cross-sections subject to axial and flexural loads.

Berger's *pcaColumn* files included analysis of the northernmost diagonal in the main span (Member 11), a 24-inch by 21-inch rectangular member with 2-#7 bars on each face. WJE used the Berger input file to re-create their *pcaColumn* analysis in accordance with the Seventh Edition of the AASHTO LRFD Code. The graphical output, including axial forces determined by Berger, is provided in Exhibit 6.2. Their analysis consider a factored axial force of 1760 kips. Presumably, this value was based on their Adina model.

The factored axial force considering construction staging is 2365 kips, 34 percent more than the value considered by Berger. The discrepancy is apparently due to the unconservative Adina model in which the stay pipes are incorrectly assumed to work with the truss members to resist dead load of the concrete structure. As noted in the previous section, the Berger model could not have been used to reasonably estimate the forces in the concrete truss members, which was required by their peer review contract.

6.1.9 Certification Letters

Berger provided certification letters, signed and sealed by their review engineer for the foundation, substructure and superstructure final plans, stating that they conducted an independent peer review in accordance with FDOT requirements.

6.2 Expected and Provided Peer Review Documents

Based on review of the Berger file, WJE compared the peer review documents produced by Berger to those expected based on Berger's contractual requirements and the standard of care for a structural peer review of a Category 2 bridge.

WJE's findings are summarized in Exhibit 6.3.1 to 6.3.3.

6.3 Discussion

6.3.1 Quality and Completeness of Berger Peer Review.

Berger's contractual obligations are defined by their agreement with FIGG, which incorporated referenced standards for peer review, including the RFP and Chapter 26 of the FDOT Plans Preparation Manual.

The language in the agreement itself required an independent peer review of the foundation, substructure, and superstructure plans, as well as development of a finite element model for estimating demands on all elements due to different load combinations. Chapter 26 of the FDOT Plans Preparation Manual clarifies that the peer review must be independent and in compliance with AASHTO, FDOT and FHWA design requirements. Furthermore, Berger was obligated to assess the design at critical stages of the construction because construction staging was explicitly shown in the superstructure plans and because Chapter 26 requires "constructibility assessment limited to looking at fatal flaws in design approach."

As described under *Expected and Provided Peer Review Documents*, Berger's file included only a fraction of the documents expected to meet their contractual obligation and the standard of care. In particular, only

a few comments on the foundation plans were provided in the file. There were no written comments or questions whatsoever on the substructure and superstructure plans.

Berger did not attempt to assess the design at critical stages of the construction, as admitted by Berger VP Nick Ivanoff in his March 15, 2018 email. Furthermore, Berger incorrectly modeled the stay pipes in their finite element model to carry the dead weight of the concrete trusses. Therefore, the Berger model could not have been used to reasonably estimate the forces in the concrete truss members during construction or in the structure's final configuration. As such, Berger's evaluation of the capacity of Member 11 considered a factored axial force that was much less than the factored force required by the project design criteria and the AASHTO Code.

6.4 Findings

The following conclusions are based on the review described above:

- The Berger agreement with FIGG required an independent peer review of the superstructure, including review of structural integrity during construction.
- As admitted in Nick Ivanoff's email of March 15, 2018, Berger failed to consider structural integrity during construction.
- Numerous documents that would be expected based on contractual requirements and standard peer review practice were missing from the file, most notably:
 - An analytical model of the main span during and after transport
 - Verification of connection strength
 - Listing of review comments for substructure and superstructure plans (if any)
- Berger's analytical model of the completed structure was incorrect and unconservative because the stay pipes were modeled to resist dead load.


In summary, contrary to the certification letters they provided, Berger's peer review fell far short of their contractual obligations. In particular, by their own admission, Berger did not even attempt to assess the conditions at the construction stages shown in the plans (including the stage of construction at the time of collapse), which was required by their contract. Furthermore, the Berger finite element model could not have been used to reasonably estimate the forces in the concrete truss members during construction or in the structure's final configuration.

**Exhibit 6.1.1. Berger peer review comments on foundation plans
(page 1 of 2)**

		UniversityCity Prosperity Project DESIGN QUALITY MANAGEMENT PLAN	
Doc. No.: DQP104FA	Rev. 0	07.27.16	Page DQP104FA - 1 of 3

REVIEW COMMENT FORM							
DESIGNER	1. PACKAGE: 100% Foundation Plans						
	2. SUBMITTAL: <input type="checkbox"/> FIU OVERSIGHT REVIEW <input type="checkbox"/> EARLY START OF CONSTRUCTION <input checked="" type="checkbox"/> 100% Foundation Plans <input type="checkbox"/> RELEASED FOR CONSTRUCTION <input type="checkbox"/> INTERNAL						
	3. REVIEW TYPE: <input type="checkbox"/> DCR <input type="checkbox"/> ITR <input type="checkbox"/> CR <input checked="" type="checkbox"/> IPR			4. DISCIPLINES: <input checked="" type="checkbox"/> Structural <input type="checkbox"/> Drainage <input type="checkbox"/> Aesthetics <input type="checkbox"/> Utilities <input type="checkbox"/> Owner <input type="checkbox"/> Traffic <input type="checkbox"/> Geotechnical			
	5. DATE: 9/9/16		6. COMMENTS DUE DATE: 9/9/16		7. RETURN COMMENTS TO: M. Feliciano		
	8. RESOLUTION MEETING DATE & TIME: 9/12/2016		9. RESOLUTION MEETING LOCATION: Conf. Call		10. Concurrent Review? Checked for overlap by Design Manager: <input type="checkbox"/> Yes <input type="checkbox"/> No (DM initials)		
	11. REVIEWER: Ayman Shama			12. ORGANIZATION: <input type="checkbox"/> FIU <input type="checkbox"/> MCM <input type="checkbox"/> FIGG <input checked="" type="checkbox"/> Louis Berger			
	No.	Dwg. / Pg.	Comment	Disp.	Response	Disp.	Ver.
	1	B-2	Please remove the statement about scour since no scour analysis was performed.	D	The scour analysis was performed for the bulkhead wall on the north side of the project. Therefore, drawing B-2 makes reference to scour since the design of the wall accounts for it.	closed	
2		Under vibrations: based on the analysis done by LB the structure satisfied the horizontal vibration criteria. AASHTO requires the first vertical natural frequency to be higher than 3 Hz. The value obtained is 2.9. We recommend reducing the thicknesses of the pipe stays to achieve higher natural vertical frequency	D	According to our analysis, the natural frequency of the bridge is approximately 3.1 Hz.	closed		
3	B-9	The table shows that scour and down drag are not accounted for. Nevertheless, the equation in the LHS shows that they are included. Please change the equation so that it reflects the factor design load only.	D	For FDOT projects, it is customary to show the entire equation even though the values for the net scour and downdrag are equal to zero or N/A. It is understood that the nominal bearing resistance is equal to the factored design load divided by the resistance factor.	closed		
4		It is not clear if the minimum tip elevation is the value started with in the FB-Deep analysis or this is the anticipated tip elevation of the pile. This tip elevation is inconsistent with the pile length of 32 ft in the table. The 32 ft pile length is consistent with the results from FB-Deep.	D	The Pile Order Length in the Pile Data Table is what is necessary in order to satisfy the required design axial loading. Length of the pile will be confirmed during construction with PDA.	closed		
RESOLUTION MEETING FINAL CONCURRENCE		13. DESIGNER Sign & Date:		14. REVIEWER Sign & Date:			
INITIAL DISPOSITION CODES:		C = Will Comply F = Further Clarify		D = Delete Comment N = Incorporate Next Submittal		FINAL DISPOSITION CODES: C D N	
Written by: ADH		Revised by:		Approved by:			
Date: 07.27.16		Date:		Date:			

Exhibit 6.1.2. Berger peer review comments on foundation plans (page 2 of 2)

		UniversityCity Prosperity Project DESIGN QUALITY MANAGEMENT PLAN	
Doc. No.: DQP104FA	Rev. 0	07.27.16	Page DQP104FA - 2 of 3

No.	Dwg. / Pg.	Comment	Disp.	Response	Disp.	Ver.
5		The geotechnical report states that it is anticipated that the required compression capacity of about 433 kips will be achieved at -15 ft. At this time we recommend adhering to the results of FB-Deep as it is the most reliable tool to evaluate the capacity until the real capacity is validated during construction by PDA. The 433 nominal capacity in the table is consistent with a tip elevation at -30 ft.	D	See response to comment 4.	closed	
6		The lateral capacity of the 24 inch pile was checked against the case of the extreme-2 load using simple hand calculations and moment curvature analysis. The capacity was found adequate.	C	Agree.	closed	
7	B-7, B-11, B-13	Please locate foundations Type-1 and Type-3 at the same bearing strata to avoid the likelihood of differential settlement effects at the south pier. Currently elevations of the bottom of foundations for the two footings are 4.00 and 0.50. Try to locate the bottom of foundations directly on top of the hard limestone, or at least use elevation 0.50 for the two footings	D	It is our opinion that the contact pressures at these foundation locations are well below the recommended bearing capacity values. Both Type 1 and Type 3 footings are bearing on top of the limestone layer and no dissimilar materials were observed at these bearing elevations based on the boring performed. Furthermore, currently, the estimated settlements at these footing locations are about ¼ inches, or significantly less than 1 inch and adequate. Hence, differential settlement is not a concern.	closed	
8	B-7, B-15, B-16	Please locate foundations Type-6 and Type-7 at the same bearing strata to avoid the likelihood of differential settlement effects at the north pier. Currently elevations of the bottom of foundations for the two footings are 4.00 and 0.50. Try to locate the bottom of foundations directly on top of the hard limestone, or at least use elevation 0.50 for the two footings	D	It is our opinion that the contact pressures at these foundation locations are well below the recommended bearing capacity values. Both Type 6 and Type 7 footings are bearing on top of the limestone layer and no dissimilar materials were observed at these bearing elevations based on the boring performed. Furthermore, currently, the estimated settlements at these footing locations are about ¼ inches, or significantly less than 1 inch and adequate. Hence, differential settlement is not a concern.	closed	
9	B-11	It seems that the bottom foundation reinforcement is governed by the minimum reinforcement ratio. It was expected for the square foundation to have the same number and size of bars in the two perpendicular directions. Currently there are 14-9F01 in one side and 14-7F01 for the other side.	D	For the Type 1 footing, the bottom flexural reinforcement is sized based on the bending moment at the face of the column. Although the design pressure is the same in both directions, the bending moment is larger in the transverse direction because the column is rectangular and the lever arm is longer than in the longitudinal direction. Therefore, more reinforcing steel was provided in the transverse direction.	closed	
10	B-26 through B-28	It is recommended for bar schedules to add one more column for the bar shape.	D	The bar lists are produced with an FDOT application; therefore, the layout of the table cannot be modified. Bar shape is shown in the 5th column (TYP BAR) and references the FDOT Standard Bar Bending Details (Index No. 21300).	closed	

RESOLUTION MEETING FINAL CONCURRENCE	13. DESIGNER Sign & Date:	14. REVIEWER Sign & Date:
INITIAL DISPOSITION CODES:	C = Will Comply F = Further Clarify	D = Delete Comment N = Incorporate Next Submittal
Written by: ADH	Revised by:	Approved by:
Date: 07.27.16	Date:	Date:

FINAL DISPOSITION CODES:
C D N

QC VERIFY: Incorporation of C or N comments and agreement with D comments.
(Design Task Mgr. Initials)

**Exhibit 6.2. pcaCOL
 interaction diagram for
 Member 11 per AASHTO
 LRFD 7th Edition**

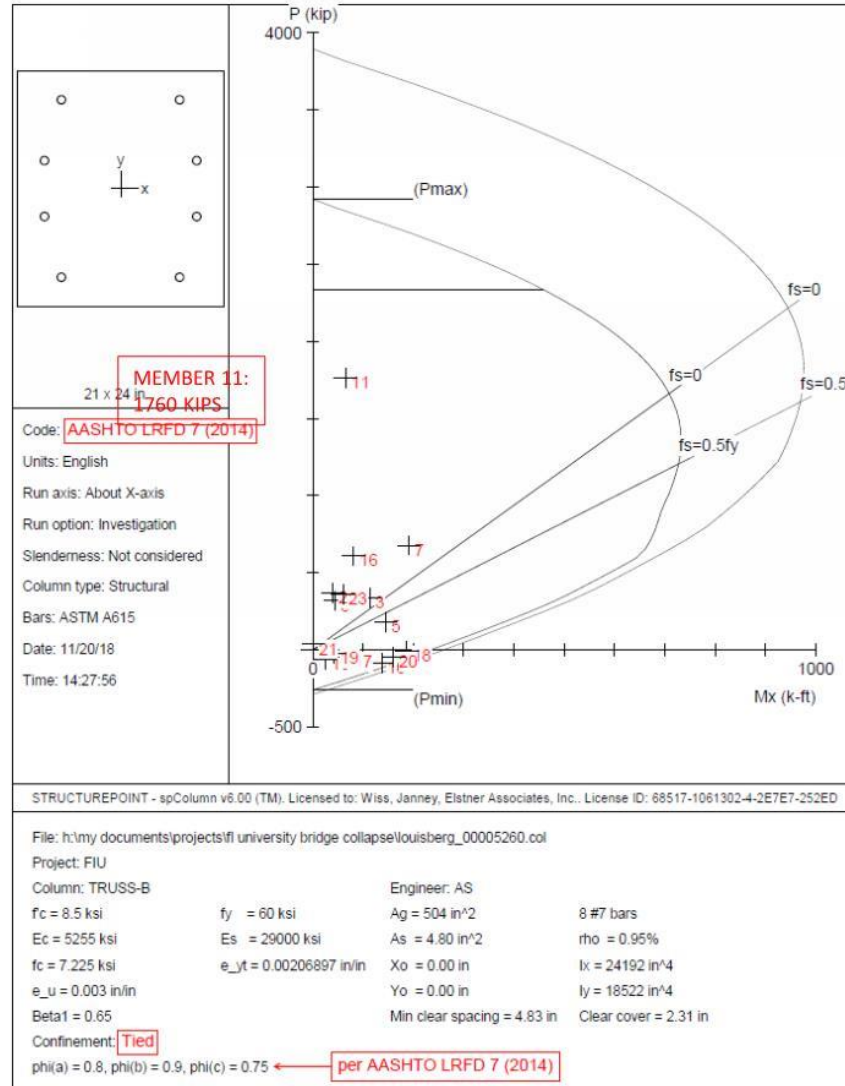


Exhibit 6.3.1

WJE EVALUATION OF EXPECTED AND PROVIDED PEER REVIEW DOCUMENTS

Items shown in **blue type** in the Expected Document(s) column were not found in the peer review file

Category	Expected Document(s)	Document(s) Provided by Berger
1. Design Criteria	Document identifying relevant FDOT, AASHTO, and FHWA criteria for structural design and peer review.	Relevant criteria were found in the file.
2. Input Calculations for Analytical Model	<p>Calculation of loads, including wind loads.</p> <p>Calculation of truss geometry, material properties, and section properties used for input into the analytical model by hand calculation, Mathcad, Excel, proprietary software or other means.</p>	None found in file
3. Analytical Model	<p>Analytical models for all relevant construction stages, including, but not necessarily limited to the following:</p> <ol style="list-style-type: none"> 1. Main span simply supported (with and without prestressing of exterior diagonals) 2. Transport with SPMTs 3. Two-span configuration (without stay pipes) 4. Final configuration <p>The model should be consistent with the construction sequence shown on the drawings. Include all relevant load combinations (construction and in-service).</p>	<p>Only an analytical model in the final configuration was provided (using ADINA).</p> <p>The model was not consistent with the construction sequence.</p> <p>In-service load combinations were considered for the final configuration.</p>
4. Verification of Analytical Modeling	<p>Peer review verification of analytical modeling would include calculations confirming model geometry, loads, units, and assumptions. Verification is done to ensure no errors were made during the modeling and the model is behaving as expected. Verification of analytical models typically is performed by hand calculation, Mathcad, or Excel and at a minimum would include the following:</p> <ol style="list-style-type: none"> 1. Confirmation the analytical model is calculating the weight of the bridge correctly 2. Confirmation external loads were applied to the bridge properly and the analytical model is distributing correctly. 	No files verifying the analytical model were found in the file.

Exhibit 6.3.2

WJE EVALUATION OF EXPECTED AND PROVIDED PEER REVIEW DOCUMENTS

Items shown in **blue type** in the Expected Document(s) column were not found in the peer review file

Category	Expected Document(s)	Document(s) Provided by Berger
5. Verification of Sectional Strength of Bridge Elements	<p>Calculation of axial, flexural, shear and torsional sectional strength of main members by hand calculation, Mathcad, Excel, proprietary software or other means. Sectional strength is to be calculated in accordance with AASHTO specifications using appropriate strength reduction factors.</p> <p>Primary members include footings, pier columns, deck elements, truss diagonals, canopy elements, pylon, and stay pipes.</p> <p>Results are compared to calculated forces from analytical model including appropriate load factors.</p>	<p>PCACOL was used to verify the combined flexural and actual strength of strength of selected substructure and truss members. The strength reduction factor used in PCACOL appears to be from ACI 318 rather than AASHTO, which is conservative but incorrect. Otherwise, no sectional strength calculations were found in the file.</p> <p>No calculations of shear or torsional strength for any members were found in the file. Examples of members in which shear or torsional strength is important include footings, pier columns, and deck diaphragms.</p>
6. Verification of Strength of Connections	<p>Calculation of connection strength by hand calculation, Mathcad, Excel, proprietary software or other means. Connection strength is to be calculated in accordance with AASHTO specifications using appropriate strength reduction factors.</p> <p>Primary connections include pier column/footing connection, superstructure bearings, connections of diagonal web members to canopy and deck, post-tensioning anchorage zones, and connection of stay pipes to pylon and canopy.</p>	<p>A Mathcad calculation of the connection strength for the connection of the stay pipes to the pylon was provided. The calculation was performed in accordance with ACI 318 criteria, which is permitted by AASHTO.</p> <p>Otherwise, no calculations of connection strength were found in the file.</p>
7. Verification of Serviceability	<p>Calculations for serviceability criteria:</p> <ul style="list-style-type: none"> • Deflection • Cracking at Service Load • Vibration <p>Such checks Please say that again re the bridge is serviceable.</p>	<p>Comment 3 on the Foundation Plans indicated that the horizontal vibration frequency met AASHTO criteria but expressed concern about the frequency of vertical vibration. Otherwise, no serviceability-related calculations were found in the file.</p>

Exhibit 6.3.3

WJE EVALUATION OF EXPECTED AND PROVIDED PEER REVIEW DOCUMENTS

Items shown in **blue type** in the Expected Document(s) column were not found in the peer review file

Category	Expected Document(s)	Document(s) Provided by Berger
8. Verification of Foundation strength	Calculation of vertical and lateral forces acting on the pile foundations relative to the resistance determined by the geotechnical report.	The expected documents were found in the file.
9. Review of Drawings for Completeness and Compliance with Design Criteria	<p>Listing of comments, questions, and/or drawing markups identifying concerns or comments relating to completeness or compliance with design criteria for each portion of the drawings included in the scope:</p> <ul style="list-style-type: none"> • Foundation Plans • Substructure Plans • Superstructure Plans 	No drawing markups were found in the file. Only a few comments on the foundation plans were provided in the file. There were no comments or questions whatsoever on the substructure and superstructure plans.
10. Constructability Assessment	Listing of comments and/or drawing markups identifying concerns or comments relating to constructability.	No drawing markups or comments relating to constructability were from the file.

7 EVALUATION OF TILT EXCEEDANCES DURING MAIN SPAN TRANSPORT

WJE studied twist exceedances during transport of the main span. The objective was to assess the possible effect of exceeding the maximum allowable transverse twist on damage to the web members at the north end of the main span.

7.1 Background on Transport of Main Span

The design drawings prepared by FIGG called for the main span to be precast. MCM set up a casting yard just south of SW 8th Street and moved the precast span into its final position using self-propelled mobile transporters (SPMTs). After an initial lift and roll test on the evening of March 9, 2018, the move started at 4:20 a.m. on March 10, and the span was set into position at 12:27 p.m. As a subcontractor to MCM, Barnhart Crane & Rigging Company (Barnhart) was responsible for transport of the main span, including design and operation of the transporter system. Barnhart subcontracted to Bridge Diagnostics, Inc. (BDI) for monitoring of strain, tilt, and twist during the move.

7.2 Document Review

Observations from review of key documents pertaining to distress in the north end and transverse tilt during the move are provided in the following sections.

7.2.1 Photos of North-End Distress before and After Move

As described in the following paragraphs, photographic evidence indicates that cracks in the north end were much worse several hours after the move than they were before. The widened cracks were observed shortly before the posttensioning bars in Member 11 were de-stressed.

Exhibit 7.1.1 and 7.1.2. Barnhart provided a close-up photograph of the west side of the north-end diaphragm taken on March 8, 2018, prior to the move. As shown in Exhibit 7.1.1, a narrow diagonal crack can be seen on top of the diaphragm. Corradino provided a photograph (also shown in Exhibit 7.1.1) of the same area taken on March 10 at 3:14 p.m., after the move but before de-stressing of Member 11. After the move and placement of the main span in its final location, the narrow crack widened by more than 0.5 inches and was accompanied by spalling of the north face of the diaphragm. Exhibit 7.1.2 provides a similar comparison for cracks on the east side of the north end diaphragm.

Exhibit 7.1.3. A photograph taken on February 24, 2018 by BPA shows a diagonal crack along the bottom of Member 11 on the east face. The crack width appears to be approximately 0.03 inches in width at that time. Shortly after the move, at 12:30 p.m., a photo by FIGG shows the crack to be about the same width, although it is difficult to be certain because the member was apparently painted by the contractor prior to the move. However, less than three hours after the move, the crack widened more than tenfold to approximately 0.50 inches, based on a photograph taken by Corradino at 3:14 p.m.

7.2.2 SPMT Bridge Movement Monitoring Plan

The SPMT Bridge Movement Monitoring Plan is Submittal #00400-6.A. Page 4 of the plan indicates a 0.5-degree tolerance for the difference in rotation angle between Nodes 2 and 4, the points at which the main span is supported during the move. These points are illustrated on Figure 7.1. The difference in rotation between the north and south supports is referred to as twist.

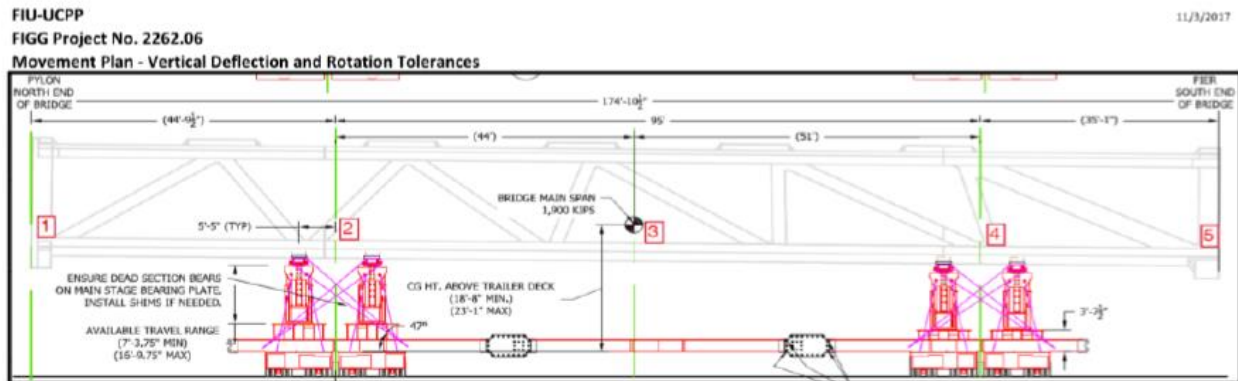


Figure 7.1. Schematic of movement plan from SPMT Bridge Movement Monitoring Plan

Submittal #00400-6.A includes the following discussion regarding the relationship between twist and cracking:

“Maximum limit for twist/torque that is achievable by Barnhart’s current equipment and methods where there likely would be temporary cracks observed on selected areas of certain struts (localized) for the temporary conditions during the bridge movements once the span is in the final position and the torque/twist is removed, any cracks that may have occurred during the movement would likely close and would be small in width, if measurable at all. There may be selected nonstructural cracks in select areas, if any, that may need to be sealed (Per FDOT Standard Specifications for Roadway Bridge Construction, 2015 – Section 400 Concrete Structures) once the span is in the final position...”

In summary, this statement acknowledges that the twisting during the main span move is likely to cause small cracks, which would close after the main span is supported in his final location. Apparently the 0.5-degree limit for the difference in rotation between support points (twist) was chosen because Barnhart believed that twist within that limit was achievable using their proposed methods and equipment²⁷.

7.2.3 BDI Monitoring Report

The BDI Monitoring Report is entitled “Florida International University Pedestrian Bridge – Monitoring of Lift and Move Procedures.” The final version is dated April 4, 2018 (20 days after the collapse), and was submitted to Barnhart. The executive summary on page 1 includes the following statements regarding monitoring of twist during the move:

- “The primary goal of the project was to monitor twist of the truss-girder span during the move and at final span placement. Vertical displacements and concrete surface strains were also measured at specified locations for the record.”
- “Measurements were recorded on a continuous basis during the initial lift and during a relatively short roll test. The roll test was done to verify twist measurement sensitivity during actual operations and BCR’s²⁸ ability to control adjustment of twist.”

²⁷ FIGG originally requested a much smaller tolerance.

²⁸ BCR refers to Barnhart Crane & Rigging

- “BCR was in charge of all rigging and moving operations while BDI’s role was to provide on-site feedback on the twist of the girder during movement and placement. BDI personnel operating the monitoring system were in direct contact with BCR’s transport operators and were authorized to stop movement at any time. Any time the girder twist approached the limit, transport movement was stopped and BCR adjusted the alignment.”

The 0.5-degree twist tolerance is acknowledged on page 9:

- “A BCR representative was with the BDI monitoring system operator and viewing the screen while tilt and rotation readouts displayed. Any time that twist data plot approached ± 0.5 degrees, an ‘All Stop’ command was given, transport movement was halted, and adjustments to the trailers were performed.”

The 0.5-degree twist limit was exceeded on at least two occasions during the move. These two points are indicated with red arrows in Exhibit 7.2.1²⁹, which is a plot of twist between support points versus time. As shown in Exhibit 7.2.1, a maximum twist of 0.84 degrees (168 percent of the maximum limit) occurred at 4:48 a.m. on March 10.

Most of the excessive twist is due to rotation of the north support. As can be seen in Exhibit 7.2.2³⁰, rotation at the north support was 0.97 degrees at 4:48 a.m. on March 10, when the maximum twist occurred. At the same moment, the south support point was rotated in the same direction (canopy rotated to the west). As shown in Exhibit 7.2.3³¹, the rotation at the south support was 0.13 degrees. Thus, the difference in rotation was $0.97 - 0.13 = 0.84$ degrees.

The BDI report discusses this tilt exceedance. Specifically, BDI points to Figure 7 in their report, which is reproduced herein as Exhibit 7.2.4. The figure shows spikes in the rotation and twist data. In particular, there is a significant spike at 4:48 a.m. on March 10 that is not matched in the strain measurements, although there is a smaller peak in the strain measurement at that time. BDI indicates that the spike “was observed to be an artifact of the tilt sensor dynamics.” However, BDI acknowledges that the “peak static twist value” at this time was approximately 0.65 degrees, which exceeds the 0.5 degree limit. Also, there is concurrent peak in strain readings at 4:48 a.m., indicating that the actual peak static twist value is greater than 0.65 degrees.

As previously described, twisting causes stresses between the support points, which may cause cracking. However, the north end of the main span is free to rotate, and cracking is not caused by twisting per se. Rather, the concern with respect to damage at the north end is transverse bending of the web members due to the rotation, which is addressed in Section 7.3 below.

7.3 Structural Analyses

A finite element model of the main span was developed and analyzed using Abacus, finite element software for structural analysis of complex systems (see Section 5.1.1). An overview of the model is shown in Exhibit 7.3.1.

²⁹ From BDI monitoring report Figure 32. Red arrows and dashed lines indicating tilt exceedances added by WJE.

³⁰ From BDI monitoring report Figure 29. Red lines and boxed note added by WJE.

³¹ From BDI monitoring report Figure 21. Red lines and boxed note added by WJE.

To evaluate stresses, the maximum observed rotation angles described above were imposed on the model. A plot of the deformed shape is shown in Exhibit 7.3.2. As can be seen in this exhibit, the rotation at the north transporter system support causes an even greater rotation at the north end. The resulting westward deformation at the north end of the canopy is 4.26 inches.

The tilt of the canopy causes transverse bending stress near the base of the web members at the north end — in the same way that tilting a patio umbrella causes bending of the support pole. A second-order³² analysis was used to capture the effect of the tilt. To isolate the effect of the canopy tilt, the effects of self-weight and post-tensioning were subtracted from the combined effects of self-weight, post-tensioning, and tilt. A plot of the tilt-induced stresses at the base of the north support members is shown in Exhibit 7.3.3. The green color indicates that the tilt causes a tensile stress of more than 500 psi on the east face of the northernmost vertical web member (Member 12), which is in the region where cracks were observed prior to the collapse. This peak stress would reduce to about 400 psi if the maximum rotation readings are reduced to account for spikes in rotation readings due to sensor dynamics.

7.4 Discussion

A 0.5-degree twist limit was established to control cracking. However, this limit was exceeded. The full degree of the exceedance is somewhat uncertain due to “spikes” in the rotation and twist readings.

Cracks in the north-end diaphragm and Member 11 were evident prior to the move and widened greatly after the move, although not immediately afterward. Obviously, the cracks occurring before the move were unrelated to the move. The nature and cause of these cracks is discussed in Section 2. There are four possible contributors to widening of the cracks:

1. The rotation associated with the twist exceedances caused high transverse bending stress near the base of the northernmost vertical. Although the calculated stress is somewhat less than that needed to initiate cracking, the stress from the tilt would tend to exacerbate cracking in the region.
2. Prior to the move, the north end diaphragm was supported on shoring at close intervals. After the move, the diaphragm was supported on temporary shims. The shims were nearly continuous except for a 38-inch gap at the centerline. The truss reaction at the center of the north-end diaphragm spanned the gap, increasing shear and bending stresses in the north-end diaphragm relative to the diaphragm stresses in the casting yard.
3. Prior to the move, the north-end diaphragm and Member 11 exhibited distress related to the northward sliding of Members 11 and 12. Immediately prior to the bridge being lifted by the transporter, the force in Member 11 would have been approximately equal to the force at the time of the failure. The horizontal force was temporarily relieved when the transport assembly lifted the main span from the casting yard and was then reapplied when the span was set in its final location. Thus, the move applied an additional load cycle to a connection that was near its strength limit. Damage can increase significantly due to even one additional load cycle when the load is near the strength limit.
4. For the reasons described in item 3, after the move, the north diagonal connection was near its strength limit. Cracks can widen over time due to sustained load near the strength limit.

There is not enough information to assess the degree to which each of these factors contributed to the increase in distress after the move. In WJE’s opinion, all of these factors could have contributed to the damage at the north end and ultimately the collapse.

³² Second-order analysis, also known as P-delta analysis, captures the effect of deformations on stress

Finally, it should be noted that the OSHA report³³ claims that cracks began to appear “as they began to de-stress the PT bars of Member 11.” For reasons explained in Section 8, WJE does not agree with this finding. In particular, the cracking shown in the right photo in Exhibit 7.1.1 occurred before de-stressing. The OSHA report also maintains that lateral bracing in the casting yard provided “considerable lateral support to diaphragm II.” Based on review of the OSHA photographs, it is WJE’s opinion that the location and stiffness of the support connected to the north diaphragm was insufficient to significantly reduce the pattern of distress.

7.5 Findings

In summary, this study shows that cracks in the region of the connection of Members 11 and 12 to the deck increased dramatically after the move from the casting yard to the final location. The tilt associated with exceeding the established twist limits caused high stresses in the region. Along with other factors, this stress may have contributed to damage in the region and ultimately to the collapse.

³³ Occupational Safety and Health Administration, "Investigation of March 15, 2018 Pedestrian Bridge Collapse at Florida International University, Miami, FL," June 2019.

Exhibit 7.1.1. Crack in west side of north end diaphragm before and after move



Photo 12 from BPA crack inspection after formwork/scaffolding removal. February 28. Crack is indicated by blue arrows. Crack width ruler appears to indicate 0.014 inches.

March 10 photo by Corradino showing same crack after move at 3:14 p.m. The yellow arrow points to the west side of the same #11 bar in each photograph.

Exhibit 7.1.2. Crack in east side of north end diaphragm before and after move



Photo 13 from BPA crack inspection after formwork/scaffolding removal. February 28.



March 10 photo by Corradino showing same crack after move at 3:14 p.m.

Exhibit 7.1.3. Diagonal “wedge” crack at Member 11 before and after move



Diagonal “wedge” crack along the bottom of Diagonal 11 on the east face. Photo taken by BPA prior to the move on February 24, 2018.



Same diagonal “wedge” crack shortly after the move. Photo taken by FIGG at about 12:30 p.m. on March 10.



Same diagonal “wedge” crack 3 hours after the move. Photo taken by Molina at about 3 p.m. on March 10.

Exhibit 7.2.1. Twist rotation between support points versus time

(From BDI monitoring report Figure 32. Red arrows and dashed lines indicating tilt exceedances added by WJE.)

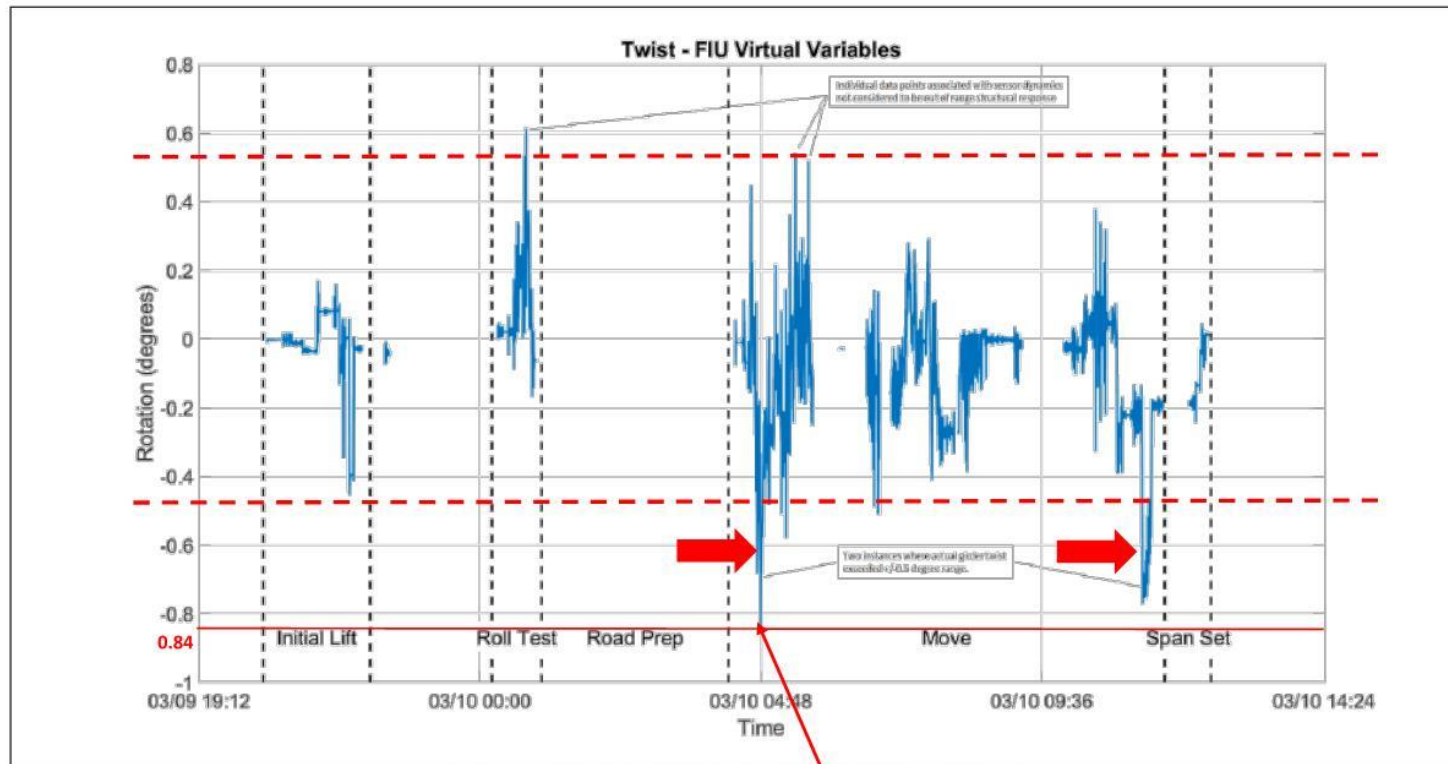


Figure 32 – Girder Twist – Difference in angle between Sections J & L

Difference in rotation between north and south supports: 0.84°

Exhibit 7.2.2. Tilt meter readings at north support versus time
 (From BDI monitoring report Figure 29. Red lines and boxed note added by WJE.)

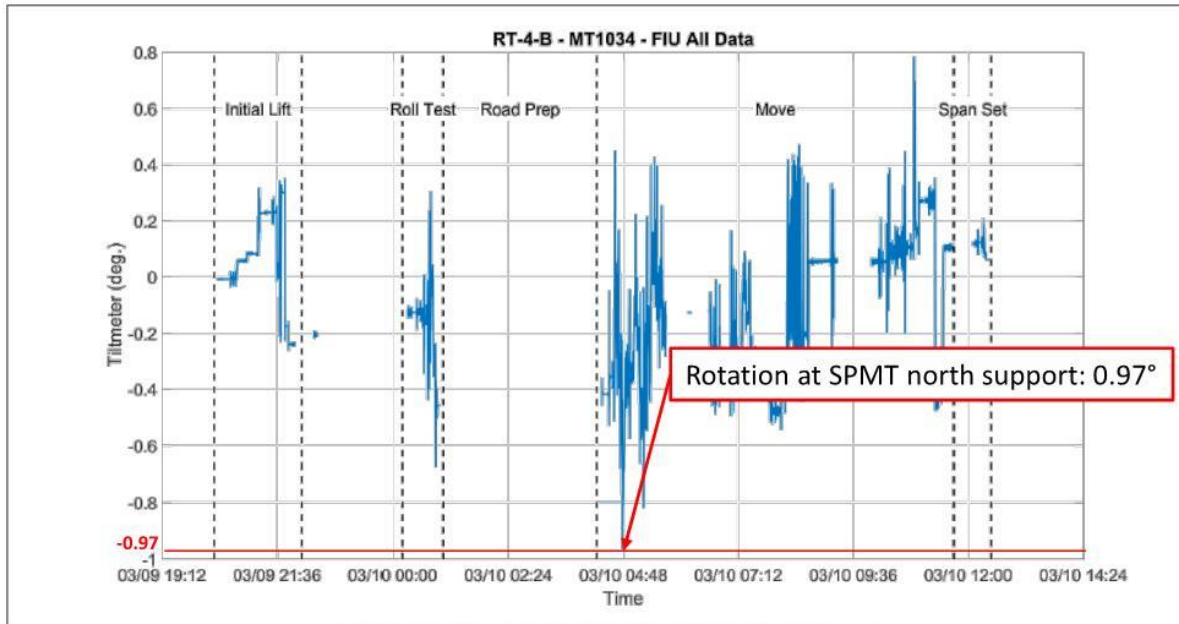


Figure 29 – Transverse rotation at Cross-Section 4 – Transverse Position B

Exhibit 7.2.3. Tilt meter readings versus time

(From BDI monitoring report Figure 21. Red lines and boxed note added by WJE.)

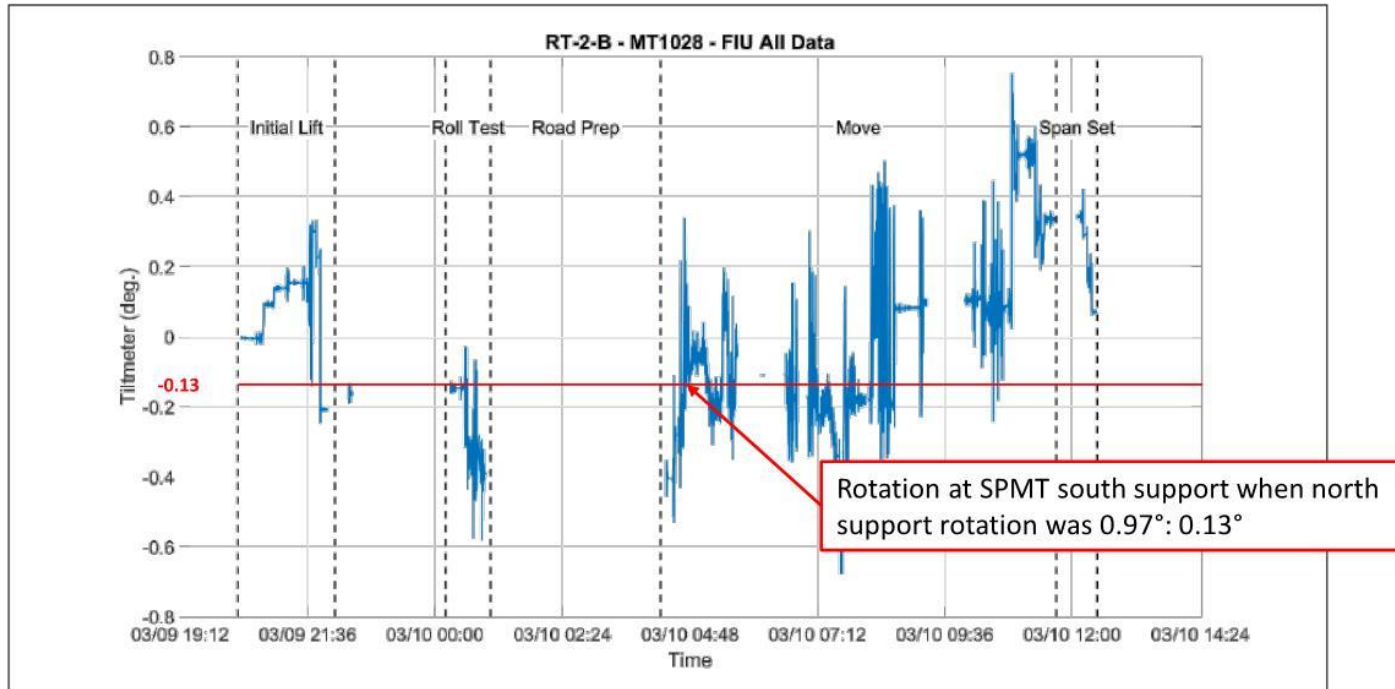


Figure 21 – Transverse rotation at Cross-Section J – Transverse Position B.

Exhibit 7.2.4. Twist, rotation and strain readings versus time
(From BDI monitoring report Figure 21. Boxed note added by WJE.)

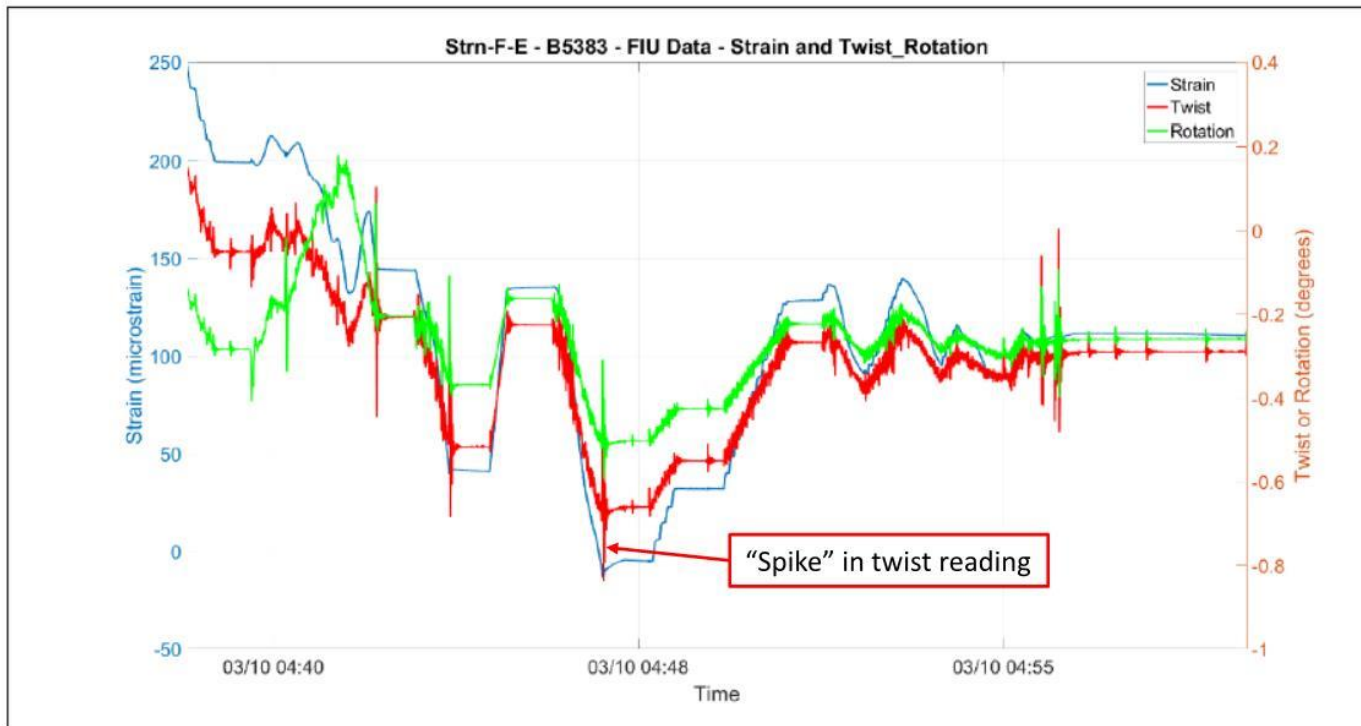
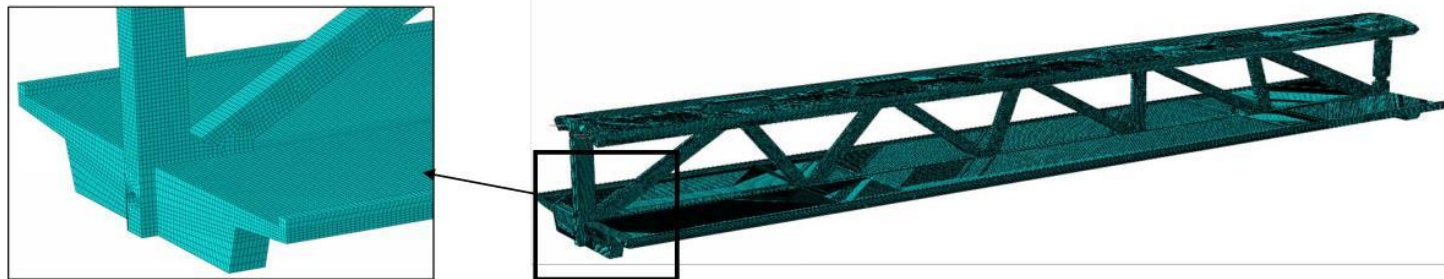


Figure 7 – Measured strain at Section F (east) with corresponding twist and rotation measurements

Exhibit 7.3.1. Finite element model



Top: Finite element model of concrete elements

Bottom: Longitudinal posttensioning tendons in finite element model.

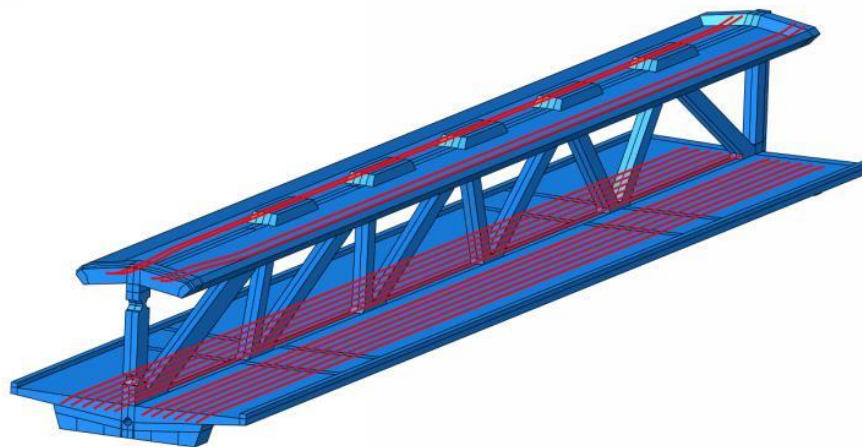


Exhibit 7.3.2. Twist deformation looking southwest (deformations exaggerated 20x)

- Self-weight and PT effects are subtracted

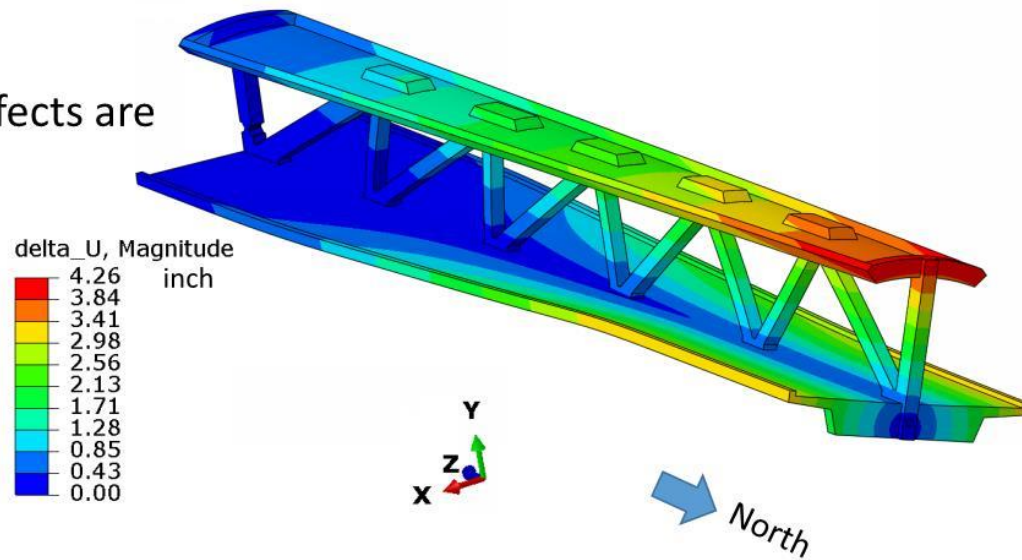
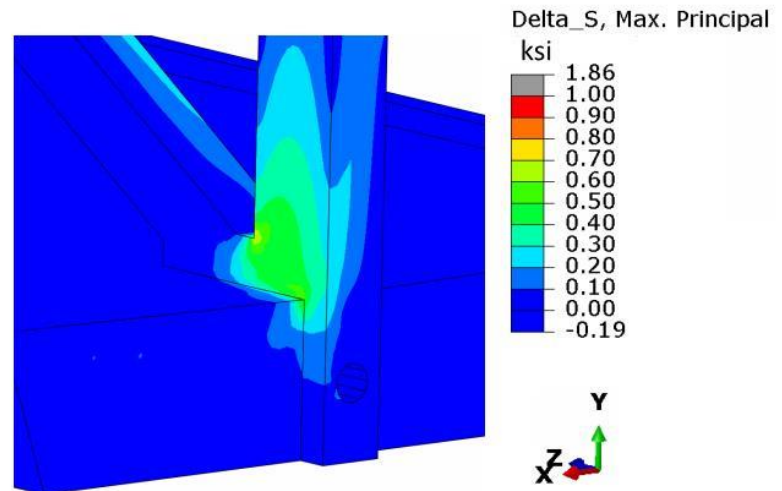


Exhibit 7.3.3. Maximum principle tensile stress due to twist only

Looking southwest at north end and east face. Green color indicates more than 500 psi tensile stress.

Dark blue areas have zero tensile stresses or they are compression dominant



8 RE-STRESSING OF MEMBER 11

WJE evaluated crack monitoring during re-stressing of Member 11 five days after the main span was set in its final position and Member 11 was de-stressed. The objective of the evaluation is twofold: 1) determine the extent to which cracks in the north diaphragm of the main span were monitored during re-stressing of the northernmost diagonal, and 2) assess the means by which changes in crack width could have been monitored and the likelihood of detecting increases in crack width.

8.1 Timeline and History of Cracking near the North End

The following is a brief timeline of events that substantially changed forces in the truss members, which led to distress near the north end and the eventual collapse.

Event	Date/Approximate Start Time
Shoring removal in casting yard	February 24, 2018
Initial lifting by transporter	March 9, 2018
Placement of the main span on the south pier and central pier	March 10, 2018, 12:27 p.m.
De-stressing of Member 11 by Structural/VSL	March 10, 2018, 4:17 p.m.
Re-stressing of Member 11 by Structural/VSL	March 15, 2018, 11:51 a.m.

The distress associated with the above events is described in the following paragraphs.

February 24-28, shoring removal. Cracks in the north-end truss members were first reported by BPA (on-site construction inspectors) in a February 28 email to FIGG. The cracks were observed shortly after removal of the shoring in the casting yard. Exhibit 8.1.1 shows narrow cracks on the top of the north-end diaphragm. Exhibit 8.1.2 shows a crack in the chamfer at the base of Member 11 visible on February 24. This crack is referred to as the “wedge” crack.

March 10, after the move. The cracks in the north end worsened significantly by mid-afternoon on March 10, 2018, after the main span was moved and supported in its final position between the south pier and central pier. Placement of the span in its final position would have resulted in a compressive force of more than 1700 kips in Member 11³⁴ due to the combined effects of dead load and post-tensioning. Exhibit 8.2.1 shows wide cracks on the top of the north-end diaphragm that were apparent several hours after the move, but prior to de-stressing. These photos were taken at about 3:10 p.m. on March 10. The cracks shown in Exhibit 8.2.1 are much wider than those visible before the move in Exhibit 8.1.1. Also, as can be seen by comparing Exhibit 8.1.2 and Exhibit 8.2.2, the wedge crack also widened significantly after the move.

March 10, after de-stressing. Even though de-stressing would have reduced the compressive force in Member 11, Structural/VSL reported that as they began to de-stress the post-tensioning (PT) bars of Member 11, cracks began to appear at multiple locations. The Structural/VSL supervisor took pictures of the cracks and forwarded them in an internal text stating “it cracked like hell.” SW 8th Street was re-open to traffic around 8 p.m. that evening.

On March 12, 2018, MCM’s project manager emailed several photographs of distress to FIGG, the first crack photos sent to FIGG since February 28. The photographs were taken near the north end of the main

³⁴ See Table 5.3

on March 12, two days after de-stressing of Member 11³⁵. Exhibits 8.3.1 and 8.3.2 show that cracking in the north-end diaphragm and near the base of Member 11 worsened somewhat after de-stressing, but the cracks were not substantially different than those visible in Exhibits 8.2.1 and 8.2.2, which were taken before de-stressing began.

March 14. Photographs taken on March 13 and 14, 2018, show that the cracks in the north-end diaphragm continue to widen, as can be seen in Exhibits 8.4.1 and 8.4.2.

8.2 Re-Stressing of Member 11

Based on the observations and events described above, as well as phone conversations between MCM and FIGG, the project team was under the impression that the worsening of the cracking was related to de-stressing of Member 11. FIGG also understood that the cracks had not grown since the de-stressing. On March 13, 2018, FIGG sent an email to MCM recommending re-stressing of Member 11. Each post-tensioning bar was to be re-stressed in 50 kip increments, alternating between the top and bottom bars, up to the originally specified prestressing force of 280 kips in each bar.

The March 13 email instructed MCM to closely monitor the north-end diaphragm “to ensure that the crack size does not increase.” FIGG anticipated the crack size would either remain the same or more probably decrease in size. Nevertheless, the FIGG email also indicated that “If the crack size increases, the post-tensioning bar stressing shall stop and FIGG be notified immediately.”

Also, the stressing safety guidelines in the Structural/VSL post-tensioning shop drawings state “Immediately cease prestressing and remove all personnel from the area if any existing crack widening, new concrete cracking, bearing plate movement, or unusual sounds are observed.” Thus, it would be expected that Structural/VSL would implement some type of monitoring of the existing cracks during re-stressing.

8.3 Actual Crack Monitoring

Wood blocks were mounted across cracks on the north face of the north-end diaphragm, as shown in Figure 8.1. Lines transcribed across the blocks indicate they were intended for monitoring changes in crack width. The extent to which these crack gauges were used is not known; however, as described below, time-lapse video does indicate they were not used to monitor changes in crack width during re-stressing.

³⁵ Occupational Safety and Health Administration, "Investigation of March 15, 2018 Pedestrian Bridge Collapse at Florida International University," June 2019, page 48.



Figure 8.1. Wood blocks mounted across cracks on the north face of the north and diaphragm

Two cameras near SW 8th Street recorded time-lapse images of construction activity: one west of the main span on the south side of SW 8th Street, and a second east of the main span on the north side of SW 8th Street. March 15 screenshots, mainly from the camera on the south side of SW 8th Street, are provided in Exhibits 8.5.1 to 8.5.10.

The following are examples of observations made from these screenshots:

Approximate Time (3/15/18)	Observation(s)
11:45 a.m.	Start of re-tensioning. Apparently, the five-person crew gained access from a green manlift (left side of screenshot). The hydraulic ram used for de-tensioning was positioned with a white crane (next to the manlift).
11:53 a.m.	Two persons (red arrows) can be seen on the east side of the deck near the railing at the north end.
1:42 p.m.	A person (red arrow) can be seen on the west side of the deck near the railing at the north end. Repositioning of the ram is evidenced by movement of the crane boom and ball on the crane line. The ram was repositioned numerous times during the course of the re-stressing. The number of times the ram was repositioned is consistent with the FIGG email to re-stress in 50 kip increments, alternating between the top and bottom bars, up to the originally specified pre-stressing force of 280 kips in each bar.
1:43 p.m.	The person seen in the previous image has moved a few feet southward.
1:44 p.m.	The person seen in the previous image has moved northward to his 1:42 p.m. position.
1:46 p.m.	One minute before collapse. No change from previous screenshot.
1:47 p.m.	First screenshot after collapse.

As described in the next section, closely monitoring cracks in the north-end diaphragm would have required electronic instrumentation or continual arm's-length or closer access to the cracks, either from a manlift on the north side of the diaphragm or on hands and knees on the deck at the north end. There is no record of electronic instrumentation and none of the time-lapse video images showed a person with arm's-length access to the cracks, either from the deck or from a manlift. Apparently, the cracks were not closely monitored as instructed by FIGG.

8.4 Possible Crack Monitoring

In light of FIGG’s email to monitor cracks during re-stressing and the Structural/VSL stressing safety guideline regarding cracking during stressing, WJE evaluated possible means for monitoring cracks in the north-end diaphragm. Figure 8.2 shows a concrete slab in WJE’s Northbrook laboratory used for evaluating anchors installed in cracked concrete. The specimen is mounted on a tensioning frame that induces cracks. A 0.1-inch-wide crack was induced in the concrete specimen to simulate an existing crack in the north-end diaphragm.

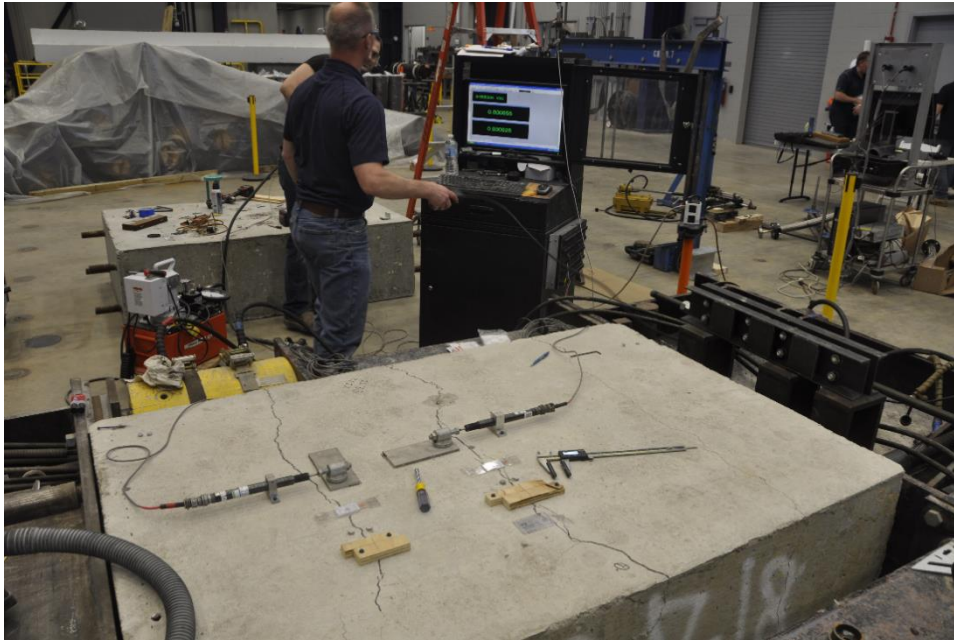


Figure 8.2. Crack induced in concrete specimen in WJE Northbrook laboratory

The crack frame was then used to increase the crack width to 0.2 inches in 0.02 inch increments, based on displacement transducer readings. Five methods for monitoring changes in crack width were evaluated:

1. Displacement transducer
2. Humboldt crack gauge
3. Dial caliper and measurement points
4. Wood block crack gauge (similar to that used at the site)
5. Crack width ruler (crack comparator)

The devices used in these five methods are shown in Figure 8.3. The numbers in the blue boxes correspond to the numbers in the above list.

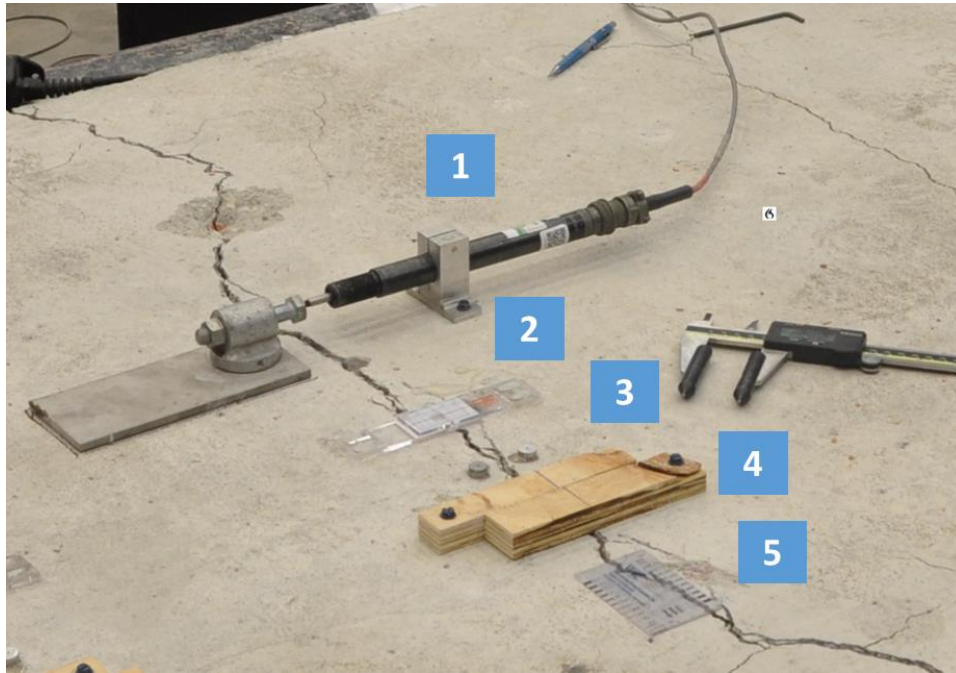


Figure 8.3. Crack monitoring methods evaluated

The effectiveness of these methods is summarized in Table 8.1. Effectiveness of crack monitoring methods. As indicated in Table 8.1. Effectiveness of crack monitoring methods, the first four methods, including the wood block crack gauge (similar to that used on the north end diaphragm), were effective in detecting changes in crack width as small as 0.02 inches. Much smaller changes could be detected with the displacement transducer or digital calipers. The crack comparator was only effective if used in combination with close-up photographs. Exhibit 8.6.1 provides photographs of the Humboldt crack gauge, wood block crack gauge, and crack comparator after a 0.02 inch increase in crack width.

Small changes in crack width could have been monitored remotely using a displacement transducer. (The readout from the displacement transducer used by WJE can be seen in Figure 8.2.) All other methods would have required arm's-length or closer access to the crack.

Table 8.1. Effectiveness of crack monitoring methods

Method	Effectiveness
Displacement transducer	Very accurate and effective; detects crack width changes of less than 0.001 inches.
Humboldt crack gauge	Requires close examination, but effective in detecting 0.02-inch increase in crack width.
Digital caliper	Very accurate and effective; detects crack width changes as small as approximately 0.002 inches.
Wood block crack gauge	Effective in detecting 0.02-inch increase in crack width.
Crack comparator	Requires close examination; effective if used in combination with close-up photographs.

8.5 Discussion and Findings

As described above, the cracks in the region of the connection of the northernmost diagonal to the deck increased dramatically during the course of the move from the casting yard to the final location. Even though the truss member forces were very similar before and after the move, several factors could have contributed to the additional damage. These factors are described in Section 7.

The damage observed after de-stressing is only slightly greater than the damage observed about three hours after the move. Therefore, the additional damage was related to the move and placement of the span in its final position, rather than de-stressing. Placement of the span in its final position would have resulted in a compressive force of almost 1700 kips in Member 11. The damage is consistent with horizontal sliding of Member 11 relative to the deck in combination with horizontal breakout failure of the north-end diaphragm, which are aggravated by additional compressive force in Member 11. On the other hand, de-stressing reduced the compressive force in Member 11, although a small increase in the post-tensioning force would have been required to loosen the nut on the post-tensioning rod in the first de-tensioning step. (No records of the de-stressing force used are available.)

Analysis of time-lapse video indicates that, contrary to FIGG instructions and Structural/VSL Safety Guidelines, no one closely monitored cracks in the north-end diaphragm during re-stressing of Member 11. Review of the time-lapse video also shows that Member 11 was re-stressed in increments. As such, Structural/VSL must have been aware of the instructions in FIGG's March 13 email to MCM. However, WJE does not know if MCM delegated responsibility for closely monitoring cracks during de-stressing to Structural/VSL.

Because the construction joint was not roughened and re-stressing Member 11 in incremental steps over two hours would have increased the compressive force by up to 560 kips, the existing cracks would have widened. If closely monitored by MCM, Structural/VSL, BPA or Corradino, increases in crack width could have been readily detected by several means, including use of wood block crack gauges, which were already used at the site. Increases in crack width would have required stopping the re-stressing in accordance with FIGG instructions and Structural/VSL safety guidelines and thereby prevented the collapse.

Exhibit 8.1.1. Crack in north end diaphragm approximately two weeks before move



East side of Member 12. Photo 13 from BPA crack inspection after formwork/scaffolding removal, February 28. Crack is indicated by blue arrows. Crack width ruler appears to indicate 0.020 inches.



West side of Member 12. Photo 12 from BPA crack inspection report after formwork/scaffolding removal, February 28. Crack is indicated by blue arrows. Crack width ruler appears to indicate 0.014 inches.

Exhibit 8.1.2. Diagonal “wedge” crack at Member11 approximately two weeks before move



Diagonal “wedge” crack along the bottom of Diagonal 11 on the east face. Photo taken by BPA on February 24, 2018, prior to the move.

Exhibit 8.2.1. Cracks in north end diaphragm approximately three hours after move



East side of Member 12. March 10 photo by Corradino showing same crack after move at 3:14 p.m.



West side of Member 12. March 10 photo by Corradino at 3:14 p.m.

Exhibit 8.2.2. Diagonal “wedge” crack at Member 11 approximately three hours after move



Diagonal “wedge” crack at base of Member 11 after the move on the east face. Photo taken by Corradino on March 10, 2018 at 3:07pm.

Exhibit 8.3.1. Cracks in north end diaphragm

PHOTO 5: Diaphragm 2, Eastside top view crack



East side of Member 12. Photo taken March 12, 2018 by MCM.

PHOTO 1: Diaphragm 2, Westside top view, crack



West side of Member 12. Photo taken March 12, 2018 by MCM.

Exhibit 8.3.2. Diagonal “wedge” crack at Member 11



Diagonal “wedge” crack at base of Member 11 on the east face. Photo taken by MCM on March 12, 2018.

Exhibit 8.4.1. Cracks in north end diaphragm



East side of Member 12. Photo taken March 14, 2018 by BPA.



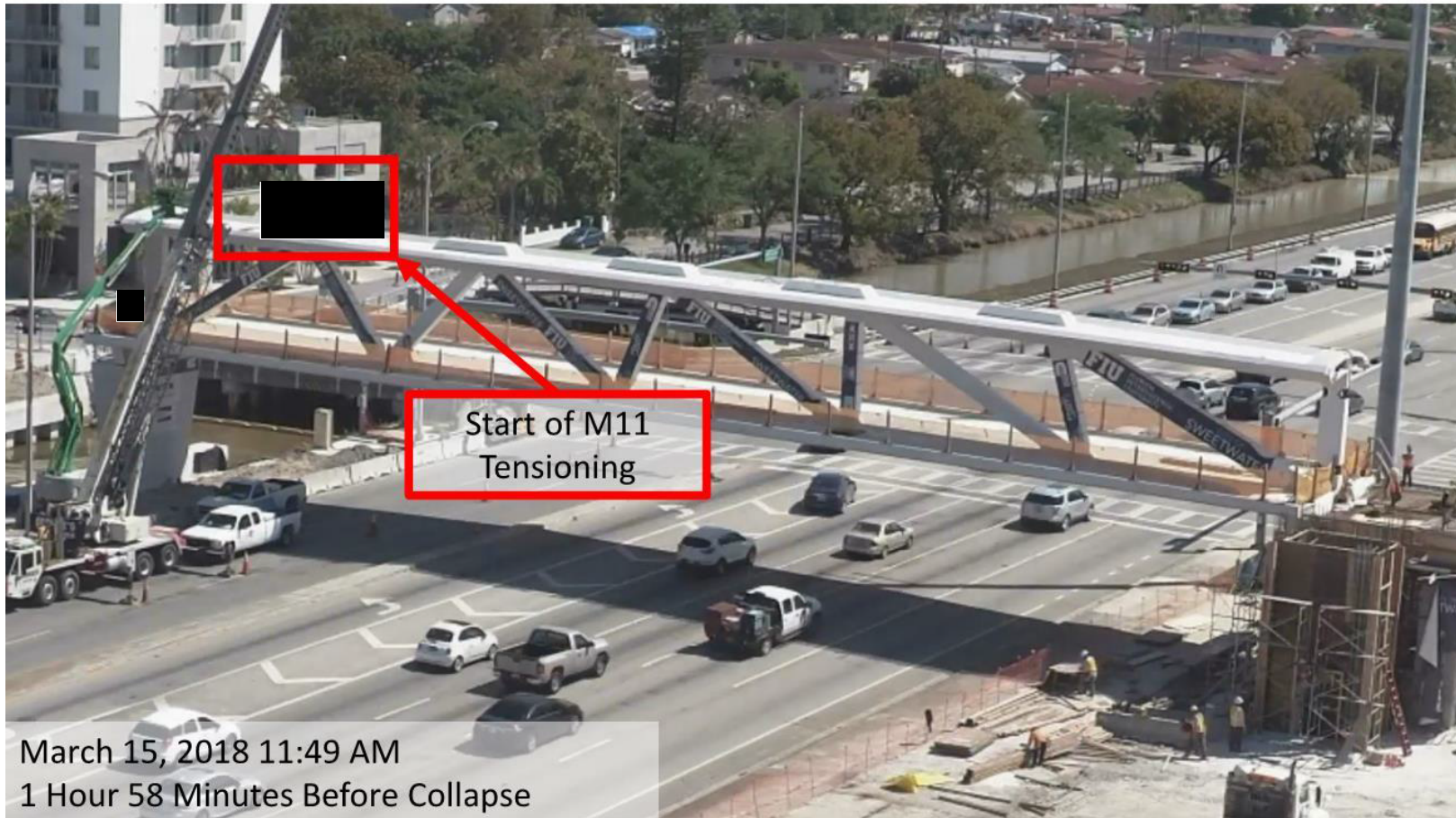
West side of Member 12. Photo taken March 13, 2018 by BPA.

Exhibit 8.4.2. Diagonal “wedge” crack at Member 11



Diagonal “wedge” crack at base of Member 11. Photo taken by BPA on March 13, 2018. Note the spall seen in Exhibit 3.2 has been removed.

Exhibit 8.5.1. Time-lapse video



Note: Redaction in "Exhibit 8.5.1 Time-lapse video" as per NTSB Operations Bulletin CIO-GEN-016.

Exhibit 8.5.2. Time-lapse video



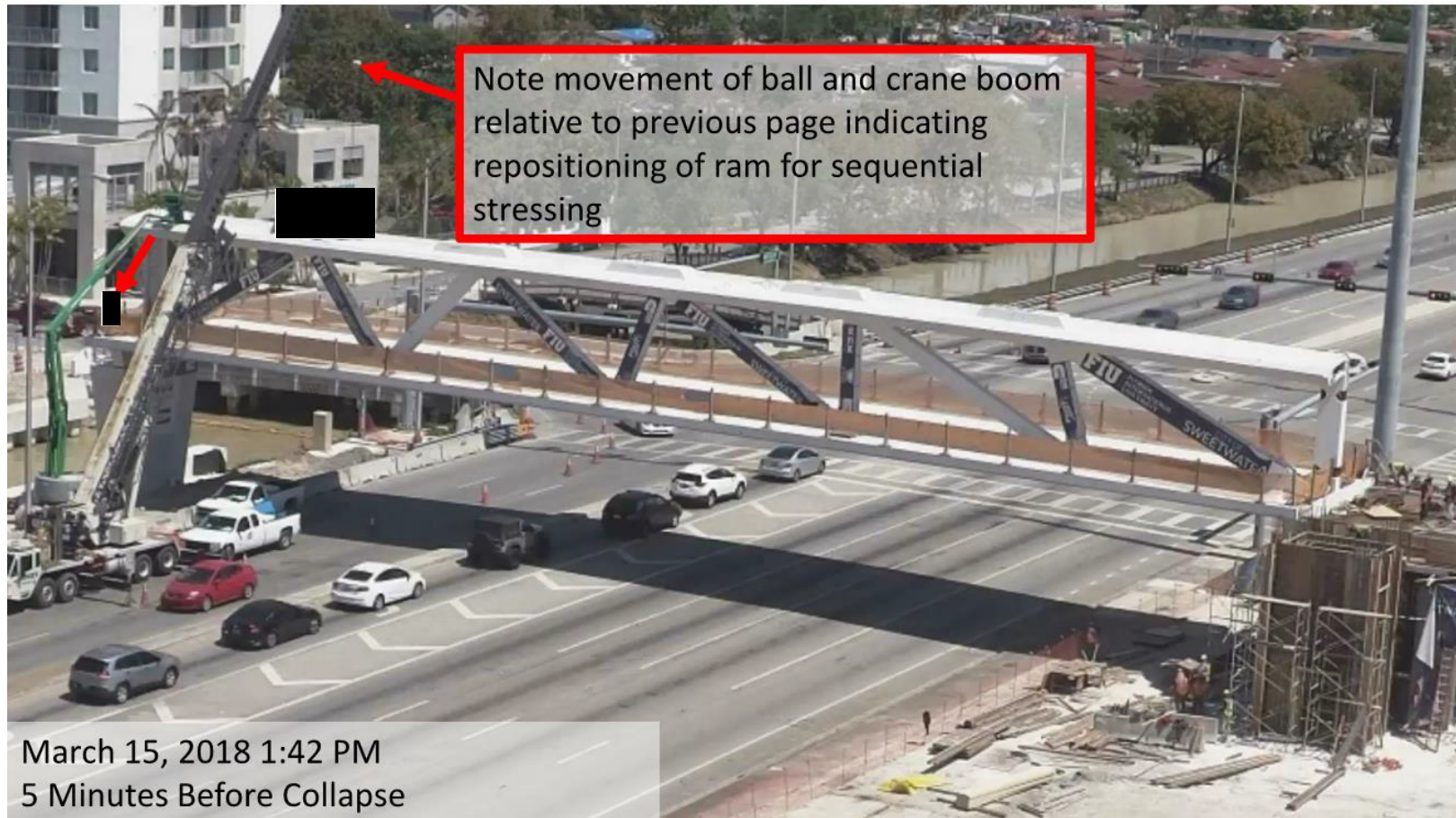
Note: Redaction in "Exhibit 8.5.2 Time-lapse video" as per NTSB Operations Bulletin CIO-GEN-016.

Exhibit 8.5.3. Time-lapse video



Note: Redaction in "Exhibit 8.5.3 Time-lapse video" as per NTSB Operations Bulletin CIO-GEN-016.

Exhibit 8.5.4. Time-lapse video



Note: Redaction in "Exhibit 8.5.4 Time-lapse video" as per NTSB Operations Bulletin CIO-GEN-016.

Exhibit 8.5.5. Time-lapse video



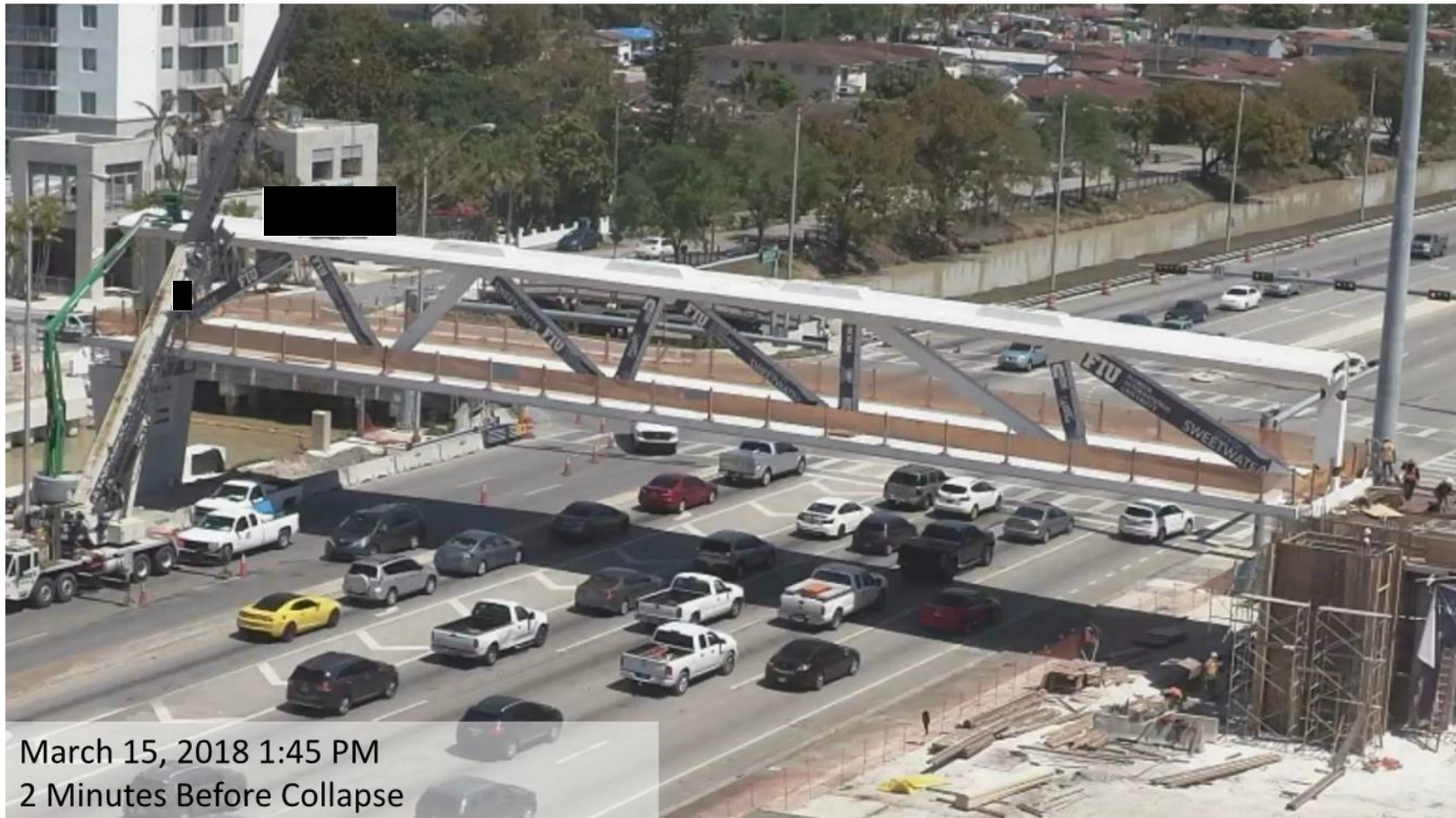
Note: Redaction in "Exhibit 8.5.5 Time-lapse video" as per NTSB Operations Bulletin CIO-GEN-016.

Exhibit 8.5.6. Time-lapse video



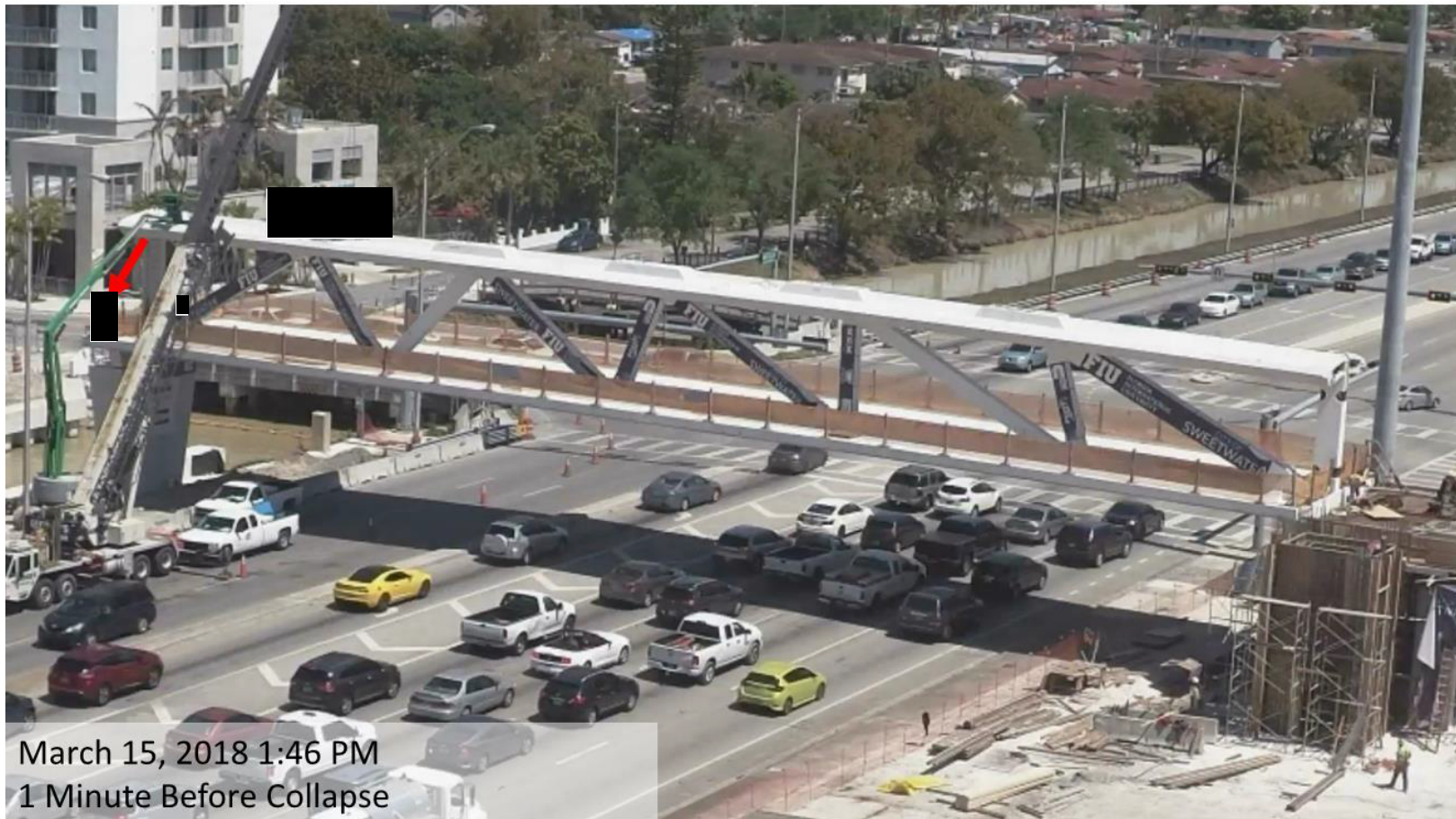
Note: Redaction in "Exhibit 8.5.6 Time-lapse video" as per NTSB Operations Bulletin CIO-GEN-016.

Exhibit 8.5.7. Time-lapse video



Note: Redaction in "Exhibit 8.5.7 Time-lapse video" as per NTSB Operations Bulletin CIO-GEN-016.

Exhibit 8.5.8. Time-lapse video



Note: Redaction in "Exhibit 8.5.8 Time-lapse video" as per NTSB Operations Bulletin CIO-GEN-016.

Exhibit 8.5.9. Time-lapse video



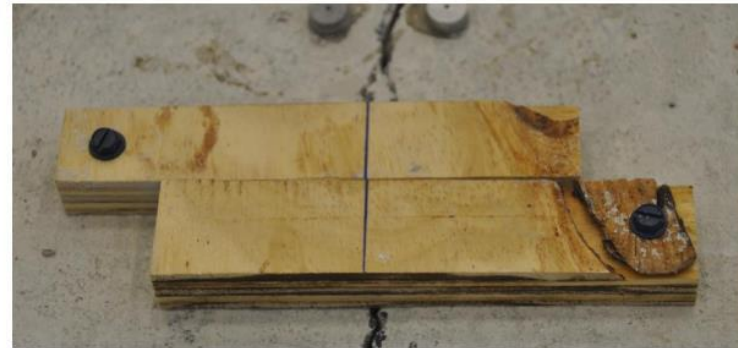
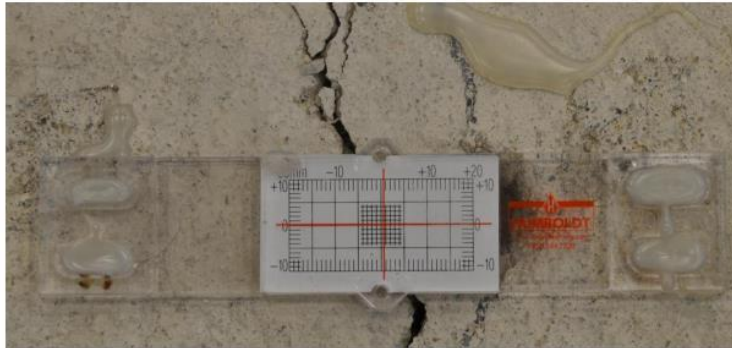
Note: Redaction in "Exhibit 8.5.9 Time-lapse video" as per NTSB Operations Bulletin CIO-GEN-016.

Exhibit 8.5.10. Time-lapse video



Note: Redaction in "Exhibit 8.5.10 Time-lapse video" as per NTSB Operations Bulletin CIO-GEN-016.

Exhibit 8.6.1. Comparison of crack monitoring methods for 0.02 inch change in crack width



*Upper left: Humboldt crack gauge
Upper right: Wood block crack gauge
Lower left: Crack comparator*

9 SUMMARY OF FINDINGS AND CONCLUSION

The following summary of findings and conclusion follow from the research and analysis described in Sections 2 through 8 of this report. The section that relates to each conclusion is indicated.

Failure Pattern (Section 2). A debonding and sliding failure at the construction joint below Member 11 led to breakout failure of the north-end diaphragm and ultimately collapse, triggered by sudden crushing of Member 11 near its base.

Construction Joint Conditions (Section 3). Despite FIGG’s confirmation to MCM that the FDOT Standard Specifications requiring roughening of the **hardened** concrete must be followed, the construction joint surface below Members 11 and 12 appeared to have been left in an as-placed (non-roughened), relatively smooth condition.

Interface Shear Transfer Testing (Section 4). The primary finding from the experimental program is that intentional roughening of the construction joint following FDOT Standard Specifications improved the shear capacity of the cracked interface by a factor of 1.78. This factor reduces by 5 to 13 percent if adjustment for Florida aggregate is made based on slant shear tests. This finding is consistent with relative difference according to the AASHTO Code: the maximum allowable shear stress for a roughened surface (1.5 ksi) is 1.88 times that for a non-roughened surface (0.8 ksi).

Comparison of observed axial strengths of the as-placed (non-roughened) specimens to the calculated force in Member 11 after the shoring was removed suggests that the construction joint was weakened or at least partially debonded when the shoring was removed.

More significantly, the axial capacities of the roughened specimens, before or after adjustment for Florida aggregate, are substantially greater than the calculated axial force in Member 11 at the time of the collapse. As such, if the construction joint were roughened as required by the FDOT specifications, the collapse would not have occurred. This conclusion is valid for hardened concrete surfaces intentionally roughened in accordance with FDOT Standard Specifications even if the surface roughness is considered to be less than the 1/4 inch amplitude referenced in the AASHTO Code. Also note that this conclusion neglects the additional capacity from breakout resistance of the north end diaphragm, which if included would provide additional capacity to the connection.

Structural Analyses (Section 5). A finite-element model of the main span was developed to determine truss member forces and bending moments during construction.

AASHTO LRFD Design Compliance. The Member 11/12 deck connection was evaluated in accordance with the AASHTO Code, assuming resistance by shear-friction across the entire construction joint. Although inconsistent with the actual failure mode, resistance by shear-friction across the entire construction joint is the likely design assumption. Based on WJE test results, the AASHTO friction coefficient for a roughened surface (which calls for 1/4-inch roughness amplitude) was assumed. However, AASHTO does not provide specifics on preparation of the joint (including intentional roughening of hardened concrete) or how roughness is measured. The FDOT Standard Specifications, as proven by laboratory testing, achieves the requirements of AASHTO Code. The capacity-to-demand ratio was found to be 1.09 if AASHTO load modifiers for ductility and redundancy are excluded, and 0.99 if they are included, indicating compliance with AASHTO design requirements.

Estimated Capacity for Non-roughened Joint. For the assumption of an un-roughened surface, factored capacity calculated in accordance with the AASHTO design code was much less than the factored demand, indicating a significant deficiency if the bridge is not built in compliance with the FDOT Standard Specifications for preparation of construction joints.

Capacity Analysis for Observed Failure Pattern. The Member 11/12 deck connection was also evaluated based on results of the interface shear transfer testing in combination with breakout resistance consistent with the actual failure pattern, ACI 318 design equations, and related research. The results indicate that the combined shear-friction and breakout resistance is consistent with the calculated horizontal force in the Member 11/12 deck connection at the time of the failure. This explains the failure due to the unroughened construction joint surface.

Evaluation of Peer Review (Section 6). Berger's peer review fell far short of their contractual obligations. In particular, by their own admission, Berger did not even attempt to assess the conditions at the construction stage shown in the plans that was being built at the time of the collapse, which was required by their contract. Furthermore, the Berger finite element model could not have been used to reasonably estimate the forces in the concrete truss members during construction or in the structure's final configuration because it did not address the construction phasing.

Evaluation of Twist Exceedances during the Main Span Transport (Section 7). Cracks in the region of the connection of Members 11 and 12 to the deck increased dramatically after the move from the casting yard to the final location, as evidenced by photographs taken before and after the move. The deformations associated with exceeding the established twist limits caused high stresses in the region. Along with other factors, this stress may have been a contributing factor to damage in the region and ultimately to the collapse.

Re-Stressing of Member 11 (Section 8). Contrary to FIGG's instructions, no one closely monitored cracks in the north-end diaphragm during re-stressing of Member 11, even though both MCM and Structural/VSL were aware of the instruction. Also, Structural/VSL's shop drawings state that stressing operations should stop if existing cracks widen or new cracks are observed. Evidence shows the construction joint was not roughened, so the existing cracks would have widened during re-stressing, and the widening could have been readily detected by several means. In accordance with FIGG's instruction and Structural/VSL's awareness of crack monitoring per their shop drawings, widening of the cracks would have required stopping the re-stressing, thereby preventing the collapse.

Conclusion. In conclusion, most significant finding from WJE's research and analysis is that full-scale tests show that if the construction joint below Members 11 and 12 were roughened as required by the FDOT Standard Specifications, the collapse would not have occurred. It is also highly significant that, for the observed failure pattern and relatively smooth as-built condition of the construction joint, the combined shear-friction and breakout resistance determined from testing and analysis is consistent with the calculated horizontal force in the deck connection at the time the failure.

B. TFHRC Factual Report

**TURNER-FAIRBANK HIGHWAY RESEARCH CENTER
FACTUAL REPORT**

Concrete Interface Under Members 11 and 12

Prepared For:

National Transportation Safety Board

NTSB Accident ID: HWY18MH009

Prepared by:

Benjamin Graybeal, Ph.D., P.E.

Zachary Haber, Ph.D.

Federal Highway Administration

Turner-Fairbank Highway Research Center

6300 Georgetown Pike, McLean, VA 22101

October 19, 2018

SCOPE

This report provides a compilation of facts related to a horizontal concrete surface between the deck and Members 11 and 12 at the north end of the bridge. This surface was an interface on which a large shear demand was placed at various times in the life of the structure. A portion of this surface under Member 11 became debonded prior to the structural failure, resulting in a pair of horizontal surfaces on which relative horizontal sliding was possible. Investigation of the competence and geometry of the concrete at this location was necessary as part of an overall performance assessment of the structure.

CONCRETING FUNDAMENTALS

Concrete is mixed and placed in a semi-liquid state, later developing mechanical properties through a series of chemical reactions that transform the semi-liquid material into a solid. Concrete is commonly placed into preconstructed formwork that is designed to hold the semi-liquid concrete in a desired shape while supporting the material's self-weight. This formwork is commonly removed after the placed and hardened concrete is capable of carrying the necessary loads. The placement of concrete progresses as multiple discrete batches of material are deposited into the formwork. These discrete batches of concrete are commonly vibrated (i.e., agitated) in order to consolidate the concrete and merge concretes from successive semi-liquid batches along locations where successive batches meet.

It is often the case that a particular portion of formwork will need to be filled to the top with concrete and that this concrete will need to harden prior to the installation of subsequent formwork and the placement of subsequent concrete batches. In these cases the subsequent castings of concrete will often rest upon the earlier, hardened casting of concrete. The plane between the earlier and later concrete castings is commonly referred to as a cold joint. The American Concrete Institute defines a cold joint as “a joint or discontinuity resulting from a delay in placement of sufficient duration to preclude intermingling and bonding of the material” and defines a cold joint line as “indicating the presence of discontinuities where one layer of concrete had reached final set before subsequent concrete was placed”.^a

The mechanical properties of a structural concrete element differ locally in a cold joint region as compared to properties in nearby monolithic concrete. As previously noted, concrete from the initial placement will have hardened prior to the placement of the secondary concrete casting. As the second casting hardens, chemical and mechanical bonds will form at the interface between the two castings; this interface constitutes the cold joint. The strength of these bonds is dependent on numerous factors. Yet, even in ideal conditions, the cold joint region will have different mechanical properties than those that occur within a monolithic pour of concrete. Thus, cold joints must be recognized within the context of the demands placed on the structural concrete and detailed to ensure appropriate overall performance.

^a ACI CT-18. (2018). “*ACI Concrete Terminology*.” American Concrete Institute. Farmington Hills, Michigan.

COLD JOINT SURFACE PREPARATION

The plane of a concrete cold joint may perform differently than an arbitrary plane of monolithic concrete within the same structural element. Thus, concrete construction commonly requires that cold joint regions receive special design considerations and receive special concrete placement techniques to enhance their performance. Of note, the Florida Department of Transportation's *Standard Specifications for Road and Bridge Construction, Division II – Construction Details* pertains to the bridge under discussion in this report and includes the following:^b

400-9 Construction Joints

400-9.3 Preparations of Surfaces: *Before depositing new concrete on or against concrete which has hardened, re-tighten the forms. Roughen the surface of the hardened concrete in a manner that will not leave loosened particles, aggregate, or damaged concrete at the surface. Thoroughly clean the surface of foreign matter and laitance, and saturate it with water.*

Additionally, the AASHTO LRFD Bridge Design Specification^c prescribes that certain structural resistance levels will be provided by cold joints that are prepared in certain ways. This design specification also requires that a minimum amount of discrete reinforcement cross a cold joint subjected to certain types of loads. Section 5.8.4 of the specification is titled “Interface Shear Transfer—Shear Friction” and discusses the resistance provided along a concrete interface depending on the characteristics of said interface. The interfaces discussed include:

- interfaces composed of monolithic concrete,
- interfaces composed of cold joints whose substrate concrete was intentionally roughened, and
- interfaces composed of cold joints whose substrate concrete was not intentionally roughened.

Roughened concrete is defined as a “clean concrete surface, free of laitance, with surface intentionally roughened to an amplitude of 0.25 in.” Surfaces that are not intentionally roughened are required to be clean and free of laitance.

Bridge elements containing cold joints that will be subjected to interface shear commonly have construction requirements that call for the roughening of the substrate concrete on the cold joint. This roughening is commonly completed after the concrete has been placed in the formwork and consolidated, but while it is still in a semi-liquid-like state. In order to complete the actions of finishing and roughening of the concrete, construction personnel must be able to access the relevant concrete surface and to impart the needed mechanical actions on the surface.

^b Florida Department of Transportation. (July 2015). *Standard Specifications for Road and Bridge Construction, Division II – Construction Details*. page 384.

^c AASHTO. (2014). “*AASHTO LRFD Bridge Design Specification, 7th Ed.*” American Association of State Highway and Transportation Officials. Washington, D.C.

INTERFACE BETWEEN MEMBERS 11 AND 12 AND THE DECK OF THE BRIDGE

The construction process for the superstructure of bridge included three distinct concrete pours. The first was for the deck of the bridge, the second was for the truss diagonal and vertical members, and the third was for the canopy of the structure. These pours were completed sequentially with significant time allotted between pours to allow for development of the mechanical properties of concrete from earlier pours. The design plans for the bridge indicated that the cold joints between pours would be at the following locations:

- between the bridge deck and the bottoms of the diagonal/vertical members, and
- between the tops of the diagonal/vertical members and the bridge canopy.

An image of the bridge superstructure captured just prior to the placement of the bridge on the piers is provided in Figure 1. This figure includes an annotation highlighting the region of interest on the north end of the bridge at the location where Members 11 and 12 framed into the deck. An elevation view of the north end of the superstructure is provided in Figure 2, again with annotations to indicate the region of interest.



Figure 1. Main span of the bridge highlighting the portion of the bridge this is of interest to this factual report.

Finally, Figure 3 provides a local view of the location where Members 11 and 12 meet the bridge deck. The provided photograph shows the east face of diagonal Member 11 and the south and east faces of vertical Member 12. The deck surface can be seen around the base of where the two members frame into the deck. The interface under discussion is annotated in this figure.

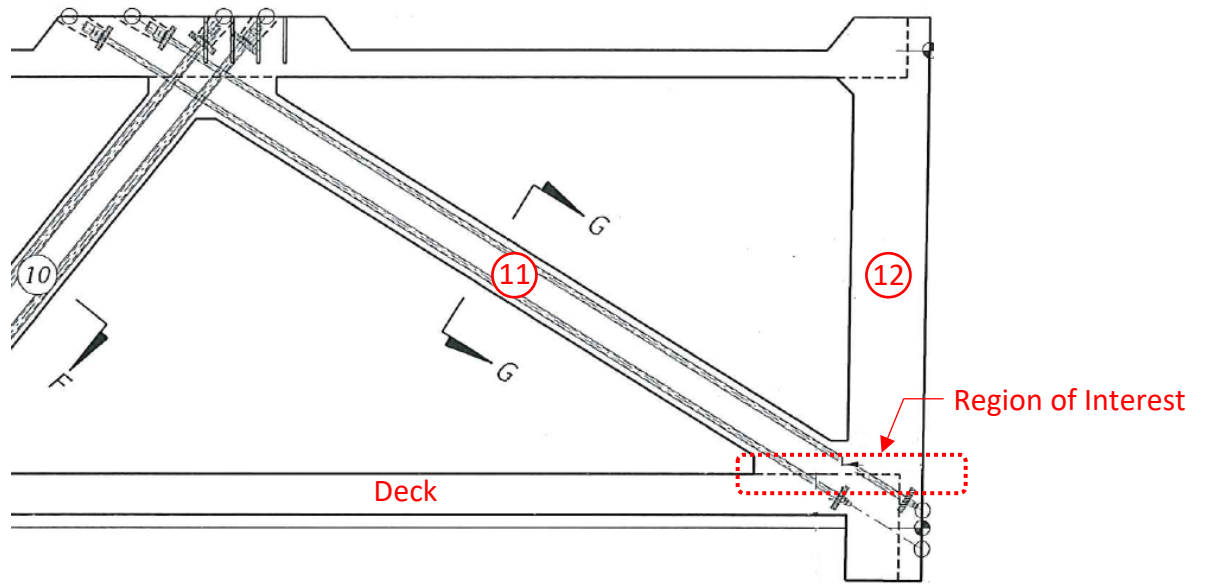


Figure 2. Elevation view of region of interest at the intersection of members 11 and 12 and the deck.

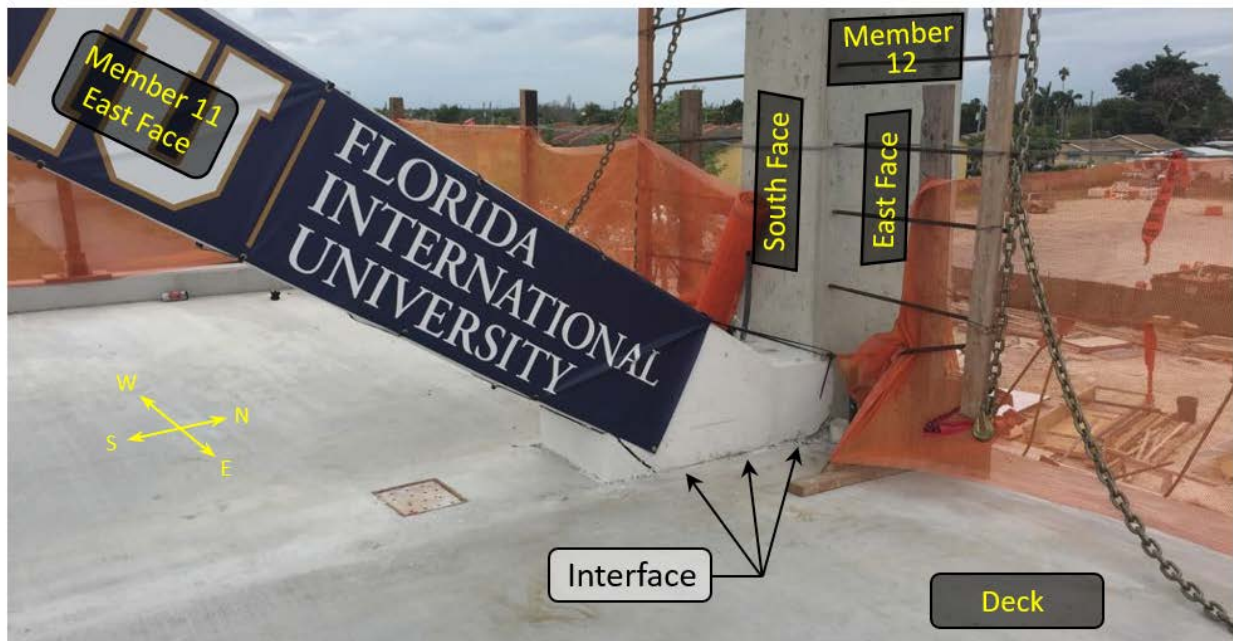


Figure 3. Annotated image showing elevation view of region of interest at the intersection of members 11 and 12 and the deck.

INTERFACE BEFORE COLLAPSE

Numerous photographs of the interface under discussion were captured prior to the collapse of the bridge. These photographs were captured in relation to the cracking and apparent relative horizontal translation of the elements immediately above and below this interface in the weeks leading up to the collapse.

Figure 4 provides a set of photographs that document a portion of the east face of the interface in the days immediately before the collapse. The compound figure shows the overall location in the structure (Part A), followed by a zoomed location in the structure (Part B), followed by three close-up photos of the interface between the bridge deck and the bottom of Member 11 (Parts C through E). The specific location shown in the three close-up photos is within the line of action of Member 11 near the intersection with Member 12. The three close-up images appear to show that the secondary pour sits slightly above the surface of the deck. It is also apparent that the secondary pour was not completely consolidated, with a small amount of less consolidated concrete visible on a portion of the bottom edge of the casting (annotated in Parts D and E). The indication of this less consolidated concrete is the observation of apparent paste-covered aggregates that reside in a void that is recessed from the vertical finished surface of the member.

Figure 5 provides a set of photographs that also document a portion of the east face of the interface in the days immediately before the collapse. This compound figure shows the overall location in the structure (Part A), followed by a zoomed location in the structure (Part B), followed by three close-up photos of the interface (Parts C through E). The specific location shown in the three close-up photos is near the southern end of the east face of where Member 11 meets the deck.

These close-up images show that the interface, labeled as “Apparent cold joint” in Parts C through E, does not appear to be roughened. Additionally, the chamfer at the southern end of the interface between Member 11 and the deck appears to have remained connected to the deck, while the crack that runs along the northern portion of the interface departed from the interface and began following the extension of the southern face of Member 11. Thus, the cold joint at the southern end of the interface being investigated may have remained intact until the collapse began.

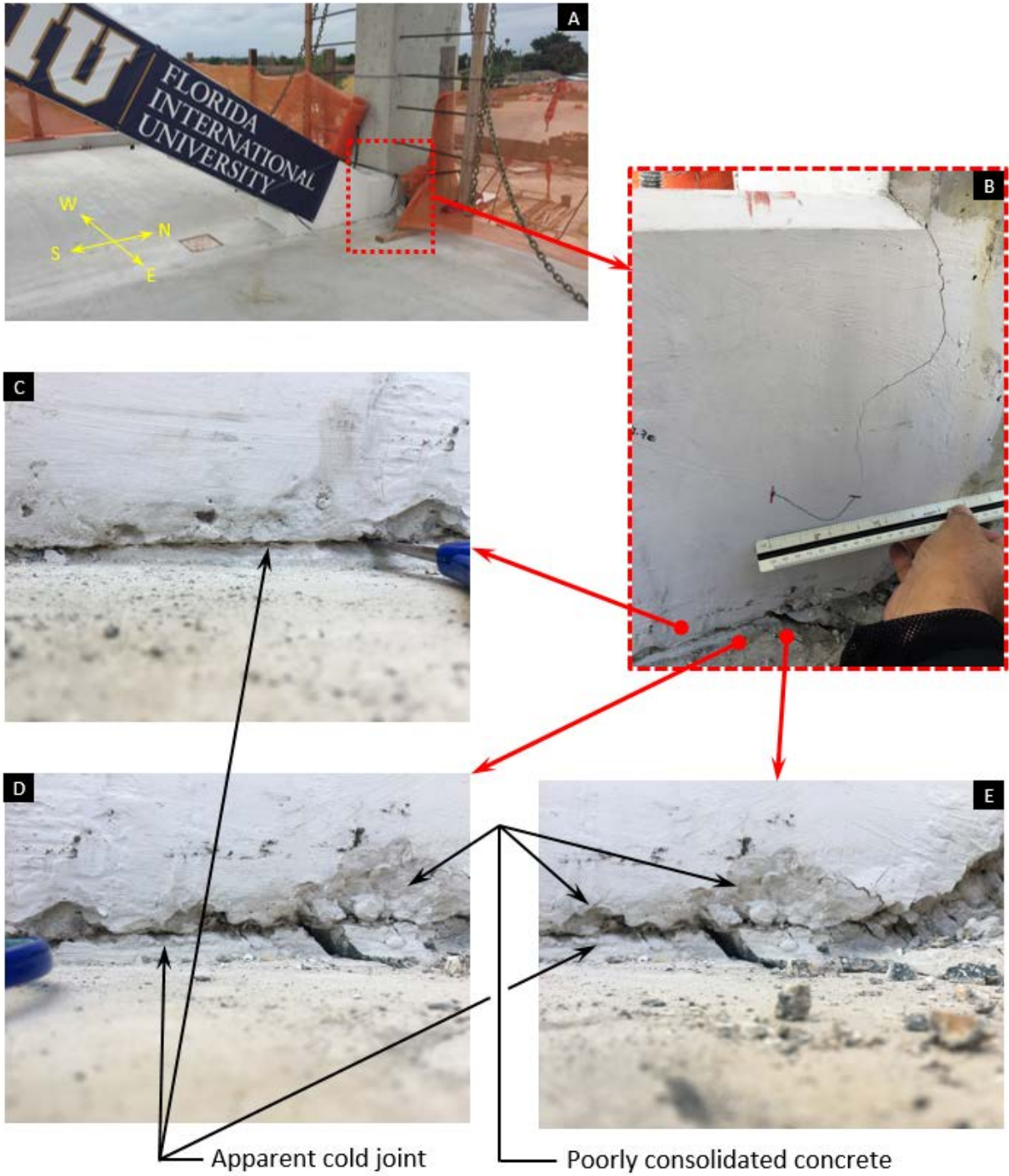


Figure 4. Annotated images demonstrating interface condition on east face of member 11 near member 12.

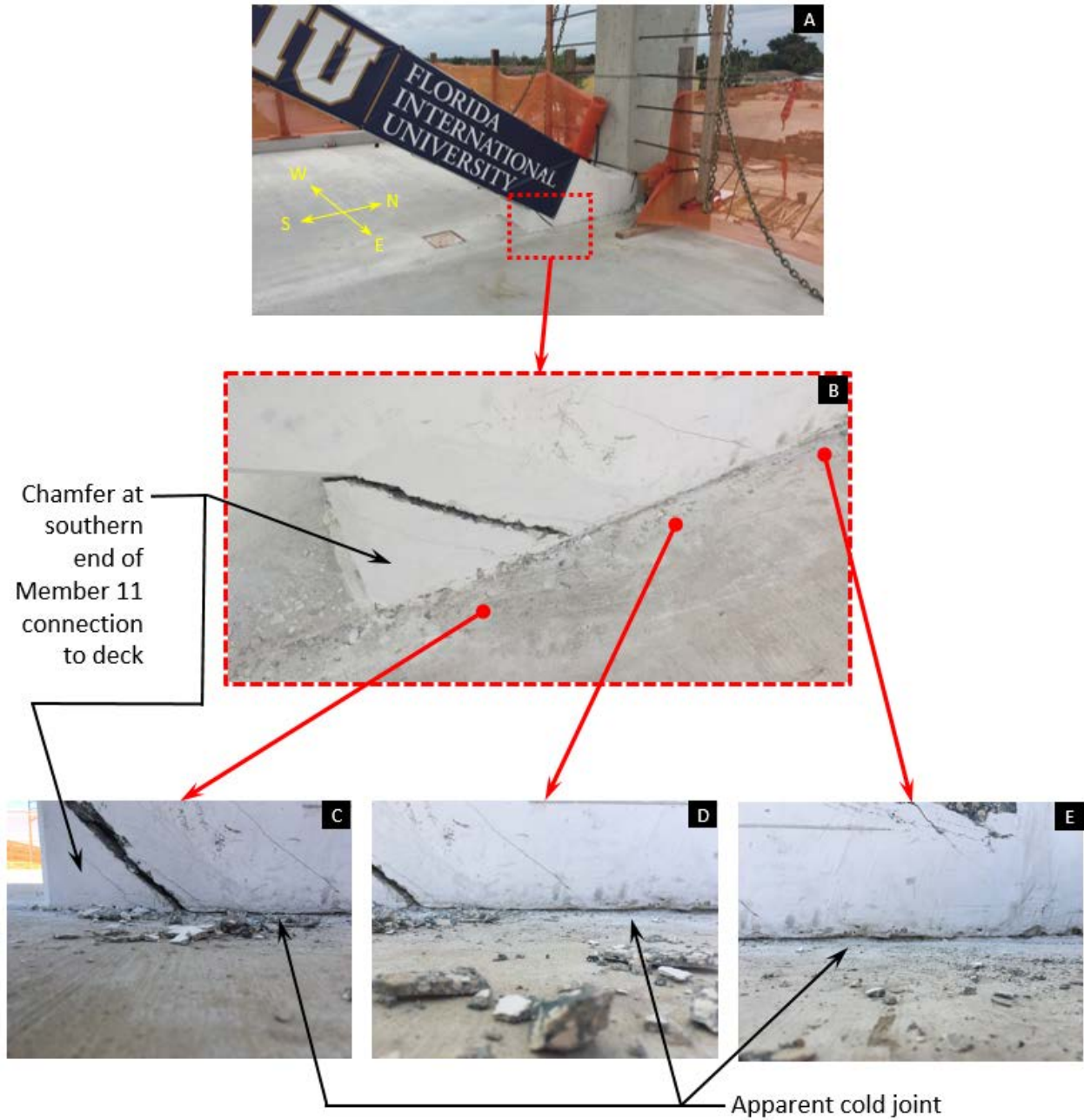


Figure 5. Annotated images demonstrating interface condition near the south end of the east face of Member 11 with the deck.

INTERFACE AFTER COLLAPSE

The collapse of the bridge superstructure caused significant damage to many parts of the structure, including portions of the structure near the region of interest; the location where Members 11 and 12 intersected with the deck. In particular, the concrete in the lower portions of Members 11 and 12 was pulverized into rubble, as was the concrete in the deck immediately under Member 12. Post-collapse assessment of the cold joint was completed using remaining intact pieces of concrete from the region of interest in the structure.

Figure 6 provides a set of photographs showing the bottom end of Member 12. The photos in Part D and E show the north face of Member 12, with the left side of the member in each photo being the bottom end of Member 12. Part E and the annotation call attention to the location of a cold joint interface between concrete pours. From a construction process standpoint, this surface feature indicates a location where vertical formwork for a secondary pour of concrete was nearly pressed against the existing hardened concrete of the first pour. The small gap between the formwork and the first pour allowed a small amount of concrete paste to flow slightly past the leading edge of the hardened concrete on the north face of the member, thus creating the ragged horizontal paste line at the cold joint location.

Parts A through C of Figure 6 show the remnants of the south face and bottom end of Member 12. The boxed area in Part A draws attention to bottom end of Member 12 where it met the bridge deck. The key feature in this image is shown in both Parts B and C. A flat, nearly smooth plane of concrete paste is visible. This plane coincides with the cold joint surface feature visible on the north face of Member 12. This plane is part of the secondary casting of concrete that was placed and hardened against the first casting of concrete. The concrete in this plane and nearby appears well consolidated, indicating that this concrete replicated the surface geometry of the surface on which it was cast. Prior to or during the collapse, the concrete from the secondary casting debonded from the concrete from the original casting, leaving behind this preserved portion of the cold joint. This flat, nearly smooth plane does not show indications of abrasion or other mechanical actions that could have left a smoother surface than was originally present after the secondary pour of concrete was completed.

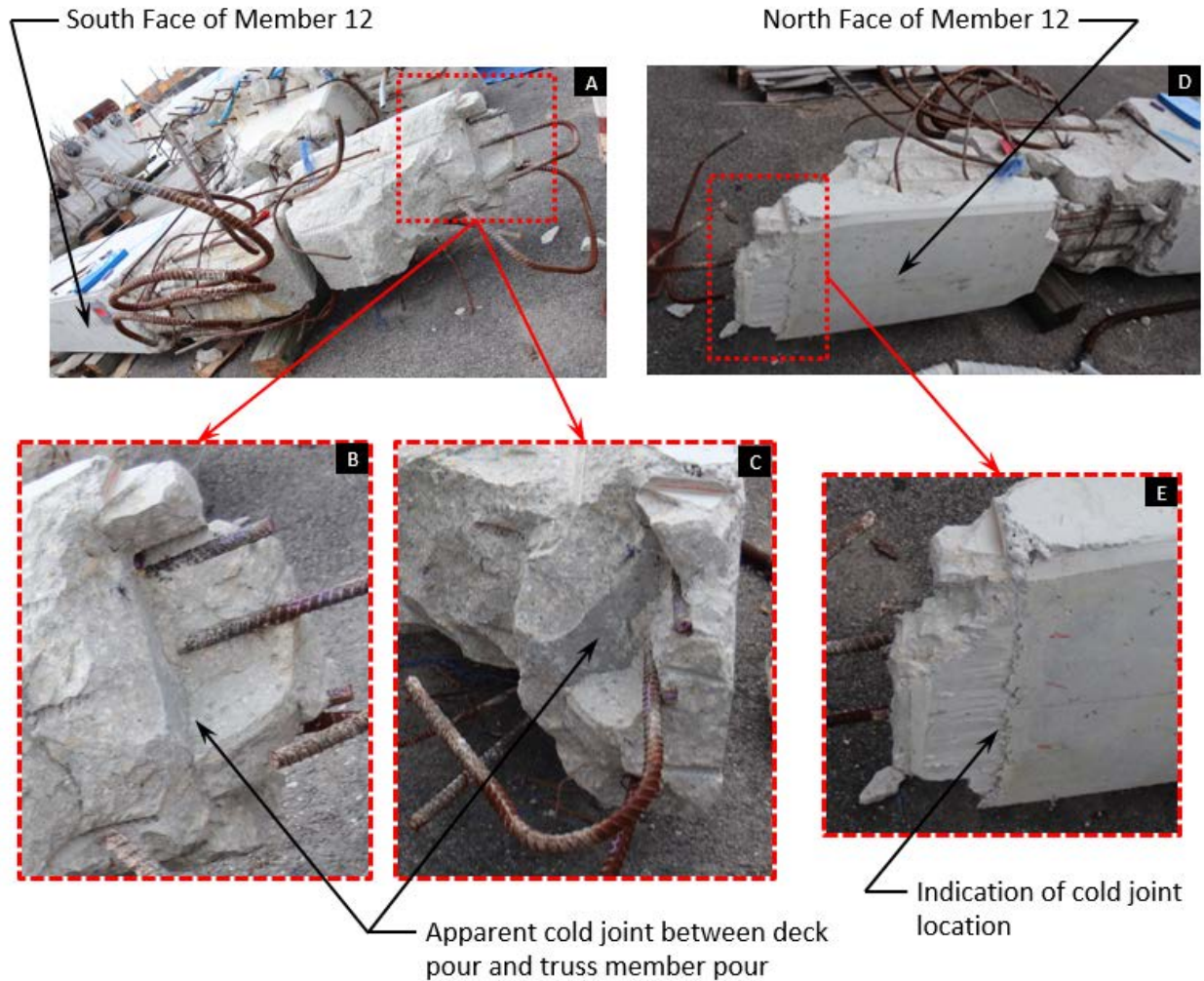
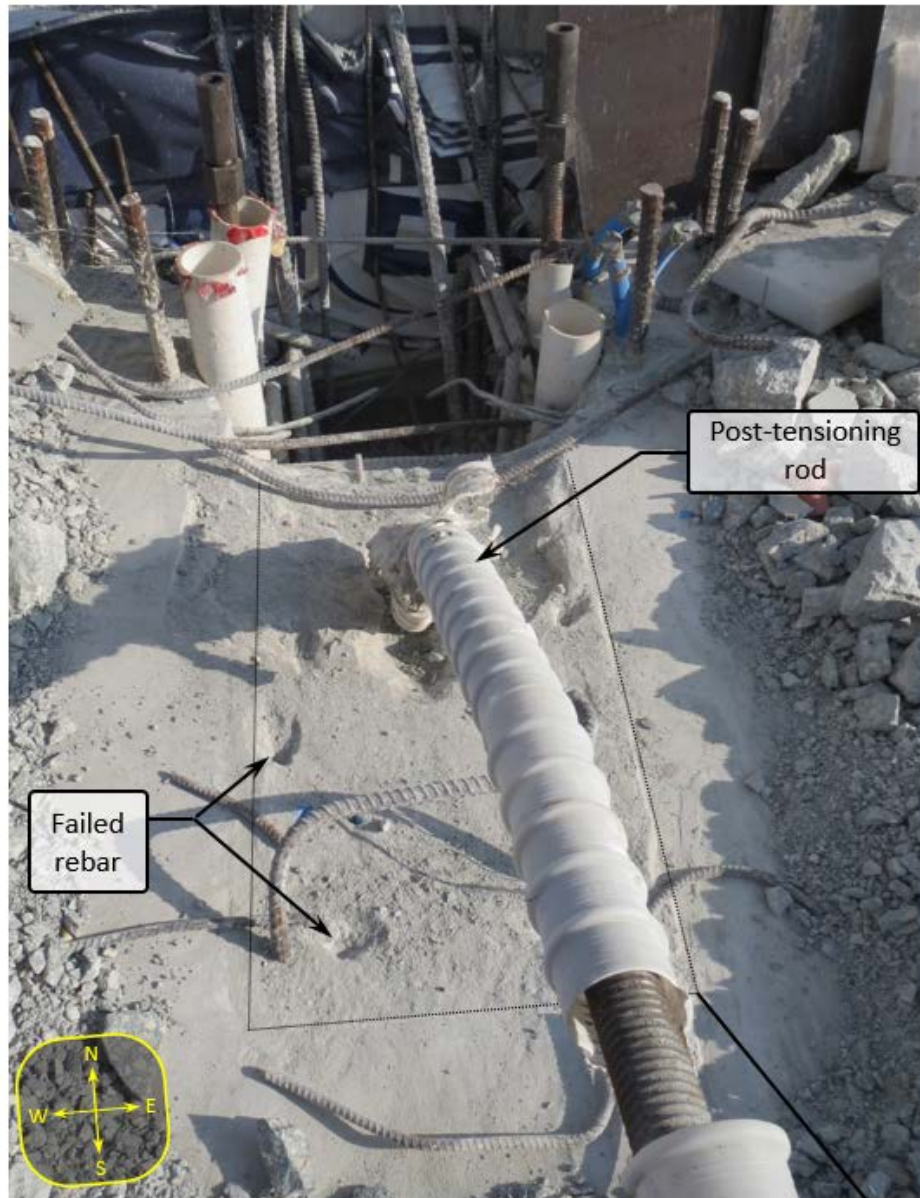


Figure 6. Indications of cold joint near the bottom end of Member 12.

After the collapse, the deck under Member 11 was partially intact; this shown in Figure 7. This photo was captured in the days after the collapse once pulverized concrete and other debris created by the collapse had been carefully removed from the surface. This northward looking photo is taken from the vantage point of where Member 11 was heading diagonally toward the deck. The hole in the north end of the deck is the location where Member 12 met the deck. The visible post-tensioning rod was the lower rod within Member 11.

The portion of the deck under the southern end of Member 11 is largely intact from the post-tensioning rod to the southern end of the interface. This surface appears relatively smooth. The isolated depressions on the concrete surface, identified in Figure 7, are locations where reinforcing bars previously passed upward through the interface between the base of Member 11 and the deck.



Footprint of Member 11 on deck indicated with superimposed dotted line

Figure 7. Interface under Member 11 after loose debris removal.

Further photographic evidence of this surface is provided in Figure 8 which shows the southeast corner of the interface after the surface had been washed with water. The foreground includes the southern end of the interface near the interface shear rebar that remained intact through the collapse. The upper portion of the photo includes the portion of the interface near the lower post-tensioning rod from Member 11. A concrete fracture surface within a cone of failed concrete near a fractured rebar is labeled. The apparent cold joint surface between Member 11 and the deck is also labeled. The visual difference between the fractured concrete surface near the fractured rebar and the apparent cold joint surface is notable. The fractured surface shows fractured aggregates as well as fractured paste, whereas the apparent cold joint surface is largely

covered in relatively smooth concrete paste. It is also important to note that the apparent cold joint surface does not show scratches or gouges near the southern end of the interface; scratches and gouges begin to appear as one traverses northward toward the lower post-tensioning rod. These scratches and gouges have a north-south orientation and appear likely to have occurred during the collapse as the concrete in the bottom end of Member 11 slid northward across the deck surface.

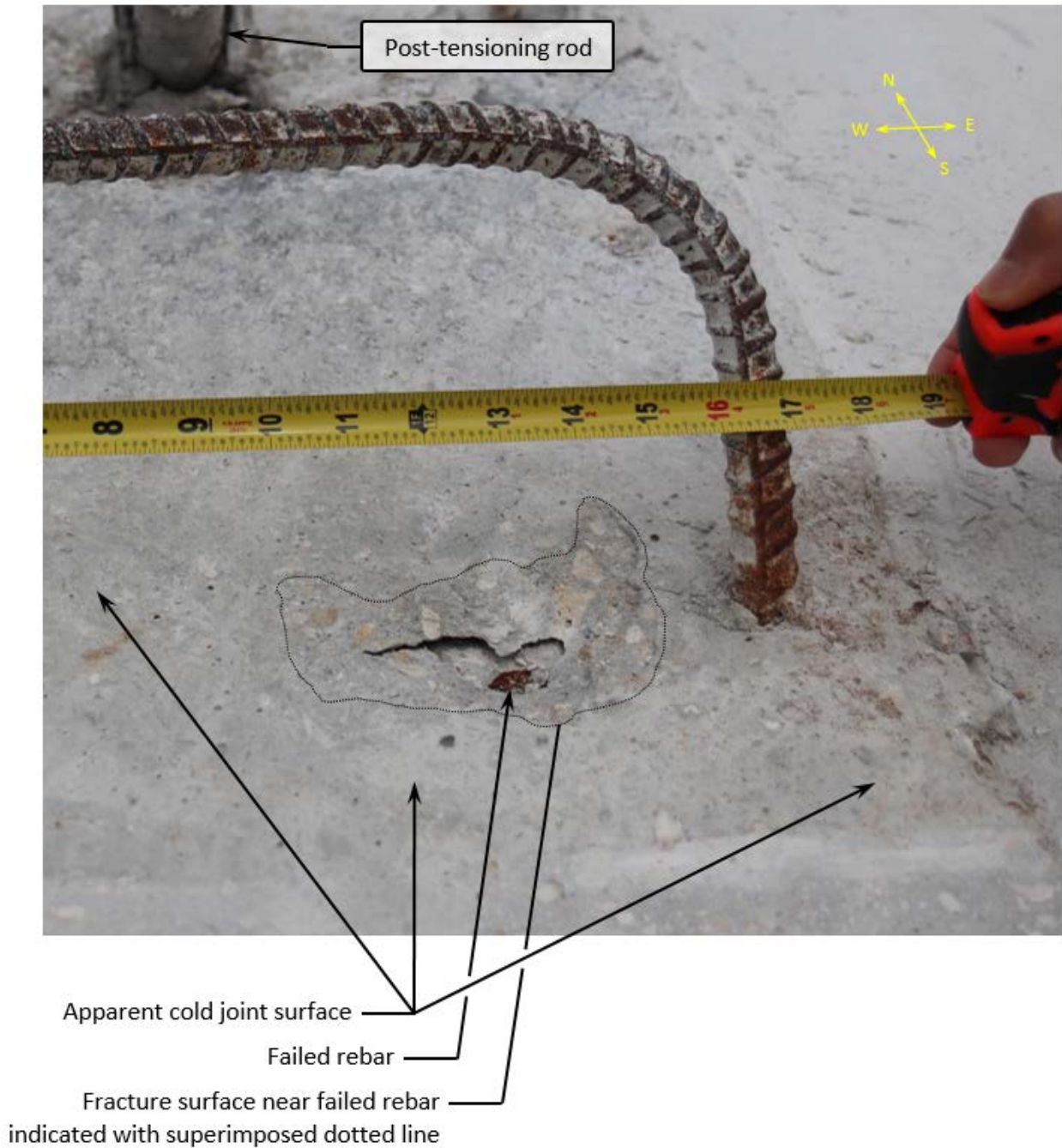


Figure 8. Interface under southeast corner of Member 11 after cleaning.

Further investigation was completed on the portion of the interface on the southern end of the connection between Member 11 and the deck. Figure 9 provides a series of photos related to the interface after it had been removed from the collapse site. The photo in Part A shows the interface, this time after the free length of the post-tensioning rod had been removed and a core hole had been cut into the south end of the interface. The concrete under the southern portion of the interface had become delaminated on a horizontal plane at a depth approximately 1 inch below the visible surface. A portion of that delaminated concrete was collected as evidence and is shown in the photo in Part B. Note that the delamination extended beyond the area under Member 11 into the area under the finished concrete surface of the deck. It is likely that this delamination occurred after the collapse initiated, quite likely in relation to the deck impacting the ground after falling off the pier.

The image in Part C shows a view along the deck looking south to north along the east edge of where Member 11 met the deck. An elevation increase from right to left is visible in the center of the photo; this location coincided with the eastern edge of Member 11. The relative smoothness of the surface of both the finished deck and the interface under Member 11 is evident.

The photo in Part D shows an east-west vertical slice of concrete that was cut from the delaminated concrete along the line identified in Part C. Note that the right side of the image shows concrete that was from the deck east of the member and the elevation change in the horizontal concrete surface indicates the eastern extent of where Member 11 met the deck. By looking at the combination of the paste and aggregates in this concrete slice, it is apparent that there is no other cold joint throughout this depth of concrete. The smoothness of the top surface of the interface is also apparent.

Part E shows a close-up isometric view of the concrete along a small portion of the interface. The vertical slice shows concrete paste and fine aggregates. The top of the image shows the interface surface. This surface is largely composed of cementitious paste, which in some locations appears to cover slightly protruding larger aggregates. Throughout the southern half of the interface between Member 11 and the deck there are relatively few locations where an aggregate piece in the concrete appears to have protruded through the interface and been sheared off prior to or during the collapse.

Further evidence related to the interface is provided by a core that was taken vertically down through the interface near the southern end of where Member 11 met the deck. This core is shown in Figure 10. As was discussed previously, there was a delamination layer under the interface surface. The photo in the figure is annotated to identify key features. The top of the core shows the apparent cold joint surface at the interface. This surface is largely concrete paste with a small number of fractured aggregates. The vertical fractured surface in the delaminated piece shows small aggregates immediately under the top surface. On this surface there are also a few larger aggregates, one of which is identified as being fractured where it crosses the delamination plane. This is indicative of the delamination plane having been caused by mechanical stressors and not by its having originally been a cold joint. Further examination through the depth of the core make apparent that 1) the concrete under Member 11 was well consolidated, and 2) the cold joint between the deck pour and the member pour was not at a location beneath the failure interface.

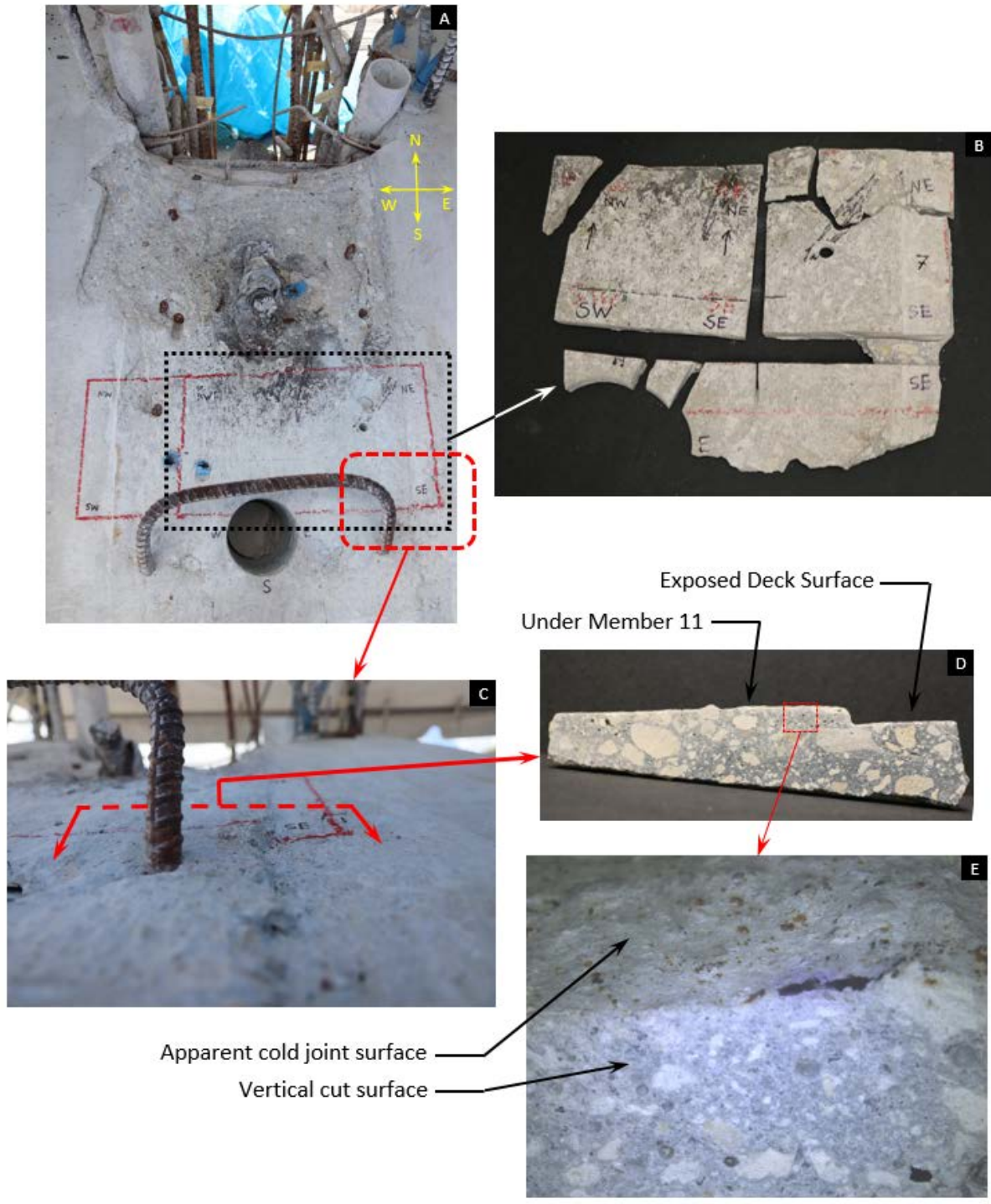


Figure 9. Interface surface under Member 11.



Figure 10. Annotated image of core extracted from south end of interface surface under Member 11.

SUMMARY

The failure interface between the bases of Members 11 and 12 and the bridge deck was investigated. Evidence was collected to assess the location of the cold joint between the deck concrete pour and the truss member pour, and also to assess the apparent roughness of the interface created at the cold joint. Photographs captured prior to the collapse provide an indication of the location of the failure interface and the apparent smoothness thereof. Evidence collected after the collapse provide an indication of the location of the cold joint within the structure and the original roughness of the cold joint. The evidence indicates that the failure interface coincides with the original cold joint and that the cold joint was not intentionally roughened.

C. NTSB Materials Laboratory Study

NATIONAL TRANSPORTATION SAFETY BOARD

Office of Research and Engineering
Materials Laboratory Division
Washington, D.C. 20594



August 27, 2019

MATERIALS LABORATORY STUDY REPORT

Report No. 19-043

A. ACCIDENT INFORMATION

Place : Miami, FL
Date : March 15, 2018
Vehicle : FIU UniversityCity Pedestrian Bridge
NTSB No. : HWY18MH009
Investigator : Robert Accetta (HS-20)

B. COMPONENTS EXAMINED

Selected surfaces on Member 12 and the deck under Member 11.

C. DETAILS OF THE STUDY

Flat areas were observed on the deck surface that was under Member 11 and on the bottom of Member 12 where it met the deck surface. A discussion of these areas is given in a Turner-Fairbank Highway Research Center (TFHRC) Factual Report entitled, "Concrete Interface Under Members 11 and 12", dated October 19, 2018.

The location of the flat area on the deck surface under Member 11 is shown in Figures 1 and 2. Yellow dashed lines indicate a lip on the surface that was consistent with the edge of a cold joint. A portion of this area was sectioned and removed from the deck surface, as shown in Figure 3. The largest pieces separated from the deck were numbered 1, 2, and 3.

The bottom of Member 12 is shown in profile in Figure 4 and perpendicular in Figure 5. The yellow dashed line in Figure 4 highlights the straight plane of the flat area observed. Figure 5 shows that the flat area on Member 12 was only a portion of the cold joint and was irregular in shape.

The extracted portion of the deck under Member 11 and the entirety of the bottom of Member 12 were examined at TFHRC. Post-collapse damage was observed on portions of the flat surfaces, thus subsequent evaluation was performed on a best effort basis on undamaged areas.

There are two methods within the concrete construction community that are widely used to characterize concrete surfaces. The first method is ICRI 310.2R-2013, *Selecting and Specifying Concrete Surface Preparation*, International Concrete Repair Institute, Inc., St. Paul, MN, 2013. This method utilizes a set of concrete surface profile chips with

varying levels of distress to use as a comparison tool for evaluating surface preparation only in a qualitative manner.

The second method follows ASTM E965-15, *Standard Test Method for Measuring Pavement Macrotexture Depth Using a Volumetric Technique*, ASTM International, West Conshohocken, PA, 2015. This method involves spreading a known volume of sand over the concrete surface to form a circle until all sand has settled in the surface cavities, with the roughness then calculated from the diameter of the circle. While this method results in quantifying the roughness of the surface, it does not directly measure surface roughness specifically. Moreover, this method was deemed unusable in the present evaluation due to the configuration of the specimens and the small size of the available surfaces.

There is no industry standard that specifies a direct method for quantitatively measuring the surface roughness of concrete.

Additional challenges to the measured surface characterization included that the post-collapse forensic evaluation was limited due to structural damage and availability of surfaces clearly identified as in the region of interest. Thus, although the surface area tested was atypical for a traditional evaluation of surface roughness, the testing documented in this report provided the best opportunity to quantify the flat areas observed on the structure in the location between Members 11 and 12.

Pieces 1, 2, and 3 on the deck and all the flat area under Member 12 were scanned using a 2G Robotics ULS-100 short-range laser scanner with a class 3R laser. An exemplar photo of a laser scan of the flat area on the bottom of Member 12 is shown in Figure 6. The laser determined the height of the surface at each positional coordinate on a specified grid.

The average scan resolution for the Member 11 pieces was 0.3 mm (0.012 in) by 0.5 mm (0.020 in) in the X and Y directions. The scan resolution for the height data was approximately 0.1 mm (0.004 in). The number of sampling points for Piece 1 was 211,744; for Piece 2 was 122,913; and for Piece 3 was 149,592.

The scan resolution for Member 12 was 0.5 mm (0.020 in) by 1.0 mm (0.039 in) in the X and Y directions, and 0.1 mm (0.004 in) in height, resulting in 109,605 total sampling points.

Because standards for this type of testing have not been established, a MatLab® (The MathWorks, Inc., Natick, Massachusetts) program was coded to quantify the surface roughness of the flat areas using the scan data¹. The program used the following general procedure:

- Import the scan data (i.e., read in the X, Y, and Height values of each point from the three-dimensional point cloud). (Figure 7)
- Tessellate the point cloud (i.e., create a three-dimensional, unstructured, triangular surface mesh, without gaps or coincident features). (Figure 8)
- Remove extreme outliers from the data set (i.e., remove points far above or far below the target cold joint region).
- Section the tessellated surface mesh with parallel planes to extract point profiles needed to calculate surface roughness parameters. Each edge of the triangular surface mesh that intersects a cutting plane is used to calculate the corresponding surface height (via linear interpolation). (Figure 9)
- Remove run-on and run-off points along each point profile. The respective run-on/run-off points are discarded from the beginning/end of each scan to prevent edge effects from biasing the surface roughness calculations. The run-on and run-off lengths were sample-specific.
- Calculate the centerline for each extracted point profile. The centerline is a straight line that divides equal areas above (defined by the centerline to surface peak distance times the incremental distance along the surface) and below (defined by the centerline to surface valley distance times the incremental distance along the surface). (Figure 10)
- Calculate the mean profile depth (MPD) from the centerline in segment lengths of 50 mm (about 2.0 in.) when at least two adjacent 50 mm segment lengths are present.² (Figure 11)
- Average all MPDs across the scanned surface to calculate the arithmetic mean roughness value (S_a) for the target cold joint areas. (Figure 12)

¹ The calculations developed in the code were based on the following sources: ISO 4287:1997, *Geometrical Product Specifications (GPS) – Surface Texture: Profile Method – Terms, Definitions, and Surface Texture Parameters*, International Organization for Standardization, Geneva, Switzerland, April 1997; ASTM E1845-15, *Standard Practice for Calculating Pavement Macrotecture Mean Profile Depth*, ASTM International, West Conshohocken, PA, 2015; and *Machine Design: An Integrated Approach, 2nd Edition*, Prentice-Hall, Inc., Upper Saddle River, NJ, 2000, p. 447.

² The evaluation length measured for surface roughness profiles has been defined as a multiple of the desired surface roughness profile amplitude by both American Concrete Institute methodology and in ISO specifications. Due to the limited amount of measurable surface in this specific case, 50 mm was chosen in order to gather a larger amount of data for evaluation.

The average S_a for the flat areas evaluated on both the Member 11 pieces as well as the Member 12 surface was approximately 1 mm (0.04 in), as measured in the partially damaged post-collapse condition.

The surface roughness on the FIU build plans was not specified for the surface between the deck and the bottom of the truss members on sheets B-37, B-38, and B-41. The surface roughness was specified as “proposed construction joint (CJ) shall be roughened to an amplitude of $\frac{1}{4}$ ” [0.25-in] prior to casting back span” on pylon diaphragm dimensions and reinforcement sheets B-24B and B-25. AASHTO LRFD Bridge Design Specifications defines surface roughness as “normal-weight concrete placed against a clean concrete surface, free of laitance, with surface intentionally roughened to an amplitude of 0.25 inch” (Section 5.8.4.3).

Adrienne V. Lamm
Materials Engineer

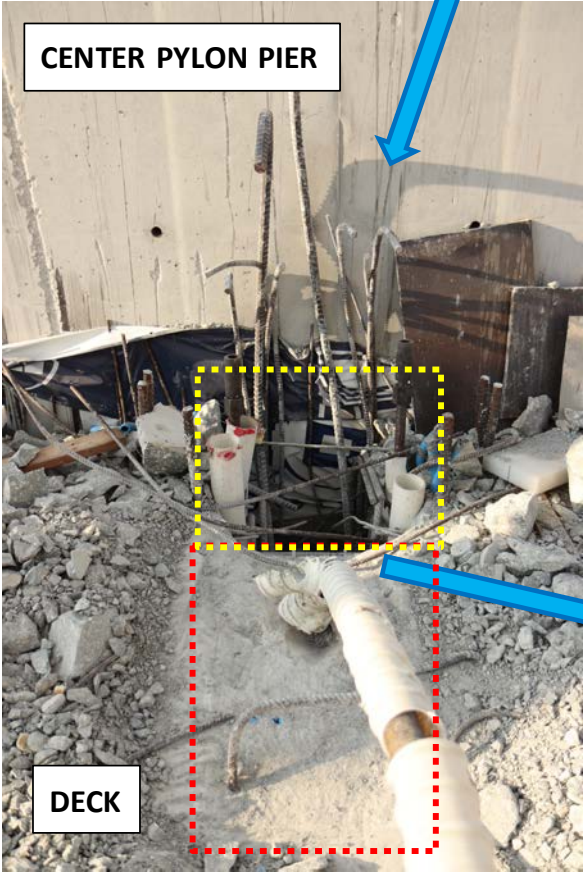


Figure 1: On-scene photos of the deck surface. The red box outlines the flat area on the deck surface under Member 11. The yellow box outlines where Member 12 was located.

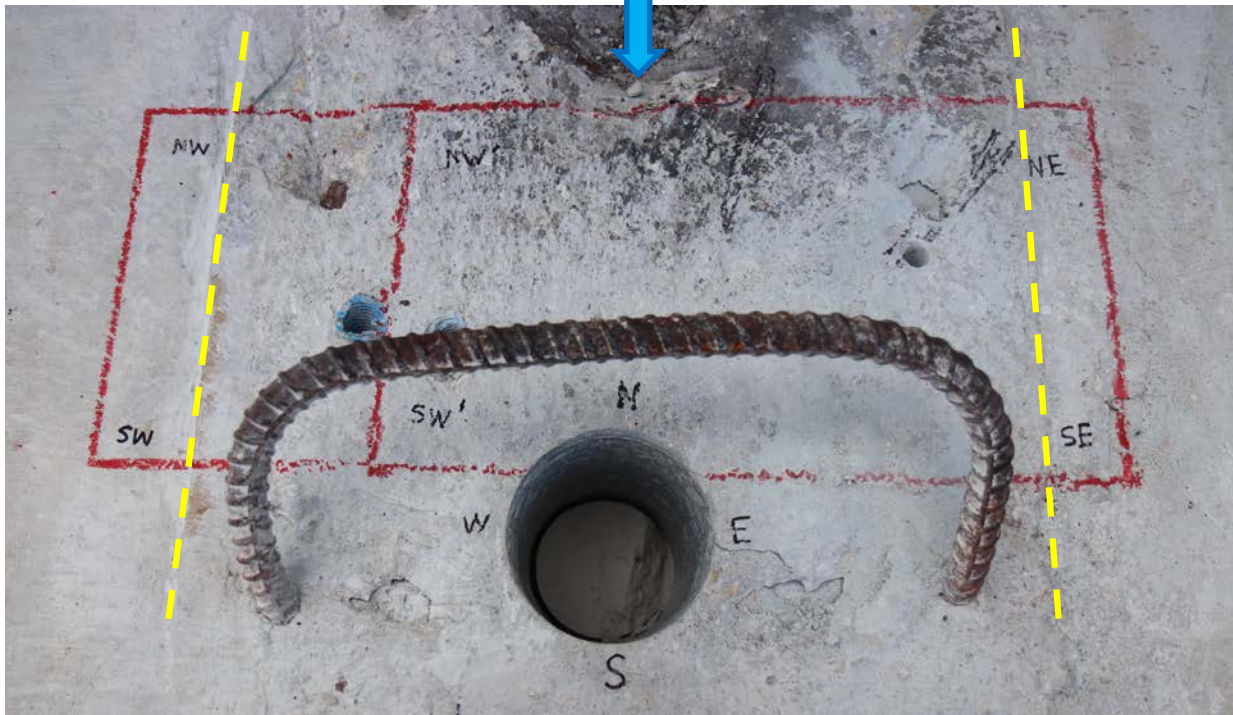


Figure 2: Close-up photos of the deck surface under Member 11. The yellow dotted lines indicate the edges of the cold joint.

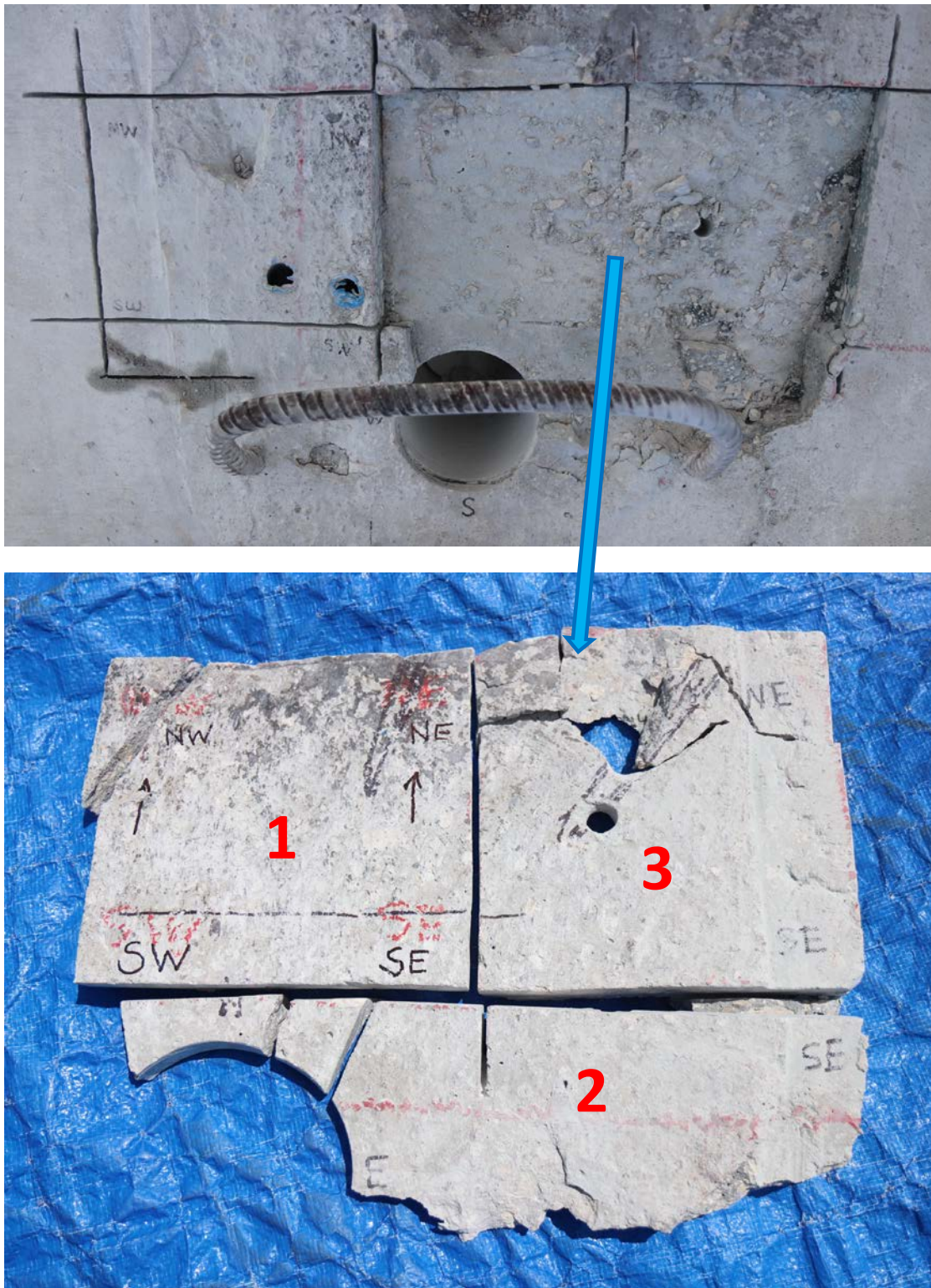


Figure 3: Close-up photos showing the portions of the deck surface under Member 11 that were sectioned for further analysis.

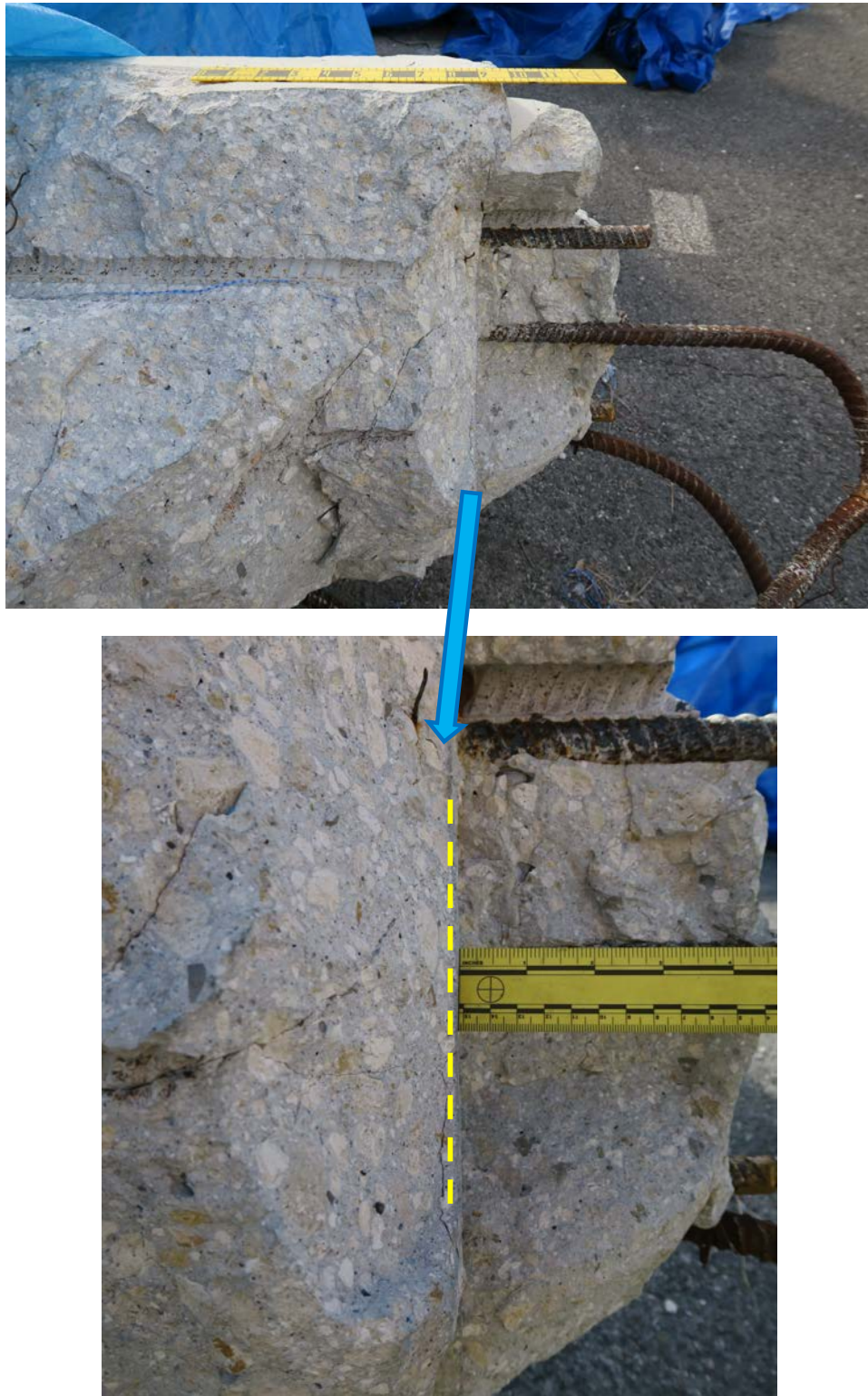


Figure 4: Macro photos of the bottom of Member 12 viewed in profile. The yellow dotted line indicates the straight plane of the flat area observed.

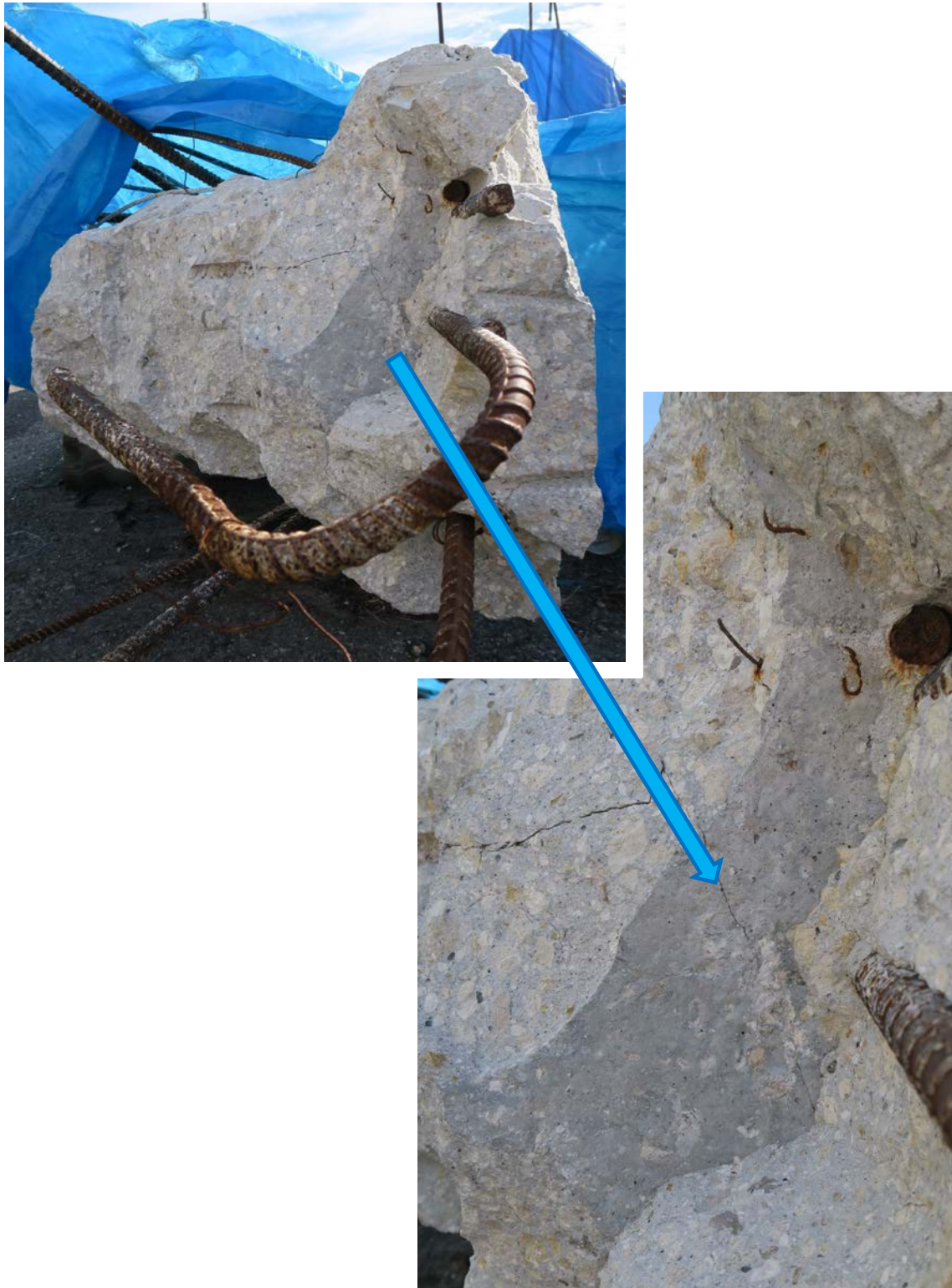


Figure 5: Macro photos of the bottom of Member 12 viewed perpendicular. The flat area observed was irregular in shape.



Figure 6: Macro photos of a laser scan of the flat area on the bottom of Member 12. The green line in the bottom image is the laser projected onto the surface.

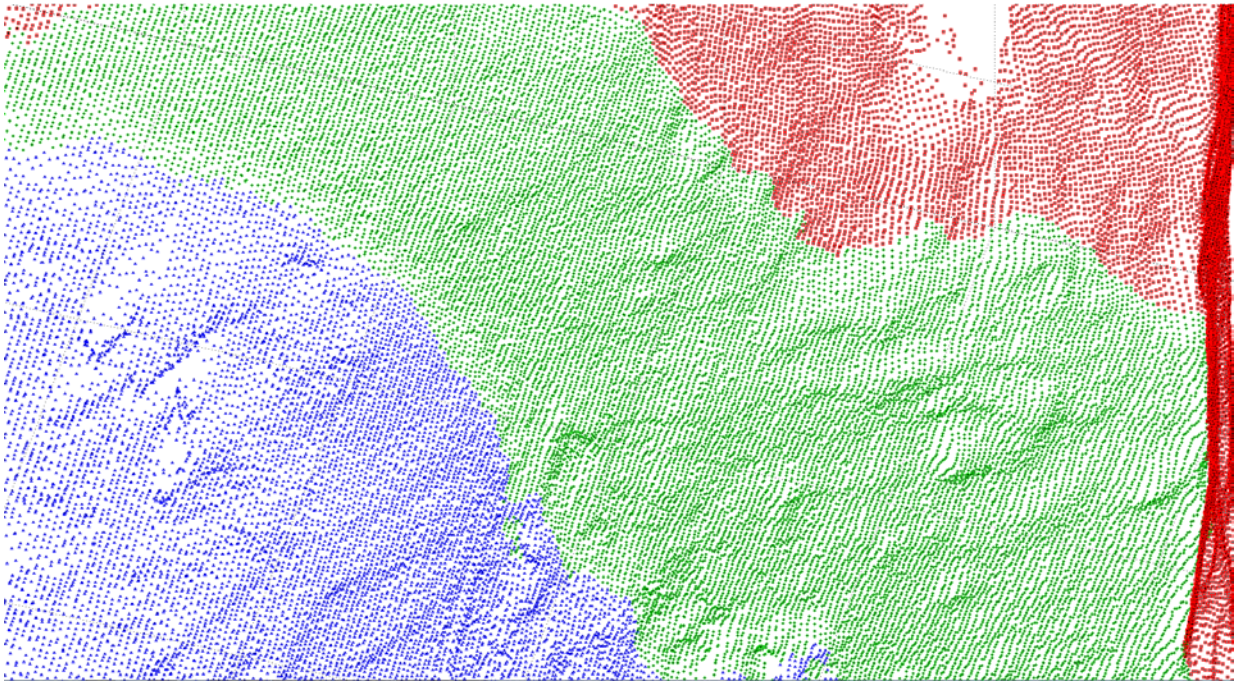


Figure 7: Subset of Member 12 point cloud obtained from digital scan (height not to scale).

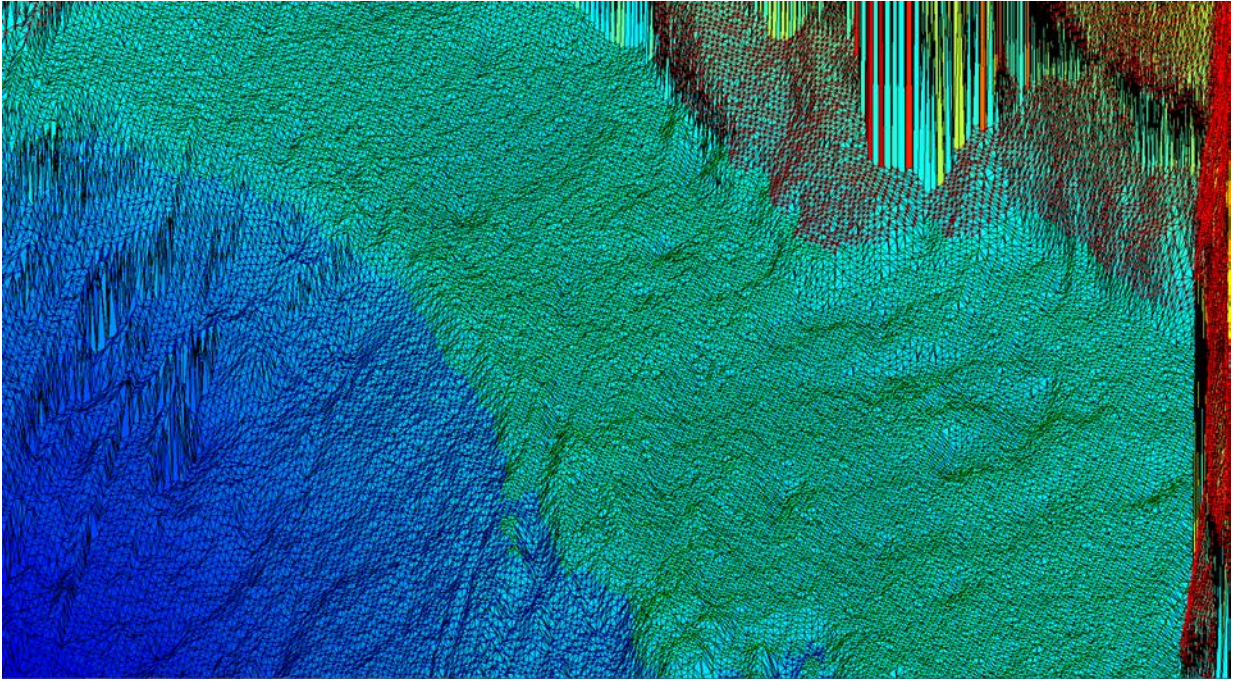


Figure 8: Subset of surface tessellation of Member 12 point cloud (height not to scale).

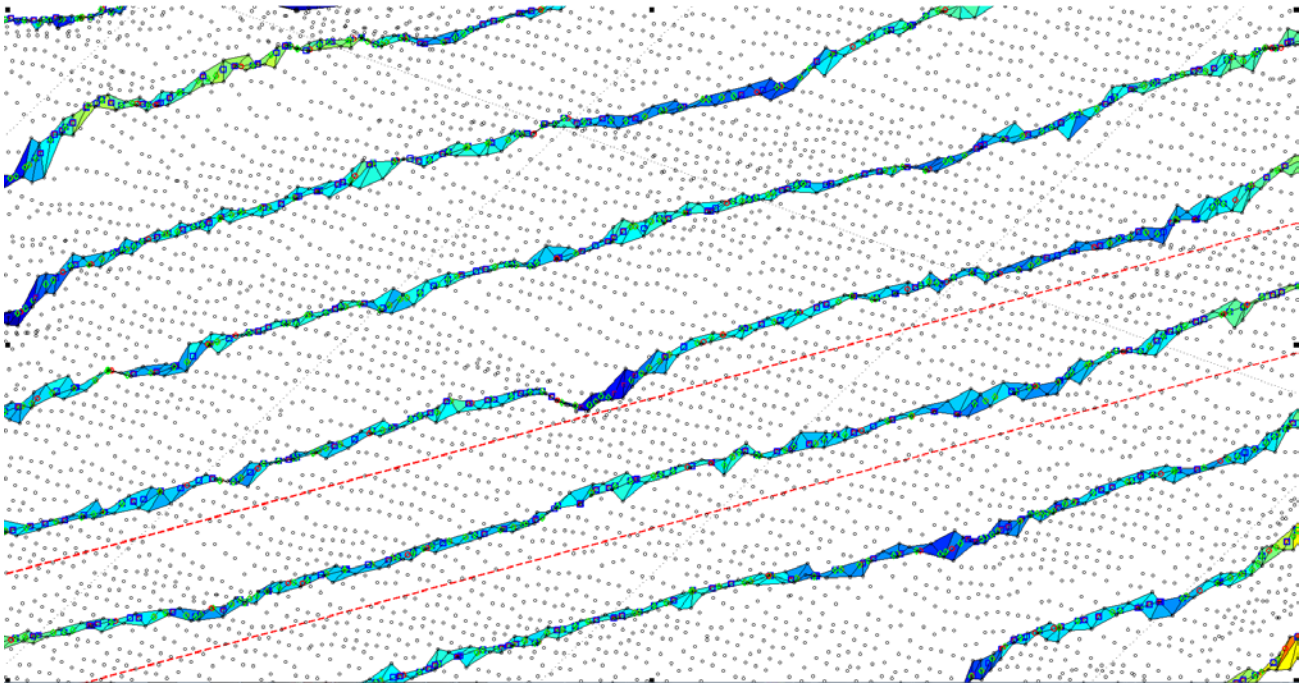


Figure 9: Exemplar intersection triangles and interpolated heights for subset of Member 12 point cloud (results shown for portions of nine parallel cutting planes).

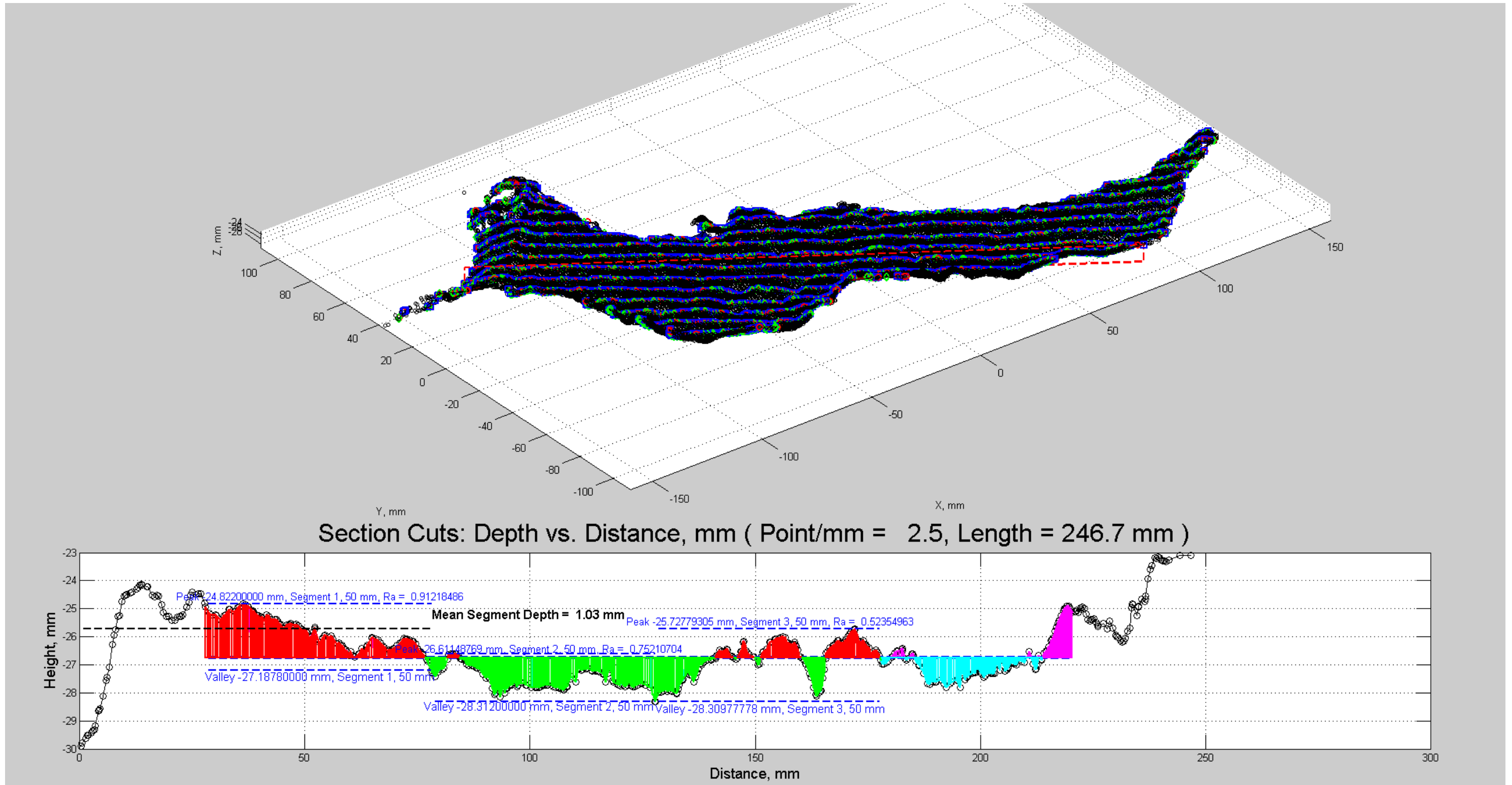


Figure 10: Exemplar section cut and MSD calculation #1 for Member 12.

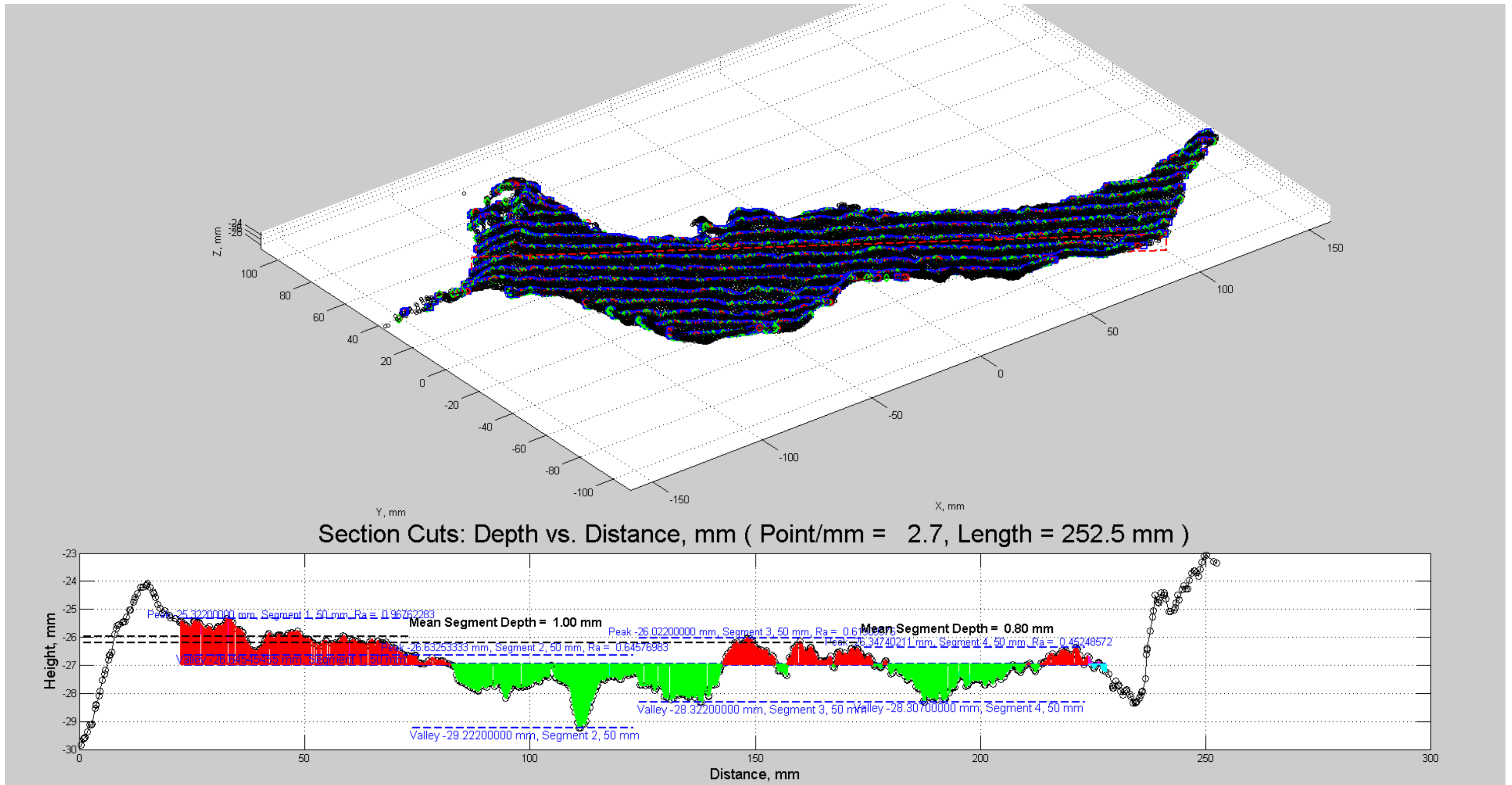


Figure 11: Exemplar section cut and MSD calculation #2 for Member 12.

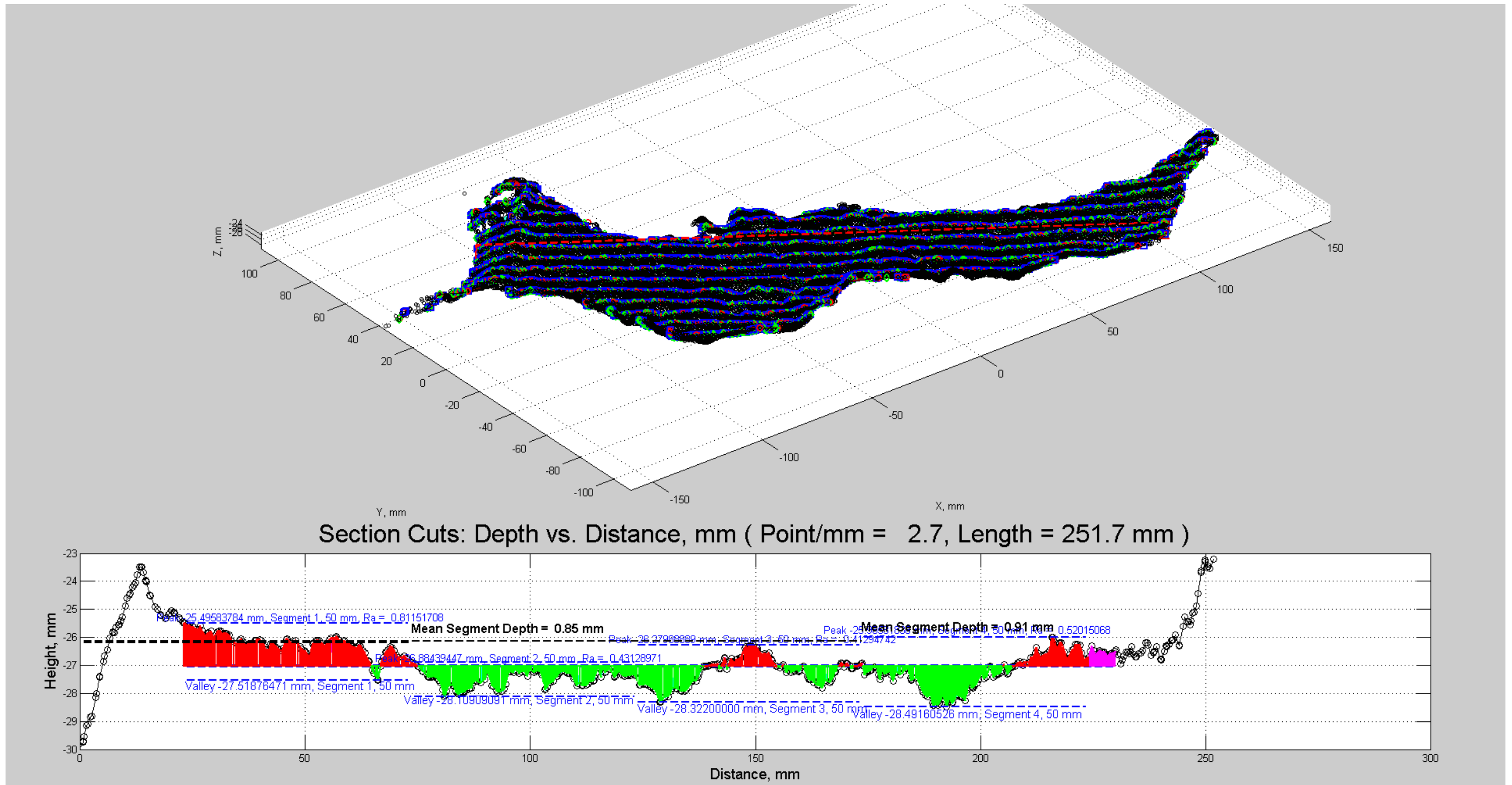


Figure 12: Exemplar section cut and MSD calculation #3 for Member 12.

D. BDI Report (Excerpts)



Florida International University Pedestrian Bridge Monitoring of Lift and Move Procedures

SUBMITTED TO:
BARNHART CRANE & RIGGING, INC.
2163 AIRWAYS BLVD
MEMPHIS, TN 38114

SUBMITTED BY:
BRIDGE DIAGNOSTICS, INC.
740 SOUTH PIERCE AVE, SUITE 15
LOUISVILLE, CO 80027

BDI Project Number: 170804-FL
Report Version: Submittal_04/04/2018
Date Submitted: April 4th, 2018



EXECUTIVE SUMMARY

Bridge Diagnostics, Inc. (BDI) was subcontracted by Barnhart Crane & Rigging (BCR) to perform monitoring during the move and placement of the 175-foot bridge span. The structure being moved was Span 1 of the pedestrian bridge which was under construction at Florida International University (FIU) using Accelerated Bridge Construction procedures. The primary goal of the project was to monitor twist of the truss-girder-span during the move and at the final span placement. Vertical displacements and concrete surface strains were also measured at specified locations for the record.

BDI mobilized to Miami, Florida on Thursday March 8th, 2018 and installed all instrumentation on Friday, March 9th. Following all instrumentation procedures and rigging operations by BCR, a baseline recording was performed while the span was still supported by the temporary piers. All subsequent measurements made during the move were relative to the initial baseline values. Measurements were recorded on a continuous basis during the initial lift and during a relatively short roll test. The roll test was done to verify twist measurement sensitivity during actual operations and BCR's ability to control adjustments of twist. This was an important step in defining the interaction between monitoring and operation during the actual move. Through the roll test, it was successfully demonstrated that measurement sensitivity was well within the desired range and that BCR could react and adjust the span tilt and twist in a timely and precise manner.

According to the monitoring specification provided to BDI through BCR by FIGG Bridge Group (FIGG), the only limiting criteria during the bridge move and final set was the amount of girder twist. Girder twist was monitored by two independent systems; BCR used two electronic levels with LED lights which provided operators immediate visual feedback, and BDI used an array of sensitive tilt sensors and a structural monitoring system to measure and record rotation values. Within the monitoring system, transverse rotation was measured at three span cross-sections; center of the two lift points and at midspan. Three tilt meters were used at the three cross-sections to provide redundancy in the measurements and minimize influence of local flange deformations at each cross-section. Twist was then computed as the difference in rotation angle between the two lift-point cross-sections. This value was calculated and displayed in real-time by the monitoring system. BCR was in charge of all rigging and moving operations while BDI's role was to provide onsite feedback on the twist of the girder during movement and placement. BDI personnel operating the monitoring system were in direct contact with BCR's transport operators and were authorized to stop movement at any time. Any time the girder twist approached the limit, transport movement was stopped and BCR adjusted the alignment.

The bridge move began once all roadway work was complete at 4:20am Saturday, March 10th. Final placement of the span and termination of the monitoring occurred approximately eight hours later at 12:27pm. The movement sequence went according to plan with several stops to adjust trailer load distribution and to troubleshoot monitoring system communication. All operations and movement of the span were stopped any time the monitoring system was inactive. The largest swing in twist occurred as the span was being lowered into position and one of the south bearings made contact. At that moment the twist angle briefly exceeded the specified tolerance by approximately 0.25 degrees, the transport operators were notified, and the system was corrected immediately. The final twist angle at span set was 0.01 degrees and overall rotation angle was 0.07 degrees relative to the initial condition on the temporary piers.

Strain measurements from specified locations were recorded for the duration of the bridge move. These values were not examined in real-time as there were no defined limits or stop criteria. Global deformation

measurements in the form of span deflection and flexural rotation were performed at the time of the lift and for the final span placement. Examination of this data was performed following the monitoring system de-mobilization. All global deformations such as rotation, twist, and deflection indicated the condition of the span after the move was nearly identical to its initial state. Changes in strain during lifting and setting events were essentially equal and opposite indicating all measured responses were linear-elastic.

All instrumentation procedures are defined in this report along with all post-processed measurement results.

SUBMITTAL NOTES

This submittal includes the following files:

1. BDI_Barnhart_FIU_BridgeMove_Report_Submittal_04042018.pdf
This is the BDI report in "pdf" format. It contains details regarding the instrumentation and monitoring procedures, qualitative data review, and appendix of equipment specifications.
2. BARNHART_FL_FIU_PED_BRIDGE_LLT_PoF.pdf
Instrumentation drawings and monitoring plan

TABLE OF CONTENTS

Executive Summary	1
Submittal Notes	3
Table of Contents	4
List of Figures	4
List of Tables	6
Instrumentation and Monitoring Procedures	7
Instrumentation	7
Monitoring Procedures	8
Examination of Monitoring Results	14
Lateral Rotation (Twist and Axial rotation)	14
Strain Measurements	18
Girder Deflection	20
Girder Flexural Rotation	23
General Conclusions	23
Appendix A – Data Plots	25
Appendix B – Data Plots Illustrating Final Bridge Set	57
Appendix C – Monitoring Specification	76
Appendix D – Equipment and Sensor Specifications	78
Appendix E – Instrumentation and Monitoring Plan	87

LIST OF FIGURES

Figure 1 – Overall instrumentation schematic.....	8
Figure 2 – Typical tilt sensor installation – transverse rotation	11
Figure 3 – Strain transducers on truss diagonal member (Section A)	11
Figure 4 – Strain transducer on steel beams	12
Figure 5 – Sash chain used to connect string-pot displacement sensors to bottom of girder	12
Figure 6 – Monitoring display during twist adjustment.....	13
Figure 7 – Measured strain at Section F (east) with corresponding twist and rotation measurements	16
Figure 8 – Measured strain at Section F (west) with corresponding twist and rotation measurements	16
Figure 9 – Measured strain at Section F (east) with corresponding twist and rotation measurements	17
Figure 10 – Measured strain at Section F (west) with corresponding twist and rotation measurements	17
Figure 11 – Strain measurements on Truss Member 2 during lift – Cross-sections A & B	19
Figure 12 – Strain measurements on Truss Member 12 during lift – Cross-sections G & H.....	19
Figure 13 – Girder displacement measurements during lift	21
Figure 14 – Girder displacement measurements during span set	21
Figure 15 – Girder deflection during lift (5-point and 3-point calculation)	22
Figure 16 – Girder deflection during placement (5-point and 3-point calculation)	22

Figure 17 –Girder rotation during span lift	24
Figure 18 –Girder rotation during span placement	24
Figure 19 – Longitudinal rotation at 5 points along girder (global deformed shape during entire move) ...	26
Figure 20 – Transverse rotation at Cross-Section J – Transverse Position A.....	27
Figure 21 – Transverse rotation at Cross-Section J – Transverse Position B.....	28
Figure 22 – Transverse rotation at Cross-Section J – Transverse Position C.....	29
Figure 23 – Transverse rotation at Cross-Section J - Positions A, B & C	30
Figure 24 – Transverse rotation at Cross-Section 3 – Transverse Position A.....	31
Figure 25 – Transverse rotation at Cross-Section 3 – Transverse Position B.....	32
Figure 26 – Transverse rotation at Cross-Section 3 – Transverse Position C	33
Figure 27 – Transverse rotation at Cross-Section 3 – Transverse Positions A, B & C	34
Figure 28 – Transverse rotation at Cross-Section 4 – Transverse Position A.....	35
Figure 29 – Transverse rotation at Cross-Section 4 – Transverse Position B.....	36
Figure 30 – Transverse rotation at Cross-Section 4 – Transverse Position C	37
Figure 31 – Transverse rotation at Cross-Section 3 – Transverse Positions A, B & C	38
Figure 32 – Girder Twist – Difference in angle between Sections J & L	39
Figure 33 – Overall Girder Rotation – Average of all transverse tilt sensors.....	40
Figure 34 – Strain Histories – Section A-E	41
Figure 35 – Strain Histories – Section A-W	42
Figure 36 – Strain Histories – Section B-E	43
Figure 37 – Strain Histories – Section B-W	44
Figure 38 – Strain Histories – Section C-E.....	45
Figure 39 – Strain Histories – Section C-W.....	46
Figure 40 – Strain Histories – Section D-E	47
Figure 41 – Strain Histories – Section D-W	48
Figure 42 – Strain Histories – Section E-E	49
Figure 43 – Strain Histories – Section E-W	50
Figure 44 – Strain Histories – Section F-E.....	51
Figure 45 – Strain Histories – Section F-W.....	52
Figure 46 – Strain Histories – Section G-E	53
Figure 47 – Strain Histories – Section G-W.....	54
Figure 48 – Strain Histories – Section H-E	55
Figure 49 – Strain Histories – Section H-W	56
Figure 50 – Girder twist between Points 2 & 4 (Section J & L) during bridge span set	57
Figure 51 – Overall girder axial rotation during bridge span set	58
Figure 52 – Longitudinal (Flexural) rotation during bridge span set	59
Figure 53 - Transverse rotation during bridge span set – Section 2-A	60
Figure 54 - Transverse rotation during bridge span set – Section 2-B	61
Figure 55 - Transverse rotation during bridge span set – Section 2-C.....	62
Figure 56 - Transverse rotation during bridge span set – Section 3-A	63
Figure 57 - Transverse rotation during bridge span set – Section 3-B.....	64
Figure 58 - Transverse rotation during bridge span set – Section 3-C.....	65
Figure 59 - Transverse rotation during bridge span set – Section 4-A.....	66
Figure 60 - Transverse rotation during bridge span set – Section 4-B.....	67
Figure 61 - Transverse rotation during bridge span set – Section 4-C.....	68
Figure 62 - Transverse rotation during bridge span set – Section 2 (J)	69
Figure 63 - Transverse rotation during bridge span set – Section 3 (K).....	70
Figure 64 - Transverse rotation during bridge span set – Section 4 (L)	71

Figure 65 - Strain history during bridge span set – Sections C & D 72
Figure 66 - Strain history during bridge span set – Sections A & B..... 73
Figure 67 - Strain history during bridge span set – Sections E & F 74
Figure 68 - Strain history during bridge span set – Sections G & H 75

LIST OF TABLES

Table 1 – Structure description & monitoring notes 9
Table 2 – Absolute maximum and final sensor values 15

INSTRUMENTATION AND MONITORING PROCEDURES

Monitoring during the bridge move was performed to ensure the truss girder remained in an acceptable geometric state from the time it was lifted from the temporary piers until it was set on the permanent girder bearings. Monitoring specifications were defined by FIGG and had the following requirements:

- Measure and record girder deformations when the span was lifted and when it was set in place
- Measure and monitor girder rotation and twist during entire span move sequence
- Measure and record strains on selected truss members during span move

The only limiting criteria of monitoring was to maintain a girder twist angle not to exceed ± 0.50 degrees between the two lift locations during the move. Based on earlier versions of the monitoring specification, final twist angle after the girder was set on the permanent bearings was not to exceed 0.22 degrees relative to the girder's initial state. FIGG's monitoring specification used to develop the instrumentation and monitoring plan is provided in Appendix C – Monitoring Specification.

INSTRUMENTATION

The span was instrumented with 16 strain transducers, 14 tilt sensors, and 5 displacement sensors. Details regarding sensor range and precision are provided in Appendix D – Equipment and Sensor Specifications. An overall schematic of the instrumentation layout, including lift points, is shown in Figure 1. Additional details of the sensor installation are provided in Appendix E – Instrumentation and Monitoring Plan. All sensors were connected to a structural monitoring system which was used to measure, record, and display results. Arrangement of the sensors was defined to achieve the goals of the FIGG monitoring specification. All strain gage locations on the truss members were defined by FIGG. Following is an outline of the various sensor and monitoring values:

- Transverse rotations were measured at three girder cross-sections; two centered at the lift points and one at midspan. Each cross-section contained three tilt sensors attached to the bottom flange and oriented to measure rotation about the girder longitudinal axis. Three sensors were used to provide redundant measurements and to verify consistent rotation within the cross-section. Two rotation sensor installations are shown in Figure 2 and a total of 9 transverse tilt sensors were utilized.
- Longitudinal rotation sensors were located at five locations along the length of the span; south end, centered between south lift points, midspan, centered between north lift points, and north end. These sensors measured the longitudinal rotation at each cross-section and provided a backup method for determining girder deflection. As with the string-pot measurements, they were influenced by rigid-body-motion and girder flexure, so results were processed after the move operation.
- Strain transducers were utilized to measure surface strain on the concrete at 8 truss member cross-sections; designated as Sections A through H. Transducers were placed at right and left sides of each cross-section making 16 strain measurement locations. Figure 3 illustrates typical strain transducer installation on the truss members. Because the strain transducers are influenced by temperature variations, the primary purpose was to measure change in strain during the short-term events of span lifting and setting.
- Eight additional strain sensors (Figure 4) were attached to the steel beams tying the pairs of Goldhofer trailers together. These strains were not part of the monitoring specification and were provided strictly for BCR's load information.
- Slide wire potentiometers (string-pots) were attached at five locations to the bottom of the girder to measure displacement relative to the ground as the girder was lifted off the bearings and

lowered back to the bearings. As shown in Figure 5, sash chain was attached to the bottom of the girder and provided the reference for the string-pot mounted to a steel plate on the ground. These measurements were influenced by rigid-body-motion and girder deflections. The recorded values were post-processed to calculate girder deflection values.

- A girder twist virtual sensor was programmed into the monitoring system software to provide real-time values along with the individual sensor data. The rotation of each cross-section was defined as the average of the three transverse tilt sensors at the location. Twist was defined by the difference in girder rotation between the girder cross-sections 2 and 4, which corresponded with the center of the south and north lift points.
- An overall girder rotation virtual sensor was also programmed to view the tilt of the girder and was computed as the average of all 9 transverse rotation sensors.

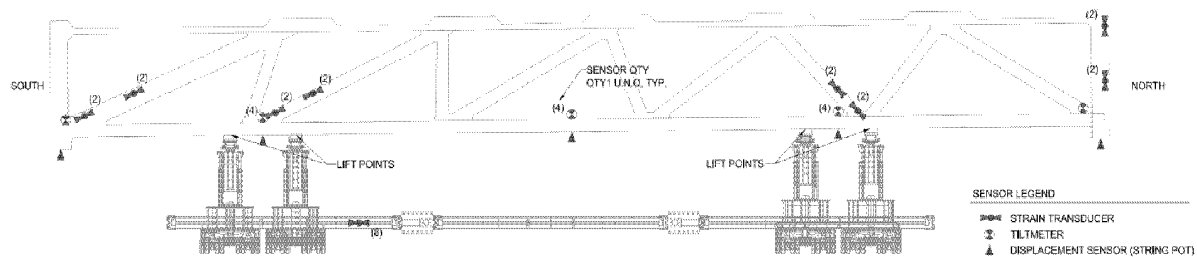


Figure 1 – Overall instrumentation schematic

MONITORING PROCEDURES

Monitoring consisted of measuring values from each sensor, recording the values digitally, and displaying real-time responses on a computer. With the exception of the displacement sensors, all measurements were recorded continuously at a rate of 10 samples per second during all lift and move operations. Displacement measurements were made relative to the ground or the piers and were only in place during the initial lift from the temporary piers and setting on the permanent piers. All measurements were made through the STS4 structural monitoring system and the recorded values were in engineering units: strain ($\mu\epsilon$); displacement (in); and rotation (degrees). Certified calibration factors were applied automatically for each sensor. All sensor calibration sheets were submitted to BCR prior to mobilization.

Just prior to the initial lift from the temporary piers, data was recorded for a brief period to establish baseline readings. All readings were “zeroed” in this state so that all subsequent readings would be relative to this initial condition. Therefore, all presented values of strain or rotation indicated change in value and should not be considered actual total stress or rotation relative to vertical.

Following the instrumentation procedures and initial baseline readings, monitoring began, and the initial girder lift was performed. Once the girder was lifted and rigging chains were connected, a series of short roll maneuvers were done to verify sensitivity of the monitoring and the precision of the operator control. In addition, BCR wanted to verify they could adjust girder twist and rotation based on reported values and stay within the tight tolerances. The roll move was highly successful in proving the monitoring system could accurately display the girder position and that BCR could perform adjustments as required. Figure 6 shows the monitoring system display during one twist adjustment period. These roll tests were performed because there was initial concern that machinery vibrations would influence the tilt sensors and that it would be difficult to accurately readout rotation and twist. While dynamic vibration was amplified within the tilt sensors, the “dynamic noise” was identified and visually eliminated from the actual tilt or twist value

during the monitoring period. This initial test allowed onsite engineers to focus on the mean value between the vibrations rather than the individual peaks or valleys associated with the sensor dynamics. Roll tests were completed while roadway preparation work was being performed.

A few hours later, the roadway prep work was complete, and the actual bridge move began. A procedure had been established that the BCR operators would move the transports using their own readings until they were informed that the monitoring readings were reaching the threshold. A BCR representative was with the BDI monitoring system operator and viewing the screen with tilt and rotation readouts displayed. Any time the twist data plot approached ± 0.5 degrees, an "All Stop" command was given, transport movement was halted, and adjustments to the trailers were performed.

At approximately 6:00am, the monitoring system began to have connectivity issues due to electronic interference. Any time connectivity to tilt-sensor data acquisition nodes was lost, the twist and tilt measurements could not be updated in real-time. The "All Stop" command was given any time the data display was disrupted. At no time was the trailer moved when the monitoring system was not functional. The majority of interruptions in data acquisition occurred between 6:00am and 9:00am.

Once the bridge was in position and lowered to approximately 1 inch off the bearing pads, the string-pot displacement sensors were reattached to the sash chains that were still attached to the bottom of the bridge. Recording and monitoring were re-established and the bridge was lowered down on the bearings. At that time, on-site readings indicated a twist angle of 0.17 degrees and an overall girder rotation angle of 0.29 degrees. This condition was within tolerance and monitoring was terminated several minutes after all load was transferred to the piers.

Individual data files were recorded for specific events such as girder lift, roll tests, girder moving, and girder setting. To keep data file size manageable, data files were broken into hourly recordings during the long move event. Table 1 contains general monitoring details along with file names associated with times and events.

Table 1 – Structure description & monitoring notes

ITEM	DESCRIPTION
STRUCTURE NAME	FIU Pedestrian Bridge – Bridge Move
BDI REFERENCE NUMBER	170804-FL
FIELD DATES	March 9-10, 2018
LOCATION/ROUTE	Miami, FL, 8 th Avenue @ FIU
STRUCTURE TYPE	Post-tensioned concrete truss girder
TOTAL LENGTH	175 ft
NUMBER/TYPE OF SENSORS	43 Sensors 9 transverse tilt sensors 5 longitudinal tilt sensors 5 vertical displacement string-pots 16 strain transducers on concrete truss 8 strain transducers on steel trailer support beams
SAMPLE RATE	10 Hz
TOTAL MONITORING TIME	3 hours monitoring during initial lift and roll tests 6 hours monitoring during bridge move

ITEM	DESCRIPTION	
	16 hours total time span	
DATA FILE INFORMATION	<i>File Name (note: times displayed in filename are in MST)</i>	<i>Description</i>
	BDI STS Project_R20_03_09_2018_18_08_33_Normal Data_RawDat.tdms	Baseline data
	BDI STS Project_R21_03_09_2018_18_21_47_Normal Data_RawDat.tdms	Initial lift
	BDI STS Project_R21_03_09_2018_19_21_54_Normal Data_RawDat.tdms	Rigging
	BDI STS Project_R22_03_09_2018_20_22_36_Normal Data_RawDat.tdms	Roll test
	BDI STS Project_R23_03_09_2018_22_18_13_Normal Data_RawDat.tdms	Roll test
	BDI STS Project_R24_03_10_2018_02_21_39_Normal Data_RawDat.tdms	Start of girder move
	BDI STS Project_R24_03_10_2018_03_21_45_Normal Data_RawDat.tdms	Girder move
	BDI STS Project_R25_03_10_2018_03_46_14_Normal Data_RawDat.tdms	Girder move
	BDI STS Project_R26_03_10_2018_04_09_19_Normal Data_RawDat.tdms	Girder move
	BDI STS Project_R27_03_10_2018_04_35_38_Normal Data_RawDat.tdms	Girder move
	BDI STS Project_R28_03_10_2018_05_00_13_Normal Data_RawDat.tdms	Girder move
	BDI STS Project_R28_03_10_2018_06_00_22_Normal Data_RawDat.tdms	Girder jacking / rigging adjustment
	BDI STS Project_R29_03_10_2018_06_10_12_Normal Data_RawDat.tdms	Girder move
	BDI STS Project_R30_03_10_2018_06_53_46_Normal Data_RawDat.tdms	Girder move
	BDI STS Project_R31_03_10_2018_07_59_06_Normal Data_RawDat.tdms	Girder move
	BDI STS Project_R31_03_10_2018_08_59_15_Normal Data_RawDat.tdms	Girder move
	BDI STS Project_R32_03_10_2018_10_05_56_Normal Data_RawDat.tdms	Girder alignment
BDI STS Project_R33_03_10_2018_10_12_59_Normal Data_RawDat.tdms	Girder alignment	
BDI STS Project_R34_03_10_2018_10_14_39_Normal Data_RawDat.tdms	Final girder placement	
ADDITIONAL COMMENTS	Strain transducers on steel beams were disconnected from nodes prior to R28 to minimize node dropping issue. Data of interest already obtained.	

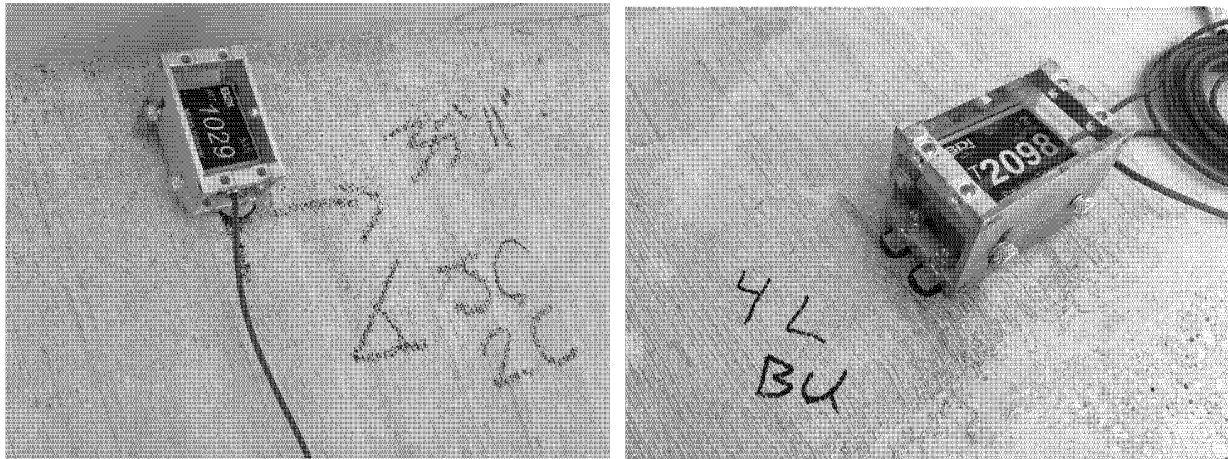


Figure 2 – Typical tilt sensor installation – transverse rotation

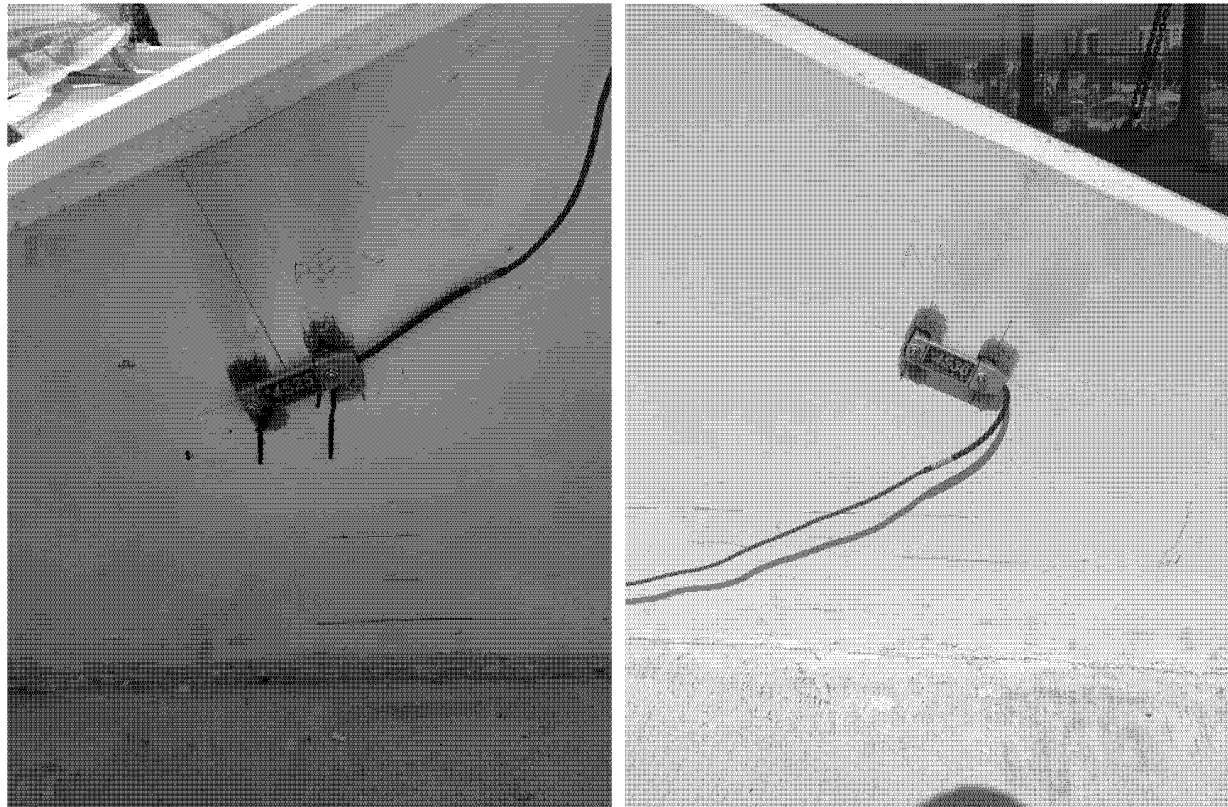


Figure 3 – Strain transducers on truss diagonal member (Section A)

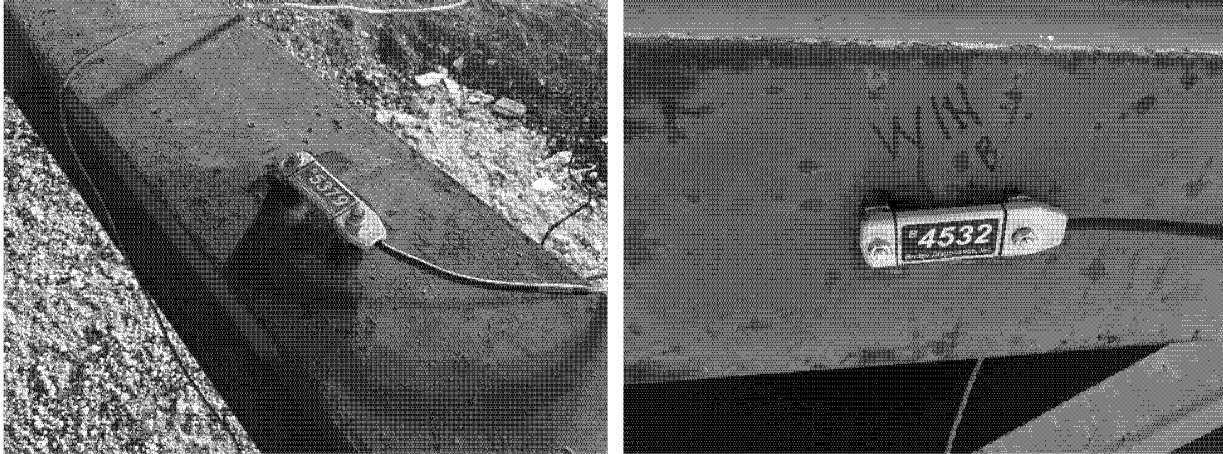


Figure 4 – Strain transducer on steel beams



Figure 5 – Sash chain used to connect string-pot displacement sensors to bottom of girder

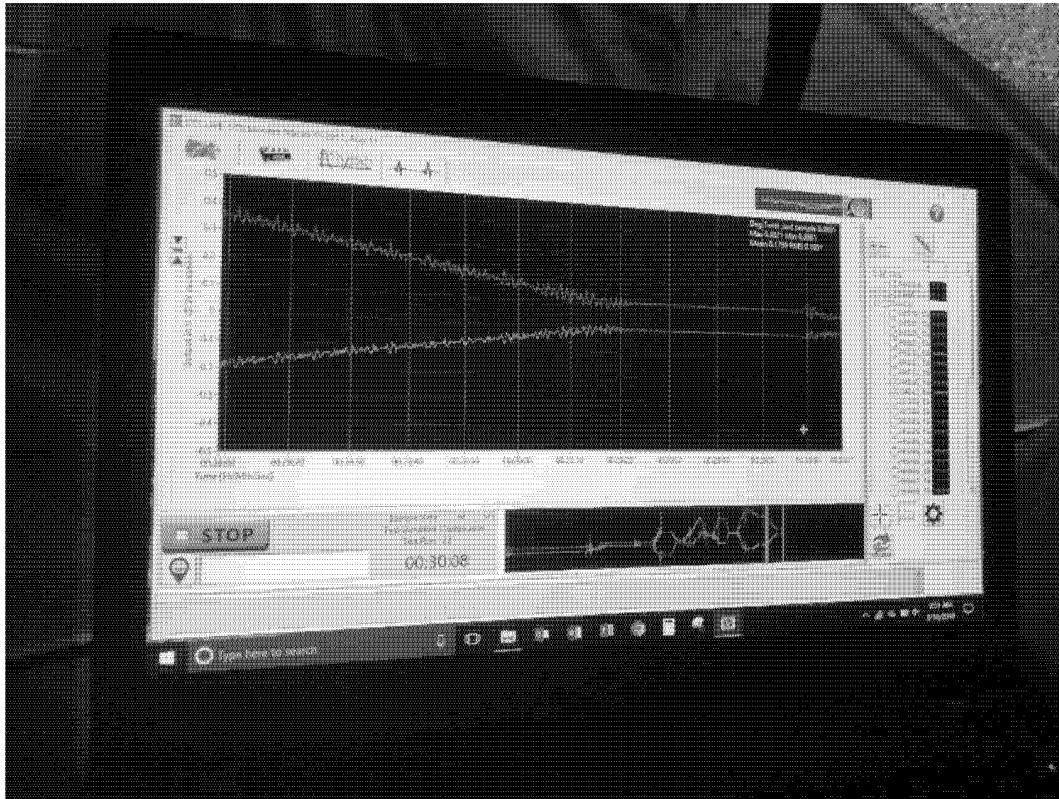


Figure 6 – Monitoring display during twist adjustment

EXAMINATION OF MONITORING RESULTS

LATERAL ROTATION (TWIST AND AXIAL ROTATION)

As previously indicated, real-time monitoring was focused on the girder twist and acceptance of the girder move was based on this value. This data was further examined along with all other data for reporting purposes. In general, all measurements were plotted and tabulated for peak and final values as listed in Table 2. Clarification was required on the tilt sensor output because they were influenced by vibration, so short term peak tilt sensor values do not correspond to actual girder tilt. It was noted during the roll test and moving operations that the largest magnitude tilt values occurred during stop events because the rapid deceleration even though the transport was moving very slow. Therefore, peak tilt values should not be considered relevant and focus should be on static conditions or trend values over a period of time. During the data post processing, it was noted that sensor offset values were not re-applied correctly before the bridge move began. The tilt sensors were physically adjusted to near zero reading during the installation, so the offsets were very small. Therefore, this shift was not noticeable during monitoring. The correct offset was applied to all sensors during the post processing and final twist and rotation values were re-calculated. As a result, the onsite values of 0.17 degrees and 0.29 degrees for twist and rotation were found to be 0.01 degrees and 0.07 degrees. All data presented in this report is the post processed data.

During the move, the ± 0.5 -degree tolerance was exceeded briefly in two instances. This was a function of the rate at which twist was occurring, the time to make an “all stop” decision, and the time to execute the command. Figure 7 and Figure 8 illustrate data plots for one of those instances, where girder twist, girder rotation, and strain on a truss member are plotted together. In this case the twist (red line) appears to have a peak value exceeding 0.80 degrees, but the spike in the data was observed to be an artifact of the tilt sensor dynamics. Examination of the strain data (blue line) at the same time period shows that the strain was in fact directly influenced by twist; strain on the east side of the member changed in the same direction as the twist, while the west side strain changed in the opposite direction. It was clear from the strain measurements that there was no dynamic component to the structural response. The peak static twist value was approximately 0.65 degrees for this instance.

The second and largest girder twist exceedance occurred during the final alignment process just prior to the bridge being placed on the piers. A peak twist angle of 0.75 degrees occurred briefly as the girder came in contact with one of the bearing pads on the south pier. During the girder alignment process, the procedure was to align the south end of the girder with the bearings and then set the north end. As the girder was being aligned the girder came into contact with the southwest bearing. This induced twist since only one bearing came in contact; the girder was not yet oriented perfectly with the pier. As the girder was lowered the induction of a new support condition at the southwest bearing caused the twist value to change quickly. An “All Stop” call was made, BCR immediately stopped movement and immediately adjusted the rotation to bring the twist back within specification. Figure 9 and Figure 10 provide zoomed in view of girder twist, rotation, and the largest measured strain variation associated with the twist event. As shown in the plot, the twist occurred relatively rapidly, over a few seconds. The correction was completed very carefully and occurred over approximately 10 minutes. Again, it was noted that measured strains were directly influenced by girder twist, but strain measurements had relatively little dynamic component compared to the tilt sensors. Note that the north end of the girder was floating and had not yet made any contact at this time. At the end of this adjustment the girder was no longer in contact with the bearing pads.

The girder axial rotation was adjusted to match the pier bearing profile and the remaining alignment procedures were completed without any girder contact with the bearings. Once the alignment was set,

displacement sensors were re-connected to the girder and the bridge was lowered down and placed on the piers. The measured girder rotation and twist angles were nearly zero, meaning the girder was in the same orientation as it was when it was lifted from the temporary piers.

Table 2 – Absolute maximum and final sensor values

Sensor_Desc	SensorID	Units	MaxValue	EndValue
RL-1-B*	MT2022	deg.	-1.144	0.107
RL-2-B*	T2100	deg.	-1.015	0.099
RL-3-B*	T2038	deg.	-0.921	0.090
RL-4-B*	T2098	deg.	-0.702	0.107
RL-5-B*	MT2027	deg.	-0.765	0.100
RT-2-A*	MT1027	deg.	0.758	0.035
RT-2-B*	MT1028	deg.	0.751	0.070
RT-2-C*	MT1029	deg.	-0.818	0.085
RT-3-A*	MT1032	deg.	0.704	0.061
RT-3-B*	MT1030	deg.	-0.701	0.040
RT-3-C*	MT1031	deg.	0.728	0.105
RT-4-A*	MT1033	deg.	0.875	0.074
RT-4-B*	MT1034	deg.	-0.966	0.060
RT-4-C*	MT1035	deg.	-1.140	0.095
Strn-A-E	B4525	με	588	-221
Strn-A-W	B4536	με	455	-142
Strn-B-E	B4542	με	836	-136
Strn-B-W	B5413	με	545	-140
Strn-C-E	B4533	με	312	-128
Strn-C-W	B5380	με	240	-113
Strn-D-E	B5414	με	368	-135
Strn-D-W	B4530	με	244	-97
Strn-E-E	B5385	με	221	-81
Strn-E-W	B4521	με	251	-155
Strn-F-E	B5383	με	277	-94
Strn-F-W	B6179	με	315	-149
Strn-G-E	B6189	με	-134	-95
Strn-G-W	B5407	με	-113	-104
Strn-H-E	B5399	με	-1021	-69
Strn-H-W	B4519	με	-459	-174
Rotation*	Rotation	deg.	0.728	0.069
Twist**	Twist	deg.	-0.75	0.013

* Peak values include sensor dynamics and are not representative of peak girder rotation

** Peak value based on visual interpretation of data plot eliminating dynamic component

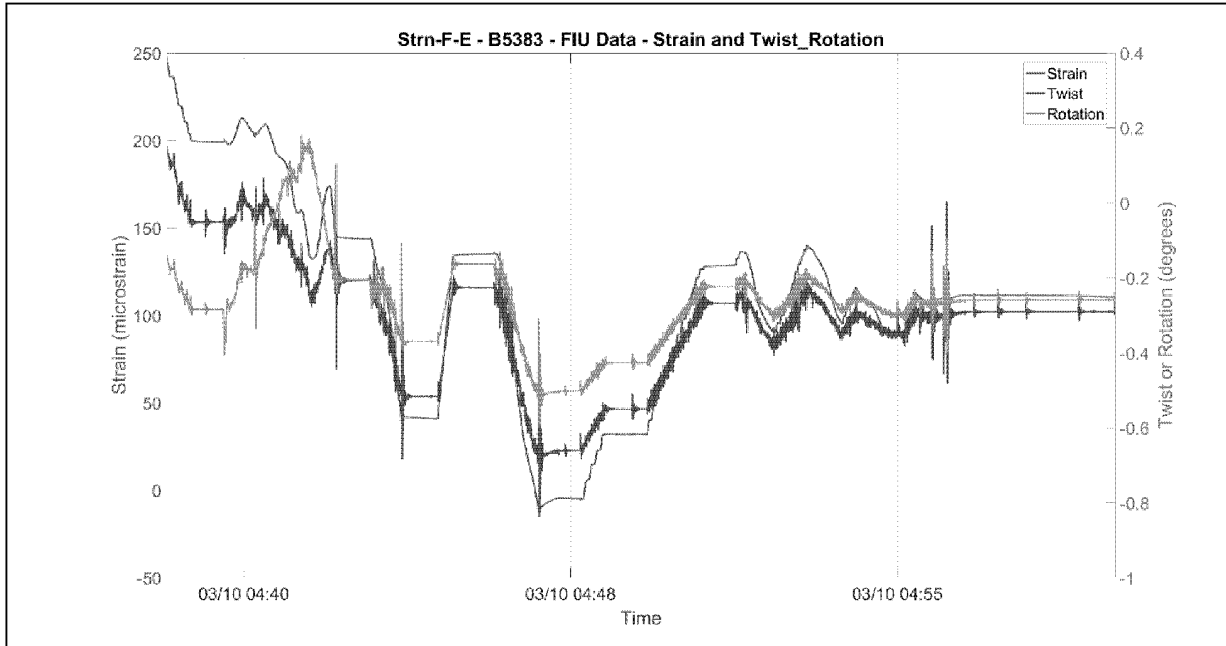


Figure 7 – Measured strain at Section F (east) with corresponding twist and rotation measurements

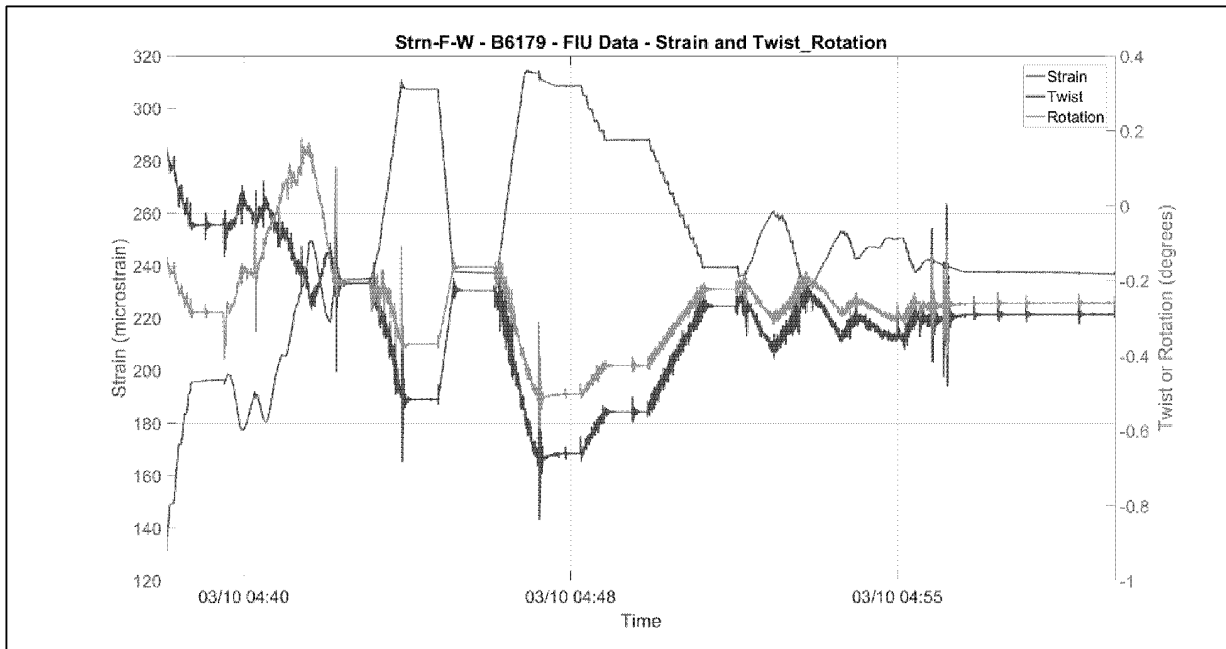


Figure 8 – Measured strain at Section F (west) with corresponding twist and rotation measurements

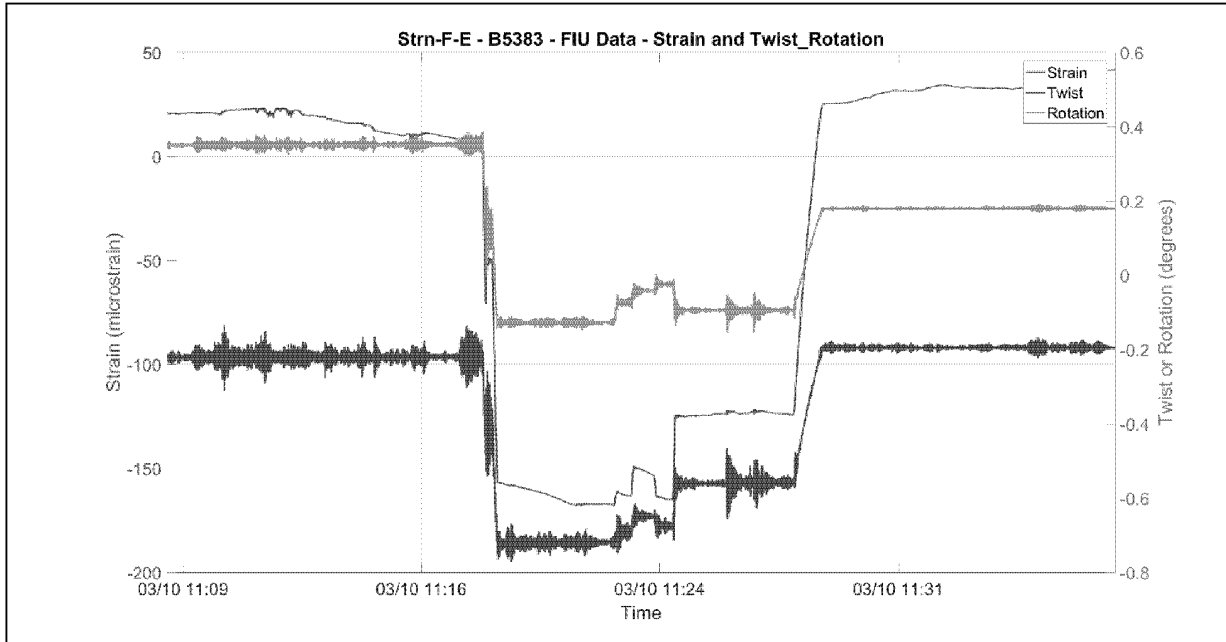


Figure 9 – Measured strain at Section F (east) with corresponding twist and rotation measurements

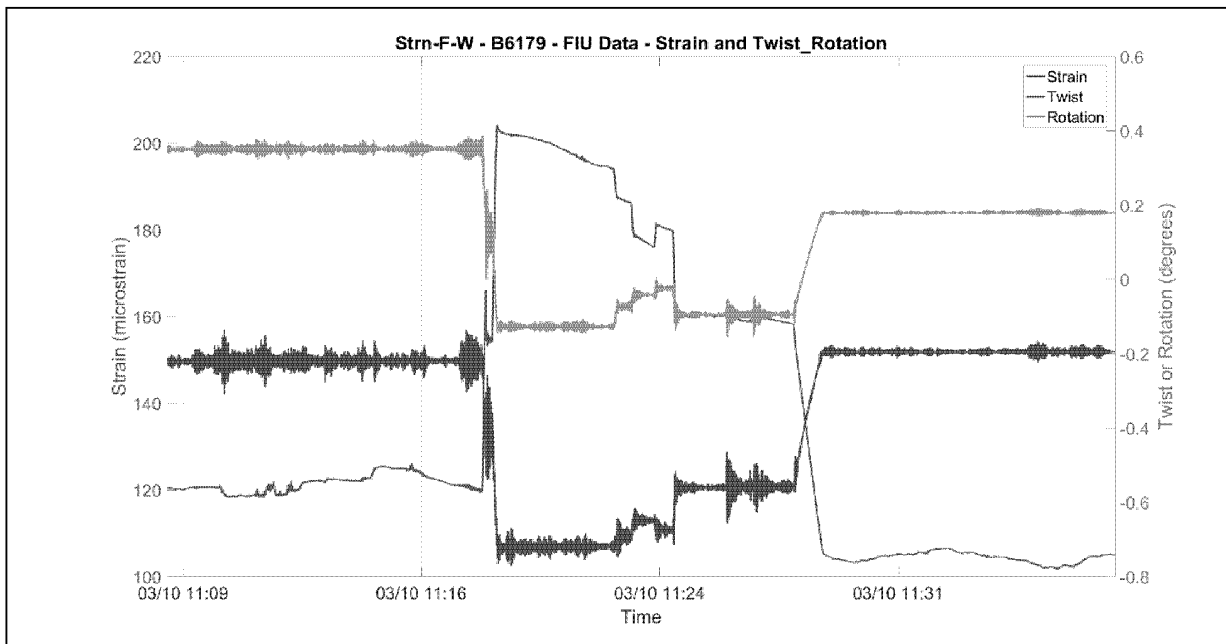


Figure 10 – Measured strain at Section F (west) with corresponding twist and rotation measurements

STRAIN MEASUREMENTS

In addition to tilt values, strains were measured on several locations on the concrete truss. As indicated previously, these sensors were zeroed prior to the lift and indicate the change in strain relative to the initial position and should not be considered to correspond with the overall in-situ stress. The existing stress prior to gage installation was not determined as this was not included in BDI's scope. In general, the largest strain changes occurred during the lift and during the girder placement due to the change in support conditions. These values were not monitored in real-time as there were no specified limits to compare with, it was not required by the monitoring specification, and the data was requested only for design verification. Gradual change in strain values during the move should not be considered structural responses since the strain transducers were influenced by temperature and rate of temperature change. The most relevant use of this data would be to examine short term events such as the lift, placement, and other short period events during the move. To examine these short-term events, the strain data is typically zeroed prior to the event and the change in strain from start to finish of the event is analyzed. Figure 11 and Figure 12 illustrate strain values on truss members 2 and 12 during the span lift. Final strain values were relatively close to zero after the bridge was set on the piers. Offsets in the range of 100 to 200 micro-strain ($\mu\epsilon$) can be expected due to thermal considerations of the sensors and the truss itself. To re-emphasize, the most appropriate use of this data to validate the condition of the truss at the beginning and end of the bridge move would be to examine change in strain during lifting and the change in strain during placement.

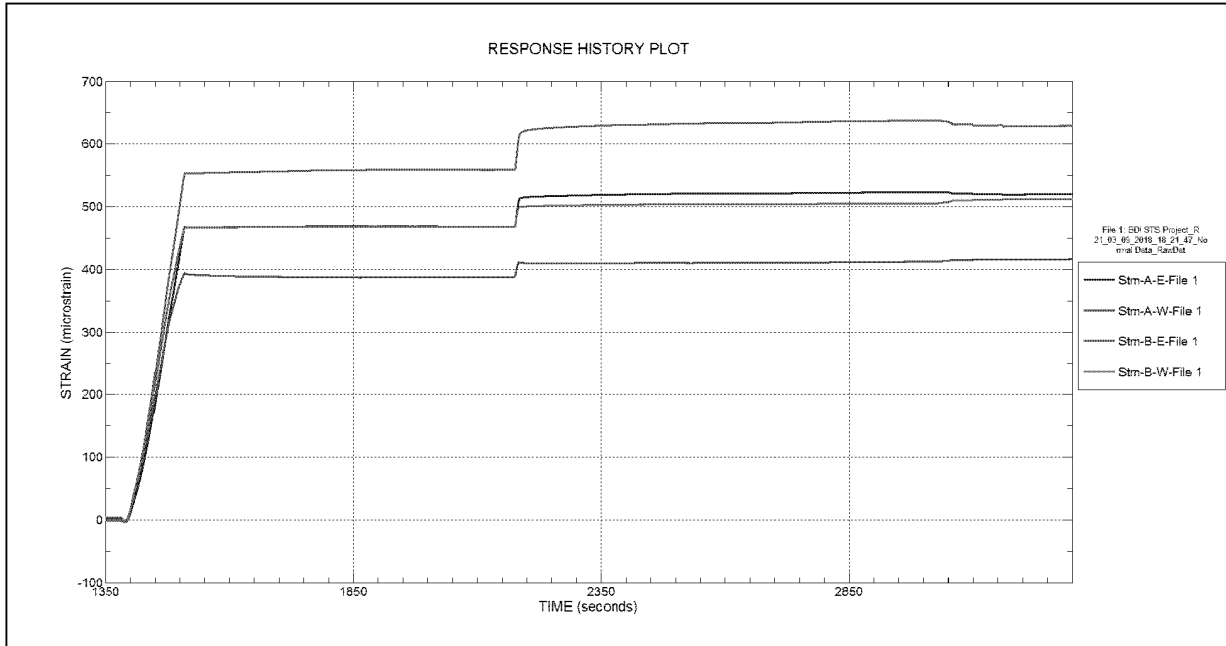


Figure 11 – Strain measurements on Truss Member 2 during lift – Cross-sections A & B

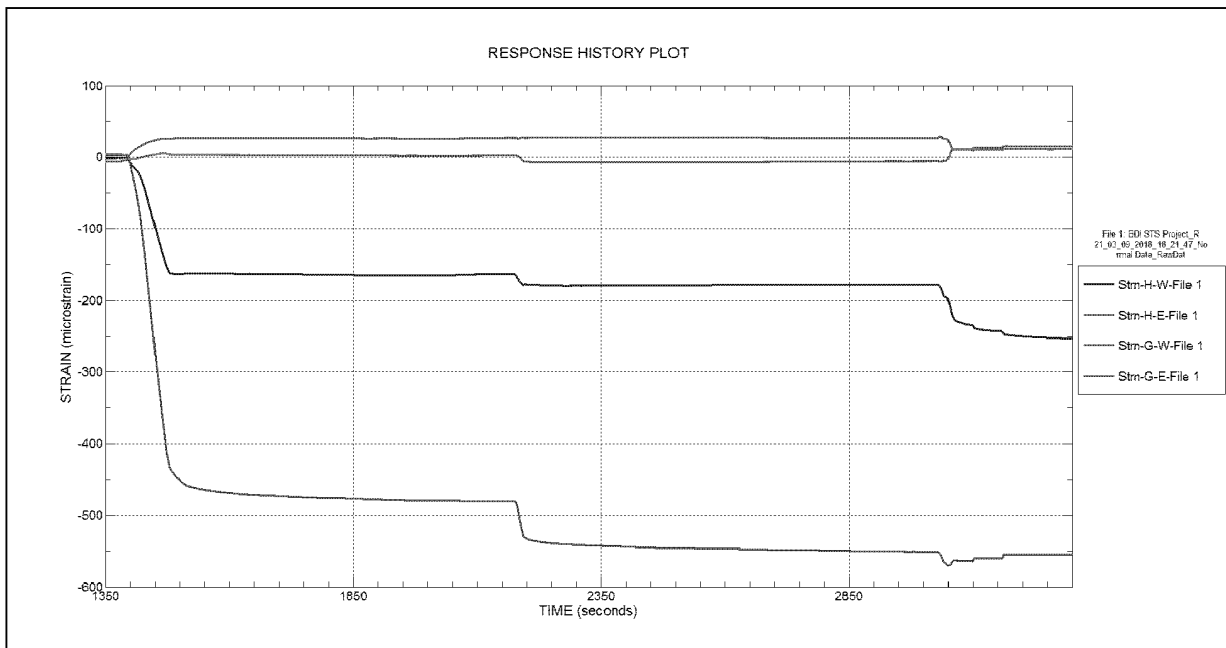


Figure 12 – Strain measurements on Truss Member 12 during lift – Cross-sections G & H

GIRDER DEFLECTION

Another requirement of the monitoring specifications was to measure girder deformation during the span lift and again during the span placement. This was primarily achieved with string-pot displacement sensors that measured movement of the girder relative to the ground during the two events. Figure 13 and Figure 14 provide displacement history measurements recorded from the five string-pots during the span lift and placement events. On-site deflected shape values were not provided during the lift as calculations needed to be performed to remove the rigid-body-motion from the raw data and there was no defined limit or course of action based on the value.

Following post processed calculations and examination of the deflected shapes, it was apparent that the measurement reference points at two locations moved. The intended static reference points for the string-pots at these locations (Location 2 & 4 centered between the lift trailers) was the ground, but the sensors were attached to the steel plates below the trailers. During the lift, the steel plates settled and deflected as the trailers acquired load during the lift and when they shed load during the span placement. Therefore, the reference point for these two measurement locations changed during the lift which resulted in amplified displacement measurements at the pick points. The effect on the deflected shape was that the relative deflections between the ends of the girder and the pick points were exaggerated and the relative displacement between the pick points and midspan were understated. However, the relative difference in displacement between the ends of the beams and midspan was accurate since these locations were measured independently of the lift point displacement measurements. This measurement discrepancy is apparent in the deflected shape diagrams in Figure 15, where the middle section of the girder is relatively flat, while the ends of the girder are very sloped. A more appropriate deflected shape is also provided in the plot using an assumed deformed shape and the three displacement sensors that had valid reference points (ends and midspan). Figure 16 contains the same deflection information during the span placement and it was apparent that the same issue of moving reference points was present, but it also shows that the girder deformation recorded during lifting and setting were nearly equal and opposite.

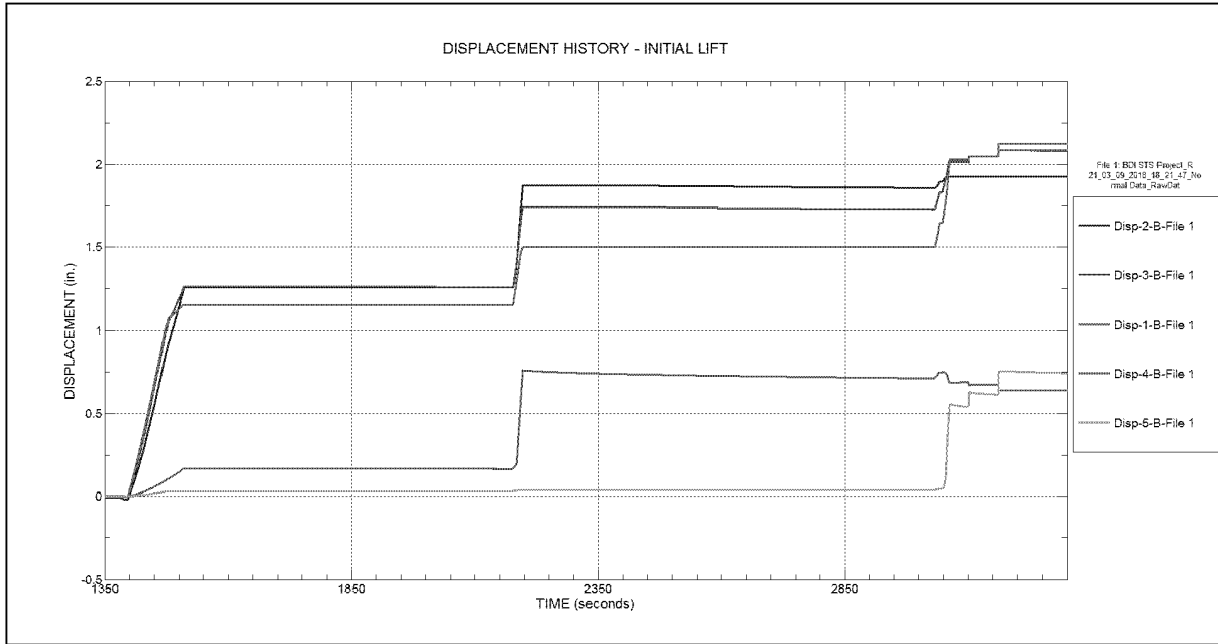


Figure 13 – Girder displacement measurements during lift

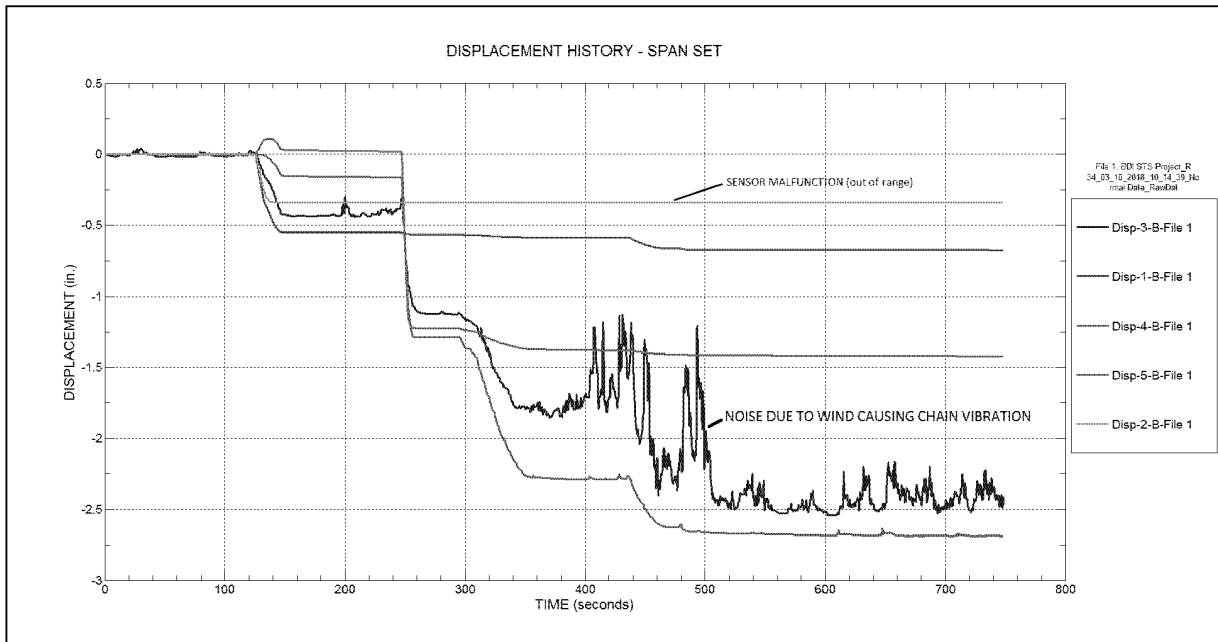


Figure 14 – Girder displacement measurements during span set

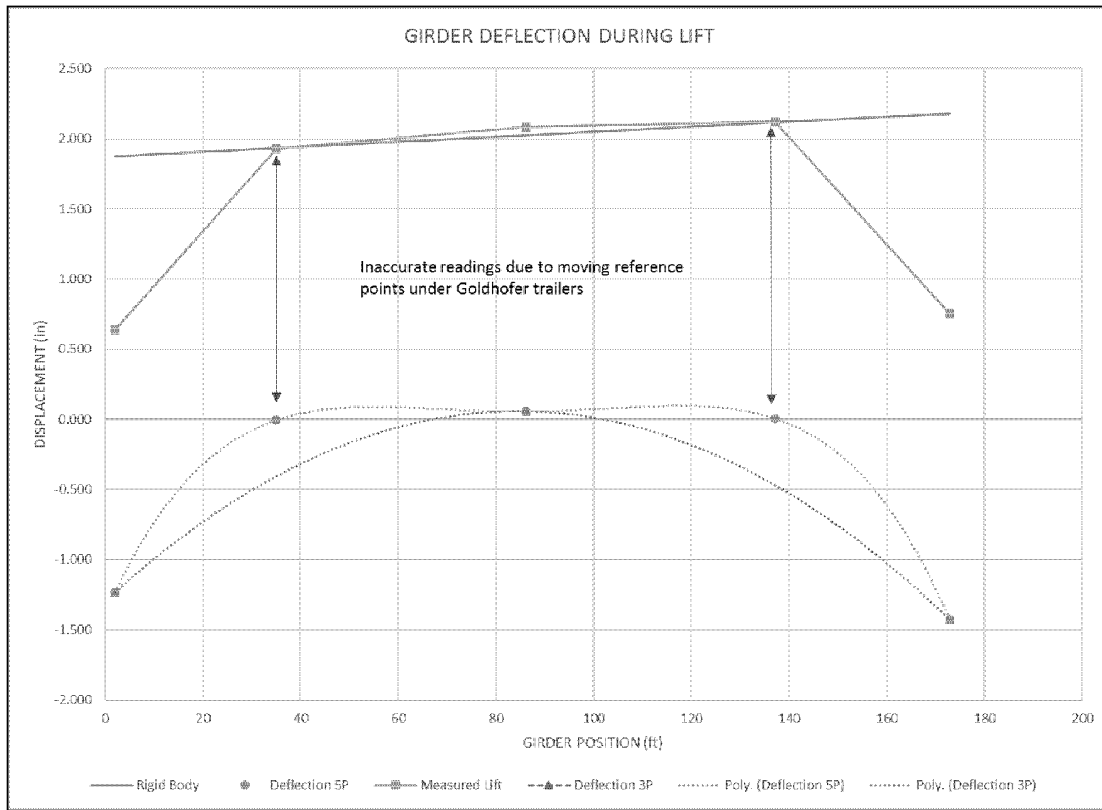


Figure 15 – Girder deflection during lift (5-point and 3-point calculation)

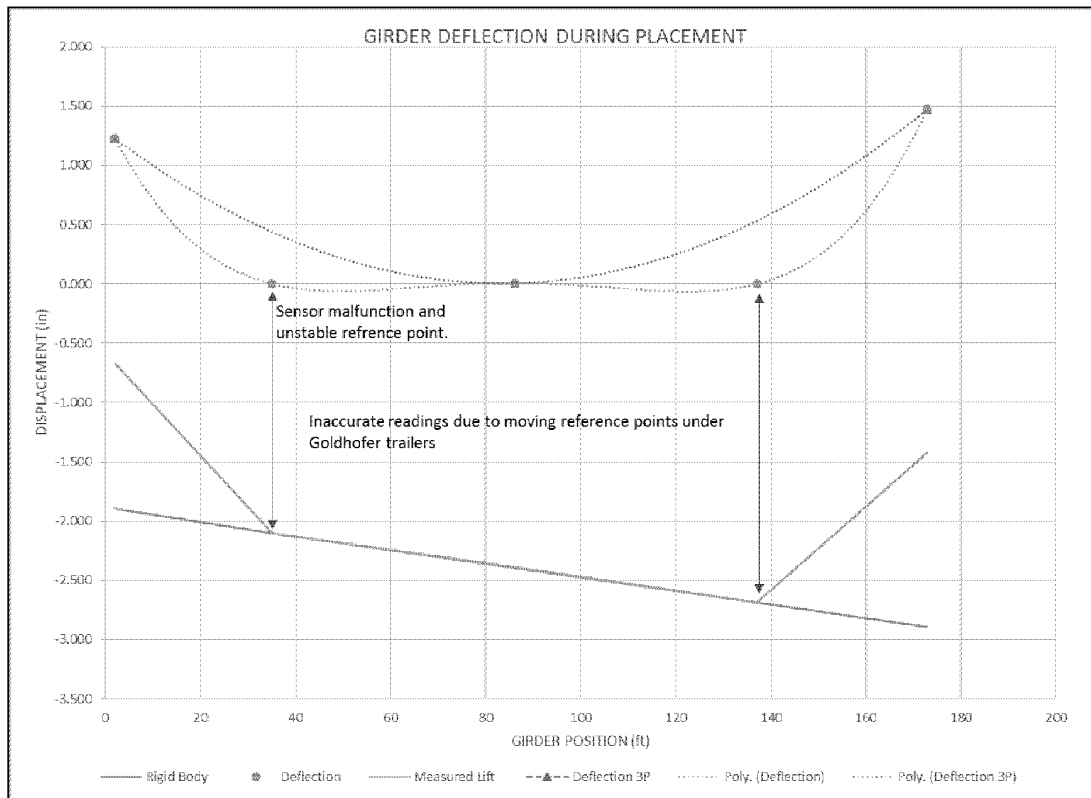


Figure 16 – Girder deflection during placement (5-point and 3-point calculation)

GIRDER FLEXURAL ROTATION

A backup global deformation measurement was performed to account for expected difficulties in obtaining direct deflection measurements; wind and unstable reference points being potential issues. Longitudinal rotation sensors were installed at the same cross-sections to provide direct measure of girder rotation at each location. Again, these measurements had a girder deformation component and a rigid-body-motion component, but the girder rotation reference was gravity and therefore stable and consistent for all locations. Examination of the girder rotation values during lifting and setting provided a direct measure of global deformation performance as shown in Figure 17 and Figure 18. As with the deflection measurements, the rotation measurements for the two loading events appeared to be equal and opposite, which was evidence of linear-elastic behavior.

GENERAL CONCLUSIONS

Monitoring results indicated that the bridge span was lifted and transported within specification aside from two minor exceedances in girder twist. The girder move was halted immediately after each occurrence and BCR corrected the twist angle prior to resuming the transport. All measurements indicate the span was placed in a condition nearly identical to the state that it was originally in prior to lifting. Local and global monitoring results showed there was no significant change in measured structural response, indicating the stress state of the structure was similar when comparing prior to and after the move. The fact that strains returned to near original values (barring thermal effects) and the global deformations during load transfer were equal and opposite between lifting and setting were direct evidence that the structure remained in a linear-elastic state through the entire move. To illustrate the final state of the bridge span, data plots are provided in Appendix B for the final segment as the span was set on the bearings.

BDI's role was to perform structural monitoring only; therefore, no structural analysis, design, or capacity calculations were performed. Monitoring results presented here do not provide any indication of safety performance or assessment of the girder performance relative to design as this was not the intent of the monitoring.

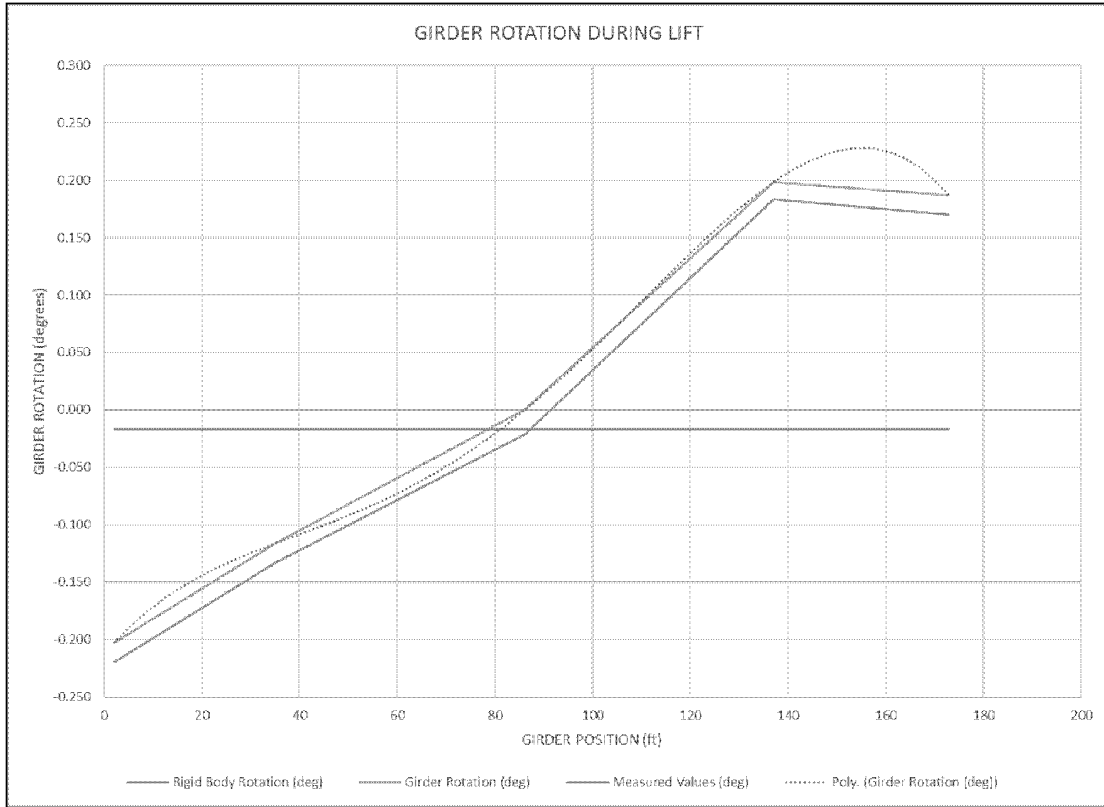


Figure 17 –Girder rotation during span lift

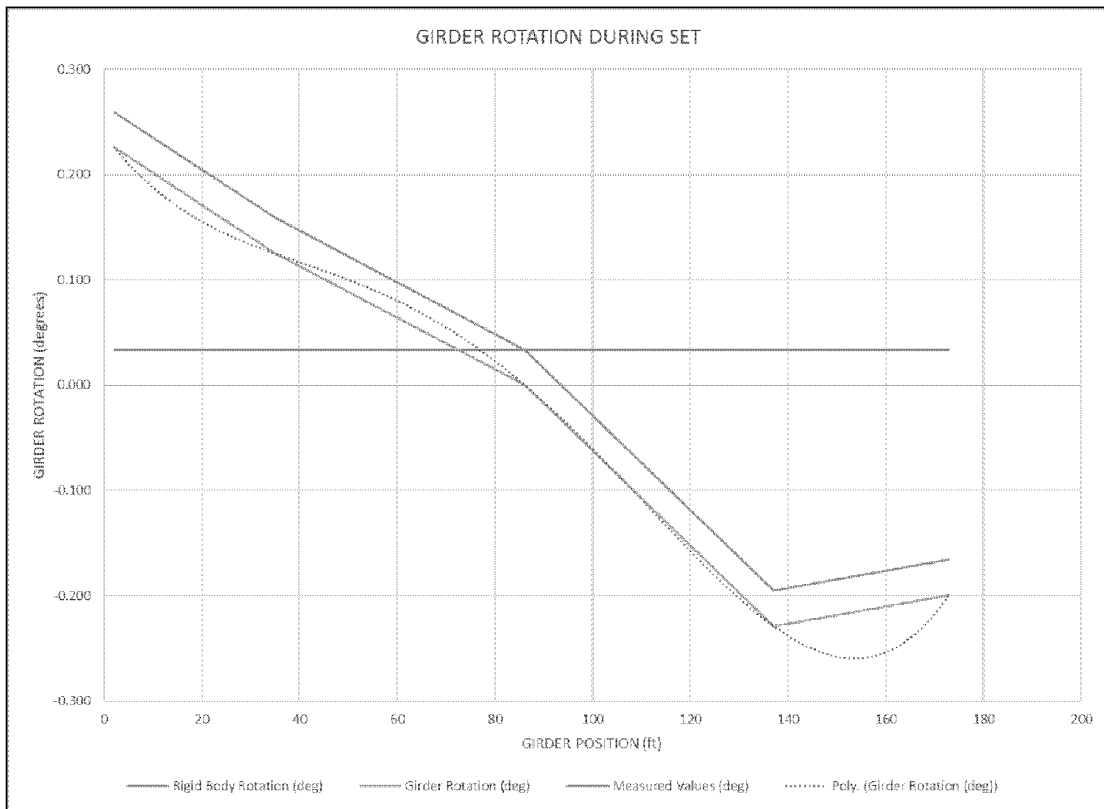


Figure 18 –Girder rotation during span placement

APPENDIX A – DATA PLOTS

The following data plots contain the entire monitoring timeline for each sensor and calculated twist and rotation angles. The horizontal axis is in time and the vertical axis is in engineering units appropriate for the sensor. Gaps in data indicate portions of time when data was not being recorded and transport operations were completely halted. These periods corresponded to data connectivity issues or during rigging chain operations before and after girder jacking. Annotations are provided to indicate the major event sequences of the move.

To reiterate, all measurements made throughout the bridge move were relative to the initial state while the span was supported on the temporary piers. For example, data plots showing positive or tensile strain do not mean the concrete was actually in tension, it just indicates that the change in strain was in the positive direction. The initial state was unknown. Sign conventions of each data plot correspond to the following rules:

Measurement Type	Sign	Description
Strain	+	Tension (or reduction in compression relative to initial state)
	-	Compression (or reduction in tension relative to initial state)
Rotation	+	Positive rotation using right-hand-rule with origin at south end of girder
	-	Negative rotation using right-hand-rule with origin at south end of girder
Twist	+	Positive rotation of north end relative to south end (right-hand-rule)
	-	Negative rotation of north end relative to south end (right-hand-rule)
Displacement	+	Upward displacement relative to ground
	-	Downward displacement relative to ground

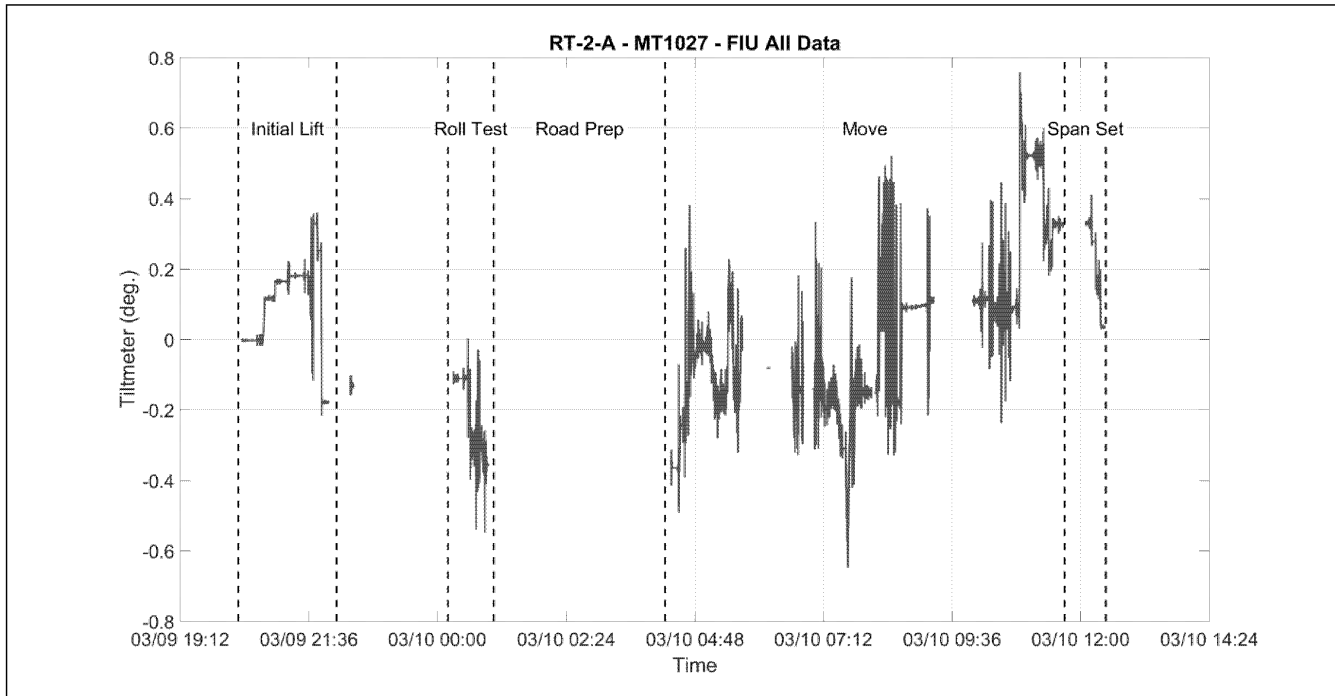


Figure 20 – Transverse rotation at Cross-Section J – Transverse Position A.

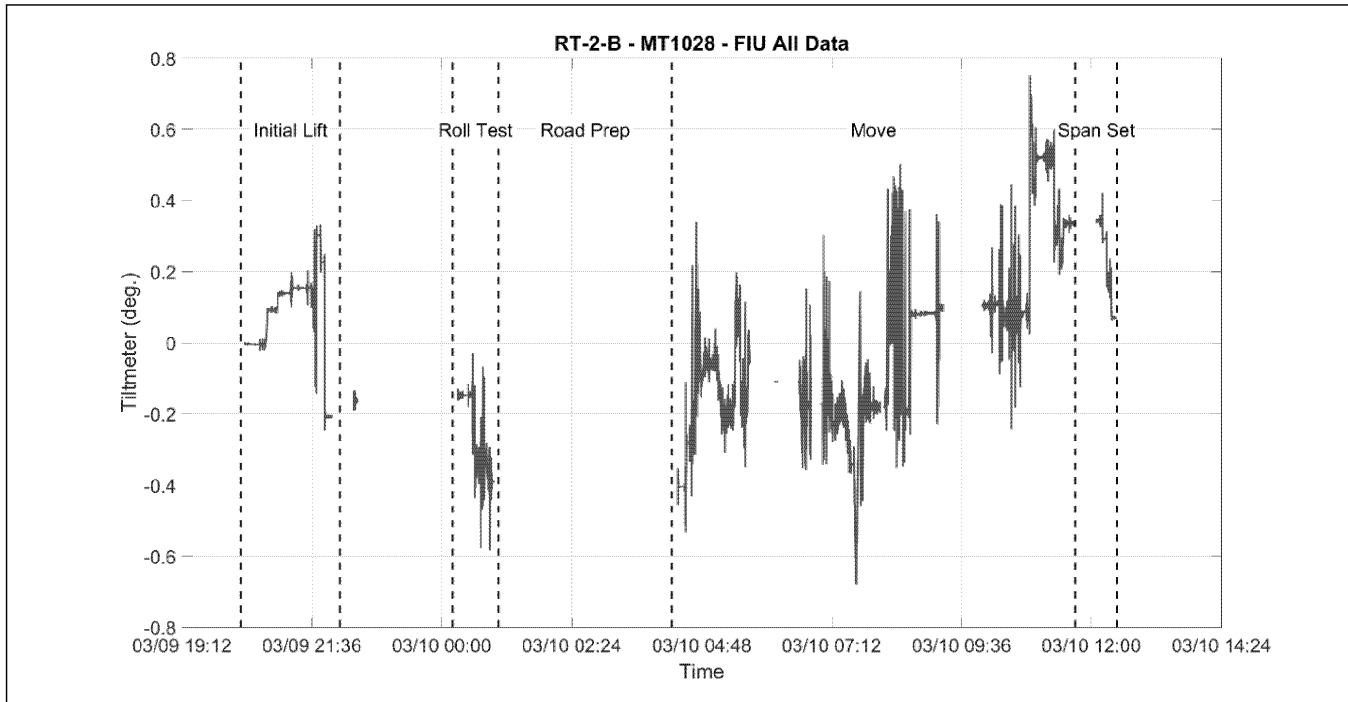


Figure 21 – Transverse rotation at Cross-Section J – Transverse Position B.

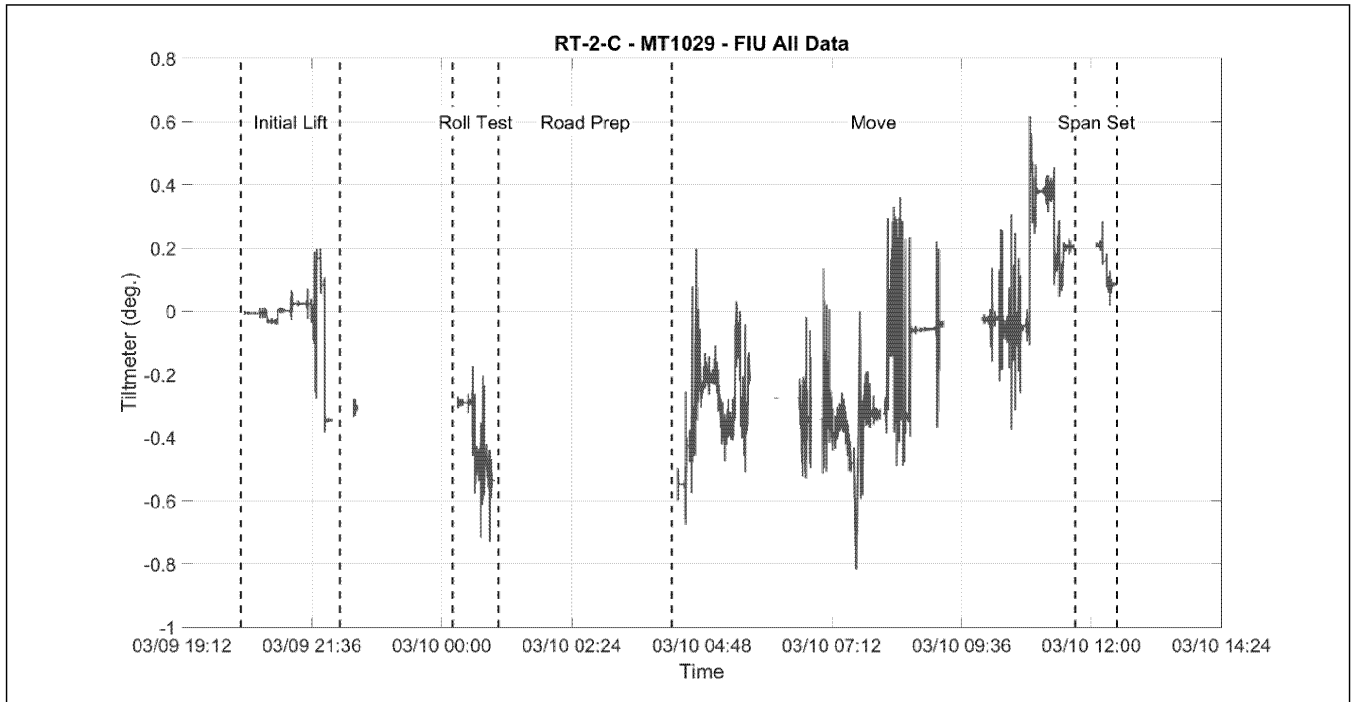


Figure 22 – Transverse rotation at Cross-Section J – Transverse Position C.

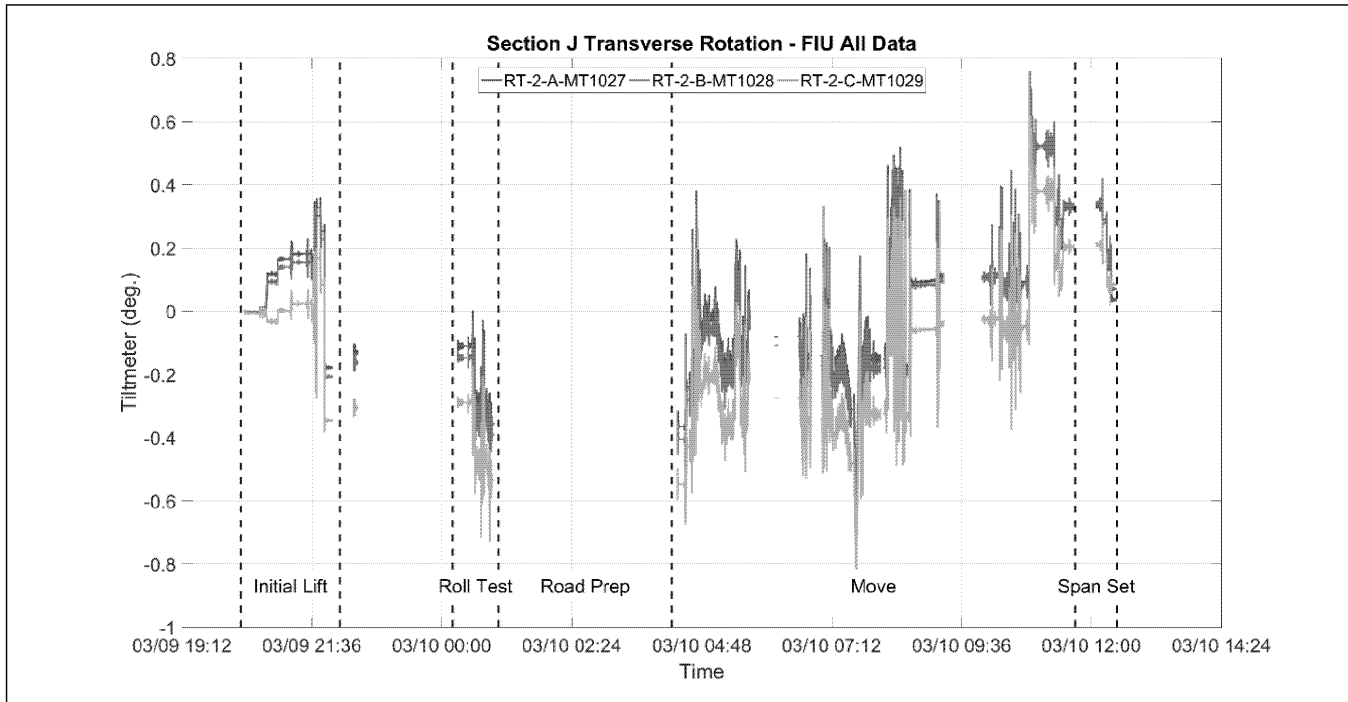


Figure 23 – Transverse rotation at Cross-Section J - Positions A, B & C

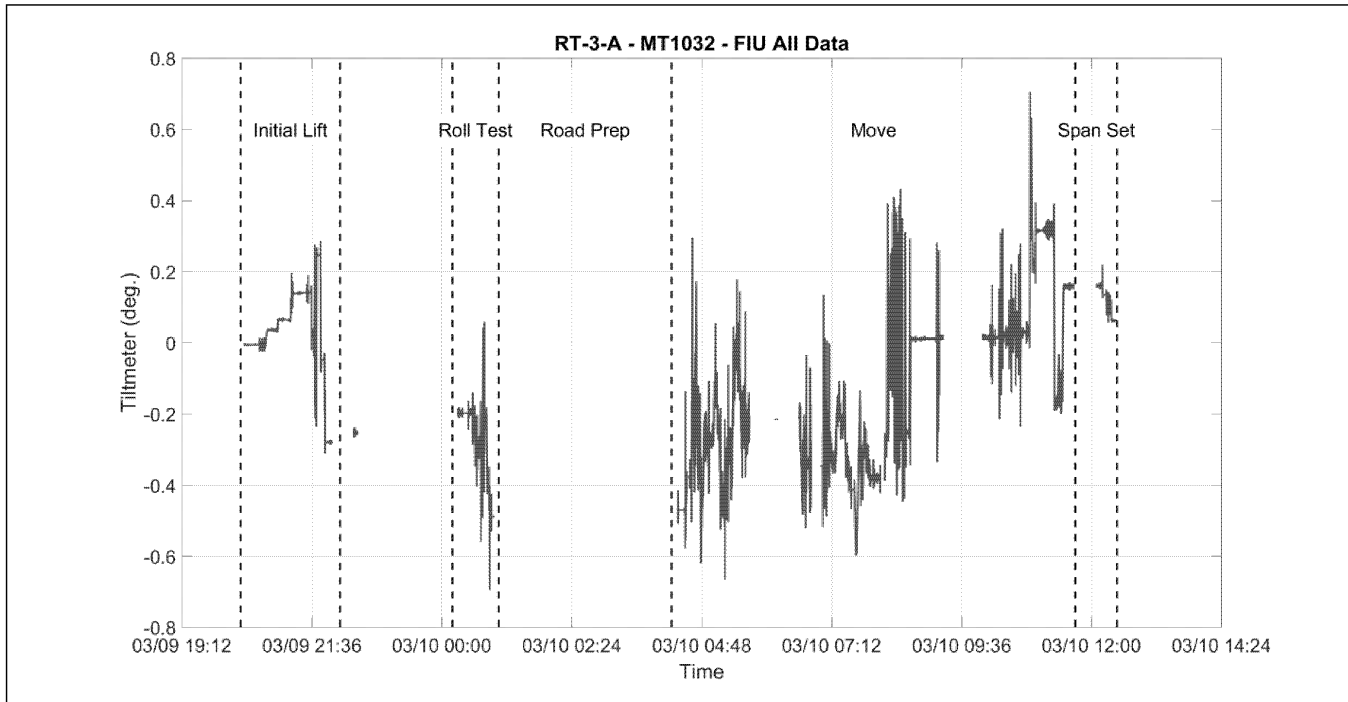


Figure 24 – Transverse rotation at Cross-Section 3 – Transverse Position A

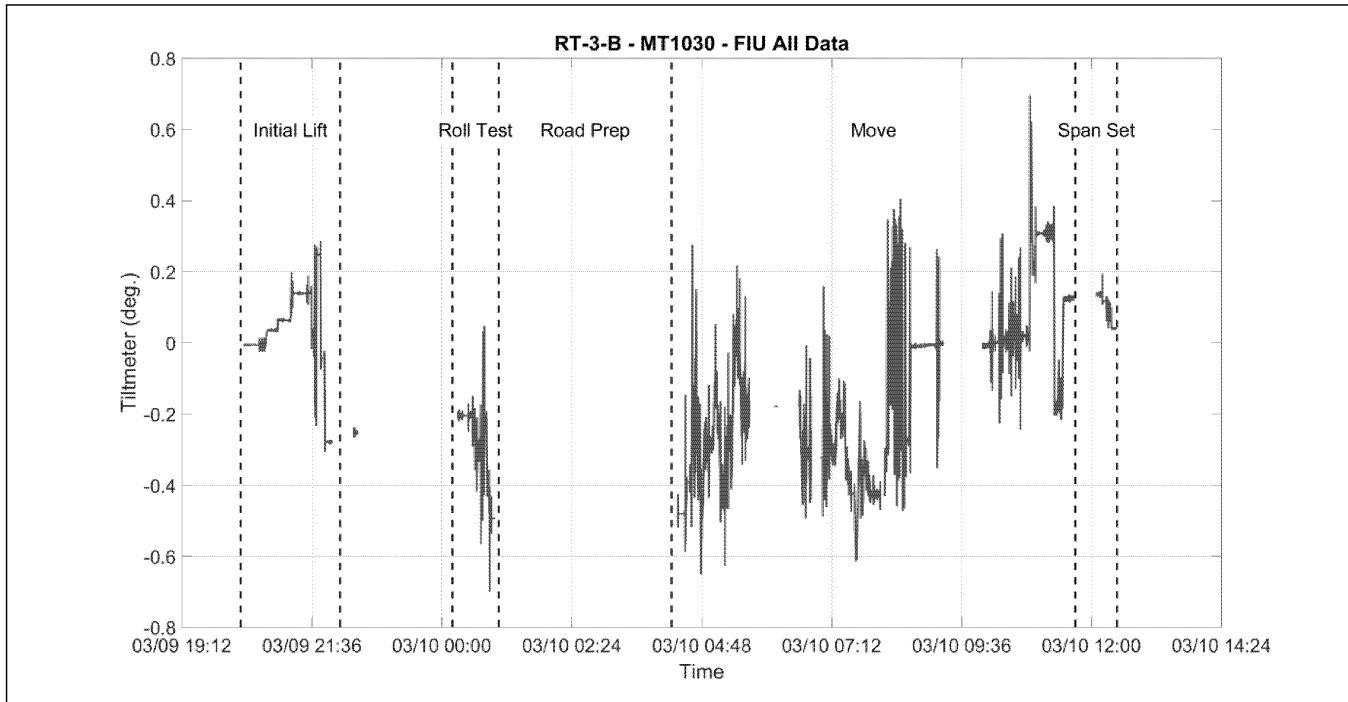


Figure 25 – Transverse rotation at Cross-Section 3 – Transverse Position B

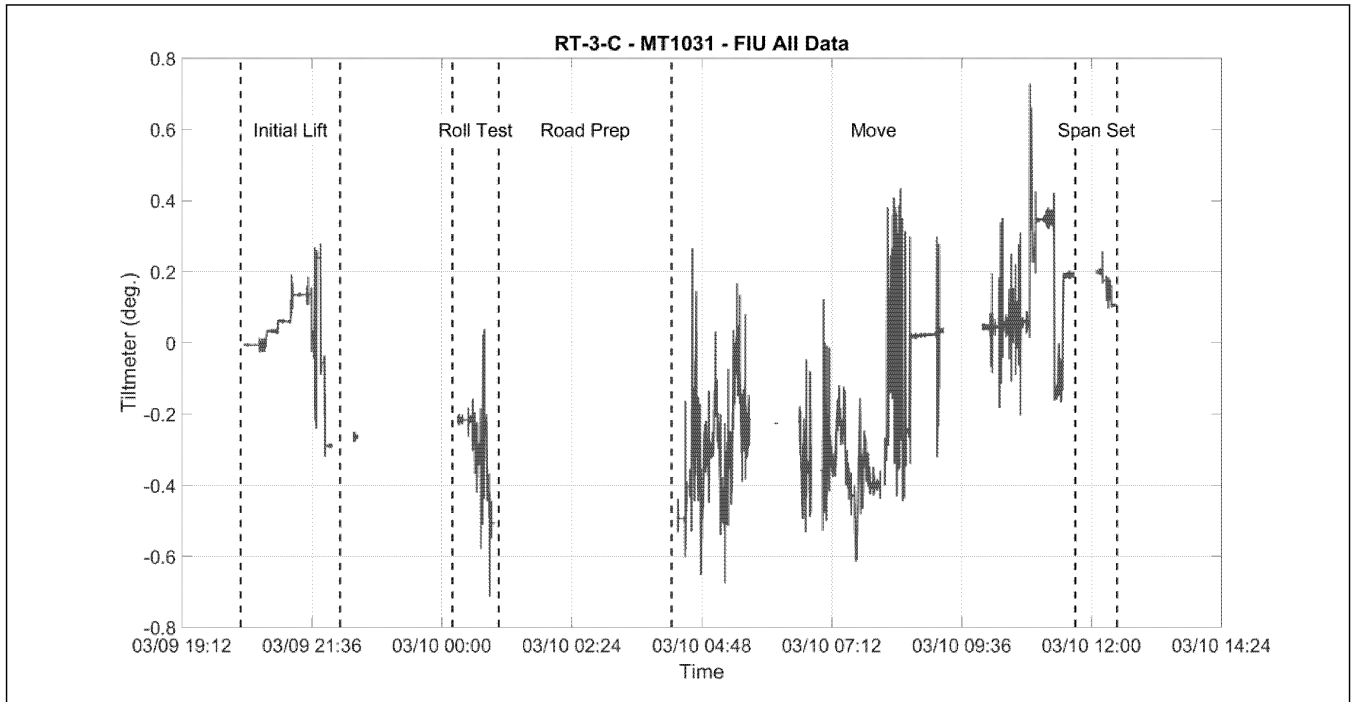


Figure 26 – Transverse rotation at Cross-Section 3 – Transverse Position C

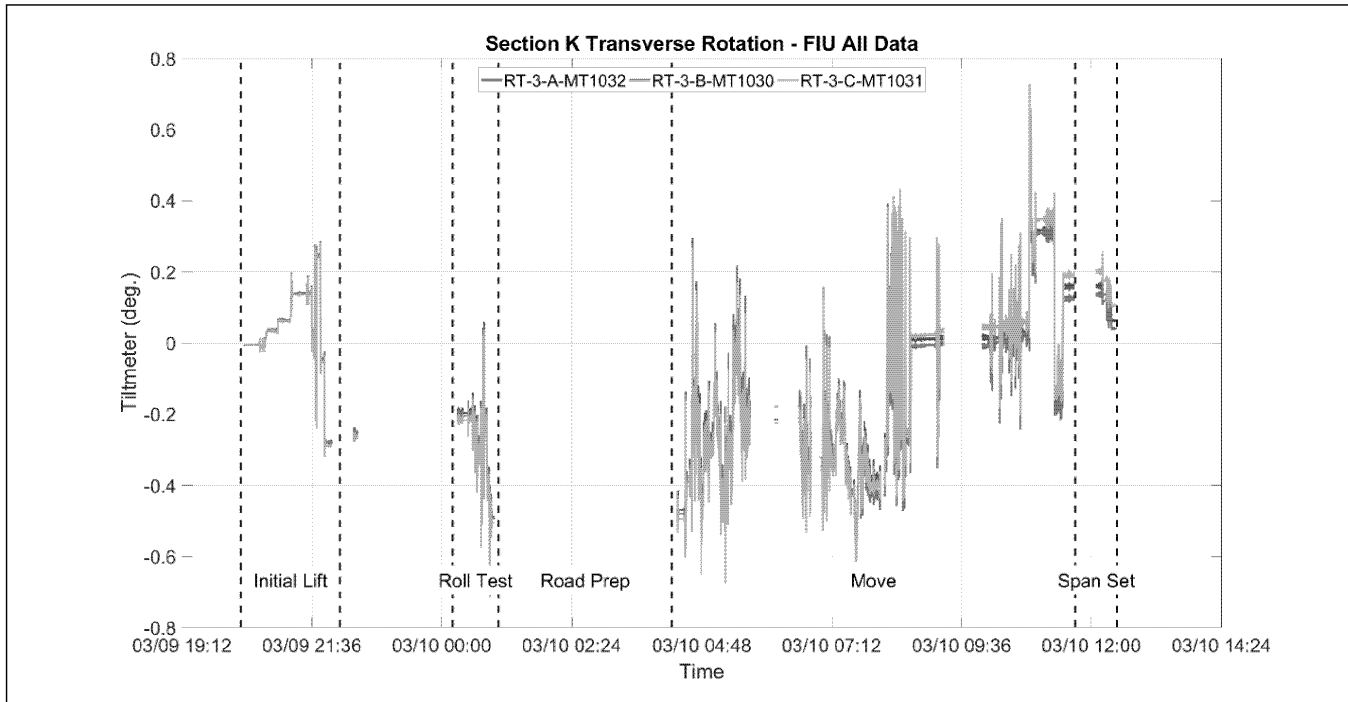


Figure 27 – Transverse rotation at Cross-Section 3 – Transverse Positions A, B & C

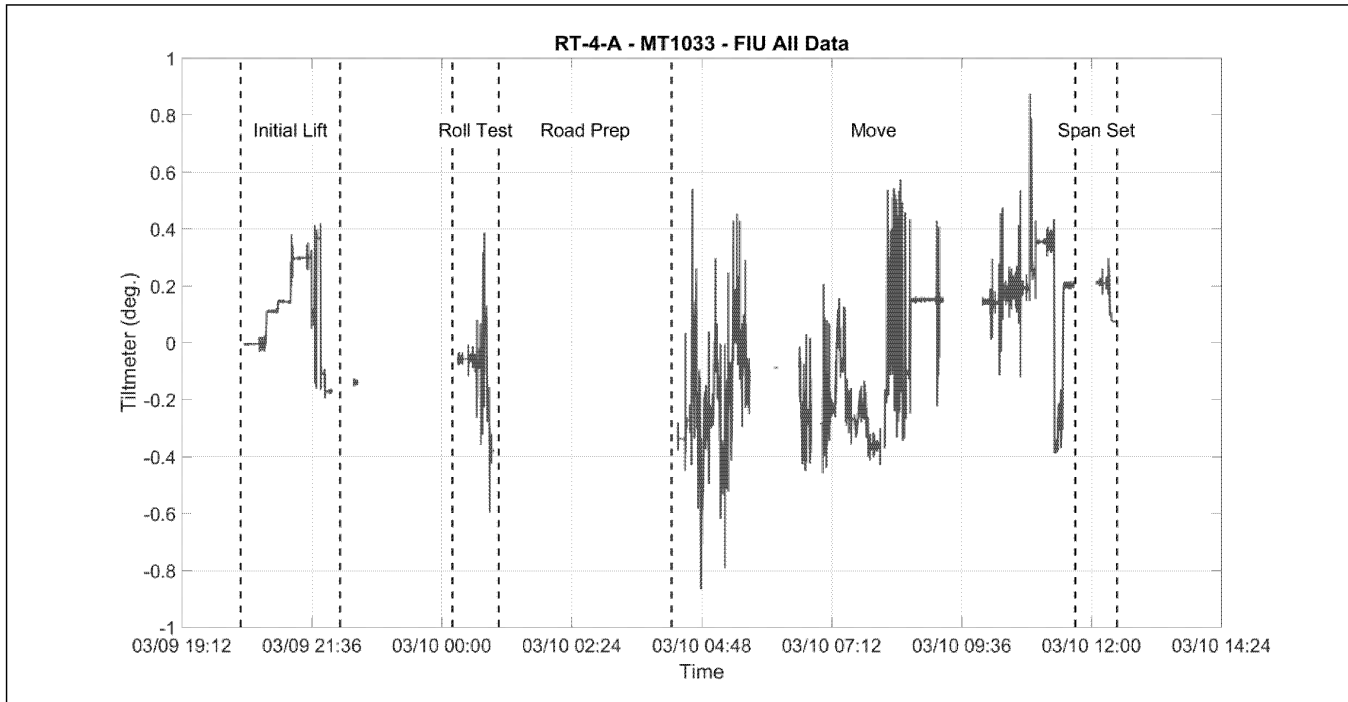


Figure 28 – Transverse rotation at Cross-Section 4 – Transverse Position A

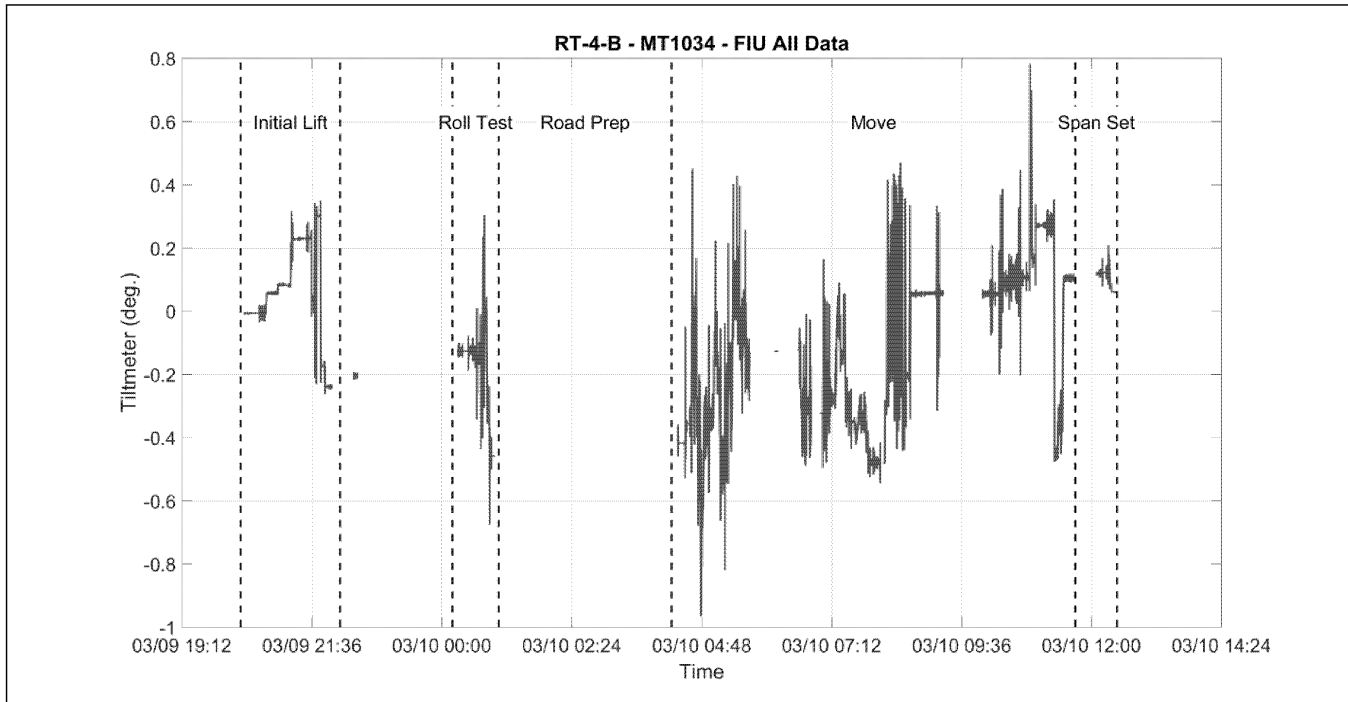


Figure 29 – Transverse rotation at Cross-Section 4 – Transverse Position B

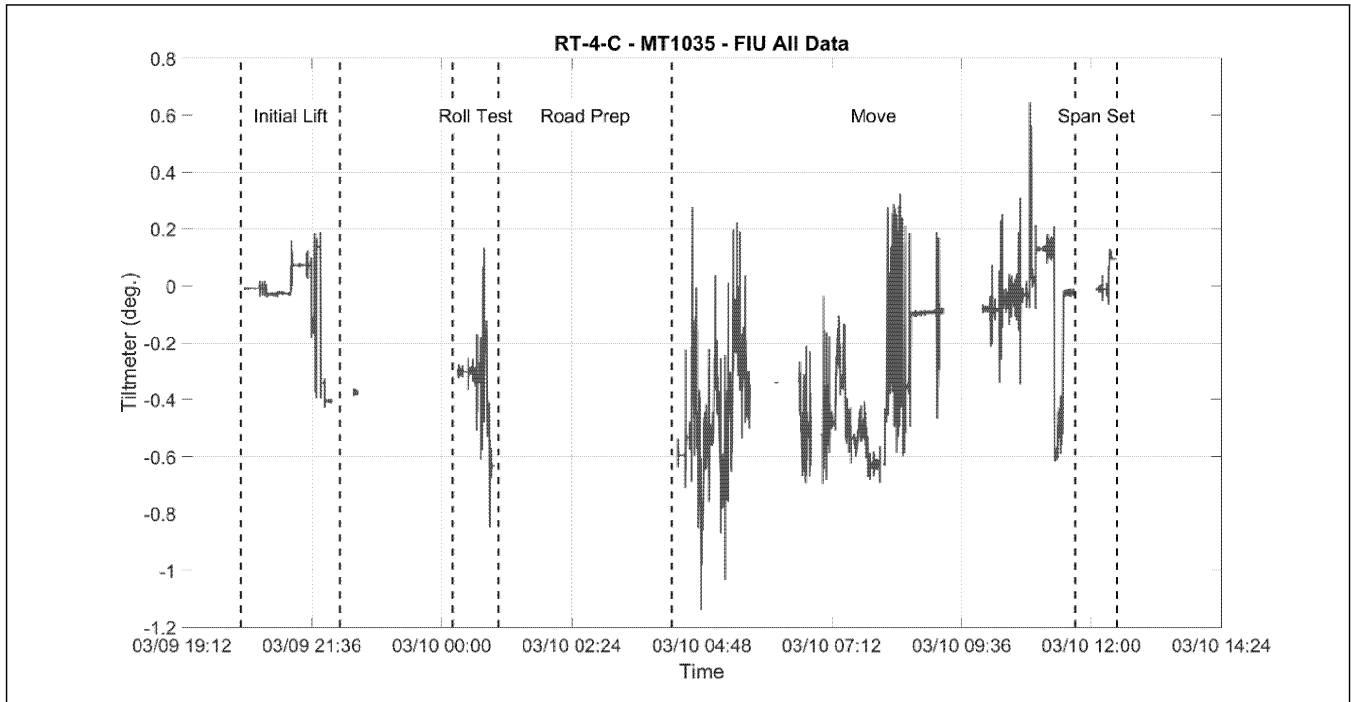


Figure 30 – Transverse rotation at Cross-Section 4 – Transverse Position C

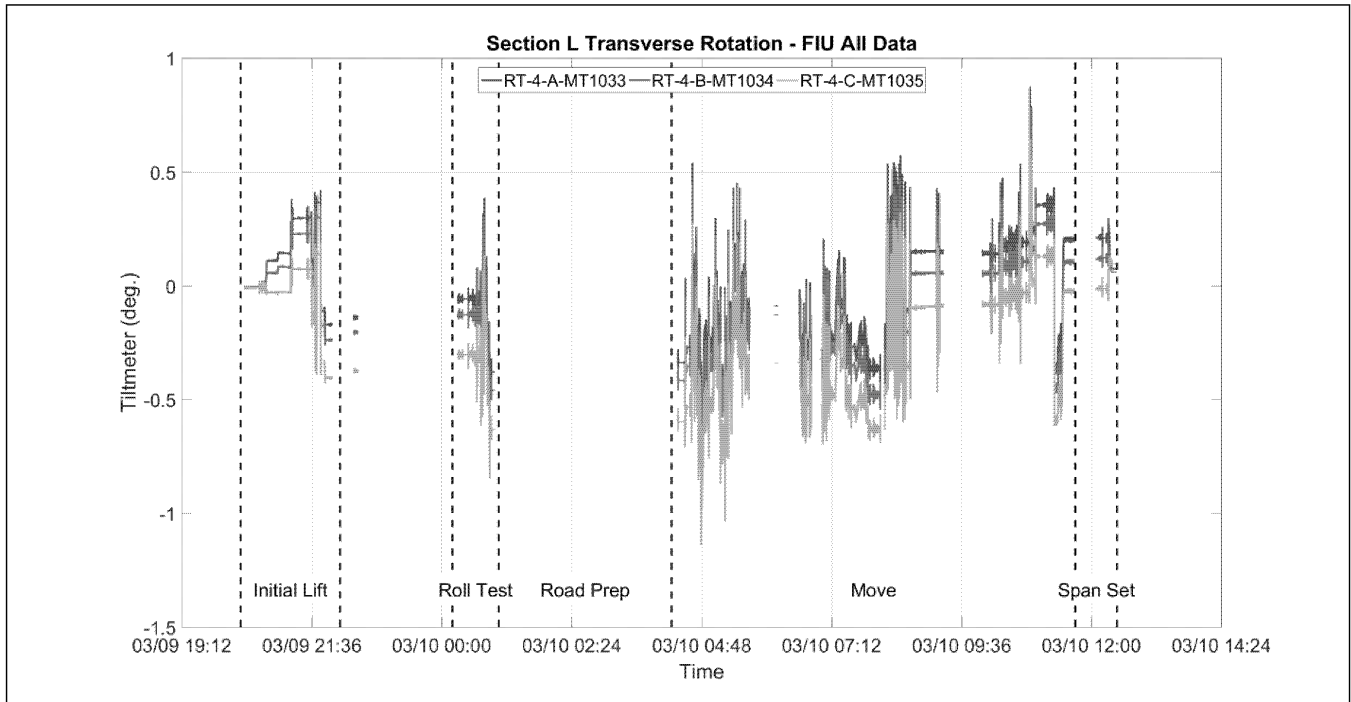


Figure 31 – Transverse rotation at Cross-Section 3 – Transverse Positions A, B & C

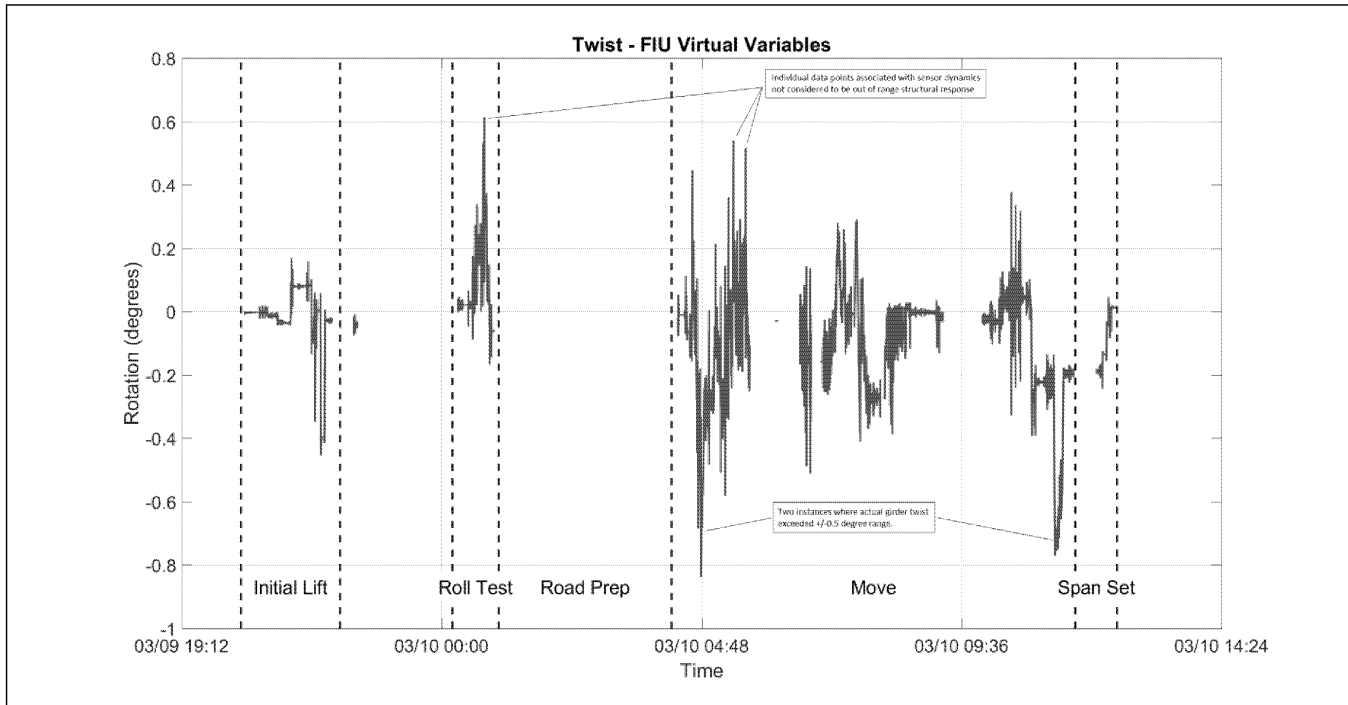


Figure 32 – Girder Twist – Difference in angle between Sections J & L